

Washington University in St. Louis

## Washington University Open Scholarship

---

Arts & Sciences Electronic Theses and  
Dissertations

Arts & Sciences

Spring 5-15-2022

### Defining the role of rare genetic variants that drive risk and pathogenesis of Alzheimer's disease

Matthew James Rosene  
*Washington University in St. Louis*

Follow this and additional works at: [https://openscholarship.wustl.edu/art\\_sci\\_etds](https://openscholarship.wustl.edu/art_sci_etds)



Part of the [Genetics Commons](#), [Molecular Biology Commons](#), and the [Neurosciences Commons](#)

---

#### Recommended Citation

Rosene, Matthew James, "Defining the role of rare genetic variants that drive risk and pathogenesis of Alzheimer's disease" (2022). *Arts & Sciences Electronic Theses and Dissertations*. 2657.  
[https://openscholarship.wustl.edu/art\\_sci\\_etds/2657](https://openscholarship.wustl.edu/art_sci_etds/2657)

This Dissertation is brought to you for free and open access by the Arts & Sciences at Washington University Open Scholarship. It has been accepted for inclusion in Arts & Sciences Electronic Theses and Dissertations by an authorized administrator of Washington University Open Scholarship. For more information, please contact [digital@wumail.wustl.edu](mailto:digital@wumail.wustl.edu).

WASHINGTON UNIVERSITY IN ST. LOUIS

Division of Biology and Biomedical Sciences  
Molecular Cell Biology

Dissertation Examination Committee:

Celeste M. Karch, Chair  
John R. Cirrito  
Carlos Cruchaga  
Jin-Moo Lee  
Jason D. Ulrich

Defining the Role of Rare Genetic Variants that Drive Risk and Pathogenesis of Alzheimer's  
Disease  
by  
Matthew James Rosene

A dissertation presented to  
The Graduate School  
of Washington University in  
partial fulfillment of the  
requirements for the degree  
of Doctor of Philosophy

May 2022  
St. Louis, Missouri

© 2022, Matthew James Rosene

# Table of Contents

List of Figures .....	iv
List of Tables .....	v
Acknowledgments.....	vi
Abstract .....	x
Chapter 1: Introduction and Overview .....	1
1.1 Introduction .....	2
1.2 Pathology of AD .....	2
1.3 Reconciling the Genetic Architecture of AD with Pathology .....	3
1.4 Using the Genetics of AD to Identify Therapeutic Targets .....	5
1.5 <i>LMNA</i> and Nucleoskeletal Integrity in AD .....	6
1.6 <i>RAB10</i> : The protective endo-lysosomal factor.....	9
1.7 <i>PLD3</i> : A mysterious protein promoting A $\beta$ clearance .....	10
1.8 References .....	12
Chapter 2: <i>LMNA</i> -mediated nucleoskeleton dysregulation in Alzheimer's disease .....	19
2.1 Abstract .....	20
2.2 Introduction .....	21
2.3 Materials and Methods.....	23
2.4 Results.....	29
2.5 Discussion .....	38
2.6 References .....	43
Chapter 3: RAB10: a protective factor in AD .....	50
3.1 Abstract .....	51
3.2 Introduction .....	52
3.3 Materials and Methods.....	56
3.4 Results.....	58
3.5 Discussion .....	63
3.6 References .....	67
Chapter 4: Phospholipase D3 contributes to Alzheimer's disease risk via disruption of A $\beta$ clearance and microglia response to amyloid plaques .....	72

4.1 Abstract .....	73
4.2 Introduction .....	75
4.3 Materials and Methods.....	76
4.4 Results.....	87
4.5 Discussion .....	101
4.6 Supplemental Figures.....	106
4.7 Supplemental Tables.....	110
4.8 References .....	120
Chapter 5: Conclusions .....	122
5.1 Introduction .....	123
5.2 Dissertation work furthers research into genetics driving AD pathology.....	123
5.3 Future directions: linking AD genetics, intracellular and extracellular processes, and AD pathology.....	126
5.4 References .....	128
Appendix 1: Genes dysregulated by forced progerin expression in iPSC-derived neurons .....	130
Appendix 2: Genes dysregulated by forced progerin expression in iPSC-derived neurons and differentially expressed in AD brains (MSBB and Mayo) .....	176
Appendix 3: Common variants near LMNA and ZMPSTE24 are not associated with risk for AD in IGAP Stage 1 .....	240
Curriculum Vitae .....	248

# List of Figures

## **Chapter 1 Figures**

<u>Figure 1.1: The complex genetic architecture of AD.</u> .....	4
<u>Figure 1.2: Cellular Functions of RAB10, PLD3, and LMNA.</u> .....	7

## **Chapter 2 Figures**

<u>Figure 2.1: Model of lamin A processing.</u> .....	22
<u>Figure 2.2: LMNA and ZMPSTE24 expression are altered in AD brains.</u> .....	30
<u>Figure 2.3: Lamin A protein levels are altered in AD brains.</u> .....	33
<u>Figure 2.4: LMNA-associated genes are disrupted in AD brains.</u> .....	34

## **Chapter 3 Figures**

<u>Figure 3.1: Diagram of APP trafficking and the role of RAB10 in these intracellular transport pathways.</u> .....	168
<u>Figure 3.2: RAB10 protein expression is elevated in AD brains.</u> .....	173
<u>Figure 3.3: RAB10 expression is not changed in the context of either the rs142787485 or the APOE genotype.</u> .....	175

## **Chapter 4 Figures**

<u>Figure 4.1: iPSC-neurons expressing PLD3 p.A442A phenocopy splicing defects observed in human brains.</u> .....	202
<u>Figure 4.2: PLD3 expression is significantly reduced in brain regions vulnerable to AD pathology</u> .....	205
<u>Figure 4.3: Bi-directional expression of Pld3 alters A<math>\beta</math> turnover in vivo.</u> .....	207
<u>Figure 4.4: Loss of Pld3 alters plaque composition in APP/PS1 mouse cortex.</u> .....	210
<u>Figure 4.5: Loss of Pld3 alters the microglial response to A<math>\beta</math> pathology.</u> .....	212
<u>Figure 4.6: PLD3 is enriched in specific microglia states in human brains.</u> .....	213
<u>Supplemental Figure 4.1: Characterization of the PLD3 p.A442A iPSC-derived neurons</u> .....	219
<u>Supplemental Figure 4.2: Generation of a Pld3-deficient amyloid mouse model.</u> .....	220
<u>Supplemental Figure 4.3: Loss of Pld3 significantly increases plaque size without changing plaque area.</u> .....	221
<u>Supplemental Figure 4.4: Loss of Pld3 does not change dense core plaques.</u> .....	222

# List of Tables

## **Chapter 2 Tables**

<a href="#">Table 2.1: Study demographics .....</a>	<a href="#">25</a>
<a href="#">Table 2.2: LMNA and ZMPSTE24 expression in brains with Pathology Aging (amyloid plaques) and FTLD-tau (tau tangles).....</a>	<a href="#">32</a>
<a href="#">Table 2.3: LMNA Network Genes are dysregulated in AD brains .....</a>	<a href="#">35</a>
<a href="#">Table 2.4: LMNA network genes disrupted in AD are enriched in lysosomal, nuclear, and apoptotic pathways .....</a>	<a href="#">37</a>

## **Chapter 3 Tables**

<a href="#">Table 3.1: Relative expression of various RAB10-targeting miRNAs across different studies</a>	<a href="#">177</a>
---	---------------------

## **Chapter 4 Tables**

<a href="#">Table 4.1: Differential microglia gene expression in APP/PS1xPld3-KO compared with APP/PS1xPld3-WT brains .....</a>	<a href="#">209</a>
<a href="#">Supplemental Table 4.1: Human brain demographics for snRNAseq.....</a>	<a href="#">223</a>
<a href="#">Supplemental Table 4.2: PLD3 expression in human brain microglia.....</a>	<a href="#">224</a>
<a href="#">Supplemental Table 4.3: PLD3 expression within microglia subclusters by disease status....</a>	<a href="#">225</a>
<a href="#">Supplemental Table 4.4: PLD3 expression in iTF-Microglia CROP-Seq.....</a>	<a href="#">226</a>

## **Acknowledgments**

First and foremost, I want to give my deepest thanks to my mentor, Celeste Karch, whose patience, wisdom, and calm guidance has been monumental as I mature into the scientist I am now and sets a high bar for the scientist I hope to be in the future. I would not be here today without your mentorship. Even though my time in the lab is coming to an end, I hope to continue working and collaborating with you in the years to come.

I would also like to thank the members of the Karch lab for sharing with me their wisdom, support, and humor when I needed it the most. It has been both an honor and a delight to call you all my colleagues.

I would like to give thanks to my committee. I always enjoyed the discussions during our meetings and appreciate the valuable advice that guided and pushed this work forward. You also played a critical role in my development and I have nothing but the deepest admiration for you all.

I also want to thank my running buddies. The countless miles we spent together on the roads kept me sane and gave me a necessary respite from the daily grind.

To Bethany, thank you for hearing me endlessly ramble on about my work, for listening to me recite my practice talks countless times, for lending an ear when I had to vent about the latest frustration, and for always having my back. It has meant the world to me.

Finally, I also want to give the deepest thanks to my family. You were there for me at my highest of highs and, most importantly, my lowest of lows. You were my biggest fans and motivators to keep pushing when things got hard, while also making sure I took the time to smell the coffee. At my darkest of moments, you reminded me that there was still light at the end.

I thank the International Genomics of Alzheimer's Project (IGAP) for providing summary results data for these analyses. The investigators within IGAP contributed to the design and implementation of IGAP and/or provided data but did not participate in analysis or writing of this dissertation. Study data were provided by the following sources: The Mayo Clinic Alzheimer's Disease Genetic Studies, led by Dr. Nilufer Taner and Dr. Steven G. Younkin, Mayo Clinic, Jacksonville, FL using samples from the Mayo Clinic Study of Aging, the Mayo Clinic Alzheimer's Disease Research Center, and the Mayo Clinic Brain Bank. Study data includes samples collected through the Sun Health Research Institute Brain and Body Donation Program of Sun City, Arizona.

This work was also funded by BrightFocus Foundation (CMK), the Alzheimer's Association (CMK), NIH U01 AG052411 (AG), R01 AG062359 (CMK), P50 AG005681 (JM, CMK), R56AG067764 (CMK, OH, CC), U01 AG072464 (ST, CMK, OH, MK), UL1 TR002345, NS090934 (DMH), AG047644 (DMH), NS094692 (JML), AG062359 (MK).

This work was supported by access to equipment made possible by the Hope Center for Neurological Disorders and the Departments of Neurology and Psychiatry at Washington University School of Medicine. I thank the Washington University in St Louis Mouse Genetics Core for assistance in generating the Pld3 KO mice. The gRNAs were generated by the Genome Engineering and iPSC Center (GEiC) at the Washington University in St. Louis. I thank the Hope Center Viral Vector Core for generating the AAV8 particles and the Hope Center Animal

Surgery Core for performing the AAV8 injections.

Confocal was generated on a Zeiss LSM 880 Airyscan Confocal Microscope, which was purchased with support from the Office of Research Infrastructure Programs (ORIP), a part of the NIH Office of the Director under grant OD021629. The recruitment and clinical characterization of research participants at Washington University were supported by NIH P50 AG05681, P01 AG03991, and P01 AG026276.

Matthew James Rosene

*Washington University in St. Louis*

*May 2022*

Dedicated to my family.  
You had faith in me when I had none in myself.

## ABSTRACT OF THE DISSERTATION

Defining the role of rare genetic variants that drive risk and pathogenesis of Alzheimer's disease

By

Matthew James Rosene

Doctor of Philosophy in Biology and Biomedical Sciences

Molecular Cell Biology

Washington University in Saint Louis, 2022

Celeste M. Karch, Chair

Alzheimer's disease (AD) is the leading cause of dementia and is pathologically defined by the aggregation of extracellular amyloid plaques and intracellular neurofibrillary tangles. Rare heritable mutations within the genes for *amyloid precursor protein* (*APP*) and *presenilin 1* (*PSEN1*), and *presenilin 2* (*PSEN2*) cause early onset AD and account for approximately 1% of AD cases. While the majority of AD cases are late-onset (LOAD), which is defined by a markedly more complex genetic architecture that is comprised of many genetic risk factors that influence AD through multiple cellular pathways. The advent of deep sequencing analyses have allowed for the identification of novel risk factors and genetic variants. By identifying these genetic risk factors, characterizing their cellular and molecular function, and then identifying the roles they play influencing AD risk, this knowledge may be leveraged for the development of more effective therapeutics. In this dissertation, I look more deeply into three risk factors: *LMNA*, *RAB10*, and *PLD3*. Through a combination of computational analysis and

functional/biochemical assays, I attain a deeper understanding of the roles of these genes as they affect AD pathogenesis.

The first of these genes, *LMNA*, encodes a nuclear lamin protein that is associated with the accelerated aging condition Hutchinson-Guilford Progeria Syndrome (HGPS). In this condition, a mutation in *LMNA* leads to the production of progerin, which is unable to be processed by *ZMPSTE24* and constitutively incorporates into the nuclear membrane, causing nucleoskeletal dysfunction. In AD, some of these same nucleoskeletal deficiencies have also been observed. Through mRNA expression analysis of laser-captured microdissected neurons, we observe a significant elevation of *LMNA* expression coupled with a reduction of *ZMPSTE24* expression in diseased brains, resulting in more immature, unprocessed prelamin A. When we induced progerin expression in iPSC-derived cortical neurons, we observed disruption in pathways associated with the oxidative stress response as well as the lysosome, which has been associated with AD pathology in the literature.

Further genomic analyses in increasingly larger datasets has led to the identification of genetic variants that protect against AD. One study by our group identified a rare SNP in the 3'-untranslated region (3'-UTR) of *RAB10* (rs142787485). As a Rab GTPase, *RAB10* plays a role in the endo-lysosomal network (ELN), a central pathway to the processing of APP and the production of A $\beta$ . In AD brains, we observe increased levels of *RAB10* mRNA and *RAB10* protein expression. Overexpressing *RAB10* in N2A695 cells increases the ratio of extracellular A $\beta$ 42/40, which is associated with increased pathogenicity. Furthermore, when investigating the rs142787485 SNP, the location of this SNP is predicted to interfere with the binding of multiple miRNAs. However, these predictions still need to be validated through functional and biochemical assays.

In our efforts to better understand AD genetics, there remain challenges posed by genes that remain uncharacterized in terms of their function. One such gene is *PLD3*, a member of the phospholipase D family, but lacks any confirmed phospholipase activity or substrate. Whole exome sequencing of families densely affected by LOAD uncovered the rare variant in *PLD3* p.V232M. Further deep sequencing uncovered additional variants associated with increased disease risk. In our work we find that one particular synonymous variant, p.A442A, activates a cryptic splice site, resulting in the reduced expression of exon 11. Furthermore, studies of AD patients show that *PLD3* is reduced in the neurons of AD brains. When we look at loss of *Pld3* in amyloid model mice, we observe significantly decreased A $\beta$  turnover and altered plaque pathology which we further attribute to reduced microglial plaques, mirroring what has been observed in *Trem2*-deficient amyloid mice. Together, these studies illustrate the critical role of nuclear and ELN function in AD risk and resilience.

# **Chapter 1: Introduction and Overview**

## **1.1 Introduction**

Alzheimer's disease (AD) is a neurodegenerative disease defined clinically by progressive memory decline [1]. AD currently affects more than 44 million people worldwide, and this number is expected to rapidly increase as the population ages (<http://www.alz.co.uk>).

Neuropathologically, AD is characterized by neuronal loss and the accumulation of amyloid plaques and neurofibrillary tangles in the brain, much of which occurs many years before the onset of clinical symptoms [2]. While clinical diagnosis of AD is challenging because it is dependent primarily on observations of family members and caregivers, changes in protein analytes in plasma and cerebrospinal fluid (CSF) and brain imaging, although not widely used in clinical practice, may facilitate AD diagnosis [2]. AD can broadly be defined as early-onset, occurring prior to age 65, or the much more common late-onset, occurring after age 65 (>96.5% of total cases).

## **1.2 Pathology of AD**

AD is clinically characterized by extracellular amyloid plaques and intracellular neurofibrillary tau tangles, both of which occur in sequential order of each other and are requisite for the development of AD [3]. Extracellular amyloid accumulation is characterized by the aggregation of pathogenic amyloid- $\beta$  (A $\beta$ ), a peptide generated through the sequential cleavage of the amyloid precursor protein (APP) by  $\beta$ -secretase and  $\gamma$ -secretase within endo-lysosomal compartments within neurons. A $\beta$  was first isolated from the cerebral amyloidosis of both AD and Down Syndrome patients [4]. While ranging in length from 38-43 amino acids in length, the largest proportion of A $\beta$  peptides are the 40 amino acid long A $\beta$ 40 peptide and the 42 amino acid

long A $\beta$ 42 peptide to a much lesser degree. Upon its release from the presynaptic neuron, A $\beta$  can be endocytosed by post-synaptic neurons for lysosomal degradation, engulfed by glial cells for lysosomal degradation, or transcytosed across the blood-brain barrier (BBB) and cleared through the cerebrovascular system. A $\beta$  that is not cleared can aggregate into the amyloid plaques, with the A $\beta$ 42 being especially aggregate prone due to increased hydrophobicity of the extra two amino acids. In the timeline of AD pathology and disease progression, accumulation of amyloid plaques is the first occurring pathology in AD, starting ~20 years before the initial onset of cognitive decline [5]. This paradigm, along with discovery of the first mutations within the genes *APP*, *PSEN1*, and *PSEN2* is what ultimately led to the formulation of the amyloid cascade hypothesis [6-8]. While this hypothesis has been called into question over the years, it still stands that amyloid has an important role to play in AD disease pathogenesis and disease progression.

### **1.3 Reconciling the Genetic Architecture of AD with Pathology**

The genetics of early-onset AD (EOAD) are relatively well understood. Autosomal dominant mutations occurring in *APP*, *PSEN1*, or *PSEN2* give rise to a subset of EOAD cases. More than 200 pathogenic mutations have been reported worldwide (<https://www.alzforum.org/mutations>) [9]. Clinically, EOAD mutation carriers exhibit disease onset prior to 65 years of age [10]. Neuropathologically, EOAD and late-onset AD (LOAD) are indistinguishable [11]. Unfortunately, the genetics of LOAD is more complex (Figure 1.1) [12].

Among individuals with LOAD, there is strong evidence for genetic heritability of disease [13-17]. The single largest genetic risk factor for LOAD is *APOE* [18]. *APOE* plays critical roles in cholesterol transport, neuroplasticity, and inflammation [19]. *APOE* regulates A $\beta$  metabolism directly through binding and clearance of A $\beta$  [20] and indirectly via the LRP1 receptor [21]. Moreover *APOE* influences tau-mediated neurodegeneration [22]. Two different

*APOE* alleles,  $\epsilon 4$  and  $\epsilon 2$ , affect risk for AD. Risk for developing AD is 3-fold higher in individuals carrying one copy of the  $\epsilon 4$  allele and 12-fold higher in individuals carrying two copies of *APOE*  $\epsilon 4$  [23]. Conversely, *APOE*  $\epsilon 2$  confers resilience to AD, while the  $\epsilon 3$  allele is considered neutral risk [23].

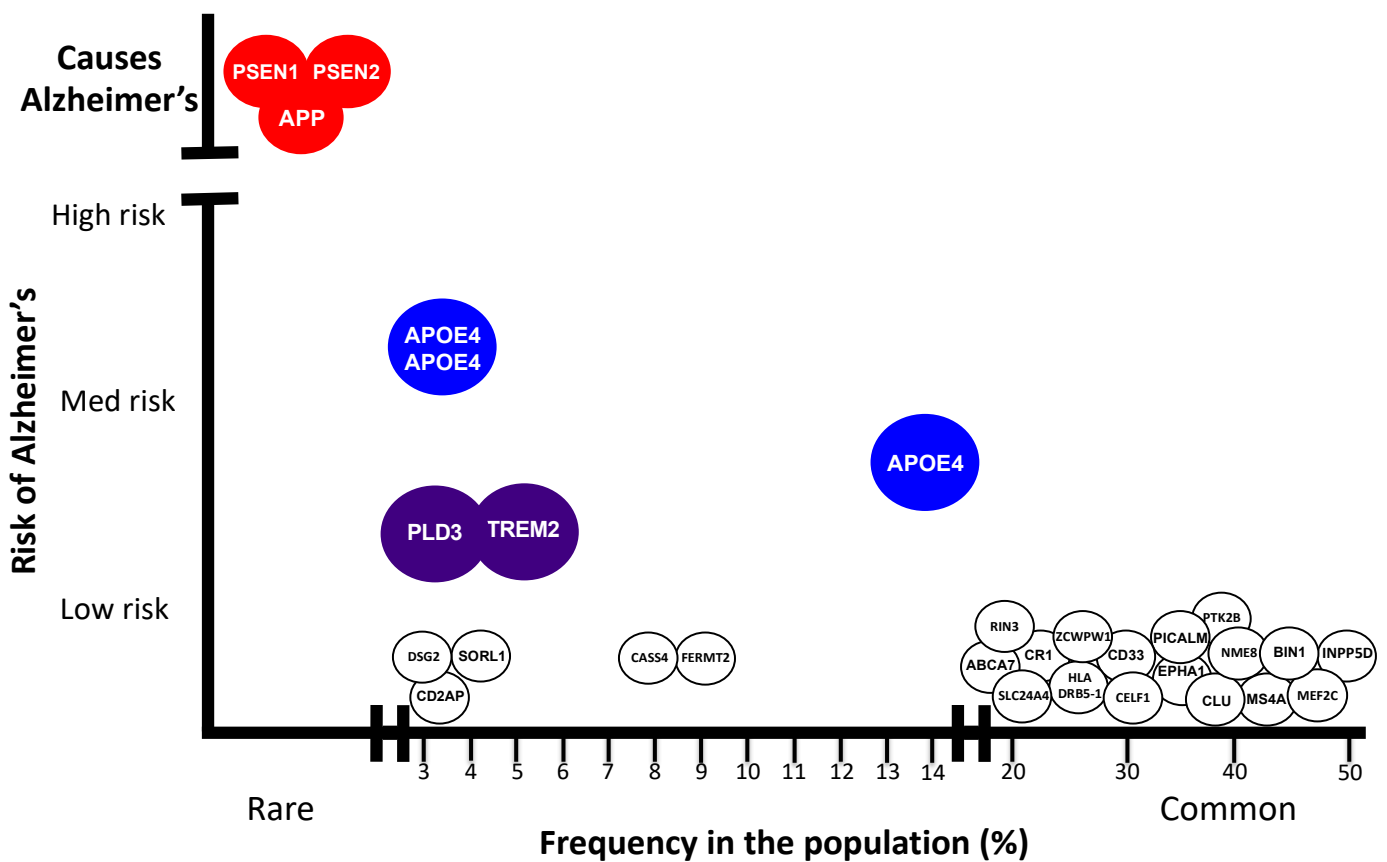


**Figure 1.1: The complex genetic architecture of AD.** While EOAD has been solely attributed to mutations in the APP metabolism genes *PSEN1/2* and *APP*, LOAD is influenced a broader range of factors that have different cellular functions and exert their own unique influence on AD risk.

Genetic variants that influence risk for AD can be broadly classified into two groups: common and rare. The majority of common variants (minor allele frequency (MAF)  $>5\%$ ) were identified using genome-wide association studies (GWAS).[15] With the exception of variants in

*APOE*, all other common variants have small effect sizes on AD risk (odds ratios=1.08-1.22, 0.73-0.94) [15]. While GWAS variants provide insights into disease processes, none of the common risk variants for AD that have been identified by GWAS have clear functional effects and efforts to identify functional variants in the regions of GWAS variants have largely been unsuccessful.

The advent of next-generation sequencing has enabled the sequencing of whole exomes and genomes, resulting in progressively larger AD datasets and providing insights into the contribution of low frequency (MAF 1-5%) and rare variants (MAF<1%) to the genetic architecture of AD. Using a variety of study designs, multiple rare variants have been identified that affect risk for AD [15, 24-27]. Rare variants typically have much larger effect sizes on disease risk than common variants identified by GWAS. Rare variants are also more likely to occur in coding or regulatory regions and thus are more likely to be functional. Thus, rare variants represent effective therapeutic targets.

Finally, alternative study designs can provide additional insights into the genetics of AD. For example, the use of quantitative endophenotypes (eg, CSF levels protein analytes such as A $\beta$  and tau [28-30]; mitochondrial copy number [31]; metabolic efficiency [32, 33]; measurements of progressive brain atrophy [34]; among others), and the analysis of mitochondrial genomic variation [35] have expanded our understanding of the genetic architecture underlying disease onset and disease course.

#### **1.4 Using the Genetics of AD to Identify Therapeutic Targets**

Genes and pathways that regulate AD pathogenesis may represent viable targets for treating disease. For example, therapies targeting the removal of A $\beta$  or inhibition of A $\beta$

production are currently in clinical trials. These strategies are based on our understanding of the mechanisms by which rare mutations in *APP*, *PSEN1* and *PSEN2* drive AD pathogenesis in EOAD and focus on inhibition of the deposition of A $\beta$  in the brain. Similarly, targeting APOE function has been investigated for its therapeutic capacity [36-38]. AD risk genes implicated in immune function, endocytosis, and lipid biology represent novel avenues of therapeutic development. Unfortunately, to date, more than 90% of all clinical trials have failed. Given the expected increase in disease incidence, developing effective therapeutics is imperative and is highly dependent on better understanding the mechanisms that drive disease. For the remainder of this dissertation, I discuss the role of three genes that have been shown to alter AD risk, *LMNA*, *RAB10*, and *PLD3*, how they influence AD pathology and mechanisms, and their potential as therapeutic targets (Figure 1.2).

## **1.4 LMNA and Nucleoskeletal Integrity in AD**

### *LMNA, HGPS, and premature aging*

In order to gain a deeper understanding of neurodegenerative disease mechanisms, we must look to analogous diseases when parallels present themselves. In Hutchinson-Guilford Progeria Syndrome (HGPS), mutations in the *LMNA* gene, which codes type-A lamins (lamin A and lamin C), results in altered splicing of the *LMNA* mRNA, yielding the truncated *LMNAΔ150* and its protein product progerin. Unable to be cleaved by the zinc metallopeptidase and become defarnesylated, the constitutively farnesylated acts in a dominant negative nature by permanently anchoring into the nuclear membrane and disrupting normal lamina functions and disrupting nucleoskeletal morphology and integrity [39]. Downstream, these defects in nucleoskeletal morphology have broader detrimental effects for the cell both within the nucleus (chromatin disorganization, genomic instability and DNA damage, and abnormal gene expression) as well as

outside the nucleus (mitochondrial dysfunction, oxidative stress, and loss of proteostasis) [40-43], all of which have been also reported within AD.

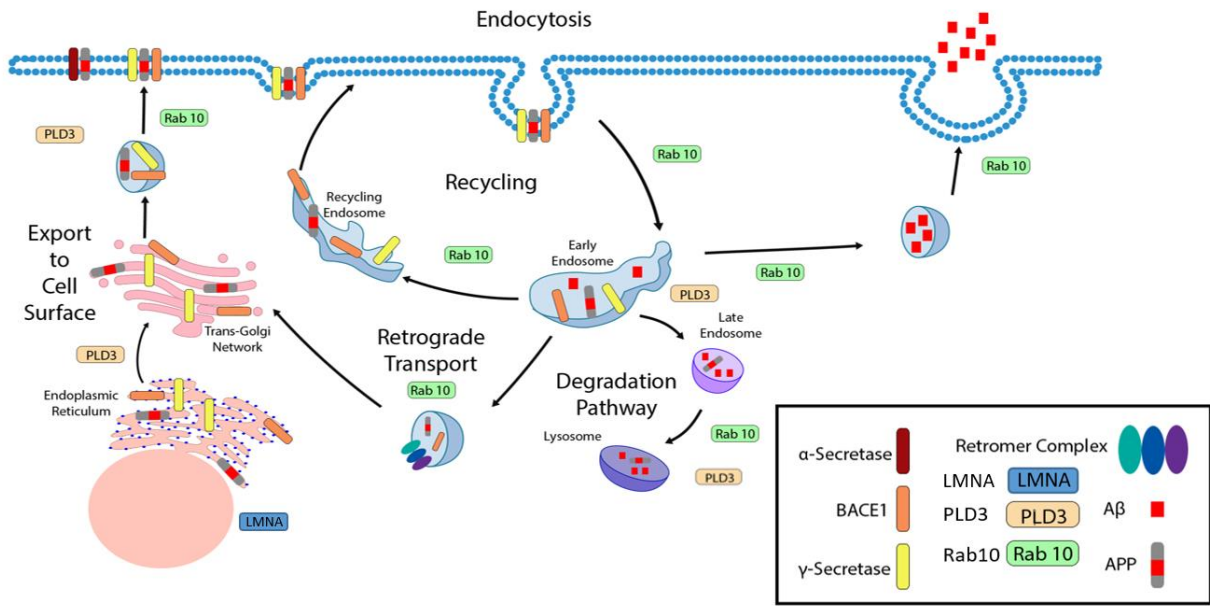


**Figure 1.2: Cellular Functions of *RAB10*, *PLD3*, and *LMNA*.** Image adapted from Tavana et al [44].

### Laminopathies

The nuclear lamina refers to the structural meshwork that exists within the inner surface of the nuclear membrane, giving nuclei its shape. Comprising of both A-type (lamins A, C, A $\Delta$ 10, and C2) and B-type (lamin B) lamins, expression of the nuclear lamina comes from the *LMNA* and *LMNB* genes. However, besides providing structure to the nucleus, research has also shown that the nuclear lamina serves important roles in the organization of heterochromatin, transcriptional regulation, and nuclear pore positioning and function [39, 45]. This broad range of roles means that dysfunctional lamins can have far-reaching consequences beyond the nucleus. Indeed, mutations in the lamin genes, in particular *LMNA*, have been linked to several serious diseases termed as laminopathies [46].

Of the known laminopathies, the most notable is Hutchinson Gilford Progeria Syndrome (HGPS), a markedly serious laminopathy that results in severe premature aging in children, resulting in death by roughly age 13. With ~90% of cases being caused by the G608G (GGC>GGT) mutation that activates a cryptic splicing site within *LMNA* to yield significantly elevated levels of progerin, a truncated form of prelamin A that is normally found to increase in the skin and liver of normal individuals with age [40, 47-49]. Unlike mature Lamin A, the missing 607-656 amino acids contain the cleavage site for ZMPSTE24, the zinc metalloproteinase that farnesylates prelamin A [47, 50]. Unable to be further processed into mature Lamin A, progerin constitutively congregates at the inner nuclear membrane in a dominant-negative manner, leading to nuclear blebbing [40, 47]. Furthermore, the missing 50 amino acids in progerin are also necessary for the binding of Lamin A to the histone modifications of heterochromatin, resulting in a loss of organization of the peripheral chromatin in the nucleus [51, 52].

### *Laminopathy in AD*

Interestingly, many of the same nuclear defects observed in laminopathies are also observed in AD. In a cohort of collected AD brains, Frost et al., observed tubular invagination in 60% of the neuronal nuclei analyzed, a level 3-fold higher than what was observed in age-matched control brains [40]. Furthermore, a link was proposed that tauopathies may exert an effect on nucleoskeletal integrity by increasing the levels of over-stabilized filamentous actin, which interacts with the nuclear lamina through the LINC (Linker of Nucleoskeleton and Cytoskeleton) complex [40, 53, 54]. When considering the role of nuclear lamina in the organization of peripheral heterochromatin, a link between tauopathies and heterochromatin disorganization can also be reasonably postulated. Additional evidence also shows that tau can

interact with the nuclear pore complex in a manner that can alter nuclear export/import. Based on these presented findings, it becomes apparent that there is a connection between AD and nuclear and Lamin dysfunction. In **Chapter 2**, I further delve into this relationship and the role of *LMNA* in AD and neurodegeneration.

## **1.5 *RAB10*: The protective endo-lysosomal factor**

### *The protective *RAB10* variant in AD*

Common and rare variants have been identified that reduce the risk for AD.[9] Those with the strongest protective effect include *APOEε2* and *APP*-A673T [55, 56]. Thus, genes and pathways involved in increasing AD risk may also confer resilience to disease. In order to identify additional genetic variants that confer resilience to AD, there is a need to develop novel study designs that focus on those individuals carrying protective factors for AD. In one such case, family pedigrees were identified with a statistical excess of AD mortality (ie, families with a higher number of AD deaths than expected relative to similarly sized pedigrees; termed high risk pedigrees). Within these high-risk pedigrees, elderly individuals with genetic risk for AD (i.e., *APOEε4* carriers) but who had escaped AD were evaluated using whole genome sequencing. Ridge et al. identified a rare variant (rs142787485) in the 3'-UTR of *RAB10* that confers resilience to AD [17]. In a cell model of *APP* metabolism, silencing of *Rab10* expression leads to a significant decrease in Aβ42 and the Aβ42/40 ratio, consistent with prior reports.[17, 57] Interestingly, independent of the *RAB10* SNP, individuals with a neuropathologic diagnosis of AD exhibited significantly higher levels of *RAB10* compared with neuropathology-free controls.[17] Thus, genetic and molecular evidence support a role for *RAB10* in AD pathogenesis. While not much work has been published to closely examine this role, in **Chapter**

3, I will discuss some of the proposed mechanisms through which RAB10 may contribute to AD and how the rs142787485 SNP contributes to this.

### **1.7 *PLD3*: A mysterious protein promoting A $\beta$ clearance**

#### *Discovery of rare variants in PLD3*

Through whole exome sequencing of families densely affected by LOAD, a rare genetic variant located within the seventh exon, V232M, was identified in the gene for phospholipase D3 (*PLD3*) and perfectly segregated with disease in two different families. Further deep sequencing of additional unrelated cohorts of AD and control patients further uncovered additional variants that were also significantly associated with disease risk, notably the M6R and A442A variants that were also associated with an increase in disease. Looking beyond variants, *PLD3* is found to accumulate on the amyloid plaques of diseased brains [58]. When analyzing at RNA expression in the brain, it was found that AD brains displayed significantly reduced expression when compared to age-matched controls, with biochemical assays using *in vitro* systems implicating this altered expression to result in an alteration of APP metabolism [15].

#### *A protein without a known function*

*PLD3* is a member of the phospholipase D family, which has seven known members. PLD family members are defined by the presence of two HKD “catalytic domains” [59]. However, of the seven known isoforms, the knockout of *PLD1* and *PLD2* together is sufficient to completely abrogate phospholipase activity [60-62]. To date, *PLD3* has no known substrate or confirmed function. However, some of the published literature have begun to shed some light on its role. On a macroscopic level, *PLD3* has been implicated in myotube formation [63] and, in tumors, is a marker of senescence and plays a role in HIF1 $\alpha$ -dependent lipid metabolism [64, 65]. At the cellular level, *PLD3* has been shown to play a wide range of roles in the endo-

lysosomal network (ELN). Within the endosome, *PLD3* has been proposed to be an endonuclease in immune cells for microbial DNA to generate short oligos for presentation to Tlr9 in mice [66]. In addition, within neurons, PLD3 colocalizes with APP in endolysosomal compartments and also has been postulated to play a role in retromer transport from the endosome, where  $\beta$ - and  $\gamma$ -secretases are rich in concentration, to the Golgi, where their concentration is much lower [67-70]. Finally, evidence both from our group as well as others have been pointed to a role for PLD3 in the lysosome. The *PLD3* promoter contains a CLEAR motif, suggesting that it is a member of the CLEAR network, a family of lysosomal enzymes regulated by TFEB, the master lysosomal transcription factor [71]. Furthermore, PLD3 not only carries a mannose-6-phosphate tag to direct it to the lysosome without being degraded and colocalizes with Lamp2 [72-74], but evidence has also demonstrated that PLD3 is trafficked to the lysosome via the endosome and requires ubiquitination of its N-terminus [66]. While the role of PLD3 in the lysosome is not fully understood, lysosomes in *Pld3*-deficient mouse neurons are increased in size and density, implying a buildup of undigested cargo [75]. Recently, it was reported that within the lysosome, PLD3 exhibits display phospholipase activity [76]. In chapters four and five of this dissertation, all of this will be further discussed and elaborated on at length.

As stated above, the genetics of LOAD is remarkably complex and, while much progress has been made, many factors still yet remain to be identified, and even more are yet to be functionally characterized. However, by better shining a light on the many genes that can influence AD risk, we stand to gain a deeper understand the pathways and mechanisms that drive disease and, by extension, we can better develop therapeutics to slow disease progression or treat the symptoms that result. For the remainder of this dissertation, I will outline and discuss my work on my own efforts to do this very thing for *LMNA*, *RAB10*, and *PLD3*.

## 1.8 References

- [1] D.M. Holtzman, J.C. Morris, A.M. Goate, Alzheimer's disease: the challenge of the second century, *Science translational medicine* 3(77) (2011) 77sr1.
- [2] C.R. Jack, Jr., D.M. Holtzman, Biomarker modeling of Alzheimer's disease, *Neuron* 80(6) (2013) 1347-58.
- [3] A.W. Bero, P. Yan, J.H. Roh, J.R. Cirrito, F.R. Stewart, M.E. Raichle, J.M. Lee, D.M. Holtzman, Neuronal activity regulates the regional vulnerability to amyloid-beta deposition, *Nature neuroscience* 14(6) (2011) 750-6.
- [4] G.G. Glenner, C.W. Wong, Alzheimer's disease: initial report of the purification and characterization of a novel cerebrovascular amyloid protein. 1984, *Biochem Biophys Res Commun* 425(3) (2012) 534-9.
- [5] S.J. Adams, M.A. DeTure, M. McBride, D.W. Dickson, L. Petrucelli, Three repeat isoforms of tau inhibit assembly of four repeat tau filaments, *PloS one* 5(5) (2010) e10810.
- [6] M.C. Chartier-Harlin, F. Crawford, H. Houlden, A. Warren, D. Hughes, L. Fidani, A. Goate, M. Rossor, P. Roques, J. Hardy, et al., Early-onset Alzheimer's disease caused by mutations at codon 717 of the beta-amyloid precursor protein gene, *Nature* 353(6347) (1991) 844-6.
- [7] Z. Amtul, P.A. Lewis, S. Piper, R. Crook, M. Baker, K. Findlay, A. Singleton, M. Hogg, L. Younkin, S.G. Younkin, J. Hardy, M. Hutton, B.F. Boeve, D. Tang-Wai, T.E. Golde, A presenilin 1 mutation associated with familial frontotemporal dementia inhibits gamma-secretase cleavage of APP and notch, *Neurobiol Dis* 9(2) (2002) 269-73.
- [8] J.L. Stein, S.E. Medland, A.A. Vasquez, D.P. Hibar, R.E. Senstad, A.M. Winkler, R. Toro, K. Appel, R. Barteczek, O. Bergmann, M. Bernard, A.A. Brown, D.M. Cannon, M.M. Chakravarty, A. Christoforou, M. Domin, O. Grimm, M. Hollinshead, A.J. Holmes, G. Homuth, J.J. Hottenga, C. Langan, L.M. Lopez, N.K. Hansell, K.S. Hwang, S. Kim, G. Laje, P.H. Lee, X. Liu, E. Loth, A. Lourdusamy, M. Mattingsdal, S. Mohnke, S.M. Maniega, K. Nho, A.C. Nugent, C. O'Brien, M. Papmeyer, B. Putz, A. Ramasamy, J. Rasmussen, M. Rijpkema, S.L. Risacher, J.C. Roddey, E.J. Rose, M. Ryten, L. Shen, E. Sprooten, E. Strengman, A. Teumer, D. Trabzuni, J. Turner, K. van Eijk, T.G. van Erp, M.J. van Tol, K. Wittfeld, C. Wolf, S. Woudstra, A. Aleman, S. Alhusaini, L. Almasy, E.B. Binder, D.G. Brohawn, R.M. Cantor, M.A. Carless, A. Corvin, M. Czisch, J.E. Curran, G. Davies, M.A. de Almeida, N. Delanty, C. Depondt, R. Duggirala, T.D. Dyer, S. Erk, J. Fagerness, P.T. Fox, N.B. Freimer, M. Gill, H.H. Goring, D.J. Hagler, D. Hoehn, F. Holsboer, M. Hoogman, N. Hosten, N. Jahanshad, M.P. Johnson, D. Kasperaviciute, J.W. Kent, Jr., P. Kochunov, J.L. Lancaster, S.M. Lawrie, D.C. Liewald, R. Mandl, M. Matarin, M. Mattheisen, E. Meisenzahl, I. Melle, E.K. Moses, T.W. Muhleisen, M. Nauck, M.M. Nothen, R.L. Olvera, M. Pandolfo, G.B. Pike, R. Puls, I. Reinvang, M.E. Renteria, M. Rietschel, J.L. Roffman, N.A. Royle, D. Rujescu, J. Savitz, H.G. Schnack, K. Schnell, N. Seiferth, C. Smith, V.M. Steen, M.C. Valdes Hernandez, M. Van den Heuvel, N.J. van der Wee, N.E. Van Haren, J.A. Veltman, H. Volzke, R. Walker, L.T. Westlye, C.D. Whelan, I. Agartz, D.I. Boomsma, G.L. Cavalleri, A.M. Dale, S. Djurovic, W.C. Drevets, P. Hagoort, J. Hall, A. Heinz, C.R. Jack, Jr., T.M. Foroud, S. Le Hellard, F. Macciardi, G.W. Montgomery, J.B. Poline, D.J. Porteous, S.M. Sisodiya, J.M. Starr, J. Sussmann, A.W. Toga, D.J. Veltman, H. Walter, M.W. Weiner, I. Alzheimer's Disease Neuroimaging, E. Consortium, I. Consortium, G. Saguenay Youth Study, J.C. Bis, M.A. Ikram, A.V. Smith, V. Gudnason, C. Tzourio, M.W. Vernooij, L.J. Launer, C.

- DeCarli, S. Seshadri, H. Cohorts for, C. Aging Research in Genomic Epidemiology, O.A. Andreassen, L.G. Apostolova, M.E. Bastin, J. Blangero, H.G. Brunner, R.L. Buckner, S. Cichon, G. Coppola, G.I. de Zubicaray, I.J. Deary, G. Donohoe, E.J. de Geus, T. Espeseth, G. Fernandez, D.C. Glahn, H.J. Grabe, J. Hardy, H.E. Hulshoff Pol, M. Jenkinson, R.S. Kahn, C. McDonald, A.M. McIntosh, F.J. McMahon, K.L. McMahon, A. Meyer-Lindenberg, D.W. Morris, B. Muller-Myhsok, T.E. Nichols, R.A. Ophoff, T. Paus, Z. Pausova, B.W. Penninx, S.G. Potkin, P.G. Samann, A.J. Saykin, G. Schumann, J.W. Smoller, J.M. Wardlaw, M.E. Weale, N.G. Martin, B. Franke, M.J. Wright, P.M. Thompson, C. Enhancing Neuro Imaging Genetics through Meta-Analysis, Identification of common variants associated with human hippocampal and intracranial volumes, *Nat Genet* 44(5) (2012) 552-61.
- [9] C.M. Karch, A.M. Goate, Alzheimer's Disease Risk Genes and Mechanisms of Disease Pathogenesis, *Biol Psychiatry* (2014).
- [10] D.C. Ryman, N. Acosta-Baena, P.S. Aisen, T. Bird, A. Danek, N.C. Fox, A. Goate, P. Frommelt, B. Ghetti, J.B. Langbaum, F. Lopera, R. Martins, C.L. Masters, R.P. Mayeux, E. McDade, S. Moreno, E.M. Reiman, J.M. Ringman, S. Salloway, P.R. Schofield, R. Sperling, P.N. Tariot, C. Xiong, J.C. Morris, R.J. Bateman, N. Dominantly Inherited Alzheimer, Symptom onset in autosomal dominant Alzheimer disease: a systematic review and meta-analysis, *Neurology* 83(3) (2014) 253-60.
- [11] N.J. Cairns, R.J. Perrin, E.E. Franklin, D. Carter, B. Vincent, M. Xie, R.J. Bateman, T. Benzinger, K. Friedrichsen, W.S. Brooks, G.M. Halliday, C. McLean, B. Ghetti, J.C. Morris, I. Alzheimer Disease Neuroimaging, N. Dominantly Inherited Alzheimer, Neuropathologic assessment of participants in two multi-center longitudinal observational studies: the Alzheimer Disease Neuroimaging Initiative (ADNI) and the Dominantly Inherited Alzheimer Network (DIAN), *Neuropathology* 35(4) (2015) 390-400.
- [12] C.M. Karch, A.M. Goate, Alzheimer's disease risk genes and mechanisms of disease pathogenesis, *Biol Psychiatry* 77(1) (2015) 43-51.
- [13] P.L. Greer, D.M. Bear, J.M. Lassance, M.L. Bloom, T. Tsukahara, S.L. Pashkovski, F.K. Masuda, A.C. Nowlan, R. Kirchner, H.E. Hoekstra, S.R. Datta, A Family of non-GPCR Chemosensors Defines an Alternative Logic for Mammalian Olfaction, *Cell* 165(7) (2016) 1734-1748.
- [14] P.G. Ridge, S. Mukherjee, P.K. Crane, J.S. Kauwe, C. Alzheimer's Disease Genetics, Alzheimer's disease: analyzing the missing heritability, *PLoS One* 8(11) (2013) e79771.
- [15] B.A. Benitez, S.C. Jin, R. Guerreiro, R. Graham, J. Lord, D. Harold, R. Sims, J.C. Lambert, J.R. Gibbs, J. Bras, C. Sassi, O. Harari, S. Bertelsen, M.K. Lupton, J. Powell, C. Bellenguez, K. Brown, C. Medway, P.C. Haddick, M.P. van der Brug, T. Bhangale, W. Ortmann, T. Behrens, R. Mayeux, M.A. Pericak-Vance, L.A. Farrer, G.D. Schellenberg, J.L. Haines, J. Turton, A. Braae, I. Barber, A.M. Fagan, D.M. Holtzman, J.C. Morris, t.E.c.t.A.s.D.G.C.A.s.D.N.I.t.G.C. C Study Group, J. Williams, J.S. Kauwe, P. Amouyel, K. Morgan, A. Singleton, J. Hardy, A.M. Goate, C. Cruchaga, Missense variant in TREML2 protects against Alzheimer's disease, *Neurobiol Aging* 35(6) (2014) 1510 e19-26.
- [16] P.G. Ridge, C.M. Karch, S. Hsu, I. Arano, C.C. Teerlink, M.T.W. Ebbert, J.D.G. Murcia, J.M. Farnham, A.R. Damato, M. Allen, X. Wang, O. Harari, V.M. Fernandez, R. Guerreiro, J. Bras, J. Hardy, R. Munger, M. Norton, C. Sassi, A. Singleton, S.G. Younkin, D.W. Dickson, T.E. Golde, N.D. Price, N. Ertekin-Taner, C. Cruchaga, A.M. Goate, C. Corcoran, J. Tschanz, L.A. Cannon-Albright, J.S.K. Kauwe, I. Alzheimer's Disease Neuroimaging, Correction to:

- Linkage, whole genome sequence, and biological data implicate variants in RAB10 in Alzheimer's disease resilience, *Genome Med* 10(1) (2018) 4.
- [17] D.E. Crombie, C.L. Curl, A.J. Raaijmakers, P. Sivakumaran, T. Kulkarni, R.C. Wong, I. Minami, M.V. Evans-Galea, S.Y. Lim, L. Delbridge, L.A. Corben, M. Dottori, N. Nakatsuji, I.A. Trounce, A.W. Hewitt, M.B. Delatycki, M.F. Pera, A. Pebay, Friedreich's ataxia induced pluripotent stem cell-derived cardiomyocytes display electrophysiological abnormalities and calcium handling deficiency, *Aging (Albany NY)* 9(5) (2017) 1440-1452.
- [18] W.J. Strittmatter, K.H. Weisgraber, D.Y. Huang, L.M. Dong, G.S. Salvesen, M. Pericak-Vance, D. Schmechel, A.M. Saunders, D. Goldgaber, A.D. Roses, Binding of human apolipoprotein E to synthetic amyloid beta peptide: isoform-specific effects and implications for late-onset Alzheimer disease, *Proceedings of the National Academy of Sciences of the United States of America* 90(17) (1993) 8098-102.
- [19] D.M. Holtzman, J. Herz, G. Bu, Apolipoprotein E and apolipoprotein E receptors: normal biology and roles in Alzheimer disease, *Cold Spring Harb Perspect Med* 2(3) (2012) a006312.
- [20] J.M. Castellano, J. Kim, F.R. Stewart, H. Jiang, R.B. DeMattos, B.W. Patterson, A.M. Fagan, J.C. Morris, K.G. Mawuenyega, C. Cruchaga, A.M. Goate, K.R. Bales, S.M. Paul, R.J. Bateman, D.M. Holtzman, Human apoE isoforms differentially regulate brain amyloid-beta peptide clearance, *Science translational medicine* 3(89) (2011) 89ra57.
- [21] P.B. Verghese, J.M. Castellano, K. Garai, Y. Wang, H. Jiang, A. Shah, G. Bu, C. Frieden, D.M. Holtzman, ApoE influences amyloid-beta (Abeta) clearance despite minimal apoE/Abeta association in physiological conditions, *Proceedings of the National Academy of Sciences of the United States of America* 110(19) (2013) E1807-16.
- [22] Y. Shi, K. Yamada, S.A. Liddelow, S.T. Smith, L. Zhao, W. Luo, R.M. Tsai, S. Spina, L.T. Grinberg, J.C. Rojas, G. Gallardo, K. Wang, J. Roh, G. Robinson, M.B. Finn, H. Jiang, P.M. Sullivan, C. Baufeld, M.W. Wood, C. Sutphen, L. McCue, C. Xiong, J.L. Del-Aguila, J.C. Morris, C. Cruchaga, I. Alzheimer's Disease Neuroimaging, A.M. Fagan, B.L. Miller, A.L. Boxer, W.W. Seeley, O. Butovsky, B.A. Barres, S.M. Paul, D.M. Holtzman, ApoE4 markedly exacerbates tau-mediated neurodegeneration in a mouse model of tauopathy, *Nature* 549(7673) (2017) 523-527.
- [23] E.H. Corder, A.M. Saunders, W.J. Strittmatter, D.E. Schmechel, P.C. Gaskell, G.W. Small, A.D. Roses, J.L. Haines, M.A. Pericak-Vance, Gene dose of apolipoprotein E type 4 allele and the risk of Alzheimer's disease in late onset families, *Science* 261(5123) (1993) 921-3.
- [24] M.K. Wetzel-Smith, J. Hunkapiller, T.R. Bhangale, K. Srinivasan, J.A. Maloney, J.K. Atwal, S.M. Sa, M.B. Yaylaoglu, O. Foreman, W. Ortmann, N. Rathore, D.V. Hansen, M. Tessier-Lavigne, C. Alzheimer's Disease Genetics, R. Mayeux, M. Pericak-Vance, J. Haines, L.A. Farrer, G.D. Schellenberg, A. Goate, T.W. Behrens, C. Cruchaga, R.J. Watts, R.R. Graham, A rare mutation in UNC5C predisposes to late-onset Alzheimer's disease and increases neuronal cell death, *Nat Med* 20(12) (2014) 1452-7.
- [25] R. Guerreiro, A. Wojtas, J. Bras, M. Carrasquillo, E. Rogeava, E. Majounie, C. Cruchaga, C. Sassi, J.S. Kauwe, S. Younkin, L. Hazrati, J. Collinge, J. Pocock, T. Lashley, J. Williams, J.C. Lambert, P. Amouyel, A. Goate, R. Rademakers, K. Morgan, J. Powell, P. St George-Hyslop, A. Singleton, J. Hardy, TREM2 variants in Alzheimer's disease, *The New England journal of medicine* 368(2) (2013) 117-27.
- [26] S.C. Jin, B.A. Benitez, C.M. Karch, B. Cooper, T. Skorupa, D. Carrell, J.B. Norton, S. Hsu, O. Harari, Y. Cai, S. Bertelsen, A.M. Goate, C. Cruchaga, Coding variants in TREM2 increase risk for Alzheimer's disease, *Hum Mol Genet* 23(21) (2014) 5838-46.

- [27] S.C. Jin, M.M. Carrasquillo, B.A. Benitez, T. Skorupa, D. Carrell, D. Patel, S. Lincoln, S. Krishnan, M. Kachadoorian, C. Reitz, R. Mayeux, T.S. Wingo, J.J. Lah, A.I. Levey, J. Murrell, H. Hendrie, T. Foroud, N.R. Graff-Radford, A.M. Goate, C. Cruchaga, N. Ertekin-Taner, TREM2 is associated with increased risk for Alzheimer's disease in African Americans, *Mol Neurodegener* 10 (2015) 19.
- [28] T.J. Maxwell, C. Corcoran, J.L. Del-Aguila, J.P. Budde, Y. Deming, C. Cruchaga, A.M. Goate, J.S.K. Kauwe, I. Alzheimer's Disease Neuroimaging, Genome-wide association study for variants that modulate relationships between cerebrospinal fluid amyloid-beta 42, tau, and p-tau levels, *Alzheimers Res Ther* 10(1) (2018) 86.
- [29] M. Allen, M. Kachadoorian, Z. Quicksall, F. Zou, H.S. Chai, C. Younkin, J.E. Crook, V.S. Pankratz, M.M. Carrasquillo, S. Krishnan, T. Nguyen, L. Ma, K. Malphrus, S. Lincoln, G. Bisceglie, C.P. Kolbert, J. Jen, S. Mukherjee, J.K. Kauwe, P.K. Crane, J.L. Haines, R. Mayeux, M.A. Pericak-Vance, L.A. Farrer, G.D. Schellenberg, J.E. Parisi, R.C. Petersen, N.R. Graff-Radford, D.W. Dickson, S.G. Younkin, N. Ertekin-Taner, Association of MAPT haplotypes with Alzheimer's disease risk and MAPT brain gene expression levels, *Alzheimers Res Ther* 6(4) (2014) 39.
- [30] Y. Deming, Z. Li, M. Kapoor, O. Harari, J.L. Del-Aguila, K. Black, D. Carrell, Y. Cai, M.V. Fernandez, J. Budde, S. Ma, B. Saef, B. Howells, K.L. Huang, S. Bertelsen, A.M. Fagan, D.M. Holtzman, J.C. Morris, S. Kim, A.J. Saykin, P.L. De Jager, M. Albert, A. Moghekar, R. O'Brien, M. Riemenschneider, R.C. Petersen, K. Blennow, H. Zetterberg, L. Minthon, V.M. Van Deerlin, V.M. Lee, L.M. Shaw, J.Q. Trojanowski, G. Schellenberg, J.L. Haines, R. Mayeux, M.A. Pericak-Vance, L.A. Farrer, E.R. Peskind, G. Li, A.F. Di Narzo, I. Alzheimer's Disease Neuroimaging, C. Alzheimer Disease Genetic, J.S. Kauwe, A.M. Goate, C. Cruchaga, Genome-wide association study identifies four novel loci associated with Alzheimer's endophenotypes and disease modifiers, *Acta Neuropathol* 133(5) (2017) 839-856.
- [31] S.H. Choi, Y.H. Kim, M. Heibisch, C. Sliwinski, S. Lee, C. D'Avanzo, H. Chen, B. Hooli, C. Asselin, J. Muffat, J.B. Klee, C. Zhang, B.J. Wainger, M. Peitz, D.M. Kovacs, C.J. Woolf, S.L. Wagner, R.E. Tanzi, D.Y. Kim, A three-dimensional human neural cell culture model of Alzheimer's disease, *Nature* (2014).
- [32] S.I. Kring, B.H. Brummett, J. Barefoot, M.E. Garrett, A.E. Ashley-Koch, S.H. Boyle, I.C. Siegler, T.I. Sorensen, R.B. Williams, Impact of psychological stress on the associations between apolipoprotein E variants and metabolic traits: findings in an American sample of caregivers and controls, *Psychosom Med* 72(5) (2010) 427-33.
- [33] S.D. Ostergaard, S. Mukherjee, S.J. Sharp, P. Proitsi, L.A. Lotta, F. Day, J.R. Perry, K.L. Boehme, S. Walter, J.S. Kauwe, L.E. Gibbons, C. Alzheimer's Disease Genetics, G. Consortium, E.P.-I. Consortium, E.B. Larson, J.F. Powell, C. Langenberg, P.K. Crane, N.J. Wareham, R.A. Scott, Associations between Potentially Modifiable Risk Factors and Alzheimer Disease: A Mendelian Randomization Study, *PLoS Med* 12(6) (2015) e1001841; discussion e1001841.
- [34] C.C. Chou, Y. Zhang, M.E. Umoh, S.W. Vaughan, I. Lorenzini, F. Liu, M. Sayegh, P.G. Donlin-Asp, Y.H. Chen, D.M. Duong, N.T. Seyfried, M.A. Powers, T. Kukar, C.M. Hales, M. Gearing, N.J. Cairns, K.B. Boylan, D.W. Dickson, R. Rademakers, Y.J. Zhang, L. Petruccielli, R. Sattler, D.C. Zarnescu, J.D. Glass, W. Rossoll, TDP-43 pathology disrupts nuclear pore complexes and nucleocytoplasmic transport in ALS/FTD, *Nat Neurosci* 21(2) (2018) 228-239.
- [35] P.W. Brownjohn, J. Smith, R. Solanki, E. Lohmann, H. Houlden, J. Hardy, S. Dietmann, F.J. Livesey, Functional Studies of Missense TREM2 Mutations in Human Stem Cell-Derived Microglia, *Stem Cell Reports* 10(4) (2018) 1294-1307.

- [36] J. Kim, J.M. Basak, D.M. Holtzman, The role of apolipoprotein E in Alzheimer's disease, *Neuron* 63(3) (2009) 287-303.
- [37] J. Kim, A.E. Eltorai, H. Jiang, F. Liao, P.B. Verghese, F.R. Stewart, J.M. Basak, D.M. Holtzman, Anti-apoE immunotherapy inhibits amyloid accumulation in a transgenic mouse model of Abeta amyloidosis, *The Journal of experimental medicine* 209(12) (2012) 2149-56.
- [38] T.V. Huynh, A.A. Davis, J.D. Ulrich, D.M. Holtzman, Apolipoprotein E and Alzheimer's disease: the influence of apolipoprotein E on amyloid-beta and other amyloidogenic proteins, *J Lipid Res* 58(5) (2017) 824-836.
- [39] B.C. Capell, F.S. Collins, Human laminopathies: nuclei gone genetically awry, *Nat Rev Genet* 7(12) (2006) 940-52.
- [40] B. Frost, Alzheimer's disease: An acquired neurodegenerative laminopathy, *Nucleus* 7(3) (2016) 275-83.
- [41] P.J. McKinnon, Maintaining genome stability in the nervous system, *Nat Neurosci* 16(11) (2013) 1523-9.
- [42] A.L. Boxer, M. Gold, E. Huey, F.B. Gao, E.A. Burton, T. Chow, A. Kao, B.R. Leavitt, B. Lamb, M. Grether, D. Knopman, N.J. Cairns, I.R. Mackenzie, L. Mitic, E.D. Roberson, D. Van Kammen, M. Cantillon, K. Zahs, S. Salloway, J. Morris, G. Tong, H. Feldman, H. Fillit, S. Dickinson, Z. Khachaturian, M. Sutherland, R. Farese, B.L. Miller, J. Cummings, Frontotemporal degeneration, the next therapeutic frontier: molecules and animal models for frontotemporal degeneration drug development, *Alzheimers Dement* 9(2) (2013) 176-88.
- [43] C. Settembre, A. Fraldi, D.L. Medina, A. Ballabio, Signals from the lysosome: a control centre for cellular clearance and energy metabolism, *Nat Rev Mol Cell Biol* 14(5) (2013) 283-96.
- [44] J.P. Tavana, M. Rosene, N.O. Jensen, P.G. Ridge, J.S. Kauwe, C.M. Karch, RAB10: an Alzheimer's disease resilience locus and potential drug target, *Clin Interv Aging* 14 (2019) 73-79.
- [45] E. Haithcock, Y. Dayani, E. Neufeld, A.J. Zahand, N. Feinstein, A. Mattout, Y. Gruenbaum, J. Liu, Age-related changes of nuclear architecture in *Caenorhabditis elegans*, *Proc Natl Acad Sci U S A* 102(46) (2005) 16690-5.
- [46] Y. Gruenbaum, R.D. Goldman, R. Meyuhas, E. Mills, A. Margalit, A. Fridkin, Y. Dayani, M. Prokocimer, A. Enosh, The nuclear lamina and its functions in the nucleus, *Int Rev Cytol* 226 (2003) 1-62.
- [47] M. Eriksson, W.T. Brown, L.B. Gordon, M.W. Glynn, J. Singer, L. Scott, M.R. Erdos, C.M. Robbins, T.Y. Moses, P. Berglund, A. Dutra, E. Pak, S. Durkin, A.B. Csoka, M. Boehnke, T.W. Glover, F.S. Collins, Recurrent de novo point mutations in lamin A cause Hutchinson-Gilford progeria syndrome, *Nature* 423(6937) (2003) 293-8.
- [48] D. McClintock, D. Ratner, M. Lokuge, D.M. Owens, L.B. Gordon, F.S. Collins, K. Djabali, The mutant form of lamin A that causes Hutchinson-Gilford progeria is a biomarker of cellular aging in human skin, *PLoS One* 2(12) (2007) e1269.
- [49] P. Scaffidi, T. Misteli, Lamin A-dependent nuclear defects in human aging, *Science* 312(5776) (2006) 1059-63.
- [50] A. De Sandre-Giovannoli, N. Levy, Altered splicing in prelamin A-associated premature aging phenotypes, *Prog Mol Subcell Biol* 44 (2006) 199-232.
- [51] F. Bruston, E. Delbarre, C. Ostlund, H.J. Worman, B. Buendia, I. Duband-Goulet, Loss of a DNA binding site within the tail of prelamin A contributes to altered heterochromatin anchorage by progerin, *FEBS Lett* 584(14) (2010) 2999-3004.

- [52] M. Columbaro, C. Capanni, E. Mattioli, G. Novelli, V.K. Parnaik, S. Squarzoni, N.M. Maraldi, G. Lattanzi, Rescue of heterochromatin organization in Hutchinson-Gilford progeria by drug treatment, *Cell Mol Life Sci* 62(22) (2005) 2669-78.
- [53] B. Frost, F.H. Bardai, M.B. Feany, Lamin Dysfunction Mediates Neurodegeneration in Tauopathies, *Curr Biol* 26(1) (2016) 129-36.
- [54] T.A. Fulga, I. Elson-Schwab, V. Khurana, M.L. Steinhilb, T.L. Spires, B.T. Hyman, M.B. Feany, Abnormal bundling and accumulation of F-actin mediates tau-induced neuronal degeneration in vivo, *Nat Cell Biol* 9(2) (2007) 139-48.
- [55] E.H. Corder, A.M. Saunders, N.J. Risch, W.J. Strittmatter, D.E. Schmechel, P.C. Gaskell, Jr., J.B. Rimmier, P.A. Locke, P.M. Conneally, K.E. Schmader, et al., Protective effect of apolipoprotein E type 2 allele for late onset Alzheimer disease, *Nature genetics* 7(2) (1994) 180-4.
- [56] T. Jonsson, J.K. Atwal, S. Steinberg, J. Snaedal, P.V. Jonsson, S. Bjornsson, H. Stefansson, P. Sulem, D. Gudbjartsson, J. Maloney, K. Hoyte, A. Gustafson, Y. Liu, Y. Lu, T. Bhangale, R.R. Graham, J. Huttenlocher, G. Bjornsdottir, O.A. Andreassen, E.G. Jonsson, A. Palotie, T.W. Behrens, O.T. Magnusson, A. Kong, U. Thorsteinsdottir, R.J. Watts, K. Stefansson, A mutation in APP protects against Alzheimer's disease and age-related cognitive decline, *Nature* 488(7409) (2012) 96-9.
- [57] V. Udayar, V. Buggia-Prevot, R.L. Guerreiro, G. Siegel, N. Rambabu, A.L. Soohoo, M. Ponnusamy, B. Siegenthaler, J. Bali, Aesg, M. Simons, J. Ries, M.A. Puthenveedu, J. Hardy, G. Thinakaran, L. Rajendran, A paired RNAi and RabGAP overexpression screen identifies Rab11 as a regulator of beta-amyloid production, *Cell Rep* 5(6) (2013) 1536-51.
- [58] J. Satoh, Y. Kino, Y. Yamamoto, N. Kawana, T. Ishida, Y. Saito, K. Arima, PLD3 is accumulated on neuritic plaques in Alzheimer's disease brains, *Alzheimers Res Ther* 6(9) (2014) 70.
- [59] J. Wang, G. Xu, H. Li, V. Gonzales, D. Fromholt, C. Karch, N.G. Copeland, N.A. Jenkins, D.R. Borchelt, Somatodendritic accumulation of misfolded SOD1-L126Z in motor neurons mediates degeneration: alphaB-crystallin modulates aggregation, *Human molecular genetics* 14(16) (2005) 2335-47.
- [60] M.A. Frohman, The phospholipase D superfamily as therapeutic targets, *Trends Pharmacol Sci* 36(3) (2015) 137-44.
- [61] T.G. Oliveira, R.B. Chan, H. Tian, M. Laredo, G. Shui, A. Staniszewski, H. Zhang, L. Wang, T.W. Kim, K.E. Duff, M.R. Wenk, O. Arancio, G. Di Paolo, Phospholipase d2 ablation ameliorates Alzheimer's disease-linked synaptic dysfunction and cognitive deficits, *J Neurosci* 30(49) (2010) 16419-28.
- [62] L. Santa-Marinha, I. Castanho, R.R. Silva, F.V. Bravo, A.M. Miranda, T. Meira, R. Morais-Ribeiro, F. Marques, Y. Xu, K. Point du Jour, M. Wenk, R.B. Chan, G. Di Paolo, V. Pinto, T.G. Oliveira, Phospholipase D1 Ablation Disrupts Mouse Longitudinal Hippocampal Axis Organization and Functioning, *Cell Rep* 30(12) (2020) 4197-4208 e6.
- [63] M. Osismi, W. Ali, M.A. Frohman, A role for phospholipase D3 in myotube formation, *PLoS One* 7(3) (2012) e33341.
- [64] M. Althubiti, L. Lezina, S. Carrera, R. Jukes-Jones, S.M. Giblett, A. Antonov, N. Barlev, G.S. Saldanha, C.A. Pritchard, K. Cain, S. Macip, Characterization of novel markers of senescence and their prognostic potential in cancer, *Cell Death Dis* 5 (2014) e1528.
- [65] A. Valli, M. Rodriguez, L. Moutsianas, R. Fischer, V. Fedele, H.L. Huang, R. Van Stiphout, D. Jones, M. McCarthy, M. Vinaxia, K. Igarashi, M. Sato, T. Soga, F. Buffa, J. McCullagh, O.

- Yanes, A. Harris, B. Kessler, Hypoxia induces a lipogenic cancer cell phenotype via HIF1alpha-dependent and -independent pathways, *Oncotarget* 6(4) (2015) 1920-41.
- [66] B. Eftekharzadeh, J.G. Daigle, L.E. Kipinos, A. Coyne, J. Schiantarelli, Y. Carlomagno, C. Cook, S.J. Miller, S. Dujardin, A.S. Amaral, J.C. Grima, R.E. Bennett, K. Tepper, M. DeTure, C.R. Vanderburg, B.T. Corjuc, S.L. DeVos, J.A. Gonzalez, J. Chew, S. Vidensky, F.H. Gage, J. Mertens, J. Troncoso, E. Mandelkow, X. Salvatella, R.Y.H. Lim, L. Petrucelli, S. Wegmann, J.D. Rothstein, B.T. Hyman, Tau Protein Disrupts Nucleocytoplasmic Transport in Alzheimer's Disease, *Neuron* 99(5) (2018) 925-940 e7.
- [67] A.S. Mukadam, S.Y. Breusegem, M.N.J. Seaman, Analysis of novel endosome-to-Golgi retrieval genes reveals a role for PLD3 in regulating endosomal protein sorting and amyloid precursor protein processing, *Cell Mol Life Sci* 75(14) (2018) 2613-2625.
- [68] L. Rajendran, A. Schneider, G. Schlechtingen, S. Weidlich, J. Ries, T. Braxmeier, P. Schwille, J.B. Schulz, C. Schroeder, M. Simons, G. Jennings, H.J. Knolker, K. Simons, Efficient inhibition of the Alzheimer's disease beta-secretase by membrane targeting, *Science* 320(5875) (2008) 520-3.
- [69] B.M. Siegenthaler, L. Rajendran, Retromers in Alzheimer's disease, *Neurodegener Dis* 10(1-4) (2012) 116-21.
- [70] S.A. Small, S. Gandy, Sorting through the cell biology of Alzheimer's disease: intracellular pathways to pathogenesis, *Neuron* 52(1) (2006) 15-31.
- [71] M. Sardiello, M. Palmieri, A. di Ronza, D.L. Medina, M. Valenza, V.A. Gennarino, C. Di Malta, F. Donaudy, V. Embrione, R.S. Polishchuk, S. Banfi, G. Parenti, E. Cattaneo, A. Ballabio, A gene network regulating lysosomal biogenesis and function, *Science* 325(5939) (2009) 473-7.
- [72] M. Palmieri, S. Impey, H. Kang, A. di Ronza, C. Pelz, M. Sardiello, A. Ballabio, Characterization of the CLEAR network reveals an integrated control of cellular clearance pathways, *Hum Mol Genet* 20(19) (2011) 3852-66.
- [73] D.E. Sleat, P. Sun, J.A. Wiseman, L. Huang, M. El-Banna, H. Zheng, D.F. Moore, P. Lobel, Extending the mannose 6-phosphate glycoproteome by high resolution/accuracy mass spectrometry analysis of control and acid phosphatase 5-deficient mice, *Mol Cell Proteomics* 12(7) (2013) 1806-17.
- [74] D.E. Sleat, H. Zheng, M. Qian, P. Lobel, Identification of sites of mannose 6-phosphorylation on lysosomal proteins, *Mol Cell Proteomics* 5(4) (2006) 686-701.
- [75] P. Fazzari, K. Horre, A.M. Arranz, C.S. Frigerio, T. Saito, T.C. Saido, B. De Strooper, PLD3 gene and processing of APP, *Nature* 541(7638) (2017) E1-E2.
- [76] A.G. Nackenoff, T.J. Hohman, S.M. Neuner, C.S. Akers, N.C. Weitzel, A. Shostak, S.M. Ferguson, B. Mobley, D.A. Bennett, J.A. Schneider, A.L. Jefferson, C.C. Kaczorowski, M.S. Schrag, PLD3 is a neuronal lysosomal phospholipase D associated with beta-amyloid plaques and cognitive function in Alzheimer's disease, *PLoS Genet* 17(4) (2021) e1009406.

## **Chapter 2: LMNA-mediated nucleoskeleton dysregulation in Alzheimer's disease**

## 2.1 Abstract

Nucleoskeleton dysfunction has been implicated in Alzheimer disease (AD). Tubular invaginations of the nuclear envelope observed in AD brains are consistent with the accumulation of farnesylated prelamin A (encoded by the *LMNA* gene) that occurs in Hutchinson-Gilford Progeria Syndrome, a premature aging disorder caused by *LMNA* mutations. Proper function of the nuclear membrane is required for neuronal survival and for maintenance of genetic architecture. To determine whether dysregulated *LMNA* expression and prelamin A processing are responsible for nucleoskeleton dysfunction in AD, we performed differential gene expression and network analyses in human AD and age-matched control brains. In AD brains, we observed a significant increase in *LMNA* and a significant decrease in *ZMPSTE24*, which encodes the zinc metallopeptidase protein that defarnesylates prelamin A. We replicated these findings in laser capture microdissected neurons from AD brains, suggesting that the effect is neuronally driven. Thus, high levels of *LMNA* paired with low levels of *ZMPSTE24* could result in the accumulation of farnesylated prelamin A and tubular invaginations in the nuclear membrane. *LMNA*-associated networks were also differentially expressed in AD brains. Genes within the dysregulated *LMNA* network were enriched in lysosomal and chromatin remodeling pathways. We propose that  $\beta$ -amyloid and tau accumulation disrupts prelamin A processing and downstream changes in the nuclear membrane. Alterations in the nucleoskeleton induce genomic instability, loss of proteostasis, and cellular senescence, which may accelerate AD pathogenesis.

## 2.2 Introduction

Alzheimer disease (AD) is a neurodegenerative disorder characterized by extensive neuronal loss and accumulation of extracellular amyloid plaques and intracellular neurofibrillary tangles. Nucleoskeleton dysfunction has also been reported in AD brains [1, 2]. Dysfunction of this kind can cause genomic instability, loss of proteostasis, epigenetic changes, mitochondrial dysfunction, deregulated nutrient sensing and cellular senescence [1, 3-5], all of which have been described in AD [2, 6, 7]. The precise mechanism by which nucleoskeleton dysfunction occurs in AD remains unclear. Thus, identifying the molecular and protein triggers that drive these defects could allow us to target and modify critical phenotypes in AD.

Genetic and cell-based evidence point to a critical role of lamin A in proper nuclear membrane function. Hutchinson-Gilford Progeria Syndrome (HGPS) is a rare premature aging disorder. HGPS is caused by mutations in *LMNA*, the gene that encodes A-type lamins (lamin A and lamin C), activating a cryptic splice site that gives rise to a truncated transcript termed *LMNAΔ150* and its protein product progerin [8, 9]. Under normal conditions, immature lamin A protein (prelamin A) is post-translationally modified at the nuclear membrane by farnesylation, cleavage, carboxyl methylation and excision of the farnesylated residue by the zinc metallopeptidase ZMPSTE24 [10-12]. The *LMNAΔ150* transcript, however, lacks the ZMPSTE24 binding site, leading to accumulation of progerin, a shorter protein with retained farnesyl modification, in the nuclear membrane and subsequent nuclear shape abnormalities, chromatin disorganization, damage to DNA and abnormal gene expression [13-15]. These progerin-induced phenotypes mimic several aspects of normal aging [16, 17]. Deficiency in

ZMPSTE24 function, which results in build-up of farnesylated prelamin A in the nuclear membrane, also causes nuclear distortion and a premature aging phenotype [18-20]. Notably, progerin builds up in the nuclear envelope even in normal cells with aging due to sporadic use of the cryptic splice site, which prevents defarnesylation (Figure 2.1) [9, 16].

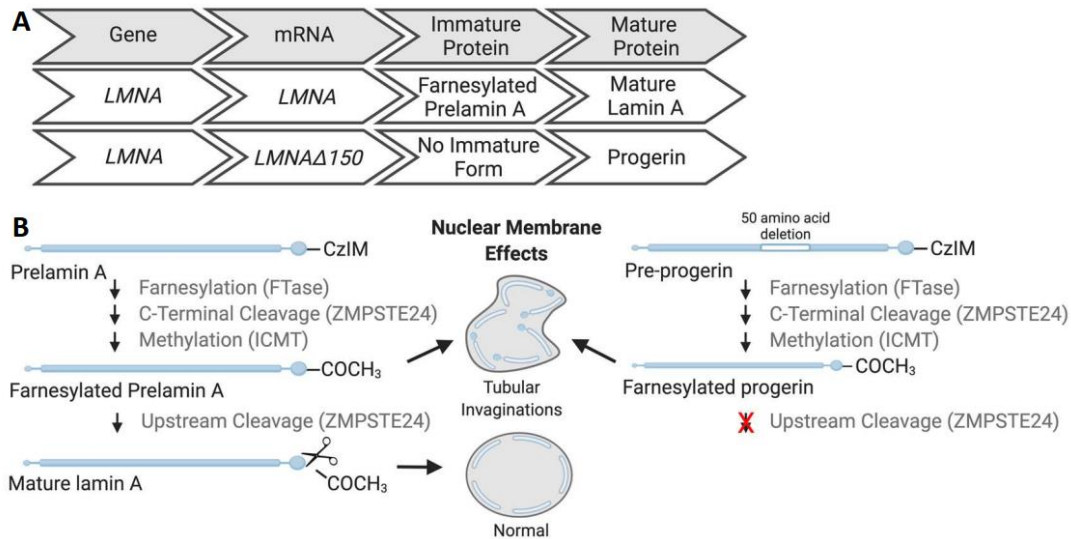


**Figure 2.1: Model of lamin A processing.** A. Schematic of lamin A and progerin processing. B. After translation, immature prelamin A is farnesylated, then cleaved by ZMPSTE24 to remove the farnesyl residue and yield mature lamin A. Farnesylated prelamin A or progerin are unable to properly incorporate into the nuclear lamina but are retained in the nuclear membrane resulting in tubular invaginations.

The changes observed in nuclear envelope morphology in AD brains are consistent with the build-up of farnesylated prelamin A or progerin, which could indicate an AD-associated change in the regulation of lamin A expression and processing [1, 2]. Here, we show that AD pathology is associated with disrupted *LMNA* and *ZMPSTE24* expression, which, in turn, brings about changes in lamin A protein levels and subsequently alters molecular networks associated with proteostasis and chromosome remodeling. Thus, nucleoskeleton defects caused by altered

lamin A processing may contribute to downstream pathways that promote neurodegeneration and AD pathogenesis.

## **2.3 Materials and Methods**

### *Human Subjects*

The Washington University IRB reviewed the Charles F. and Joanne Knight Alzheimer Disease Research Center (Knight ADRC) Neuropathology Cores (from whom the brains were obtained) operating protocol as well as this specific study and determined it was exempt from approval. In the state of Missouri, individuals can give prospective consent for autopsy. Our participants provide this consent by signing the hospital's autopsy form. If the participant does not provide future consent before death the DPOA or next of kin provide it after death. All data were analyzed anonymously.

### *Laser Capture Microdissected Neurons*

The GSE5281 dataset was obtained from laser capture microdissected neurons from AD and control brains (Table 2.1) [21]. Brain samples from individuals of European descent that were collected from Washington University, Duke University, and Sun Health Research Institute were included in the study. Samples were obtained from the entorhinal cortex, hippocampus, medial temporal gyrus, posterior cingulate, superior frontal gyrus, and primary visual cortex and were clinically and neuropathologically confirmed AD (N=33) or controls (N=14). RNA expression was measured using an Affymetrix GeneChip for gene expression. To analyze RNA expression, the log transformed expression values were analyzed with brain region, age, and gender as covariates as previously described [22].

### *Mount Sinai Brain Bank*

Mount Sinai Brain Bank (MSBB) RNA sequencing (RNAseq) study was accessed from the Accelerating Medicines Partnership – Alzheimer’s Disease (AMP-AD) portal (syn8690199; accessed December 2017). We examined gene expression in the parahippocampal gyrus (PHG; BA36) of brains with a neuropathologic diagnosis of AD (N=135) and neuropathology free, age matched controls (N=85; Table 2.1). RNAseq was performed using the Illumina HiSeq 2500 System with an average of 38.7 million reads per sample [23, 24]. The gene count data generated from RNAseq analysis was imported into RStudio, an integrated development environment that supports R, a programming language for statistical computations. Differential gene expression analysis was performed using the package *DESeq2* with covariates including age at death, post-mortem interval, sex, and RNA integrity number.

### *Mayo Clinic Brain Bank*

Mayo Clinic Brain Bank (Mayo) RNAseq study was accessed from the AMP-AD portal (syn6090813). We examined gene expression in the temporal cortex of brains with neuropathologic diagnosis of AD (N=82), pathologic aging (N=29), and elderly control brains that lacked a diagnosis of neurodegenerative disease (N=80; Table 2.1). Pathologic aging is defined as the presence of amyloid plaques (CERAD neuritic and cortical plaque densities of 2 or more) without neurofibrillary tangles (Braak NFT stage of less than 3 and no other co-morbid pathology) [25]. These brains were part of the Mayo Clinic RNAseq cohort, as described previously [25]. RNAseq was performed using Illumina HiSeq 2000, 101-base-pair, paired-end sequencing at the Mayo Clinic Genomic Core Facility. After applying quality control steps, raw read counts were normalized according to conditional quantile normalization (CQN) using the

Bioconductor package. Differential gene expression comparing AD to controls used a “Simple Model.” In this model, multi-variable linear regression analyses were conducted in R, using CQN normalized gene expression measures and including age-at-death, gender, RNA integrity number (RIN), brain tissue source, and flowcell as biological and technical covariates.

### *Frontotemporal Lobar Dementia-tau (FTLD-tau) Brains*

Insular cortex from autopsy-confirmed, FTLD-tau with a causative mutation at *MAPT* p.R406W (N=2) and age-matched, cognitively normal control brains (N=2) were obtained from the Knight ADRC (Table 2.1) [26]. RNAseq paired end reads were generated using Illumina HiSeq 4000 with a mean coverage of 80 million reads per sample. FastQC was applied to the data to evaluate sequencing quality [27]. Data were aligned to GRCh37 primary assembly using STAR (ver 2.5.2b) [28]. Reads alignment were further evaluated by applying Picard CollectRnaSeqMetrics (ver 2.8.2) to examine reads distribution on the genome [29]. The gene count data generated from RNAseq analysis was imported into RStudio. Differential gene expression analysis was performed using the package *DESeq2* with covariates including age at death, post-mortem interval, sex, and RNA integrity number as previously described [30].

**Table 2.1:** Study demographics

Dataset	Brain Region	N	Male (%)	Mean Age at Death	AD	PA	FTLD-MAPT	Control
MSBB	PHG*	220	36	83.3	135	0	0	85
GSE5281	EC, HPC, MTG, PC, SFG, PVC**	47	53.2	79.9	33	0	0	14
Mayo [25]	Temporal Cortex	191	50.2	80.2	82	29	0	80
Knight ADRC [26]	Insular Cortex	4	50	69.5	0	0	2	2

\*PHG, Parahippocampal Gyrus. \*\*, EC, Entorhinal Cortex; HPC, Hippocampus; MTG, Medial Temporal Gyrus; PC, Posterior Cingulate; SFG, Superior Frontal Gyrus; PVC, Primary Visual Cortex. AD, Alzheimer's disease. PA, pathological aging. FTLD-tau, frontotemporal lobar dementia with tau inclusions.

### *Developmental expression of LMNA and ZMPSTE24*

Developmental gene expression for *LMNA* and *ZMPSTE24* were evaluated using a spatial and temporal microarray expression data set focusing on the prenatal brain [31]. These exon-level expression data originate from 25 areas and 9 layers (fetal mitotic and post-mitotic zones) of the human brain sampled in 40 clinically normal postmortem brains of diverse ethnicity that span 32 consecutive periods of neurodevelopment and adulthood from 8 post-conception weeks (PCW) to 40 years (for additional details see <http://www.brainspan.org/>). We downloaded expression values, calculated using z-score normalization. Using line and bar plots we visualized patterns of gene expression, across region and over time (from 8 PCW to 40 years of age). Using a repeated measure analysis of variance (ANOVA), we evaluated whether gene expression patterns over time showed statistically significant differences between brain regions.

### *Network Analysis*

*LMNA*-associated gene networks were defined as those genes that were significantly differentially expressed in response to forced progerin expression (GEO: GSE52431) [5]. Briefly, these expression profiles were generated in a prior study of Parkinson disease models by differentiating human induced pluripotent cells (iPSC) into dopaminergic (mDA) neurons using a modified Dual-SMAD protocol [5]. RNAseq was performed in 70-day iPSC-derived mDA neurons expressing nuclear-GFP or progerin-GFP [5].

Briefly, paired-end reads were generated on an Illumina HiSeq2000. Reads were mapped to the human genome (Hg19) using STAR 2.3.0e [28] using default mapping parameters, and read counts were assessed using HTSeq. Differentially expressed genes were identified with limma voom in R. A low read count filter was used such that all samples were required to contain non-zero read counts for a gene to be assessed. Differentially expressed genes were identified using a fold change cut off of +/- 2 and a Bonferroni adjusted p-value of 0.05.

Forced progerin expression in iPSC-derived mDA neurons resulted in 113 up-regulated and 1,318 down-regulated genes (FDR<0.05; Supplemental Table 2.1) [5]. We used these genes to construct a *LMNA* network in the Mayo and MSBB-PHG datasets. In the Mayo dataset (Table 2.1), 1,273 genes were identified. In the MSBB dataset (Table 2.1; PHG), 693 genes were identified. Subsequent analyses were then focused on those genes that were differentially expressed in the same direction across all three datasets: iPSC-derived mDA, Mayo, and MSBB.

### *Pathway Analysis*

To identify enrichments in gene ontology associated with the genes within the *LMNA* network, we used the Consensus Path Database (CPDB). Gene ontology analyses were performed using CPDB (Release 31; <http://cpdb.molgen.mpg.de/>) [32, 33]. CPDB compares gene ontology terms between background and candidate gene sets using the hypergeometric test and generates p-values that are corrected for multiple testing using FDR. We used the default background gene set, which includes 18,043 genes. Biological, cellular and molecular gene ontology terms were included in a single analysis.

### *GWAS*

Single Nucleotide Polymorphisms (SNPs) within 10kb of *LMNA* and *ZMPSTE24* were identified using NCBI. To determine whether these SNPs were associated with AD risk, we used the International Genomics of Alzheimer's Project (IGAP), a large two-stage study based upon genome-wide association studies (GWAS) on individuals of European ancestry. In stage 1, IGAP used genotyped and imputed data on 7,055,881 SNPs to meta-analyze four previously-published GWAS datasets consisting of 17,008 Alzheimer's disease cases and 37,154 controls (The European Alzheimer's Disease Initiative–EADI the Alzheimer Disease Genetics Consortium–ADGC The Cohorts for Heart and Aging Research in Genomic Epidemiology consortium–CHARGE The Genetic and Environmental Risk in AD consortium–GERAD).

### *Lamin A and ZMPSTE24 protein analyses in human AD brains*

Parietal lobes from autopsy-confirmed AD (CDR 3; N = 3) and age-matched, cognitively normal control (CDR 0; N = 3) brains were obtained from the Knight ADRC. Brains were homogenized in RIPA lysis buffer (50mM Tris pH 7.6, 2.5mM EDTA, 150mM NaCl, 0.5% SDS, 1.0% Triton X-100, 0.5% sodium deoxycholate, protease inhibitor cocktail) on ice by sonication and centrifuged at 14,000g for 10 minutes at 4°C as previously described [34]. The resulting supernatants were analyzed for total protein levels by bicinchoninic acid assay (Thermo Fisher). Standard SDS-PAGE was performed with 10μg of protein for each sample using NuPAGE Novex 4-12% Bis-Tris Protein Gels (Thermo Fisher) in NuPAGE MOPS SDS Running Buffer (Thermo Fisher). Samples were boiled for 5 min in Laemmli sample buffer prior to electrophoresis [35]. Proteins were subsequently transferred onto Immobilon-P polyvinylidene fluoride (PVDF) Membrane, 0.45μm (Millipore) in Tris-Glycine buffer with 20% methanol. Immunoblots were stained with Ponceau S solution (0.1 % (w/v) in 5% acetic acid) to evaluate total protein. Immunoblots were probed with antibodies to lamin A/C (Santa Cruz sc-376248

1:200), or lamin B2 (Abcam ab8983 1:500). Primary antibodies were detected with goat anti-mouse IgG (H+L) HRP secondary antibody (KPL 074-1806 1:6000). Immunoblots were exposed with Pierce ECL Western Blotting Substrate (Thermo Fisher) on a G:BOX Gel Documentation System (Syngene). Band intensities were quantified using GeneTools software (Syngene) manual band quantification. Band intensities were normalized to quantified levels of Ponceau S staining and then expressed relative to the average band intensity of control samples.

## 2.4 Results

### *LMNA and ZMPSTE24 are dysregulated in AD brains*

To determine whether *LMNA* expression is altered in AD, we analyzed publicly available transcriptomic data generated from a large collection of neuropathologically defined AD and control brains (MSBB). In the parahippocampal gyrus of AD brains, a region affected early in disease pathogenesis, we observed a significant increase in *LMNA* expression and a significant reduction in *ZMPSTE24* (Figure 2.2A). To begin to understand the contribution of AD pathology to lamin A processing, we examined the correlation between *LMNA* and *ZMPSTE24* with plaque and tangle load in human brains. *LMNA* was significantly positively correlated with plaque load and tau Braak stage in the parahippocampal gyrus (Figure 2.2A). Conversely, *ZMPSTE24* was marginally negatively correlated with plaque load, but not statistically significant (Figure 2.2A). In control brains, *LMNA* and *ZMPSTE24* are expressed at similar levels across the cortex (Appendix 1).

When interpreting gene expression data in tissue homogenates from brains with neurodegenerative disease, changes in gene expression may be driven by the cellular composition of the tissue (e.g. extensive neuronal loss) [36]. To replicate our findings and to

begin to understand the cell-type specific impact of *LMNA* and *ZMPSTE24* expression in AD, we examined a publicly available dataset containing RNA expression data from laser capture microdissected neurons from AD and age-matched, control brains (Figure 2.2B) [21]. Consistent with our findings in tissue homogenates from MSBB, we found that *LMNA* was significantly elevated (Figure 2.2C;  $p=9.79\times10^{-4}$ ) and *ZMPSTE24* was significantly reduced (Figure 2.2D;  $p=1.0\times10^{-3}$ ) in neurons isolated from AD brains compared with neurons isolated from neuropathology free control brains. These findings suggest that the impact of AD on *LMNA* and *ZMPSTE24* occurs in neurons.

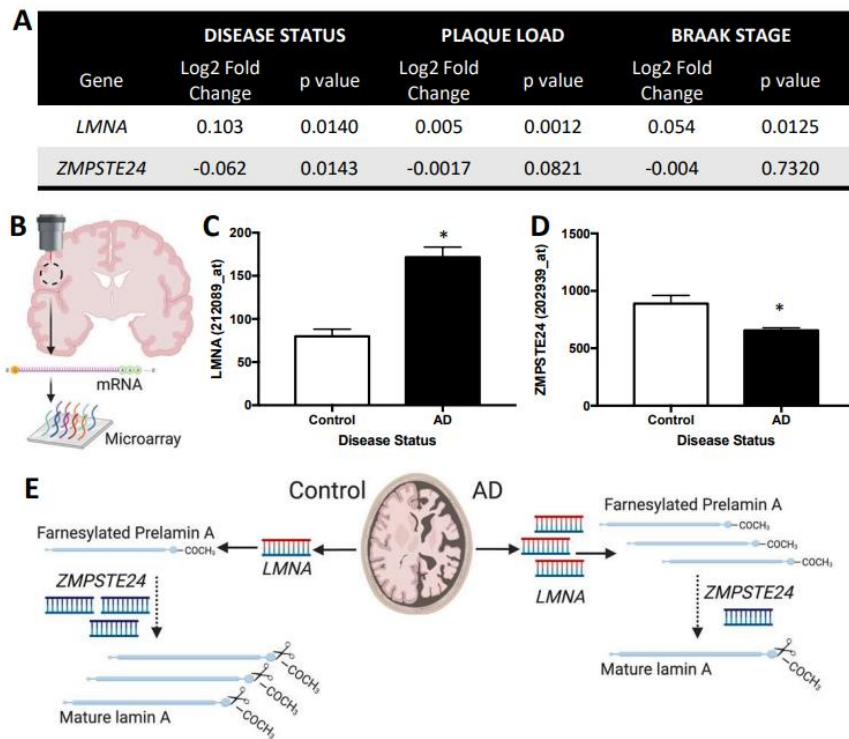


**Figure 2.2: *LMNA* and *ZMPSTE24* expression are altered in AD brains.** A. *LMNA* and *ZMPSTE24* gene expression are associated with disease status, plaque load (amyloid), and Braak Stage (tau) in brain homogenates from AD and control brains. Parahippocampal gyrus (BA36; MSBB). B-D. *LMNA* and *ZMPSTE24* expression are altered in neurons isolated from AD brains. B. RNA expression was evaluated in laser capture microdissected

neurons isolated from AD and control brains (GSE4281). C-D. Graphs of mean expression (AU)  $\pm$  SEM. C. *LMNA* expression is significantly elevated in AD neurons.  $p=9.79\times10^{-4}$ . D. *ZMPSTE24* expression is significantly reduced in AD neurons.  $p=1.0\times10^{-3}$ . E. In AD brains, increased *LMNA* expression coupled with decreased *ZMPSTE24* may result in an accumulation of immature, farnesylated prelamin A. \*  $<0.05$ .

To determine whether amyloid plaques are sufficient to trigger dysregulation of *LMNA* progressing, we examined *LMNA* and *ZMPSTE24* expression in the temporal cortices of brains with pathologic aging [37]. Pathologic aging is defined as the presence of amyloid plaques (CERAD neuritic and cortical plaque densities of 2 or more) with minimal neurofibrillary tangle burden (Braak NFT stage of less than 3 and no other co-morbid pathology) [25]. Interestingly, we found that *LMNA* was significantly reduced in brains with pathologic aging ( $p=0.01$ ), while *ZMPSTE24* levels were unchanged ( $p=0.69$ ; Table 2.2). Thus, these findings suggest that the observed effects of *LMNA* and *ZMPSTE24* are not solely  $\beta$ -amyloid dependent.

**Table 2.2:** *LMNA* and *ZMPSTE24* expression in brains with Pathology Aging (amyloid plaques) and FTLD-tau (tau tangles)

	Pathologic Aging		FTLD-Tau	
Gene	Fold Change (Log2)	p value	Fold Change (Log2)	p value
<i>LMNA</i>	-0.40	0.0126	1.25	7.60E-03
<i>ZMPSTE24</i>	0.03	0.6970	-0.92	1.51E-04

To determine whether tau aggregation is sufficient to alter lamin A processing, we measured *LMNA* and *ZMPSTE24* expression in FTLD-tau brains [30]. In brains with FTLD-tau caused by autosomal dominant mutations in *MAPT* p.R406W, we observed a significant increase

in *LMNA* ( $p=7.6\times10^{-3}$ ) and a significant decrease in *ZMPSTE24* expression ( $p=1.51\times10^{-4}$ ; Table 2.2).

### *Prelamin A accumulates in AD brains*

We predict that the molecular phenotypes of increased *LMNA* and decreased *ZMPSTE24* that we observed in AD brains result in lamin A dysregulation at the protein level (Figure 2.2E). To test whether our molecular observations lead to a change in the total levels of mature lamin A protein, we measured lamin A in tissue homogenates from AD and control brains (Figure 2.4). Lamin A protein levels were significantly lower in AD brains compared with control brains (Figure 2.4). Of the two protein products that *LMNA* encodes, lamin A requires sequential processing to produce a mature form of the protein that can be normally incorporated into the nuclear lamina, while lamin C does not. As a control, we evaluated lamin C and lamin B2 protein levels and found that these nuclear proteins were unchanged across the brain samples (Figure 2.4). Together, these findings point to a specific effect on lamin A processing in AD brains (Figure 2.4) and as a result, altered ratios of lamins which can change the mechanophenotype of the nuclear membrane [38].

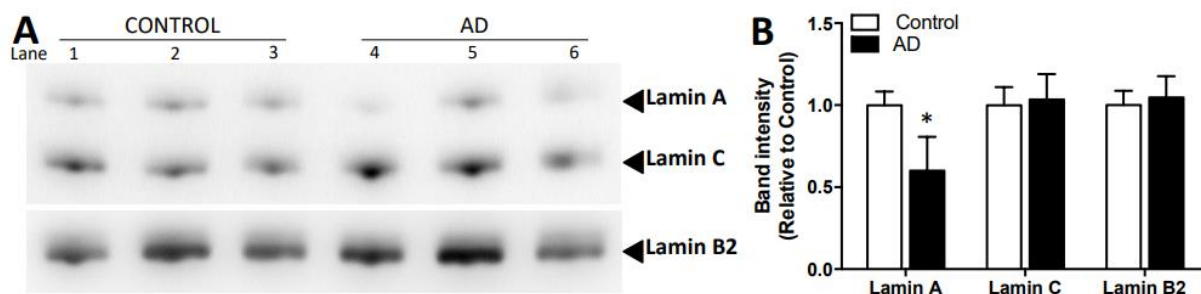


**Figure 2.3: Lamin A protein levels are altered in AD brains.** Autopsy confirmed AD (CDR 3; N=3) and control (CDR 0; N=3) parietal brain tissue were analyzed by SDS-PAGE and immunoblotting. A. Immunoblotting of

human control and AD brain tissue with antibodies specific to mature lamin A, lamin C, and lamin B2. B.

Quantification of immunoblots. Graph represents mean  $\pm$  SEM. \*, p<0.05.

### *The LMNA network is dysregulated in AD brains*

We next sought to determine whether genes associated with *LMNA* were dysregulated in AD brains. To do this, we constructed a supervised *LMNA* network using publicly available data from a stem cell model in which a mutant form of *LMNA*, progerin, was expressed in iPSC-derived mDA neurons (Figure 2.5A) [5]. Forced progerin expression resulted in 113 upregulated genes and 1,318 downregulated genes compared to iPSC-derived mDA neurons expressing GFP (FDR<0.05; Appendix 1) [5]. Importantly, forced progerin expression resulted in a significant increase in *LMNA* ( $\beta=9.38$ ;  $p=1.33\times 10^{-5}$ ; 82y mDA neurons; Appendix 1).

To determine whether genes that are altered in response to progerin expression were also differentially expressed in AD, we next extracted these 1,431 genes from two publicly available transcriptomics datasets of AD and control brains (MSBB and Mayo Clinic). In the MSBB dataset (PHG), 74 genes were significantly differentially expressed between AD and control brains in the same direction as the iPSC-derived mDA neurons (FDR<0.05; Appendix 2). In the Mayo Clinic dataset (temporal cortex), 239 genes were significantly differentially expressed between AD and control brains in the same direction as the iPSC-derived mDA neurons (FDR<0.05; Appendix 2). In total, 53 genes were differentially expressed in AD brains in the same direction in Mayo Clinic and MSBB datasets and in iPSC-derived mDA neurons (Figure 2.5B; Table 2.3; Appendix 2).

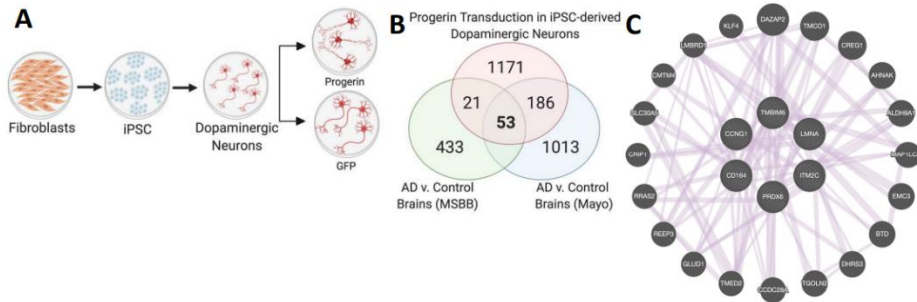


**Figure 2.4: LMNA-associated genes are disrupted in AD brains.** A. *LMNA* networks were defined as those genes altered by expression of progerin in human iPSC-derived dopaminergic neurons [5]. B. Overlap in genes altered by progerin expression *in vitro* and differentially expressed (FDR<0.05) in the same direction in AD versus control brains from two independent datasets (MSBB and Mayo). C. Relatedness of genes significantly elevated in the presence of progerin and in AD brains. Purple lines indicate prior evidence of co-expression.

The six genes that were significantly upregulated in response to progerin treatment and elevated in AD brains (Table 2.3) were highly co-expressed with one another (Figure 2.5C) and were enriched in pathways associated with lysosomal function and apoptotic signaling (Table 2.4). Genes that were downregulated in response to progerin treatment and reduced in AD brains were enriched in pathways associated with chromatin remodeling and nuclear division (Table 2.4). Together, these studies suggest that dysregulation of lamin A processing may be central to the chromatin and lysosomal abnormalities that are characteristic in AD.

**Table 2.3:** LMNA Network Genes are dysregulated in AD brains

Gene	MSBB		Mayo	
	Fold Change (Log2)	FDR	Fold Change (Log2)	FDR
<i>PRDX6</i>	0.32	1.13E-04	0.58	6.12E-05
<i>LMNA</i>	0.42	4.69E-04	0.34	4.41E-02
<i>CD164</i>	0.25	3.14E-03	0.39	4.08E-05

<i>TMBIM6</i>	0.18	1.07E-02	0.46	2.69E-06
<i>CCNG1</i>	0.23	1.47E-02	0.53	7.07E-06
<i>ITM2C</i>	0.21	1.65E-02	0.62	3.45E-04
<i>HTR4</i>	-0.39	3.43E-05	-0.66	1.08E-02
<i>BCL11A</i>	-0.38	4.13E-05	-0.67	3.60E-03
<i>OTOG</i>	-0.58	4.13E-05	-0.59	1.12E-02
<i>BMPER</i>	-0.37	5.66E-05	-0.57	5.16E-03
<i>CACNA2D3</i>	-0.33	1.01E-04	-0.44	2.48E-02
<i>CNIH3</i>	-0.26	1.71E-04	-0.73	1.97E-04
<i>FRMPD4</i>	-0.39	2.64E-04	-0.72	8.21E-03
<i>ANO3</i>	-0.52	8.51E-04	-1.11	1.33E-03
<i>LRRC2</i>	-0.37	1.36E-03	-0.86	3.59E-04
<i>MYOZ3</i>	-0.35	1.37E-03	-0.89	5.69E-05
<i>CLSPN</i>	-0.40	1.41E-03	-0.60	2.19E-02
<i>CCDC158</i>	-0.31	1.48E-03	-0.35	2.52E-02
<i>TRPA1</i>	-0.47	1.71E-03	-0.61	1.25E-02
<i>TNIP3</i>	-0.66	2.21E-03	-0.71	2.67E-02
<i>NRXN3</i>	-0.32	2.25E-03	-0.95	2.09E-06
<i>SLC26A4</i>	-0.37	3.26E-03	-0.57	7.53E-03
<i>TOMIL1</i>	-0.22	3.64E-03	-0.40	9.14E-06
<i>GRHL1</i>	-0.27	4.92E-03	-0.62	1.64E-04
<i>TPX2</i>	-0.30	5.51E-03	-0.56	3.36E-04
<i>TNFRSF11A</i>	-0.25	5.59E-03	-0.69	2.42E-04
<i>SATB2</i>	-0.25	5.89E-03	-0.39	2.60E-02
<i>TPTE2PI</i>	-0.27	6.20E-03	-0.68	2.33E-05
<i>ACRVI</i>	-0.41	7.24E-03	-0.68	1.08E-03
<i>MACROD2</i>	-0.26	7.32E-03	-0.69	2.59E-05
<i>CASQ1</i>	-0.34	8.07E-03	-0.60	4.73E-03
<i>SLC12A1</i>	-0.41	9.10E-03	-0.86	7.36E-05
<i>EXTL1</i>	-0.28	1.12E-02	-0.41	3.65E-02
<i>MIR137HG</i>	-0.35	1.20E-02	-0.48	3.79E-02

<i>RTKN2</i>	-0.42	1.25E-02	-0.95	1.59E-04
<i>ABCA10</i>	-0.28	1.32E-02	-0.48	3.68E-04
<i>EFNA5</i>	-0.27	1.67E-02	-0.45	1.07E-02
<i>IGF1</i>	-0.34	1.67E-02	-1.10	2.40E-04
<i>DGKH</i>	-0.17	1.68E-02	-0.32	4.24E-03
<i>P2RX5</i>	-0.30	2.12E-02	-0.55	3.45E-03
<i>PPARGC1B</i>	-0.15	2.16E-02	-0.28	2.83E-02
<i>C3orf49</i>	-0.18	2.23E-02	-0.34	4.81E-02
<i>TIAM2</i>	-0.20	2.27E-02	-0.37	6.11E-03
<i>PXDNL</i>	-0.23	2.59E-02	-0.37	3.78E-02
<i>USP43</i>	-0.21	2.59E-02	-0.38	1.54E-02
<i>GRB7</i>	-0.49	2.62E-02	-0.90	4.39E-03
<i>MOV10L1</i>	-0.25	2.67E-02	-0.42	3.11E-03
<i>KIAA1456</i>	-0.22	2.95E-02	-0.51	4.62E-03
<i>FMNI</i>	-0.26	3.04E-02	-0.47	2.28E-02
<i>NME9</i>	-0.13	3.07E-02	-0.36	6.74E-05
<i>PRR16</i>	-0.23	3.17E-02	-0.63	8.99E-05
<i>DMKN</i>	-0.26	3.71E-02	-0.58	2.84E-04
<i>BMP3</i>	-0.33	3.83E-02	-0.76	6.72E-03

**Table 2.4:** *LMNA* network genes disrupted in AD are enriched in lysosomal, nuclear, and apoptotic pathways

GO Term	Pathway Name	FDR	Genes	Direction
GO:0005764	lysosome	9.92E-03	<i>ITM2C, PRDX6, CD164</i>	Up
GO:2001233	apoptotic signaling	1.43E-04	<i>LMNA, ITM2C, TMBIM6</i>	Up
GO:0000280	nuclear division	8.19E-03	<i>BMP3, EXTL1, PPARGC1B, IGF1, FMNL1, SATB2</i>	Down
GO:0000793	condensed chromosome	1.69E-03	<i>CASQ1, SLC12A1, P2RX5, SLC26A4, TRPA1, CACNA2D3, CNIH3, ANO3</i>	Down

#### *Genetic association with AD risk*

Candidate gene studies have previously implicated *LMNA* in AD risk [39-41]. To determine whether common variants in *LMNA* or *ZMPSTE24* contribute to AD risk, we extracted all SNPs in the 10kb region around *LMNA* and *ZMPSTE24*, and we then determined whether these SNPs were associated with risk for AD in IGAP Stage 1 [42]. We identified 133 SNPs near *LMNA* and present in the IGAP Stage 1 dataset; however, no SNPs were significantly associated with AD risk (Appendix 3). Past candidate gene studies implicated rs505058 near *LMNA* in AD risk; however, in IGAP Stage 1, rs505058 was not associated with AD risk ( $p=0.3578$ ). Similarly, of the 52 SNPs near *ZMPSTE24* and present in the IGAP Stage 1 dataset, we failed to observe any SNPs significantly associated with AD risk (Appendix 3). Together, these findings suggest that the observed dysregulation of lamin A processing occurs at the protein rather than the genetic level, which is consistent with previously observed sporadic use of the cryptic splice site [9, 16].

## 2.5 Discussion

AD is defined neuropathologically by the presence of amyloid plaques and neurofibrillary tangles. However, the underlying cellular and molecular mechanisms connecting disease pathology to neurodegeneration and cognitive decline are still not clearly understood. In our study, we demonstrate an association between lamin A-mediated nucleoskeletal dysfunction and AD. We also provide evidence demonstrating that lamin A misprocessing may influence other well-established AD-related pathways.

Nuclear membrane integrity is largely dependent on the highly controlled processing of lamin A. The *LMNA* transcript is translated into immature prelamin A, which is post-translationally modified with a farnesyl group. The zinc metallopeptidase ZMPSTE24 then cleaves this farnesyl group, producing mature lamin A [9, 43]. Interestingly, we observe an imbalance in the key components of this pathway with the elevation of *LMNA* and a reduction in *ZMPSTE24* expression. Together, this can cause a reduction of mature lamin A protein in the brain, leading to an accumulation of nuclear, immature prelamin A which constitutively interacts with and induces irregularities in the nuclear membrane [44].

Genomic integrity and global gene expression are linked to nuclear membrane integrity. In *Drosophila* and mouse models of tauopathy, defects in nuclear morphology were associated with oxidative stress, DNA damage, and loss of heterochromatin [1, 2]. Heterochromatin regulates gene expression. Global relaxation of heterochromatin can lead to aberrant gene expression [45], which has been described in AD. We aimed to more clearly define genes that are downstream of lamin A dysfunction and also change during AD pathology. Importantly,

genes upregulated due to altered lamin A processing and in AD brains are enriched for lysosomal function. The nucleus plays a critical role in lysosomal function. Nutrient sensing between the lysosome and the nucleus control energy metabolism [4]. Lysosomal biogenesis is regulated through transcription factor EB (TFEB) translocation from the cytosol to nucleus in a calcium-dependent manner [46]. Nuclear calcium is a potent regulator of gene transcription, and nuclear defects can significantly alter this signaling pathway. Moreover, nuclear calcium plays a central role in acquired neuroprotection by promoting the build-up of a neuroprotective “shield” through the induction of synaptic activity and by guarding against excitotoxic damage and classical apoptosis [47-50]. In addition, many calcium regulated genes are implicated in the protection of hippocampal and cortical neurons [47, 49-51]. Together, these findings suggest that dysregulation of lamin A processing may be upstream of the well-described lysosomal dysfunction during AD pathogenesis.

Growing evidence points to some mechanistic link between nuclear defects and AD. In a recent study, as many as 60% of nuclei from AD brains display nuclear invaginations [1]. Our data further builds on this by suggesting that the association between nuclear defects and AD is driven by accumulation of pathological tau. This association is consistent with previous reports that also show lamin-mediated nucleoskeletal dysfunction in *Drosophila* and mouse models of tauopathy. Specifically, *Drosophila* expressing tau<sup>R406W</sup> exhibit nuclear deformities along with a decrease in mature lamin protein [1, 52]. Tau-transgenic mice and *Drosophila* display a senescent-like phenotype along with other nuclear defects such as abnormal morphology, dysfunctional nuclear pores, loss of heterochromatin, and changes in gene expression [1, 2, 6, 53]. These defects may occur by altered actin and microtubule dynamics in the cytoskeleton. Both fibrillar-actin (F-actin) and microtubules interact with the nuclear lamina through the

nuclear-envelope-spanning linker of nucleoskeleton and cytoskeleton (LINC) complex such that changes to the cytoskeleton also disrupt the nuclear lamina [1, 44]. In iPSC-derived neurons from *MAPT* mutation carriers, microtubule and actin-mediated deformation of the nucleus is observed with microtubule filaments invading the nucleus through the tubular invaginations [54]. Thus in model systems and human brain tissue, tau-induced alterations in the actin and microtubule cytoskeleton lead to nuclear invaginations containing mislocalized nuclear pores, disrupting nucleocytoplasmic transport [1, 44, 54-56]. Thus, the lamin A processing defects we describe could be driven by tau pathology.

Here, we leveraged data from progerin-transduced iPSC-derived neurons in order to define those genes that change upon disrupted lamin A processing [5]. Miller and colleagues demonstrated that progerin expression was sufficient to capture aging and disease-associated phenotypes that were absent in the naïve cells [5]. This was an important breakthrough in overcoming the relative immaturity of neuronal cultures derived from iPSC [57]. Yet, an important question remained: does altered lamin A processing truly model diseases related to aging? We identified a number of genes that were differentially expressed in this iPSC model due to progerin expression that were also differentially expressed in AD brains in a similar manner. Additionally, these genes were enriched in pathways previously implicated in AD, such as lysosomal dysfunction, apoptosis, and nuclear function. Additionally, another gene of interest that we identified was *SLC30A5*, which codes for a zinc transporter [58, 59]. Zinc transporters have been previously implicated as potential therapeutic targets due to both differential expression in AD as well as brain zinc dyshomeostasis also being linked to AD progression [60]. The effect on *SLC30A5* expression in AD is currently unknown [60], but considering that we find this gene to be altered after forced progerin expression, this finding implies the possibility

that this zinc transporter may have a regulatory role on ZMPSTE24 function and subsequently on *LMNA* processing. Taken together, these results support the notion that forced *LMNA* expression could be used to model aging *in vitro*.

While our study provides evidence for the association of dysfunction of lamin A processing with AD, there remain some important questions. While the mutation known to cause progerin expression in HGPS, *LMNAΔ150*, results in disrupted nuclear integrity in the hippocampal neurons of transgenic mice, neurodegeneration is not observed in HGPS patients [61-63]. It has been proposed that a microRNA miR-9 represses *LMNA* expression in the brain [44, 61-63]. However, we and others demonstrate that *LMNA* transcripts and lamin A protein levels are highly abundant in human brain tissue [64]. HGPS patients may succumb to cardiovascular disease prior to demonstrating neurological effects [44]. Alternatively, given progerin-associated toxicity is increased in the presence of wild-type lamin A [65], it is conceivable that specific inter-lamin interactions might occur in AD patients and result in greater neurotoxicity. Indeed, lamin A may be just one of the lamins that contributes to nuclear defects in AD. Interestingly, it has been demonstrated that lamin B-mediated dysfunction occurs in both tau-transgenic *Drosophila* and mice as well in AD brains [1, 44, 61]. Changes in the relative levels and processing of individual lamins are known to contribute to abnormal nuclear structure and function [44]. Progerin disrupts the normal homotypic biding of A-type and B-type lamins leading to abnormal A-B heteropolymers [18]. Further, changes in the ratio of A and B lamins can significantly alter the mechanical properties and stiffness of the nuclear membrane, leading to alterations in several downstream functions including heterochromatin organization and cell signaling [66]. Moreover, failure to assemble an appropriate nuclear lamina can signal apoptosis [67]. Abnormal nuclear morphology and altered trafficking between the nucleus and cytoplasm

has also been described in Huntington's disease, amyotrophic lateral sclerosis, and FTLD [68-71]. Hence our observations of increased expression of *LMNA* and potential deficits in processing through reduced *ZMPSTE24* in affected AD brain tissue are consistent with alterations in the structure of the nuclear envelope and nuclear lamina and far-reaching effects on gene expression, cell signaling and behavior.

## Conclusions

Here, we show that *LMNA* and *ZMPSTE24* expression are disrupted in AD, which leads to changes in lamin A protein levels and alters molecular networks associated with proteostasis and chromosome remodeling. Thus, nucleoskeleton defects induced by lamin A processing abnormalities may contribute to downstream pathways that promote neurodegeneration and AD pathogenesis. Together, these findings provide compelling evidence for new therapeutic avenues.

## 2.6 References

- [1] B. Frost, F.H. Bardai, M.B. Feany, Lamin Dysfunction Mediates Neurodegeneration in Tauopathies, *Curr Biol* 26(1) (2016) 129-36.
- [2] B. Frost, M. Hemberg, J. Lewis, M.B. Feany, Tau promotes neurodegeneration through global chromatin relaxation, *Nat Neurosci* 17(3) (2014) 357-66.
- [3] P.J. McKinnon, Maintaining genome stability in the nervous system, *Nat Neurosci* 16(11) (2013) 1523-9.
- [4] C. Settembre, A. Fraldi, D.L. Medina, A. Ballabio, Signals from the lysosome: a control centre for cellular clearance and energy metabolism, *Nat Rev Mol Cell Biol* 14(5) (2013) 283-96.
- [5] J.D. Miller, Y.M. Ganat, S. Kishinevsky, R.L. Bowman, B. Liu, E.Y. Tu, P.K. Mandal, E. Vera, J.W. Shim, S. Kriks, T. Taldone, N. Fusaki, M.J. Tomishima, D. Krainc, T.A. Milner, D.J. Rossi, L. Studer, Human iPSC-based modeling of late-onset disease via progerin-induced aging, *Cell Stem Cell* 13(6) (2013) 691-705.
- [6] N. Musi, J.M. Valentine, K.R. Sickora, E. Baeuerle, C.S. Thompson, Q. Shen, M.E. Orr, Tau protein aggregation is associated with cellular senescence in the brain, *Aging Cell* 17(6) (2018) e12840.
- [7] M.S. Hipp, P. Kasturi, F.U. Hartl, The proteostasis network and its decline in ageing, *Nat Rev Mol Cell Biol* 20(7) (2019) 421-435.
- [8] B.C. Capell, F.S. Collins, Human laminopathies: nuclei gone genetically awry, *Nat Rev Genet* 7(12) (2006) 940-52.
- [9] Y. Gruenbaum, R. Foisner, Lamins: nuclear intermediate filament proteins with fundamental functions in nuclear mechanics and genome regulation, *Annu Rev Biochem* 84 (2015) 131-64.
- [10] J. Barrowman, P.A. Wiley, S.E. Hudon-Miller, C.A. Hrycyna, S. Michaelis, Human ZMPSTE24 disease mutations: residual proteolytic activity correlates with disease severity, *Hum Mol Genet* 21(18) (2012) 4084-93.
- [11] A.M. Pendas, Z. Zhou, J. Cadinanos, J.M. Freije, J. Wang, K. Hultenby, A. Astudillo, A. Wernerson, F. Rodriguez, K. Tryggvason, C. Lopez-Otin, Defective prelamin A processing and muscular and adipocyte alterations in Zmpste24 metalloproteinase-deficient mice, *Nat Genet* 31(1) (2002) 94-9.
- [12] M.O. Bergo, B. Gavino, J. Ross, W.K. Schmidt, C. Hong, L.V. Kendall, A. Mohr, M. Meta, H. Genant, Y. Jiang, E.R. Wisner, N. Van Bruggen, R.A. Carano, S. Michaelis, S.M. Griffey, S.G. Young, Zmpste24 deficiency in mice causes spontaneous bone fractures, muscle weakness, and a prelamin A processing defect, *Proc Natl Acad Sci U S A* 99(20) (2002) 13049-54.
- [13] R.D. Goldman, D.K. Shumaker, M.R. Erdos, M. Eriksson, A.E. Goldman, L.B. Gordon, Y. Gruenbaum, S. Khuon, M. Mendez, R. Varga, F.S. Collins, Accumulation of mutant lamin A causes progressive changes in nuclear architecture in Hutchinson-Gilford progeria syndrome, *Proc Natl Acad Sci U S A* 101(24) (2004) 8963-8.
- [14] E. Haithcock, Y. Dayani, E. Neufeld, A.J. Zahand, N. Feinstein, A. Mattout, Y. Gruenbaum, J. Liu, Age-related changes of nuclear architecture in *Caenorhabditis elegans*, *Proc Natl Acad Sci U S A* 102(46) (2005) 16690-5.
- [15] B. Liu, J. Wang, K.M. Chan, W.M. Tjia, W. Deng, X. Guan, J.D. Huang, K.M. Li, P.Y. Chau, D.J. Chen, D. Pei, A.M. Pendas, J. Cadinanos, C. Lopez-Otin, H.F. Tse, C. Hutchison, J. Chen, Y. Cao, K.S. Cheah, K. Tryggvason, Z. Zhou, Genomic instability in laminopathy-based premature aging, *Nat Med* 11(7) (2005) 780-5.

- [16] P. Scaffidi, T. Misteli, Lamin A-dependent nuclear defects in human aging, *Science* 312(5776) (2006) 1059-63.
- [17] A.M. Aliper, A.B. Csoka, A. Buzdin, T. Jetka, S. Roumiantsev, A. Moskalev, A. Zhavoronkov, Signaling pathway activation drift during aging: Hutchinson-Gilford Progeria Syndrome fibroblasts are comparable to normal middle-age and old-age cells, *Aging (Albany NY)* 7(1) (2015) 26-37.
- [18] B.S. Davies, L.G. Fong, S.H. Yang, C. Coffinier, S.G. Young, The posttranslational processing of prelamin A and disease, *Annu Rev Genomics Hum Genet* 10 (2009) 153-74.
- [19] C.L. Navarro, J. Cadinanos, A. De Sandre-Giovannoli, R. Bernard, S. Courrier, I. Boccaccio, A. Boyer, W.J. Kleijer, A. Wagner, F. Giuliano, F.A. Beemer, J.M. Freije, P. Cau, R.C. Hennekam, C. Lopez-Otin, C. Badens, N. Levy, Loss of ZMPSTE24 (FACE-1) causes autosomal recessive restrictive dermopathy and accumulation of Lamin A precursors, *Hum Mol Genet* 14(11) (2005) 1503-13.
- [20] C.L. Navarro, A. De Sandre-Giovannoli, R. Bernard, I. Boccaccio, A. Boyer, D. Genevieve, S. Hadj-Rabia, C. Gaudy-Marqueste, H.S. Smitt, P. Vabres, L. Faivre, A. Verloes, T. Van Essen, E. Flori, R. Hennekam, F.A. Beemer, N. Laurent, M. Le Merrer, P. Cau, N. Levy, Lamin A and ZMPSTE24 (FACE-1) defects cause nuclear disorganization and identify restrictive dermopathy as a lethal neonatal laminopathy, *Hum Mol Genet* 13(20) (2004) 2493-503.
- [21] W.S. Liang, E.M. Reiman, J. Valla, T. Dunckley, T.G. Beach, A. Grover, T.L. Niedzielsko, L.E. Schneider, D. Mastroeni, R. Caselli, W. Kukull, J.C. Morris, C.M. Hulette, D. Schmeichel, J. Rogers, D.A. Stephan, Alzheimer's disease is associated with reduced expression of energy metabolism genes in posterior cingulate neurons, *Proc Natl Acad Sci U S A* 105(11) (2008) 4441-6.
- [22] C.M. Karch, L.A. Ezerskiy, S. Bertelsen, ADGC, A.M. Goate, Alzheimer's disease risk polymorphisms regulate gene expression in ZCWPW1 and CELF1 loci., *PLoS One* (2016).
- [23] W. van Rheenen, A. Shatunov, A.M. Dekker, R.L. McLaughlin, F.P. Diekstra, S.L. Pulit, R.A. van der Spek, U. Vosa, S. de Jong, M.R. Robinson, J. Yang, I. Fogh, P.T. van Doormaal, G.H. Tazelaar, M. Koppers, A.M. Blokhuis, W. Sproviero, A.R. Jones, K.P. Kenna, K.R. van Eijk, O. Harschnitz, R.D. Schellevis, W.J. Brands, J. Medic, A. Menelaou, A. Vajda, N. Ticozzi, K. Lin, B. Rogelj, K. Vrabec, M. Ravnik-Glavac, B. Koritnik, J. Zidar, L. Leonardis, L.D. Groselj, S. Millecamps, F. Salachas, V. Meininger, M. de Carvalho, S. Pinto, J.S. Mora, R. Rojas-Garcia, M. Polak, S. Chandran, S. Colville, R. Swingler, K.E. Morrison, P.J. Shaw, J. Hardy, R.W. Orrell, A. Pittman, K. Sidle, P. Fratta, A. Malaspina, S. Topp, S. Petri, S. Abdulla, C. Drepper, M. Sendtner, T. Meyer, R.A. Ophoff, K.A. Staats, M. Wiedau-Pazos, C. Lomen-Hoerth, V.M. Van Deerlin, J.Q. Trojanowski, L. Elman, L. McCluskey, A.N. Basak, C. Tunca, H. Hamzeiy, Y. Parman, T. Meitinger, P. Lichtner, M. Radivojkov-Blagojevic, C.R. Andres, C. Maurel, G. Bensimon, B. Landwehrmeyer, A. Brice, C.A. Payan, S. Saker-Delye, A. Durr, N.W. Wood, L. Tittmann, W. Lieb, A. Franke, M. Rietschel, S. Cichon, M.M. Nothen, P. Amouyel, C. Tzourio, J.F. Dartigues, A.G. Uitterlinden, F. Rivadeneira, K. Estrada, A. Hofman, C. Curtis, H.M. Blauw, A.J. van der Kooi, M. de Visser, A. Goris, M. Weber, C.E. Shaw, B.N. Smith, O. Pansarasa, C. Cereda, R. Del Bo, G.P. Comi, S. D'Alfonso, C. Bertolin, G. Soraru, L. Mazzini, V. Pensato, C. Gellera, C. Tiloca, A. Ratti, A. Calvo, C. Moglia, M. Brunetti, S. Arcuti, R. Capozzo, C. Zecca, C. Lunetta, S. Penco, N. Riva, A. Padovani, M. Filosto, B. Muller, R.J. Stuit, P. Registry, S. Group, S. Registry, F.S. Consortium, S. Consortium, N.S. Group, I. Blair, K. Zhang, E.P. McCann, J.A. Fifita, G.A. Nicholson, D.B. Rowe, R. Pamphlett, M.C. Kiernan, J. Grosskreutz, O.W. Witte, T. Ringer, T. Prell, B. Stubendorff, I. Kurth, C.A. Hubner, P.N. Leigh,

- F. Casale, A. Chio, E. Beghi, E. Pupillo, R. Tortelli, G. Logroscino, J. Powell, A.C. Ludolph, J.H. Weishaupt, W. Robberecht, P. Van Damme, L. Franke, T.H. Pers, R.H. Brown, J.D. Glass, J.E. Landers, O. Hardiman, P.M. Andersen, P. Corcia, P. Vourc'h, V. Silani, N.R. Wray, P.M. Visscher, P.I. de Bakker, M.A. van Es, R.J. Pasterkamp, C.M. Lewis, G. Breen, A. Al-Chalabi, L.H. van den Berg, J.H. Veldink, Genome-wide association analyses identify new risk variants and the genetic architecture of amyotrophic lateral sclerosis, *Nat Genet* 48(9) (2016) 1043-8.
- [24] M. Wang, N.D. Beckmann, P. Roussos, E. Wang, X. Zhou, Q. Wang, C. Ming, R. Neff, W. Ma, J.F. Fullard, M.E. Hauberg, J. Bendl, M.A. Peters, B. Logsdon, P. Wang, M. Mahajan, L.M. Mangravite, E.B. Dammer, D.M. Duong, J.J. Lah, N.T. Seyfried, A.I. Levey, J.D. Buxbaum, M. Ehrlich, S. Gandy, P. Katsel, V. Haroutunian, E. Schadt, B. Zhang, The Mount Sinai cohort of large-scale genomic, transcriptomic and proteomic data in Alzheimer's disease, *Sci Data* 5 (2018) 180185.
- [25] M. Allen, M.M. Carrasquillo, C. Funk, B.D. Heavner, F. Zou, C.S. Younkin, J.D. Burgess, H.S. Chai, J. Crook, J.A. Eddy, H. Li, B. Logsdon, M.A. Peters, K.K. Dang, X. Wang, D. Serie, C. Wang, T. Nguyen, S. Lincoln, K. Malphrus, G. Bisceglie, M. Li, T.E. Golde, L.M. Mangravite, Y. Asmann, N.D. Price, R.C. Petersen, N.R. Graff-Radford, D.W. Dickson, S.G. Younkin, N. Ertekin-Taner, Human whole genome genotype and transcriptome data for Alzheimer's and other neurodegenerative diseases, *Sci Data* 3 (2016) 160089.
- [26] Z. Li, J.L. Del-Aguila, U. Dube, J. Budde, R. Martinez, K. Black, Q. Xiao, N.J. Cairns, N. Dominantly Inherited Alzheimer, J.D. Dougherty, J.M. Lee, J.C. Morris, R.J. Bateman, C.M. Karch, C. Cruchaga, O. Harari, Genetic variants associated with Alzheimer's disease confer different cerebral cortex cell-type population structure, *Genome Med* 10(1) (2018) 43.
- [27] B. Winckler, V. Faundez, S. Maday, Q. Cai, C. Guimas Almeida, H. Zhang, The Endolysosomal System and Proteostasis: From Development to Degeneration, *J Neurosci* 38(44) (2018) 9364-9374.
- [28] A. Dobin, C.A. Davis, F. Schlesinger, J. Drenkow, C. Zaleski, S. Jha, P. Batut, M. Chaisson, T.R. Gingeras, STAR: ultrafast universal RNA-seq aligner, *Bioinformatics* 29(1) (2013) 15-21.
- [29] E.M. Abud, R.N. Ramirez, E.S. Martinez, L.M. Healy, C.H.H. Nguyen, S.A. Newman, A.V. Yeromin, V.M. Scarfone, S.E. Marsh, C. Fimbres, C.A. Caraway, G.M. Fote, A.M. Madany, A. Agrawal, R. Kayed, K.H. Gylys, M.D. Cahalan, B.J. Cummings, J.P. Antel, A. Mortazavi, M.J. Carson, W.W. Poon, M. Blurton-Jones, iPSC-Derived Human Microglia-like Cells to Study Neurological Diseases, *Neuron* 94(2) (2017) 278-293 e9.
- [30] S. Jiang, N. Wen, Z. Li, U. Dube, J. Del Aguila, J. Budde, R. Martinez, S. Hsu, M.V. Fernandez, N.J. Cairns, N. Dominantly Inherited Alzheimer, F.T.D.G.C. International, O. Harari, C. Cruchaga, C.M. Karch, Integrative system biology analyses of CRISPR-edited iPSC-derived neurons and human brains reveal deficiencies of presynaptic signaling in FTLD and PSP, *Transl Psychiatry* 8(1) (2018) 265.
- [31] H.J. Kang, Y.I. Kawasawa, F. Cheng, Y. Zhu, X. Xu, M. Li, A.M. Sousa, M. Pletikos, K.A. Meyer, G. Sedmak, T. Guennel, Y. Shin, M.B. Johnson, Z. Krsnik, S. Mayer, S. Fertuzinhos, S. Umlauf, S.N. Lisgo, A. Vortmeyer, D.R. Weinberger, S. Mane, T.M. Hyde, A. Huttner, M. Reimers, J.E. Kleinman, N. Sestan, Spatio-temporal transcriptome of the human brain, *Nature* 478(7370) (2011) 483-9.
- [32] A. Kamburov, K. Pentchev, H. Galicka, C. Wierling, H. Lehrach, R. Herwig, ConsensusPathDB: toward a more complete picture of cell biology, *Nucleic Acids Res* 39(Database issue) (2011) D712-7.

- [33] A. Kamburov, U. Stelzl, H. Lehrach, R. Herwig, The ConsensusPathDB interaction database: 2013 update, Nucleic Acids Res 41(Database issue) (2013) D793-800.
- [34] C.M. Karch, A.T. Jeng, A.M. Goate, Calcium phosphatase calcineurin influences tau metabolism, Neurobiology of Aging (2012).
- [35] U.K. Laemmli, Cleavage of structural proteins during the assembly of the head of bacteriophage T4, Nature 227(5259) (1970) 680-5.
- [36] C.M. Karch, A.T. Jeng, P. Nowotny, J. Cady, C. Cruchaga, A.M. Goate, Expression of novel Alzheimer's disease risk genes in control and Alzheimer's disease brains, PloS one 7(11) (2012) e50976.
- [37] B. Allen, E. Ingram, M. Takao, M.J. Smith, R. Jakes, K. Virdee, H. Yoshida, M. Holzer, M. Craxton, P.C. Emson, C. Atzori, A. Miglieli, R.A. Crowther, B. Ghetti, M.G. Spillantini, M. Goedert, Abundant tau filaments and nonapoptotic neurodegeneration in transgenic mice expressing human P301S tau protein, The Journal of neuroscience : the official journal of the Society for Neuroscience 22(21) (2002) 9340-51.
- [38] R.D. Gonzalez-Cruz, K.N. Dahl, E.M. Darling, The Emerging Role of Lamin C as an Important LMNA Isoform in Mechanophenotype, Front Cell Dev Biol 6 (2018) 151.
- [39] A. Grupe, R. Abraham, Y. Li, C. Rowland, P. Hollingworth, A. Morgan, L. Jehu, R. Segurado, D. Stone, E. Schadt, M. Karnoub, P. Nowotny, K. Tacey, J. Catanese, J. Sninsky, C. Brayne, D. Rubinsztein, M. Gill, B. Lawlor, S. Lovestone, P. Holmans, M. O'Donovan, J.C. Morris, L. Thal, A. Goate, M.J. Owen, J. Williams, Evidence for novel susceptibility genes for late-onset Alzheimer's disease from a genome-wide association study of putative functional variants, Hum Mol Genet 16(8) (2007) 865-73.
- [40] B.M. Schjeide, M.B. McQueen, K. Mullin, J. DiVito, M.F. Hogan, M. Parkinson, B. Hooli, C. Lange, D. Blacker, R.E. Tanzi, L. Bertram, Assessment of Alzheimer's disease case-control associations using family-based methods, Neurogenetics 10(1) (2009) 19-25.
- [41] T.M. Feulner, S.M. Laws, P. Friedrich, S. Wagenpfeil, S.H. Wurst, C. Riehle, K.A. Kuhn, M. Krawczak, S. Schreiber, S. Nikolaus, H. Forstl, A. Kurz, M. Riemenschneider, Examination of the current top candidate genes for AD in a genome-wide association study, Mol Psychiatry 15(7) (2010) 756-66.
- [42] J.C. Lambert, C.A. Ibrahim-Verbaas, D. Harold, A.C. Naj, R. Sims, C. Bellenguez, G. Jun, A.L. Destefano, J.C. Bis, G.W. Beecham, B. Grenier-Boley, G. Russo, T.A. Thornton-Wells, N. Jones, A.V. Smith, V. Chouraki, C. Thomas, M.A. Ikram, D. Zelenika, B.N. Vardarajan, Y. Kamatani, C.F. Lin, A. Gerrish, H. Schmidt, B. Kunkle, M.L. Dunstan, A. Ruiz, M.T. Bihoreau, S.H. Choi, C. Reitz, F. Pasquier, P. Hollingworth, A. Ramirez, O. Hanon, A.L. Fitzpatrick, J.D. Buxbaum, D. Campion, P.K. Crane, C. Baldwin, T. Becker, V. Gudnason, C. Cruchaga, D. Craig, N. Amin, C. Berr, O.L. Lopez, P.L. De Jager, V. Deramecourt, J.A. Johnston, D. Evans, S. Lovestone, L. Letenneur, F.J. Moron, D.C. Rubinsztein, G. Eiriksdottir, K. Sleegers, A.M. Goate, N. Fievet, M.J. Huentelman, M. Gill, K. Brown, M.I. Kamboh, L. Keller, P. Barberer-Gateau, B. McGuinness, E.B. Larson, R. Green, A.J. Myers, C. Dufouil, S. Todd, D. Wallon, S. Love, E. Rogaeva, J. Gallacher, P. St George-Hyslop, J. Clarimon, A. Lleo, A. Bayer, D.W. Tsuang, L. Yu, M. Tsolaki, P. Bossu, G. Spalletta, P. Proitsi, J. Collinge, S. Sorbi, F. Sanchez-Garcia, N.C. Fox, J. Hardy, M.C. Naranjo, P. Bosco, R. Clarke, C. Brayne, D. Galimberti, M. Mancuso, F. Matthews, S. Moebus, P. Mecocci, M. Del Zompo, W. Maier, H. Hampel, A. Pilotto, M. Bullido, F. Panza, P. Caffarra, B. Nacmias, J.R. Gilbert, M. Mayhaus, L. Lannfelt, H. Hakonarson, S. Pichler, M.M. Carrasquillo, M. Ingelsson, D. Beekly, V. Alvarez, F. Zou, O. Valladares, S.G. Younkin, E. Coto, K.L. Hamilton-Nelson, W. Gu, C. Razquin, P. Pastor, I.

- Mateo, M.J. Owen, K.M. Faber, P.V. Jonsson, O. Combarros, M.C. O'Donovan, L.B. Cantwell, H. Soininen, D. Blacker, S. Mead, T.H. Mosley, Jr., D.A. Bennett, T.B. Harris, L. Fratiglioni, C. Holmes, R.F. de Brujin, P. Passmore, T.J. Montine, K. Bettens, J.I. Rotter, A. Brice, K. Morgan, T.M. Foroud, W.A. Kukull, D. Hannequin, J.F. Powell, M.A. Nalls, K. Ritchie, K.L. Lunetta, J.S. Kauwe, E. Boerwinkle, M. Riemschneider, M. Boada, M. Hiltunen, E.R. Martin, R. Schmidt, D. Rujescu, L.S. Wang, J.F. Dartigues, R. Mayeux, C. Tzourio, A. Hofman, M.M. Nothen, C. Graff, B.M. Psaty, L. Jones, J.L. Haines, P.A. Holmans, M. Lathrop, M.A. Pericak-Vance, L.J. Launer, L.A. Farrer, C.M. van Duijn, C. Van Broeckhoven, V. Moskvina, S. Seshadri, J. Williams, G.D. Schellenberg, P. Amouyel, Meta-analysis of 74,046 individuals identifies 11 new susceptibility loci for Alzheimer's disease, *Nature genetics* (2013).
- [43] J. Barrowman, C. Hamblet, M.S. Kane, S. Michaelis, Requirements for efficient proteolytic cleavage of prelamin A by ZMPSTE24, *PLoS One* 7(2) (2012) e32120.
- [44] B. Frost, Alzheimer's disease: An acquired neurodegenerative laminopathy, *Nucleus* 7(3) (2016) 275-83.
- [45] J.A. Mellad, D.T. Warren, C.M. Shanahan, Nesprins LINC the nucleus and cytoskeleton, *Curr Opin Cell Biol* 23(1) (2011) 47-54.
- [46] D.L. Medina, S. Di Paola, I. Peluso, A. Armani, D. De Stefani, R. Venditti, S. Montefusco, A. Scotto-Rosato, C. Prezioso, A. Forrester, C. Settembre, W. Wang, Q. Gao, H. Xu, M. Sandri, R. Rizzuto, M.A. De Matteis, A. Ballabio, Lysosomal calcium signalling regulates autophagy through calcineurin and TFEB, *Nat Cell Biol* 17(3) (2015) 288-99.
- [47] H. Bading, Nuclear calcium signalling in the regulation of brain function, *Nat Rev Neurosci* 14(9) (2013) 593-608.
- [48] S. Papadia, P. Stevenson, N.R. Hardingham, H. Bading, G.E. Hardingham, Nuclear Ca<sup>2+</sup> and the cAMP response element-binding protein family mediate a late phase of activity-dependent neuroprotection, *J Neurosci* 25(17) (2005) 4279-87.
- [49] S.J. Zhang, M.N. Steijaert, D. Lau, G. Schutz, C. Delucinge-Vivier, P. Descombes, H. Bading, Decoding NMDA receptor signaling: identification of genomic programs specifying neuronal survival and death, *Neuron* 53(4) (2007) 549-62.
- [50] S.J. Zhang, M. Zou, L. Lu, D. Lau, D.A. Ditzel, C. Delucinge-Vivier, Y. Aso, P. Descombes, H. Bading, Nuclear calcium signaling controls expression of a large gene pool: identification of a gene program for acquired neuroprotection induced by synaptic activity, *PLoS Genet* 5(8) (2009) e1000604.
- [51] S.J. Zhang, B. Buchthal, D. Lau, S. Hayer, O. Dick, M. Schwaninger, R. Veltkamp, M. Zou, U. Weiss, H. Bading, A signaling cascade of nuclear calcium-CREB-ATF3 activated by synaptic NMDA receptors defines a gene repression module that protects against extrasynaptic NMDA receptor-induced neuronal cell death and ischemic brain damage, *J Neurosci* 31(13) (2011) 4978-90.
- [52] G.L. Cornelison, S.A. Levy, T. Jenson, B. Frost, Tau-induced nuclear envelope invagination causes a toxic accumulation of mRNA in *Drosophila*, *Aging Cell* 18(1) (2019) e12847.
- [53] B. Eftekharzadeh, J.G. Daigle, L.E. Kapinos, A. Coyne, J. Schiantarelli, Y. Carlomagno, C. Cook, S.J. Miller, S. Dujardin, A.S. Amaral, J.C. Grima, R.E. Bennett, K. Tepper, M. DeTure, C.R. Vanderburg, B.T. Corjuc, S.L. DeVos, J.A. Gonzalez, J. Chew, S. Vidensky, F.H. Gage, J. Mertens, J. Troncoso, E. Mandelkow, X. Salvatella, R.Y.H. Lim, L. Petrucelli, S. Wegmann, J.D. Rothstein, B.T. Hyman, Tau Protein Disrupts Nucleocytoplasmic Transport in Alzheimer's Disease, *Neuron* 99(5) (2018) 925-940 e7.

- [54] F. Paonessa, L.D. Evans, R. Solanki, D. Larrieu, S. Wray, J. Hardy, S.P. Jackson, F.J. Livesey, Microtubules Deform the Nuclear Membrane and Disrupt Nucleocytoplasmic Transport in Tau-Mediated Frontotemporal Dementia, *Cell Rep* 26(3) (2019) 582-593 e5.
- [55] T.A. Fulga, I. Elson-Schwab, V. Khurana, M.L. Steinhilb, T.L. Spires, B.T. Hyman, M.B. Feany, Abnormal bundling and accumulation of F-actin mediates tau-induced neuronal degeneration in vivo, *Nat Cell Biol* 9(2) (2007) 139-48.
- [56] D.M. Moraga, P. Nunez, J. Garrido, R.B. Maccioni, A tau fragment containing a repetitive sequence induces bundling of actin filaments, *J Neurochem* 61(3) (1993) 979-86.
- [57] K.J. Brennand, Inducing cellular aging: enabling neurodegeneration-in-a-dish, *Cell Stem Cell* 13(6) (2013) 635-6.
- [58] R.A. Cragg, G.R. Christie, S.R. Phillips, R.M. Russi, S. Kury, J.C. Mathers, P.M. Taylor, D. Ford, A novel zinc-regulated human zinc transporter, hZTL1, is localized to the enterocyte apical membrane, *J Biol Chem* 277(25) (2002) 22789-97.
- [59] T. Kambe, H. Narita, Y. Yamaguchi-Iwai, J. Hirose, T. Amano, N. Sugiura, R. Sasaki, K. Mori, T. Iwanaga, M. Nagao, Cloning and characterization of a novel mammalian zinc transporter, zinc transporter 5, abundantly expressed in pancreatic beta cells, *J Biol Chem* 277(21) (2002) 19049-55.
- [60] Y. Xu, G. Xiao, L. Liu, M. Lang, Zinc transporters in Alzheimer's disease, *Mol Brain* 12(1) (2019) 106.
- [61] J.H. Baek, E. Schmidt, N. Viceconte, C. Strandgren, K. Pernold, T.J. Richard, F.W. Van Leeuwen, N.P. Dantuma, P. Damberg, K. Hultenby, B. Ulfhake, E. Mugnaini, B. Rozell, M. Eriksson, Expression of progerin in aging mouse brains reveals structural nuclear abnormalities without detectable significant alterations in gene expression, hippocampal stem cells or behavior, *Hum Mol Genet* 24(5) (2015) 1305-21.
- [62] H.J. Jung, C. Coffinier, Y. Choe, A.P. Beigneux, B.S. Davies, S.H. Yang, R.H. Barnes, 2nd, J. Hong, T. Sun, S.J. Pleasure, S.G. Young, L.G. Fong, Regulation of prelamin A but not lamin C by miR-9, a brain-specific microRNA, *Proc Natl Acad Sci U S A* 109(7) (2012) E423-31.
- [63] X. Nissan, S. Blondel, C. Navarro, Y. Maury, C. Denis, M. Girard, C. Martinat, A. De Sandre-Giovannoli, N. Levy, M. Peschanski, Unique preservation of neural cells in Hutchinson-Gilford progeria syndrome is due to the expression of the neural-specific miR-9 microRNA, *Cell Rep* 2(1) (2012) 1-9.
- [64] I. Mendez-Lopez, I. Blanco-Luquin, J. Sanchez-Ruiz de Gordoa, A. Urdanoz-Casado, M. Roldan, B. Acha, C. Echavarri, V. Zelaya, I. Jerico, M. Mendioroz, Hippocampal LMNA Gene Expression is Increased in Late-Stage Alzheimer's Disease, *Int J Mol Sci* 20(4) (2019).
- [65] S.H. Yang, X. Qiao, E. Farber, S.Y. Chang, L.G. Fong, S.G. Young, Eliminating the synthesis of mature lamin A reduces disease phenotypes in mice carrying a Hutchinson-Gilford progeria syndrome allele, *J Biol Chem* 283(11) (2008) 7094-9.
- [66] S. Osmanagic-Myers, T. Dechat, R. Foisner, Lamins at the crossroads of mechanosignaling, *Genes Dev* 29(3) (2015) 225-37.
- [67] B. Burke, Lamins and apoptosis: a two-way street?, *J Cell Biol* 153(3) (2001) F5-7.
- [68] C.C. Chou, Y. Zhang, M.E. Umoh, S.W. Vaughan, I. Lorenzini, F. Liu, M. Sayegh, P.G. Donlin-Asp, Y.H. Chen, D.M. Duong, N.T. Seyfried, M.A. Powers, T. Kukar, C.M. Hales, M. Gearing, N.J. Cairns, K.B. Boylan, D.W. Dickson, R. Rademakers, Y.J. Zhang, L. Petrucelli, R. Sattler, D.C. Zarnescu, J.D. Glass, W. Rossoll, TDP-43 pathology disrupts nuclear pore complexes and nucleocytoplasmic transport in ALS/FTD, *Nat Neurosci* 21(2) (2018) 228-239.

- [69] B.D. Freibaum, Y. Lu, R. Lopez-Gonzalez, N.C. Kim, S. Almeida, K.H. Lee, N. Badders, M. Valentine, B.L. Miller, P.C. Wong, L. Petrucelli, H.J. Kim, F.B. Gao, J.P. Taylor, GGGGCC repeat expansion in C9orf72 compromises nucleocytoplasmic transport, *Nature* 525(7567) (2015) 129-33.
- [70] F. Gasset-Rosa, C. Chillon-Marinas, A. Goginashvili, R.S. Atwal, J.W. Artates, R. Tabet, V.C. Wheeler, A.G. Bang, D.W. Cleveland, C. Lagier-Tourenne, Polyglutamine-Expanded Huntingtin Exacerbates Age-Related Disruption of Nuclear Integrity and Nucleocytoplasmic Transport, *Neuron* 94(1) (2017) 48-57 e4.
- [71] A.C. Woerner, F. Frottin, D. Hornburg, L.R. Feng, F. Meissner, M. Patra, J. Tatzelt, M. Mann, K.F. Winklhofer, F.U. Hartl, M.S. Hipp, Cytoplasmic protein aggregates interfere with nucleocytoplasmic transport of protein and RNA, *Science* 351(6269) (2016) 173-6.

## **Chapter 3: RAB10: a protective factor in AD**

### **3.1 Abstract**

Research into Alzheimer's disease (AD) has revealed a complex genetic architecture that comprises a multitude of genes across many different pathways. Furthermore, each of these differing risk factors exert different affects on AD risk. In a 2017 study by our group, a rare SNP in the 3'-untranslated region (3'-UTR) of *RAB10* was found to confer AD resilience in individuals who would normally be at higher risk of disease. A Rab GTPase, *RAB10* regulates subcellular trafficking within the endo-lysosomal network (ELN) a pathway central to APP metabolism. We find that, in AD, RAB10 protein is elevated, which is shown in *in vitro* models to alter the A $\beta$ 42/40 ratio in a manner that promotes protein aggregation and plaque formation. While the rare SNP, rs142787485, appears to have no influence on mRNA expression as a whole or on an allele specific level, we hypothesize that it instead affects post-transcriptional gene expression through the interference of miRNAs, with at least 5 miRNAs that bind at the SNP site and all of which are differentially expressed in AD. While this remains to be replicated *in vitro*, these findings, along with what has been published in the literature, presents interesting opportunities to the field of AD medicine for potential therapeutics against disease.

### **3.2 Introduction**

Understanding the genetic architecture of AD can provide critical insights into genes and pathways that drive disease risk, and this has been a major focus of genetic studies in the AD field. However, genetic architecture may also include variants, genes and pathways that confer resilience to AD. While understanding variants that increase risk allow us to better understand disease mechanisms, understanding protective variants also allow us to better understand successful aging without dementia [1]. In addition, due to the complex nature of AD genetics, successful therapeutics of many individual cases of LOAD may very well require a deep understanding of both risk and protective variants.

This is further demonstrated by a case study of an individual from the largest autosomal dominant AD (ADAD) kindred who carried the *PSEN1* E280A variant but remained cognitively normal until developing mild cognitive impairment (MCI) at well into her seventies, 30 years beyond her estimated age at onset [2]. Whole exome sequencing showed that, while this individual did indeed carry the *PSEN1* mutation, she also carried two copies of the rare *APOE3* R136S variant, known as the Christchurch mutation (*APOE3ch*), which was identified in select patients with hyperlipoproteinemia type III (HLP-III) [2, 3]. These findings serve to demonstrate how a protective variant can counteract a disease-driving mutation, resulting in a normal aging phenotype.

RAB10 is a member of the RAB family of small GTPases, which are key regulators of vesicular trafficking. RAB proteins are cyclically controlled. RAB activation requires a GDP-GTP exchange that is facilitated by RAB guanine nucleotide exchange factors [4]. This requires

phosphorylation at Thr73, which is mediated by Leucine-rich repeat kinase 2 (*LRRK2*), a protein kinase associated with Parkinson's disease [5, 6]. Unlike most of the other RAB proteins, which have relatively specific roles within intracellular transport, RAB10 is relatively unique because it carries out a wide variety of functions and has multiple subcellular localizations [7].

*Rab10* plays essential functional roles in development: mice are embryonic lethal when both alleles are deleted [8]. In addition, RAB10 plays a role in maintenance and regulation of endoplasmic reticulum (ER) morphology [9-11]. When RAB10 is mutated or constitutively inactive (e.g. GDP-locked), the ER contains more cisternae, suggesting that RAB10 plays a critical role in maintaining and/or generating tubule extension and fusion in the ER [10]. RAB10 function has also been linked to neuronal morphology and polarization, playing a critical role in axonal development and dendrite arborization [12, 13]. During neuronal development, RAB10 associates with plasmalemmal precursor vesicles, which are linked to kinesin 1 via c-Jun N-terminal protein kinase-interacting protein 1 [14]. Together this complex mediates anterograde transport of RAB10-positive vesicles to axonal tips, promoting axonal growth [14]. Thus, RAB10 function is critical for proper neuronal function.

RAB10 has been linked to many roles involved in intracellular transport (Figure 3.1). RAB10 plays a role in endocytic recycling. In *C. elegans*, *rab10* is required for AMPA-type glutamate receptor recycling in postsynaptic membranes [15]. RAB10 is likely functional upstream of RME-1/EHD, a protein involved in recycling endosome tubulization and endosome function [16-18]. RAB10 is expressed at the interface of early endosomes and recycling endosomes. These structures are morphologically defective in *rab-10* mutant *C. elegans* models [16, 18]. RAB10 is required for endosomal recruitment of CNT-1 [19]. This likely contributes to biogenesis and/or maintenance of recycling endosome compartments. RAB10 could also play a

role in promoting the maturation of early endosomes to recycling endosome. RAB10 is also involved in protein degradation. RAB10 and RAB3A are essential for lysosomal exocytosis and plasma membrane repair [20, 21]. RAB10-mediated lysosomal secretion is also found to play a role in the cellular response to stressed lysosomes [5]. RAB10 associates with lipid droplets [22]. Complexes of RAB10-EHBP1-EHD2 promote autophagic engulfment and degradation of lipid droplets [23]. Thus, these functional roles for RAB10 in recycling and degradation make it an interesting candidate protein in AD pathogenesis.

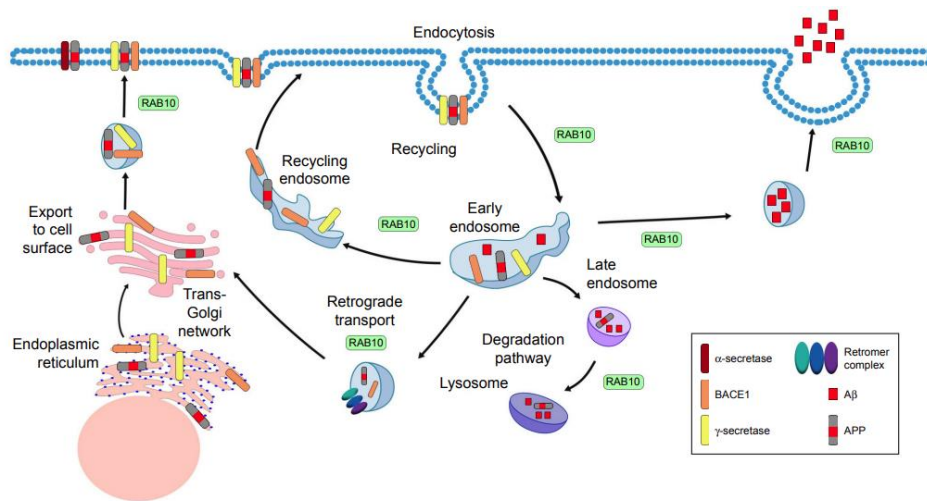


**Figure 3.1:** Diagram of APP trafficking and the role of RAB10 in these intracellular transport pathways.

RAB10 is involved in transport of proteins from the early endosome to the Trans-Golgi Network (TGN), where it may also function in the retromer pathway [24]. The retromer complex consists of Vps26, Vps35, Vps29, SNX1, SNX2, SNX5, and SNX6 [25]. The retromer complex regulates transport of protein cargo from endosomes to the TGN by the retrograde pathway or to the cell surface through the recycling pathway [26].

In order to form the amyloid plaques that define a primary component of AD pathology, the transmembrane APP must first be processed into A $\beta$  peptides. APP is thought to be retrieved

from the cell surface and trafficked to the early endosomes where it is initially cleaved by β-site APP-cleaving enzyme 1 (BACE1) to generate a C-terminal fragment (β-CTF) [27, 28]. The β-CTF fragments are then trafficked via retromer-dependent transport to the TGN, which facilitates further cleavage by γ-secretase to produce Aβ40 [29]. The retromer complex and its receptors can transport APP and BACE1 from endosomes to the TGN, ultimately regulating production of Aβ [26]. The retromer complex sorts APP and BACE, either through direct or indirect binding to the transmembrane adaptor protein SORLA [30]. Interestingly, common variants in the gene that encodes SORLA have been associated with AD risk [31]. Thus, genes that are involved in retromer function may influence AD pathogenesis and represent promising therapeutic targets.

Retromer complex dysfunction promotes APP accumulation in neurons and Aβ production. In addition, the retromer also appears to have a differential effect on Aβ isoforms, with evidence that retromer dysfunction alters Aβ40 secretion, which results in increasing the Aβ42/40 ratio [32]. In mouse models, reduction of a single component within the retromer complex, Vps26, is sufficient to increase soluble Aβ and APP [33]. Stabilization of the retromer in human induced pluripotent stem cell-derived neurons using the pharmacological chaperone R33 has been shown to significantly reduce the phosphorylation of Tau in a manner that correlated with, but ultimately independent of, Aβ production [34].

In 2017, our group sought to identify genes that conferred resilience upon otherwise high-risk individuals. To this end, we selected individuals who were at least 75 years of age, cognitively normal, and carried at least one copy of *APOE ε4*, a genotype that carries a significantly elevated risk of AD [35]. These individuals were determined to be “AD resilient”. Through this analysis, a genetic SNP in the 3'-untranslated region (3'-UTR) of *RAB10*, rs142787485 that was linked to AD resilience [35].

An RNAi screen of RABs that modify APP processing revealed that the silencing of *RAB10* reduces A $\beta$  without altering sAPP $\beta$  levels [36]. The LRRK2-RAB10 signaling pathway also causes an overproduction of A $\beta$  [6]. In this chapter I describe the link we discovered between *RAB10* and sporadic AD as well as some of the working hypotheses we have regarding how the rs142787485 ameliorates AD risk.

### **3.3 Materials and Methods**

#### *Patient Consent*

Brains were collected post-mortem following written informed consent from the donor. The Washington University School of Medicine Institutional Review Board and Ethics Committee approved the informed consent (IRB 201104178, 201306108). The consent allows for the use of tissue by all parties, commercial and academic, for research but not for human therapy.

#### *Protein extraction and Western blot of human brain tissue*

Small sections of tissue were cut from the parietal lobe of frozen brain cross sections donated by AD patients and cognitively normal individuals. 10 volumes of lysis buffer (50 mM Tris, 150 mM NaCl, 2 mM EDTA, 0.01% NP40, and 0.5% Triton X100, 1:100 protease inhibitor) were added to the tissue samples based on weight (to 0.1 g tissue, add 1 mL of lysis buffer) before the samples were sonicated 3 times for 30 seconds each. Samples were then pelleted at 14,000xg at 4°C for 10 minutes before the supernatant was collected. Protein concentration was assayed through a BCA and 20 ug of protein was run on a 4-12% bis-tris gel (10-well) (Invitrogen) in MOPS buffer (Life Technologies). The protein was then transferred to a 0.45  $\mu$ m PVDF membrane activated in methanol using 1x tris-glycine buffer supplemented with

20% methanol. Membranes were then probed with  $\alpha$ -pRAB10 (ab230261 [MJF-R21]; 1:200) or  $\alpha$ -RAB10 (ab237703 [MJF-R23]; 1:1000) at 4°C overnight. Blots were then washed and probed with goat-anti-rabbit secondary antibody (Seracare; 1:5000.) for 2 hours. Bands were visualized with either Lumigen (Lumigen) for pRAB10 or SuperSignal™ West Pico PLUS (Thermo Scientific).

### *Preparation of cDNA*

Tissue samples cut from human brains were dissolved in Qiazol lysis reagent (Qiagen) and mRNA was extracted with a phenol/chloroform extraction. The concentration of the mRNA was assayed and converted to complementary DNA (cDNA) through a reverse transcription PCR using the High Capacity cDNA Reverse Transcription kit (Thermofisher Scientific).

### *qPCR*

For the standard Taqman assays, 10 ng of cDNA is loaded with and run using the PerfeCTa FastMix II qPCR master mix (QuantaBiosciences) and Low Rox (QuantaBiosciences). RAB10 was targeted using the Hs00794658\_m1 TaqMan assay (Thermofisher Scientific). The qPCR was run using the QuantStudio 12k Flex Real-Time PCR thermocycler (ThermoFisher) using the Comparative CT method and the standard default cycling settings.

To assess whether rs142787485 had any allele specific effects on *RAB10* expression, cDNA from the parietal lobe of eight individual heterozygous carriers of the rs142787485 SNP were obtained and analyzed with a Kompetitive allele specific PCR (KASP) (LGC Genomics). Differential Ct (dCt) was obtained by comparing Ct values for both alleles from each sample. Three technical replicates were used for each individual and the dCts were averaged. Genomic

DNA (gDNA) from each individual was also used as an internal control. Differential expression across the minor and WT alleles were analyzed through Student's t-test.

### *miRNA analyses*

To identify potential miRNA binding sites affected by rs142787485, the SNP was entered into the miRSNP database. From the six miRNAs given in the readout, only has-miR-378h was excluded since its affinity was only predicted to decrease in the context of the rs142787485 SNP. The remaining five miRNAs were then cross-referenced with the TargetScan database to identify the type of interaction and miRDB to identify the binding site in the 3'-UTR. To examine the relative expression of these different miRNAs in the context of AD by looking at four different online datasets: GSE16759 (parietal lobe tissue from AD [n=4] and control brains [n=4]) [37], GSE63501 (RNAseq from AD brains [n=6], tangle-prominent demented brains [n=3], and control brains [n=7]) [38], GSE46131 (temporal neocortex gray matter tissue from AD brains [n=5], demented with Lewy Bodies brains [n=4], hippocampal sclerosis of aging brains [n=4], frontotemporal lobar demented brains [n=5], and non-demented brains [n=2]) [39], and GSE48552 (prefrontal cortex tissues from late stage AD brains [n=6] and early stage AD/control brains [n=6]) [40].

## **3.4 Results**

### *RAB10 is elevated in sporadic AD*

Due to its role in subcellular vesicle transport, RAB10 is expressed in all cell types in the brain. However, in brains affected by LOAD, there was a significant increase in the level of expressed Rab10 protein (Figure 3.2A and 3.2B).

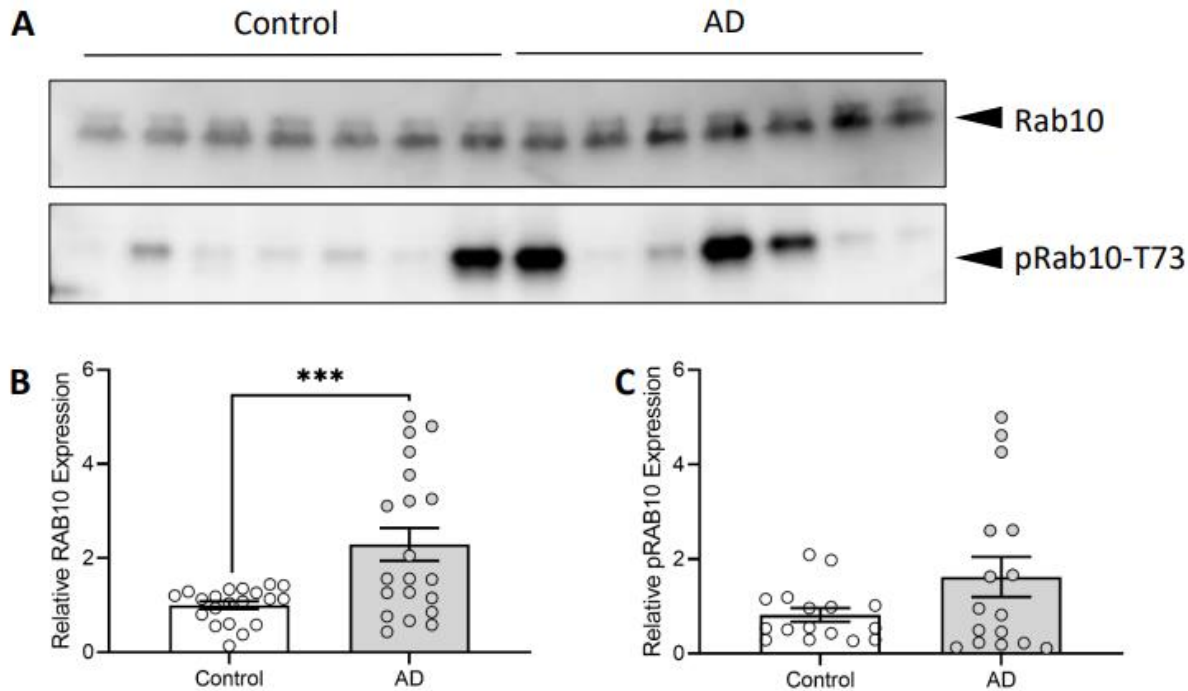


**Figure 3.2: RAB10 protein expression is elevated in AD brains.** A. representative Western blot of parietal brain tissue from case control and AD patients. B and C. Quantification of (A) for relative RAB10 protein expression (B) and RAB10 phosphorylation (C). Graphs display standard error of mean. \*\*\* p<0.0005. Analyzed by Student's two-tailed t-test.

Rab10 cycles between its inactive, GDP-bound role and its active, GTP-bound role. When inactive, Rab10 is bound by guanine dissociation inhibitors (GDIs). GDIs extract inactive Rab proteins from their target membranes and bind them in the cytosol. However, upon phosphorylation by leucine rich repeat kinase 2 (LRRK2), a genetic risk factor for Parkinson's Disease, GDI is dissociated from Rab10 and is able to be inserted into the target membrane where it can be activated with the addition of a GTP by a guanine exchange factors (GEFs) [41]. However, beyond Parkinson's, this phosphorylation event may represent a pathological feature in the brains of AD patients [6]. Immunoblotting of parietal brain tissue shows marginal elevation of Rab10 phosphorylation (Figure 3.2A and 3.2C; p=0.0822). pRab10-Thr73 was

observed to co-localize with neurofibrillary tangles in AD brains as well as with granulovascular degeneration, neuropil threads, and dystrophic neurons [6]. Double immunofluorescence staining of these structures further revealed positive staining for phosphorylated tau. However, this co-localization of pRab10-Thr73 and phosphorylated tau was not complete, with some instances showing neuropil threads or dystrophic neurons containing only phosphorylated tau or pRab10-Thr73. Interestingly, dystrophic neurons near amyloid plaques stained positive for pRab10-Thr73, while the amyloid plaques themselves were negative for pRab10 [6]. Total Rab10 staining, however, did not differ between AD and control brains [6]. Thus, while pRab10-Thr73 is associated with AD pathology, it remains unclear whether this represents excess activation or aberrant function of Rab10.

*Rs142787485 SNP is not differentially expressed*

Among AD resilient individuals, a rare SNP in the *RAB10* 3'-UTR was found to be significantly associated with a decreased risk of LOAD (OR=0.69 [0.47-0.99]; p=0.028; MAF [controls/cases]=0.045/0.031), in the presence of at least a single copy of the harmful *APOE4* isoform [35]. Existing outside the coding exons of the mRNA transcript, rs142787485 has no effect on the amino acid coding of the final protein. Indeed, data also shows that there is no difference in relative expression of *RAB10* mRNA in the context of the rs142787485 variant (Figure 3.3A and 3.3B).

*Rs142787485 may alter miRNA-mediated post-transcriptional regulation of RAB10*

Alternatively, the 3'-UTR is a common binding site for many different protein complexes and molecules that regulate post-transcriptional expression, with a notable example being micro

RNAs (miRNAs). MiRNAs are endogenous peptides of non-coding RNAs, spanning roughly 20–22 nucleotides in length. In molecular biology, miRNAs serve a key role in post-transcriptional regulation by mainly inhibiting translation of protein from the mRNA or outright facilitating the degradation of the transcripts [42]. For some time, miRNAs have mostly been researched in the context of cancer, but a growing number of studies has also begun to implicate these miRNAs in AD, with the field showing much promise for both the future development of therapeutics as well as for another type of diagnostic biomarker [43]. By looking at miRNA expression in AD patients, it was in fact observed that many miRNAs that targeted genes associated with A $\beta$  production were differentially expressed, such as miR-29a/b and miR-107, which both target the  $\beta$ -secretase BACE1 [44, 45].

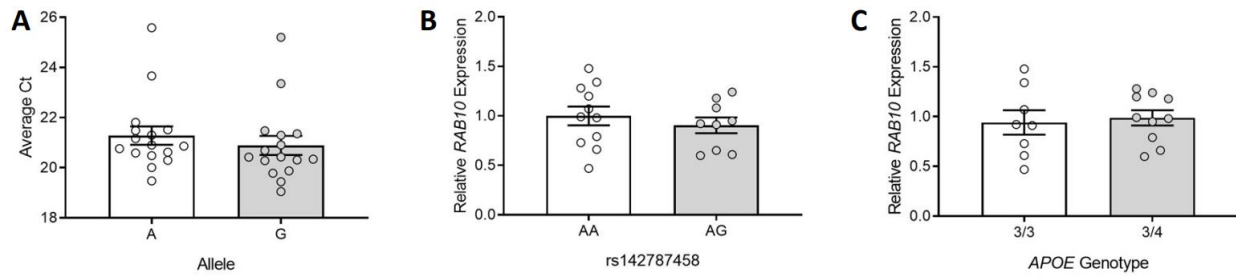


**Figure 3.3: *RAB10* expression is not changed in the context of either the rs142787485 or the *APOE* genotype.**

A. Allele specific expression in the both the wildtype *RAB10* allele (A) and the SNP allele (G) in rs142787485. B. Relative expression of *RAB10* between wildtype (AA) and single allele carriers (AG) for the rs142787485 SNP. C. Relative *RAB10* between individuals with either the neutral *APOE3/3* genotype or the higher pathogenic *APOE3/4* genotype. Graphs display standard error of mean. Analyzed by Student's two-tailed t-test.

The location of the rs142787485 SNP in the 3'-UTR of the *RAB10* gene led us to question whether miRNA-mediated regulation may be affected. To investigate this, the rs142787485 SNP was plugged into the online tool miRSNP [46], which identifies miRNA binding sites that correlate with particular SNPs and predicts the effect of the SNP on binding affinity using a

variety of different algorithms. This includes generating a ranking of miRNA target sites at SNP loci using a machine learning method, miRSVR, which trains a regression model for the features of the binding duplex, the local context features, and the global context features to generate a down-regulation score [47]. Using this tool, six miRNAs were predicted to be affected by the rs142787485 SNP (hsa-miR-369-3p, hsa-miR-374a-5p, hsa-miR-374b-5p, hsa-miR-374c-5p, hsa-miR-378h, and hsa-miR-655). For five of the six miRNAs, the protective *RAB10* SNP is predicted to prevent, or break, the interaction between the miRNA and the *RAB10* transcript, while the interaction between the sixth miRNA (hsa-miR-378h), is only predicted to decrease in affinity [46].

Furthermore, miRNAs have been implicated in multiple instances to play a role in neurodegeneration. As discussed earlier in Chapter 2, *LMNA* is regulated by miR-9 [48], while in AD, APP is targeted by multiple miRNAs that are blocked by identified genetic variants [49]. For *RAB10*, two of the predicted variants, hsa-miR-369-3p and hsa-miR-655, were both identified to be downregulated in AD along with *RAB10* [37-40, 50] (Table 3.1). Therefore, one hypothesis is that rs142787485 is providing protection against AD by disrupting the binding affinity of select miRNAs. Of course, there are some limitations with this hypothesis. Using the Mayo Clinic Brain Bank, it is shown that *RAB10* is upregulated in AD which is associated with an increase in the A $\beta$ 42/40 ratio in the brain, which is more likely to result in toxic plaque formation [35]. Therefore, it seems unlikely that a protective SNP would reduce disease risk by interfering with the binding of miRNA that serve to keep expression down. However, until further experimental work is done, more will have yet to be seen. In addition to miRNAs, the 3'-UTR also serves as a binding site for proteins that also carry out post-transcriptional regulation. These RNA binding proteins (RBPs) bind the 3'-UTR and recruit various effectors [51].

Therefore, there is a possibility that rs142787485 also influences *RAB10* expression through differential binding of RBPs to the 3'-UTR. However, further research is required to further explore this.

**Table 3.1:** Relative expression of various *RAB10*-targeting miRNAs across different studies.

miRNA	Family	Genome Context	miRNA Sequence (Seed Sequence; SNP site underlined)	Interaction Type	Conserved Species	GSE16759	GSE63501	GSE46131	GSE48552
hsa-miR-369-3p	miR-154	chr14: 101065598-101065667 [+]	AAUAAA <u>CAUGGUUGA</u> UCUUU ( <u>GU<u>A</u>UAUA</u> )	8mer	Conserved among human, chimp, rhesus, squirrel, mouse, rat, rabbit, pig, cow, cat, dog, brown bat, elephant, opossum	⬇️	⬆️ *	—	⬇️
hsa-miR-655-3p	miR-154	chr14: 101049550-101049646 [+]	AUAAA <u>CAUGGUUAC</u> CUCUUU ( <u>UG<u>U</u>UAUA</u> )	7mer-m8	Conserved among human, chimp, rhesus, squirrel, mouse, rat, rabbit, pig, cow, cat, dog, brown bat, elephant, opossum	⬇️	—	—	⬆️
hsa-miR-374a-5p	miR-374	chrX: 74287286-74287357 [-]	UUAAA <u>UACACCUGA</u> UAAGUG ( <u>U<u>GU</u>UAUA</u> )	7mer-m8	Conserved among human, chimp, rhesus, squirrel, mouse, rat, rabbit, pig, cow, cat, dog, brown bat, elephant, opossum				
hsa-miR-374b-5p	miR-374	chrX: 74218547-74218618 [-]	AUAAA <u>UACACCUGC</u> UAAGUG ( <u>U<u>GU</u>UAUA</u> )	7mer-m8	Conserved among human, chimp, rhesus, squirrel, mouse, rat, rabbit, pig, cow, cat, dog, brown bat, elephant, opossum		—	—	⬆️
hsa-miR-374c-5p	miR-374	chrX: 74218549-74218618 [+]	AUAAA <u>UACACCUGCUAA</u> GUGCU ( <u>U<u>GU</u>UAUA</u> )	7mer-m8	Conserved among human, chimp, rhesus, squirrel, mouse, rat, rabbit, pig, cow, cat, dog, brown bat, elephant, opossum				

\*Insignificant

### 3.5 Discussion

In a 2012 study, a coding variant for *APP* (A673T) was identified from whole genome sequencing data from 1,795 Icelanders [52]. Since then, more variants have been discovered across many different genes, including, but not limited to, *APOE*, *SORLI*, *ABCA1*, and *MS4A* [1].

Novel genes and pathways that contribute to the pathogenesis of AD provide insights into strategies to prevent or treat the disease. The amyloid hypothesis, which proposes that the accumulation of A $\beta$  triggers the cascade of events that lead to AD, has been the focus of AD therapeutic development for decades. The development of anti-A $\beta$  therapeutics remains the primary approach to treating AD based on our current understanding of the earliest features of this disease [53]. In this review, we emphasize the importance of *RAB10* in the processing of

APP and the production of A $\beta$ . The function of RAB10 in intracellular trafficking and evidence that a reduction of *Rab10* results in a reduction of the A $\beta$ 42/40 ratio makes inhibition of RAB10 a potential therapeutic avenue.

There are several existing strategies for therapeutic inhibition of a gene product. Potential technologies for targeting of RAB10 are small molecules, antibodies, and antisense oligodeoxynucleotide technologies. For each of these approaches the challenge of delivery across the blood brain barrier (BBB) is a significant one [54]. A molecule with high lipid solubility and molecular mass less than 400Da generally can diffuse across the BBB. These criteria limit the classes of small molecules that can be considered as potential therapeutic molecules for AD. Generally, the BBB does not permit the crossing of many antibodies to achieve an adequate therapeutic concentration without severe peripheral consequences. Several approaches have been developed to deliver antibodies to the brain. Bispecific antibodies have been developed that leverage the Transferrin receptor to successfully increase BBB penetration [55, 56]. In addition, antibody analogs that can cross the BBB are in development (Patent #EP3309171). However, even if successful across the BBB could be achieved, the targeting of intracellular proteins by these antibodies also poses a significant challenge. Antisense oligonucleotides do not readily cross the BBB [57]. However, at present, intrathecal bolus injection is an effective method for ensuring distribution in neurons and glial cells in the brain [58].

Approaches to the development and delivery of small molecule therapeutics are mature and the path, and pitfalls, are well established. Small molecules are effective enzyme inhibitors, receptor ligands, or allosteric modulators. The nature of small molecule activity can make it difficult to find the balance between efficacy and side effects when treating humans [54]. Despite these challenges, small molecule drug development has seen many successes and greater than

90% of existing therapeutics use small molecules. Small GTPases similar to RAB10 have been successfully targeted using small molecules in the past. One important use is the development of molecules to block oncogenic properties of the RAS protein to treat cancer [59]. Recent discoveries about the structure of small GTPases and advances in targeting strategies have further increased efforts to use these important proteins as therapeutic targets [60]. Targeting approaches, including interference with nucleotide binding, inactivation by irreversible covalent modification, inhibition of GTPase-GEF interactions, inhibition of GTPase-Effector interactions, and stabilization of GTPase-Protein Complexes have been successful and are reviewed by Cromm et. Al. 2015 [60]. While challenges regarding specificity and crossing the blood brain barrier remain, these advances create some optimism about the use of small molecules to inhibit RAB10 and impact AD pathology.

Antibodies function in extra- and intracellular immunity to recognize foreign or abnormal agents and target them for destruction with very high specificity. The production of monoclonal antibodies (mAb) has resulted in their use for the treatment of a wide range of human diseases [55]. There are currently >60 approved mAbs for human therapy and >50 in late-stage clinical trials [61].

Rnase H-dependent antisense oligonucleotides technology is a popular method for knockdown in cell culture. It offers specific and efficient knockdown and is a powerful tool for functional studies of genes with unknown function [62]. Antisense technology has challenges such as site specificity, toxicity at high concentrations, and the difficulty of targeting specific cell-types. However, it is a mature technology and antisense oligonucleotides offer a means to manipulate specific steps in mRNA processing, for example splicing [53]. As discussed previously, *in vitro* reduction of *Rab10/RAB10* expression using shRNA and RNAi has been

successful [36]. Expansion of antisense oligodeoxynucleotide from *in vitro* to *in vivo* represents a promising therapeutic avenue given recent successes with Spinal muscular atrophy and Huntington's disease [63, 64].

As the field of AD genetics has progressed, it has become increasingly clear that critical work needs to be done to understand not only the variants that increase disease risk, but also the variants that confer resilience to disease. Not only will such important work shed increasing light on the cellular and molecular mechanisms for how the brain combats AD, but will also assist researchers in developing more effective novel therapeutics to treat AD as well as other devastating forms of dementia and neurodegeneration.

### 3.6 References

- [1] S.J. Andrews, B. Fulton-Howard, A. Goate, Protective Variants in Alzheimer's Disease, *Curr Genet Med Rep* 7(1) (2019) 1-12.
- [2] J.F. Arboleda-Velasquez, F. Lopera, M. O'Hare, S. Delgado-Tirado, C. Marino, N. Chmielewska, K.L. Saez-Torres, D. Amarnani, A.P. Schultz, R.A. Sperling, D. Leyton-Cifuentes, K. Chen, A. Baena, D. Aguilera, S. Rios-Romenets, M. Giraldo, E. Guzman-Velez, D.J. Norton, E. Pardilla-Delgado, A. Artola, J.S. Sanchez, J. Acosta-Uribe, M. Lalli, K.S. Kosik, M.J. Huentelman, H. Zetterberg, K. Blennow, R.A. Reiman, J. Luo, Y. Chen, P. Thiyyagura, Y. Su, G.R. Jun, M. Naymik, X. Gai, M. Bootwalla, J. Ji, L. Shen, J.B. Miller, L.A. Kim, P.N. Tariot, K.A. Johnson, E.M. Reiman, Y.T. Quiroz, Resistance to autosomal dominant Alzheimer's disease in an APOE3 Christchurch homozygote: a case report, *Nat Med* 25(11) (2019) 1680-1683.
- [3] M.R. Wardell, S.O. Brennan, E.D. Janus, R. Fraser, R.W. Carrell, Apolipoprotein E2-Christchurch (136 Arg----Ser). New variant of human apolipoprotein E in a patient with type III hyperlipoproteinemia, *J Clin Invest* 80(2) (1987) 483-90.
- [4] F. Barr, D.G. Lambright, Rab GEFs and GAPs, *Curr Opin Cell Biol* 22(4) (2010) 461-70.
- [5] T. Eguchi, T. Kuwahara, M. Sakurai, T. Komori, T. Fujimoto, G. Ito, S.I. Yoshimura, A. Harada, M. Fukuda, M. Koike, T. Iwatsubo, LRRK2 and its substrate Rab GTPases are sequentially targeted onto stressed lysosomes and maintain their homeostasis, *Proc Natl Acad Sci U S A* 115(39) (2018) E9115-E9124.
- [6] T. Yan, L. Wang, J. Gao, S.L. Siedlak, M.L. Huntley, P. Termsarasab, G. Perry, S.G. Chen, X. Wang, Rab10 Phosphorylation is a Prominent Pathological Feature in Alzheimer's Disease, *J Alzheimers Dis* 63(1) (2018) 157-165.
- [7] C.E.L. Chua, B.L. Tang, Rab 10-a traffic controller in multiple cellular pathways and locations, *J Cell Physiol* 233(9) (2018) 6483-6494.
- [8] P. Lv, Y. Sheng, Z. Zhao, W. Zhao, L. Gu, T. Xu, E. Song, Targeted disruption of Rab10 causes early embryonic lethality, *Protein Cell* 6(6) (2015) 463-467.
- [9] J. Chang, C. Blackstone, Rab10 joins the ER social network, *Nat Cell Biol* 15(2) (2013) 135-6.
- [10] A.R. English, G.K. Voeltz, Rab10 GTPase regulates ER dynamics and morphology, *Nat Cell Biol* 15(2) (2013) 169-78.
- [11] A. Schuldt, Membrane dynamics: ER trailblazing by RAB10, *Nat Rev Mol Cell Biol* 14(2) (2013) 63.
- [12] Y. Liu, X.H. Xu, Q. Chen, T. Wang, C.Y. Deng, B.L. Song, J.L. Du, Z.G. Luo, Myosin Vb controls biogenesis of post-Golgi Rab10 carriers during axon development, *Nat Commun* 4 (2013) 2005.
- [13] W. Zou, S. Yadav, L. DeVault, Y. Nung Jan, D.R. Sherwood, RAB-10-Dependent Membrane Transport Is Required for Dendrite Arborization, *PLoS Genet* 11(9) (2015) e1005484.
- [14] C.Y. Deng, W.L. Lei, X.H. Xu, X.C. Ju, Y. Liu, Z.G. Luo, JIP1 mediates anterograde transport of Rab10 cargos during neuronal polarization, *J Neurosci* 34(5) (2014) 1710-23.

- [15] D.R. Glodowski, C.C. Chen, H. Schaefer, B.D. Grant, C. Rongo, RAB-10 regulates glutamate receptor recycling in a cholesterol-dependent endocytosis pathway, *Mol Biol Cell* 18(11) (2007) 4387-96.
- [16] C.C. Chen, P.J. Schweinsberg, S. Vashist, D.P. Mareiniss, E.J. Lambie, B.D. Grant, RAB-10 is required for endocytic recycling in the *Caenorhabditis elegans* intestine, *Mol Biol Cell* 17(3) (2006) 1286-97.
- [17] S. Pant, M. Sharma, K. Patel, S. Caplan, C.M. Carr, B.D. Grant, AMPH-1/Amphiphysin/Bin1 functions with RME-1/Ehd1 in endocytic recycling, *Nat Cell Biol* 11(12) (2009) 1399-410.
- [18] A. Shi, C.C. Chen, R. Banerjee, D. Glodowski, A. Audhya, C. Rongo, B.D. Grant, EHBP-1 functions with RAB-10 during endocytic recycling in *Caenorhabditis elegans*, *Mol Biol Cell* 21(16) (2010) 2930-43.
- [19] A. Shi, O. Liu, S. Koenig, R. Banerjee, C.C. Chen, S. Eimer, B.D. Grant, RAB-10-GTPase-mediated regulation of endosomal phosphatidylinositol-4,5-bisphosphate, *Proc Natl Acad Sci U S A* 109(35) (2012) E2306-15.
- [20] M. Encarnacao, L. Espada, C. Escrevente, D. Mateus, J. Ramalho, X. Michelet, I. Santarino, V.W. Hsu, M.B. Brenner, D.C. Barral, O.V. Vieira, A Rab3a-dependent complex essential for lysosome positioning and plasma membrane repair, *J Cell Biol* 213(6) (2016) 631-40.
- [21] A. Reddy, E.V. Caler, N.W. Andrews, Plasma membrane repair is mediated by Ca(2+)-regulated exocytosis of lysosomes, *Cell* 106(2) (2001) 157-69.
- [22] S. Sato, M. Fukasawa, Y. Yamakawa, T. Natsume, T. Suzuki, I. Shoji, H. Aizaki, T. Miyamura, M. Nishijima, Proteomic profiling of lipid droplet proteins in hepatoma cell lines expressing hepatitis C virus core protein, *J Biochem* 139(5) (2006) 921-30.
- [23] Z. Li, R.J. Schulze, S.G. Weller, E.W. Krueger, M.B. Schott, X. Zhang, C.A. Casey, J. Liu, J. Stockli, D.E. James, M.A. McNiven, A novel Rab10-EHBP1-EHD2 complex essential for the autophagic engulfment of lipid droplets, *Sci Adv* 2(12) (2016) e1601470.
- [24] C.M. Babbey, N. Ahktar, E. Wang, C.C. Chen, B.D. Grant, K.W. Dunn, Rab10 regulates membrane transport through early endosomes of polarized Madin-Darby canine kidney cells, *Mol Biol Cell* 17(7) (2006) 3156-75.
- [25] J.S. Bonifacino, J.H. Hurley, Retromer, *Curr Opin Cell Biol* 20(4) (2008) 427-36.
- [26] Q.Y. Zhang, M.S. Tan, J.T. Yu, L. Tan, The Role of Retromer in Alzheimer's Disease, *Mol Neurobiol* 53(6) (2016) 4201-4209.
- [27] J.T. Huse, D.S. Pijak, G.J. Leslie, V.M. Lee, R.W. Doms, Maturation and endosomal targeting of beta-site amyloid precursor protein-cleaving enzyme. The Alzheimer's disease beta-secretase, *J Biol Chem* 275(43) (2000) 33729-37.
- [28] A. Kinoshita, H. Fukumoto, T. Shah, C.M. Whelan, M.C. Irizarry, B.T. Hyman, Demonstration by FRET of BACE interaction with the amyloid precursor protein at the cell surface and in early endosomes, *J Cell Sci* 116(Pt 16) (2003) 3339-46.
- [29] R.W. Choy, Z. Cheng, R. Schekman, Amyloid precursor protein (APP) traffics from the cell surface via endosomes for amyloid beta (Abeta) production in the trans-Golgi network, *Proc Natl Acad Sci U S A* 109(30) (2012) E2077-82.
- [30] S. Gandy, O.d.C.e. Silva, E.d.C.e. Silva, T. Suzuki, M. Ehrlich, S. Small, Amyloid Precursor Protein Sorting and Processing: Transmitters, Hormones, and Protein Phosphorylation Mechanisms, *Intracellular Traffic and Neurodegenerative Disorders* (2008) 1-9.
- [31] J.C. Lambert, C.A. Ibrahim-Verbaas, D. Harold, A.C. Naj, R. Sims, C. Bellenguez, A.L. DeStafano, J.C. Bis, G.W. Beecham, B. Grenier-Boley, G. Russo, T.A. Thorton-Wells, N. Jones,

- A.V. Smith, V. Chouraki, C. Thomas, M.A. Ikram, D. Zelenika, B.N. Vardarajan, Y. Kamatani, C.F. Lin, A. Gerrish, H. Schmidt, B. Kunkle, M.L. Dunstan, A. Ruiz, M.T. Bihoreau, S.H. Choi, C. Reitz, F. Pasquier, C. Cruchaga, D. Craig, N. Amin, C. Berr, O.L. Lopez, P.L. De Jager, V. Deramecourt, J.A. Johnston, D. Evans, S. Lovestone, L. Letenneur, F.J. Moron, D.C. Rubinsztein, G. Eiriksdottir, K. Sleegers, A.M. Goate, N. Fievet, M.W. Huentelman, M. Gill, K. Brown, M.I. Kamboh, L. Keller, P. Barberger-Gateau, B. McGuiness, E.B. Larson, R. Green, A.J. Myers, C. Dufouil, S. Todd, D. Wallon, S. Love, E. Rogaeva, J. Gallacher, P. St George-Hyslop, J. Clarimon, A. Lleo, A. Bayer, D.W. Tsuang, L. Yu, M. Tsolaki, P. Bossu, G. Spalletta, P. Proitsi, J. Collinge, S. Sorbi, F. Sanchez-Garcia, N.C. Fox, J. Hardy, M.C. Deniz Naranjo, P. Bosco, R. Clarke, C. Brayne, D. Galimberti, M. Mancuso, F. Matthews, I. European Alzheimer's Disease, Genetic, D. Environmental Risk in Alzheimer's, C. Alzheimer's Disease Genetic, H. Cohorts for, E. Aging Research in Genomic, S. Moebus, P. Mecocci, M. Del Zompo, W. Maier, H. Hampel, A. Pilotto, M. Bullido, F. Panza, P. Caffarra, B. Nacmias, J.R. Gilbert, M. Mayhaus, L. Lannefelt, H. Hakonarson, S. Pichler, M.M. Carrasquillo, M. Ingelsson, D. Beekly, V. Alvarez, F. Zou, O. Valladares, S.G. Younkin, E. Coto, K.L. Hamilton-Nelson, W. Gu, C. Razquin, P. Pastor, I. Mateo, M.J. Owen, K.M. Faber, P.V. Jonsson, O. Combarros, M.C. O'Donovan, L.B. Cantwell, H. Soininen, D. Blacker, S. Mead, T.H. Mosley, Jr., D.A. Bennett, T.B. Harris, L. Fratiglioni, C. Holmes, R.F. de Bruin, P. Passmore, T.J. Montine, K. Bettens, J.I. Rotter, A. Brice, K. Morgan, T.M. Foroud, W.A. Kukull, D. Hannequin, J.F. Powell, M.A. Nalls, K. Ritchie, K.L. Lunetta, J.S. Kauwe, E. Boerwinkle, M. Riemenschneider, M. Boada, M. Hiltuenen, E.R. Martin, R. Schmidt, D. Rujescu, L.S. Wang, J.F. Dartigues, R. Mayeux, C. Tzourio, A. Hofman, M.M. Nothen, C. Graff, B.M. Psaty, L. Jones, J.L. Haines, P.A. Holmans, M. Lathrop, M.A. Pericak-Vance, L.J. Launer, L.A. Farrer, C.M. van Duijn, C. Van Broeckhoven, V. Moskvina, S. Seshadri, J. Williams, G.D. Schellenberg, P. Amouyel, Meta-analysis of 74,046 individuals identifies 11 new susceptibility loci for Alzheimer's disease, *Nat Genet* 45(12) (2013) 1452-8.
- [32] C.P. Sullivan, A.G. Jay, E.C. Stack, M. Pakaluk, E. Wadlinger, R.E. Fine, J.M. Wells, P.J. Morin, Retromer disruption promotes amyloidogenic APP processing, *Neurobiol Dis* 43(2) (2011) 338-45.
- [33] A. Muhammad, I. Flores, H. Zhang, R. Yu, A. Staniszewski, E. Planell, M. Herman, L. Ho, R. Kreber, L.S. Honig, B. Ganetzky, K. Duff, O. Arancio, S.A. Small, Retromer deficiency observed in Alzheimer's disease causes hippocampal dysfunction, neurodegeneration, and Abeta accumulation, *Proc Natl Acad Sci U S A* 105(20) (2008) 7327-32.
- [34] J.E. Young, L.K. Fong, H. Frankowski, G.A. Petsko, S.A. Small, L.S.B. Goldstein, Stabilizing the Retromer Complex in a Human Stem Cell Model of Alzheimer's Disease Reduces TAU Phosphorylation Independently of Amyloid Precursor Protein, *Stem Cell Reports* 10(3) (2018) 1046-1058.
- [35] P.G. Ridge, C.M. Karch, S. Hsu, I. Arano, C.C. Teerlink, M.T.W. Ebbert, J.D. Gonzalez Murcia, J.M. Farnham, A.R. Damato, M. Allen, X. Wang, O. Harari, V.M. Fernandez, R. Guerreiro, J. Bras, J. Hardy, R. Munger, M. Norton, C. Sassi, A. Singleton, S.G. Younkin, D.W. Dickson, T.E. Golde, N.D. Price, N. Ertekin-Taner, C. Cruchaga, A.M. Goate, C. Corcoran, J. Tschanz, L.A. Cannon-Albright, J.S.K. Kauwe, I. Alzheimer's Disease Neuroimaging, Linkage, whole genome sequence, and biological data implicate variants in RAB10 in Alzheimer's disease resilience, *Genome Med* 9(1) (2017) 100.
- [36] V. Udayar, V. Buggia-Prevot, R.L. Guerreiro, G. Siegel, N. Rambabu, A.L. Soohoo, M. Ponnusamy, B. Siegenthaler, J. Bali, Aesg, M. Simons, J. Ries, M.A. Puthenveedu, J. Hardy, G.

- Thinakaran, L. Rajendran, A paired RNAi and RabGAP overexpression screen identifies Rab11 as a regulator of beta-amyloid production, *Cell Rep* 5(6) (2013) 1536-51.
- [37] J. Nunez-Iglesias, C.C. Liu, T.E. Morgan, C.E. Finch, X.J. Zhou, Joint genome-wide profiling of miRNA and mRNA expression in Alzheimer's disease cortex reveals altered miRNA regulation, *PLoS One* 5(2) (2010) e8898.
- [38] I. Santa-Maria, M.E. Alaniz, N. Renwick, C. Cela, T.A. Fulga, D. Van Vactor, T. Tuschl, L.N. Clark, M.L. Shelanski, B.D. McCabe, J.F. Crary, Dysregulation of microRNA-219 promotes neurodegeneration through post-transcriptional regulation of tau, *J Clin Invest* 125(2) (2015) 681-6.
- [39] S.S. Hebert, W.X. Wang, Q. Zhu, P.T. Nelson, A study of small RNAs from cerebral neocortex of pathology-verified Alzheimer's disease, dementia with lewy bodies, hippocampal sclerosis, frontotemporal lobar dementia, and non-demented human controls, *J Alzheimers Dis* 35(2) (2013) 335-48.
- [40] P. Lau, K. Bossers, R. Janky, E. Salta, C.S. Frigerio, S. Barbash, R. Rothman, A.S. Sierksma, A. Thathiah, D. Greenberg, A.S. Papadopoulou, T. Achsel, T. Ayoubi, H. Soreq, J. Verhaagen, D.F. Swaab, S. Aerts, B. De Strooper, Alteration of the microRNA network during the progression of Alzheimer's disease, *EMBO Mol Med* 5(10) (2013) 1613-34.
- [41] M. Steger, F. Tonelli, G. Ito, P. Davies, M. Trost, M. Vetter, S. Wachter, E. Lorentzen, G. Duddy, S. Wilson, M.A. Baptista, B.K. Fiske, M.J. Fell, J.A. Morrow, A.D. Reith, D.R. Alessi, M. Mann, Phosphoproteomics reveals that Parkinson's disease kinase LRRK2 regulates a subset of Rab GTPases, *Elife* 5 (2016).
- [42] R. Maoz, B.P. Garfinkel, H. Soreq, Alzheimer's Disease and ncRNAs, *Adv Exp Med Biol* 978 (2017) 337-361.
- [43] Y. Zhang, Y. Zhao, X. Ao, W. Yu, L. Zhang, Y. Wang, W. Chang, The Role of Non-coding RNAs in Alzheimer's Disease: From Regulated Mechanism to Therapeutic Targets and Diagnostic Biomarkers, *Front Aging Neurosci* 13 (2021) 654978.
- [44] S.S. Hebert, K. Horre, L. Nicolai, A.S. Papadopoulou, W. Mandemakers, A.N. Silahtaroglu, S. Kauppinen, A. Delacourte, B. De Strooper, Loss of microRNA cluster miR-29a/b-1 in sporadic Alzheimer's disease correlates with increased BACE1/beta-secretase expression, *Proc Natl Acad Sci U S A* 105(17) (2008) 6415-20.
- [45] M. Wang, L. Qin, B. Tang, MicroRNAs in Alzheimer's Disease, *Front Genet* 10 (2019) 153.
- [46] C. Liu, F. Zhang, T. Li, M. Lu, L. Wang, W. Yue, D. Zhang, MirSNP, a database of polymorphisms altering miRNA target sites, identifies miRNA-related SNPs in GWAS SNPs and eQTLs, *BMC Genomics* 13 (2012) 661.
- [47] D. Betel, A. Koppal, P. Agius, C. Sander, C. Leslie, Comprehensive modeling of microRNA targets predicts functional non-conserved and non-canonical sites, *Genome Biol* 11(8) (2010) R90.
- [48] B. Frost, Alzheimer's disease: An acquired neurodegenerative laminopathy, *Nucleus* 7(3) (2016) 275-83.
- [49] C. Delay, F. Calon, P. Mathews, S.S. Hebert, Alzheimer-specific variants in the 3'UTR of Amyloid precursor protein affect microRNA function, *Mol Neurodegener* 6 (2011) 70.
- [50] Y. Zhao, W. Tan, W. Sheng, X. Li, Identification of Biomarkers Associated With Alzheimer's Disease by Bioinformatics Analysis, *Am J Alzheimers Dis Other Demen* 31(2) (2016) 163-8.
- [51] C. Mayr, What Are 3' UTRs Doing?, *Cold Spring Harb Perspect Biol* 11(10) (2019).

- [52] T. Jonsson, J.K. Atwal, S. Steinberg, J. Snaedal, P.V. Jonsson, S. Bjornsson, H. Stefansson, P. Sulem, D. Gudbjartsson, J. Maloney, K. Hoyte, A. Gustafson, Y. Liu, Y. Lu, T. Bhangale, R.R. Graham, J. Huttenlocher, G. Bjornsdottir, O.A. Andreassen, E.G. Jonsson, A. Palotie, T.W. Behrens, O.T. Magnusson, A. Kong, U. Thorsteinsdottir, R.J. Watts, K. Stefansson, A mutation in APP protects against Alzheimer's disease and age-related cognitive decline, *Nature* 488(7409) (2012) 96-9.
- [53] J. Hardy, D.J. Selkoe, The amyloid hypothesis of Alzheimer's disease: progress and problems on the road to therapeutics, *Science* 297(5580) (2002) 353-6.
- [54] W.M. Pardridge, The blood-brain barrier: bottleneck in brain drug development, *NeuroRx* 2(1) (2005) 3-14.
- [55] J.K. Atwal, Y. Chen, C. Chiu, D.L. Mortensen, W.J. Meilandt, Y. Liu, C.E. Heise, K. Hoyte, W. Luk, Y. Lu, K. Peng, P. Wu, L. Rouge, Y. Zhang, R.A. Lazarus, K. Scearce-Levie, W. Wang, Y. Wu, M. Tessier-Lavigne, R.J. Watts, A therapeutic antibody targeting BACE1 inhibits amyloid-beta production in vivo, *Sci Transl Med* 3(84) (2011) 84ra43.
- [56] Y.J. Yu, Y. Zhang, M. Kenrick, K. Hoyte, W. Luk, Y. Lu, J. Atwal, J.M. Elliott, S. Prabhu, R.J. Watts, M.S. Dennis, Boosting brain uptake of a therapeutic antibody by reducing its affinity for a transcytosis target, *Sci Transl Med* 3(84) (2011) 84ra44.
- [57] J.A. Phillips, S.J. Craig, D. Bayley, R.A. Christian, R. Geary, P.L. Nicklin, Pharmacokinetics, metabolism, and elimination of a 20-mer phosphorothioate oligodeoxynucleotide (CGP 69846A) after intravenous and subcutaneous administration, *Biochem Pharmacol* 54(6) (1997) 657-68.
- [58] F. Rigo, S.J. Chun, D.A. Norris, G. Hung, S. Lee, J. Matson, R.A. Fey, H. Gaus, Y. Hua, J.S. Grundy, A.R. Krainer, S.P. Henry, C.F. Bennett, Pharmacology of a central nervous system delivered 2'-O-methoxyethyl-modified survival of motor neuron splicing oligonucleotide in mice and nonhuman primates, *J Pharmacol Exp Ther* 350(1) (2014) 46-55.
- [59] J.B. Gibbs, A. Oliff, N.E. Kohl, Farnesyltransferase inhibitors: Ras research yields a potential cancer therapeutic, *Cell* 77(2) (1994) 175-8.
- [60] P.M. Cromm, J. Spiegel, T.N. Grossmann, H. Waldmann, Direct Modulation of Small GTPase Activity and Function, *Angew Chem Int Ed Engl* 54(46) (2015) 13516-37.
- [61] J.M. Reichert, Antibodies to watch in 2017, *MAbs* 9(2) (2017) 167-181.
- [62] S.L. DeVos, T.M. Miller, Antisense oligonucleotides: treating neurodegeneration at the level of RNA, *Neurotherapeutics* 10(3) (2013) 486-97.
- [63] M.A. Passini, J. Bu, A.M. Richards, C. Kinnecom, S.P. Sardi, L.M. Stanek, Y. Hua, F. Rigo, J. Matson, G. Hung, E.M. Kaye, L.S. Shihabuddin, A.R. Krainer, C.F. Bennett, S.H. Cheng, Antisense oligonucleotides delivered to the mouse CNS ameliorate symptoms of severe spinal muscular atrophy, *Sci Transl Med* 3(72) (2011) 72ra18.
- [64] A.L. Southwell, H.B. Kordasiewicz, D. Langbehn, N.H. Skotte, M.P. Parsons, E.B. Villanueva, N.S. Caron, M.E. Ostergaard, L.M. Anderson, Y. Xie, L.D. Cengio, H. Findlay-Black, C.N. Doty, B. Fitzsimmons, E.E. Swayze, P.P. Seth, L.A. Raymond, C. Frank Bennett, M.R. Hayden, Huntingtin suppression restores cognitive function in a mouse model of Huntington's disease, *Sci Transl Med* 10(461) (2018).

**Chapter 4: Phospholipase D3 contributes to  
Alzheimer's disease risk via disruption of A $\beta$   
clearance and microglia response to amyloid  
plaques**

## 4.1 Abstract

Alzheimer's disease (AD) is characterized by the accumulation of amyloid- $\beta$  (A $\beta$ ) plaques and neurofibrillary tangles in the brain. AD is also the result of complex genetic architecture that can be leveraged to understand pathways central to disease processes. We have previously identified coding variants in the *phospholipase D3* (*PLD3*) gene that double the late-onset AD risk. However, the mechanism by which *PLD3* impacts AD risk is unknown. One AD risk variant, *PLD3* p.A442A, disrupts a splicing enhancer-binding site and reduces *PLD3* splicing in human brains. Using differentiated induced pluripotent stem cells from a *PLD3* p.A442A carrier and CRISPR-reverted, isogenic control, we show that *PLD3* p.A442A cortical neurons exhibit a *PLD3* splicing defect and a significant increase in A $\beta$ 42 and A $\beta$ 40, both of which are corrected upon reversion of the risk allele in isogenic control neurons. Thus, *PLD3* p.A442A is sufficient to alter *PLD3* splicing and A $\beta$  metabolism. While the normal function of *PLD3* is poorly understood, *PLD3* is highly expressed in neurons and brain regions most susceptible to amyloid pathology. *PLD3* expression is significantly lower in AD brains than controls, suggesting that *PLD3* may play a role in sporadic AD. Thus, we sought to determine whether *PLD3* contributes to A $\beta$  accumulation in AD. In a mouse model of amyloid accumulation, loss of *Pld3* increases interstitial fluid (ISF) A $\beta$  and reduces A $\beta$  turnover. AAV-mediated overexpression of *PLD3* in the hippocampus decreased ISF A $\beta$  levels and accelerated A $\beta$  turnover. To determine whether *PLD3*-mediated reduction of ISF A $\beta$  impacts amyloid accumulation, we measured amyloid plaque abundance and size after significant A $\beta$  deposition. We found that in the absence of *Pld3*, amyloid plaques were less compact and more diffuse. Additionally, we observed reduced recruitment of microglia to amyloid plaques in the absence of

*Pld3*. PLD3 may impact amyloid accumulation and AD risk through disrupted microglia function as *PLD3* is enriched in disease associated microglia in human brains. Together, our findings demonstrate that PLD3 regulates A $\beta$  clearance through cell-autonomous and non-cell-autonomous pathways in a manner that likely contributes to AD risk.

## 4.2 Introduction

Alzheimer's disease (AD) is pathologically defined by neuronal loss and the accumulation of amyloid- $\beta$  (A $\beta$ ) plaques and neurofibrillary tangles in the brain. Genetic, biochemical, and neuropathologic data suggest that A $\beta$  aggregation is central to initiating AD pathogenesis [1]. Rare mutations in *APP*, *PSEN1*, and *PSEN2* cause dominantly inherited AD. Late-onset AD (LOAD) also has a strong genetic component [2]. Identifying novel loci that affect LOAD risk is critical to our understanding of the underlying etiology of AD and novel therapeutic pathways.

The genetic architecture that underlies LOAD is complex [2]. Large-scale genomic studies have led to the identification of novel genes and risk loci that contribute to AD [2, 3]. Whole exome sequencing of densely affected LOAD families has revealed a rare genetic variant within *PLD3* (p.V232M) that perfectly segregated with disease in two independent families and doubled AD risk in seven independent case-control series (4,998 AD cases/6,356 controls; OR=2.10, p=2.93 $\times$ 10 $^{-5}$ ) [4]. Gene-based analyses indicated that multiple variants in *PLD3* increase AD risk in European (EA) and African American (AA) populations (e.g.: p.M6R, p.V232M, p.A442A; EA: OR=2.75, p=1.44 $\times$ 10 $^{-11}$ ; AA: OR=5.48, p=1.40 $\times$ 10 $^{-3}$ ) [4].

*PLD3* is a non-classical member of the phospholipase D (PLD) family of enzymes, with no known function [5-7]. *PLD3* is expressed in pyramidal neurons within the brain, and in AD brains, *PLD3* co-localizes with amyloid plaques [8, 9]. Common variants in *PLD3* are associated with CSF A $\beta$  levels, an AD biomarker [10]. *In vitro*, *PLD3* expression is correlated with extracellular A $\beta$  levels: *Pld3* silencing is associated with increased A $\beta$  levels, and *PLD3*

overexpression is associated with reduced A $\beta$  levels [4]. Thus, PLD3 may play a broader role in LOAD.

Here, we sought to define the contribution of *PLD3* risk variants to AD-related phenotypes in human stem cell models and the role of PLD3 in amyloid pathology in mouse models. We found that a *PLD3* risk variant is sufficient to increase A $\beta$  levels in stem cell-derived neurons. In animal models of amyloid accumulation, *Pld3* silencing reduces A $\beta$  turnover and alters the composition of amyloid plaques. In the absence of *Pld3*, microglia recruitment to plaques is attenuated. Together, this study suggests that PLD3 contributes AD pathogenesis via A $\beta$  clearance through cell-autonomous and non-cell-autonomous pathways.

### **4.3 Materials and Methods**

#### *Patient Consent*

Skin biopsies were collected following written informed consent from the donor. The Washington University School of Medicine Institutional Review Board and Ethics Committee approved the informed consent (IRB 201104178, 201306108). The consent allows for the use of tissue by all parties, commercial and academic, for research but not for human therapy.

#### *Dermal Fibroblast Isolation*

Dermal fibroblasts were isolated from skin biopsies obtained from the Knight Alzheimer Disease Research Center (ADRC) research participants. Briefly, skin biopsies were collected by surgical punch and stored in Fibroblast Growth Media (Lonza). To isolate dermal fibroblasts from a skin biopsy, the biopsies were rinsed with PBS and cut lengthwise with dissecting scissors. The resulting tissue sections were then plated into a dry 24-well tissue culture-treated

plate (approximately 6-12 sections). After removing excess PBS from the wells, 300ul of fibroblast growth media (Lonza) was carefully added and tissue was incubated at 37°C and 5% CO<sub>2</sub>. After 24 hours, tissue was supplemented with 1mL fibroblast growth media and media changes were repeated every 3-4 days. Fibroblast cells migrated from the tissue within two weeks of culture. Dermal fibroblasts were maintained in fibroblast growth media (Lonza) supplemented with penicillin/streptomycin.

### *iPSC Generation, Characterization, and Maintenance*

Human fibroblasts (F13504) were transduced with non-integrating Sendai virus carrying the four factors required for reprogramming: OCT3/4, SOX2, KLF4, and cMYC [11, 12]. Cells showing morphological evidence of reprogramming were selected by manual dissection.

Human iPSCs were cultured using feeder-free conditions (Matrigel, BD Biosciences, Franklin Lakes, NJ, USA). Human iPSCs were thawed (1-2 x 10<sup>6</sup> cells/mL), diluted in DMEM/F12, and centrifuged at 750 rpm for 3 minutes. The resulting iPSC pellet was then diluted in mTeSR1 supplemented with Rock inhibitor (Y-27632; 10µM final). iPSC were subsequently cultured in 37°C, 5% CO<sub>2</sub> with daily medium changes (mTesR1, STEMCELL Technologies, Vancouver, BC, CA).

All iPSC lines were characterized using standard methods [11]. Each line was analyzed for pluripotency markers (OCT4A, SOX2, SSEA4, TRA1-80) by immunocytochemistry (ICC) (Invitrogen A24881) and quantitative PCR (qPCR); for chromosomal abnormalities by karyotyping; and for *PLD3* variant status by Sanger sequencing (Supplemental Figure 4.1).

### *Genome editing*

We used CRISPR/Cas9 to generate isogenic control lines for the *PLD3* p.A442A iPSC as previously described [13]. The p3s-Cas9HC Cas9 expression plasmid (Addgene 43945) and CRISPR reagents (Addgene plasmid 43860) were used [14]. Guide RNAs were designed to overlap with the allele to be modified and have at least 3bp of mismatch to any other gene in the human genome. The activity of the guide was validated using a mismatch detection assay to determine non-homologous end-joining efficiency in K562 cells. A correctly edited clone and an unmodified clone were identified, expanded and characterized as described above for karyotyping and pluripotency markers. Sanger sequencing was performed for the on-target and predicted off-target sites.

### *Cortical neuron differentiation*

iPSCs were differentiated into neuronal cells using a two-step approach as previously described [13]. iPSCs were plated at a density of 65,000 cells per well in neural induction media (STEMCELL Technologies) in a 96-well v-bottom plate to form highly uniform neural aggregates and, after five days, transferred onto culture plates. The resulting neural rosettes were then isolated by enzymatic selection (Neural Rosette Selection Reagent; STEMCELL Technologies) and cultured as neural progenitor cells (NPCs). NPCs were differentiated in planar culture in neuronal maturation medium (neurobasal medium supplemented with B27, GDNF, BDNF, cAMP). Neurons typically arise within one week after plating, identified using immunocytochemistry for β-tubulin III (Tuj1). The cells continued to mature and were analyzed at six weeks.

### *Immunocytochemistry*

IPSC-derived neurons were grown on PLO/laminin-coated 8-well chamber slides (Millipore). Culture media was aspirated, and cells were then washed and fixed with 4% paraformaldehyde (Sigma). After several washes, cells were permeabilized with 0.1% Triton X-100 in PBS. Cells were then blocked in 0.1% bovine serum albumin (BSA; Sigma) and treated with primary (Tuj1) and secondary antibodies diluted in 0.1% BSA. Immunostained cells were then imaged (Nikon Eclipse 80i fluorescent microscope).

### *Transcriptomics and Digital Deconvolution*

RNA was extracted from iPSC-derived neurons from *PLD3* p.A442A vs. the isogenic controls using Tissue Lyser LT and RNeasy Mini Kit (Qiagen, Hilden, Germany). RNA-seq paired-end reads with read lengths of 2 × 150 bp were generated using Illumina HiSeq 4000 with a mean coverage of 80 million reads per sample. FastQC was applied to perform quality control and aligned to human GRCh37 primary assembly using Star (ver 2.5.2b). We applied Salmon transcript expression quantification (ver 0.7.2) to infer the gene expression. To estimate the relative proportion of major brain cell types in the dish, digital deconvolution was performed as previously described using a reference marker panel [15].

### *PLD3 Splicing Assay*

RNA was extracted from cell lysates with an Rneasy kit (Qiagen) according to the manufacturer's protocol. Extracted RNA (10ug) was converted to cDNA by PCR using the High-Capacity cDNA Reverse Transcriptase kit (ABI). SYBR-green primers were designed using Primer Express software, Version 3 (ABI). Real-time PCR assays were used to quantify *PLD3* exon 7 (forward primer: GCAGCTCCATCCCATCAACT; reverse: CTTGGTTGTAGCGGGTGTCA), exon 8 (forward primer: CTCAACGTGGTGGACAATGC;

reverse: AGTGGGCAGGTAGTCATGACA), exon 9 (forward primer: ACGAGCGTGGCGTCAAG; reverse: CATGGATGGCTCCGAGTGT), exon 10 (forward primer: GGTCCCCGCGGATGA; reverse: GGTTGACACGGGCATATGG) and exon 11 (forward primer: GCTGCTGGTGACGCAGAAT; reverse: AGTCCCAGTCCCTCAGGAAAA). Each qPCR analysis included technical replicates and biological triplicates. Real-time data were analyzed using the comparative Ct method. Only samples with a standard error of <15% were analyzed. The Ct values for exon 11 were normalized with the Ct value for exons 7-10. The relative exon 11 levels for the iPSC-derived neurons from *PLD3* p.A442A vs. the isogenic control were compared using a Tukey's t-test.

### *A $\beta$ Measurements*

Conditioned medium was collected from neurons after six weeks in culture and centrifuged at 3,000xg at 4°C for 10 minutes to remove cell debris. The levels of A $\beta$ 42 and A $\beta$ 40 were measured in cell culture media by sandwich ELISA as described by the manufacturer (Life Technologies). To account for variability in transfection efficiency between experiments, ELISA values were obtained (pg/mL) and corrected for total intracellular protein (ug/mL). Statistical difference was measured using an unpaired Student's t-test.

### *PLD3 expression in AD and neuropathology free human brains*

Laser microdissected neurons from AD and control brains were previously reported and deposited as GSE5281 [38]. Brain samples were analyzed from 47 individuals of European descent clinically and neuropathologically confirmed AD cases or controls. The 33 AD samples were 54.5% female with a mean age of 79.9 years (range 73–86.8) and an average postmortem interval (PMI) of 2.5 hours. The 14 control brains were 28.6% female with a mean age of 79.8

years (range 70.1–88.9). Samples were obtained from the entorhinal cortex, hippocampus, medial temporal gyrus, posterior cingulate, superior frontal gyrus, and primary visual cortex. RNA expression was measured using an Affymetrix GeneChip for gene expression. The log-transformed expression values were analyzed with brain region, age, and sex as covariates to analyze RNA expression.

Gene expression was analyzed in a second, independent, publicly available dataset of the temporal cortex of 76 control and 80 AD brains (syn6090813). Differential gene expression comparing controls v. AD was performed using a “Simple Model”, multi-variable linear regression analyses were conducted in R, using normalized gene expression measures including sex, age-at-death, RNA integrity number, brain tissue source, and flowcell as covariates [16]. Statistical difference was measured using an unpaired Student’s t-test.

### *Single nuclei RNAseq in human brains*

Human parietal cortices were processed to isolate nuclei, and the nuclei were then sequenced using the 10X Chromium single cell Reagent Kit v3, with 10,000 cells per sample and 50,000 reads per cell for each of the 74 samples as previously described [17, 18]. The CellRanger (v3.0.2 10Xgenomics) software was used to align the sequences and quantify gene expression. We used the GRCh38 (3.0.0) reference to prepare a pre-mRNA reference. Filtering and QC were done using the Seurat package (3.0.1) on each subject individually. After the Uniform Manifold Approximation and Projection (UMAP) analysis was performed with the top 14 PCs, we then used Seurat *FindNeighbors* and *FindClusters* functions to identify unique cell states or subclusters. Samples included in the subsequent analyses are summarized in Supplemental Table 4.1. To identify associations between cell-type transcriptional state and

disease status or genetic strata (control, sporadic AD (sAD), TREM2), we applied linear regression models to test the cell state compositions of each subject. The proportions were normalized using a cube root transformation and were corrected by sex and age of death. Differentially expressed genes among the individual cell states were identified using a linear mixed model that corrected for sex and subject. To determine if there was unique functionality or potentially altered expression levels associated with disease/genetic carriers in the alternative cell states, we employed linear mixed model that predicted the expression level of each gene, modeled as zero-inflated negative binomial distributions and corrected for sex and age of death. Donors were modeled as random variables as previously described [17]. Data can be publicly accessed at <http://ngi.pub/SNARE>.

### *Mouse Models*

Animal care and surgical procedures were approved by the Animal Studies Committee of Washington University School of Medicine in accordance with guidelines of the United States National Institutes of Health. APPswe/PS1 $\Delta$ E9 transgenic mice (APP/PS1; The Jackson Laboratory; 034829) [19] of both sexes were used in this study. APP/PS1 mice were maintained on a C57Bl6;C3B6 mixed background.

*Pld3-KO* mice were generated using CRISPR/Cas9 technology. gRNAs were designed to target an early conserved exon (mPld3.g19; TGCTGTGAGCACCGCAAGGNGG). Guide activity was assessed in mouse neuroblastoma cells (N2A) using a T7E1 mismatch detection assay as previously described [13]. RNA was injected into the pronuclei of fertilized, viable murine oocytes isolated from a set of C57Bl/6xCBA (hybrid) female mice. Founders were identified using mPLD3 screening primers SM406.Cel.F 5' CATGGGCACTGTATCCCATCT

3' and SM406.Cel.R 5' AGGACACAAAAACGTCACCCCT 3', which generated a parental band (575bp) and fragments (307 and 268bp). Subsequent generations were backcrossed to C57Bl/6;C3B6 (Supplemental Figure 4.2).

APP/PS1 mice were crossed with the *Pld3*-KO mice to generate APP/PS1x*Pld3*<sup>+/−</sup>. APP/PS1x*Pld3*<sup>+/−</sup> were crossed to obtain APP/PS1x*Pld3*-KO (APP/PS1x*Pld3*<sup>−/−</sup>) mice and APP/PS1x*Pld3*-WT (APP/PS1x*Pld3*<sup>+/+</sup>) littermates. Animals of both sexes were used in the study.

### *Intracranial AAV-mediated expression of PLD3 and shPLD3*

Adeno-associated virus (AAV8) particles were generated that express AAV-CMV-hPLD3-WT-GFP, AAV-CMV-GFP (control), AAV-U6-shPLD3-GFP, and AAV-U6-shScrambled-GFP (control). Viral particles were injected into the hippocampus of APP/PS1 mice of both sexes to produce widespread transduction in hippocampal neurons as previously described [20, 21]. Two uL of AAV particles ( $1.5 \times 10^{12}$  vg/ml) were stereotactically injected bilaterally hippocampi (2μl over 10 minutes) in 3-month-old APP/PS1 transgenic mice (prior to plaque appearance) [22, 23]. Virus is detectable at least 4-5 months post-injection [21, 24].

### *In Vivo Microdialysis*

Prior to plaque accumulation (5 months of age) and two months post AAV8-injection, hippocampal ISF Aβ levels were quantified using microdialysis in APP/PS1 mice as previously described [25, 26]. The use of a 38-kDa MWCO semi-permeable membrane allows for molecules smaller than this cut-off to diffuse into the probe. The probe was flushed with perfusion buffer at a constant rate (1.0μl/minute) and collected into a refrigerated fraction

collector, and then assayed by sandwich ELISA ( $A\beta_{x-40}$ ). A mouse monoclonal anti- $A\beta_{40}$  capture antibody (mHJ2) made in-house was used in conjunction with a biotinylated central domain detection antibody (mHJ5.1) and streptavidin-poly-HRP-40 (Fitzgerald Industries, Acton, MA)[27]. During microdialysis, mice were housed in cages that permit free movement and ad-libitum food/water, while ISF  $A\beta$  was sampled. Baseline levels of ISF  $A\beta$  were sampled every 60 minutes between hours 5-12 (after the microdialysis probe insertion) and averaged to determine the baseline ISF  $A\beta$  levels in each mouse. At hour 12, mice were administered the  $\gamma$ -secretase inhibitor Compound E (20mg/kg), intraperitoneally, which enabled us to determine the elimination half-life of ISF  $A\beta$  [28].  $A\beta$  half-life was calculated using first-order kinetics. Microdialysis was performed with sham and littermate controls. Statistical difference was measured using an unpaired Student's t-test.

To evaluate the impact of *Pld3* on  $A\beta$  kinetics, APP/PS1x*Pld3*-WT and APP/PS1x*Pld3*-KO mice were implanted at one-month post-injection with a microdialysis probe with a 38-kDa MWCO probe, and ISF was collected as described above. After 12 hours,  $\gamma$ -secretase inhibitor LY411575 (3mg/kg in 50:50PBS:PEG400) was administered intraperitoneally to define the elimination half-life of ISF  $A\beta$ .  $A\beta$  half-life was calculated as described above. Microdialysis was performed with sham and littermate controls. Statistical difference was measured using an unpaired Student's t-test.

### *Brain Tissue Preparation*

APP/PS1x*Pld3*-WT and APP/PS1x*Pld3*-KO mice were anesthetized with sodium pentobarbital and perfused with 0.3% heparin in PBS at nine months of age. Brains were dissected and cut into two hemispheres. The right hemisphere was snap-frozen on dry ice and

stored at 80°C for biochemical analyses. The left hemisphere was fixed in 4% paraformaldehyde for 24 hours, followed by 30% sucrose in PBS at 4°C. Coronal sections (50 µm) were cut on a freezing-sliding microtome. Collected slices were stored in cryoprotectant solution (0.2 M phosphate-buffered saline, 30% sucrose, and 30% ethylene glycol) at -20°C.

### *Immunohistochemistry*

APP/PS1x*Pld3*-WT and APP/PS1x*Pld3*-KO brains were cut into 50µm sections from the rostral anterior commissure to the caudal hippocampus. Brains sections (n=20 mice per group) were incubated in 0.3% H<sub>2</sub>O<sub>2</sub> in Tris-buffered saline (TBS) for 10 minutes and blocked in 3% milk in TBS-X for 30 minutes. Tissue was incubated in HJ3.4B antibody (anti-Aβ-1-13; 2.4 µg/ml; a generous gift from the Holtzman lab) overnight [29]. Sections are then incubated in Vectastain ABC elite solution in TBS (1:400) for 1 hour before incubating in 3,3'-Diaminobenzidine (DAB) solution. Sections were then mounted onto slides with Cytoseal (Thermo Scientific 8312-4). A Nanozoomer Digital Scanner (Hamamatsu Photonics) was used to create high-resolution digital images for the HJ3.4-stained brain slices. Total plaque coverage, total plaque count, and average plaque size were analyzed using NIH ImageJ software. Total plaque coverage was expressed as a percentage of the total area for each slice and averaged across the three slices per animal. Plaque count was expressed as the plaque count per nm<sup>2</sup> averaged across the three slices per animal. Plaque size was expressed in µm<sup>2</sup> averaged across all three slices for each mouse. Both the hippocampus and cortex were analyzed separately for each slice. Statistical difference for plaque size, percentage of total area, and plaque count per square millimeter was measured using an unpaired Student's t-test.

### *X-34 Plaque Staining*

To evaluate X-34 positive plaque burden, frozen coronal brain sections (50 µm) were mounted on Superfrost Plus slides, permeabilized with 0.25% Triton X-100 in PBS for 30 minutes and stained with X-34 (0.01mM; Sigma SML1954) dissolved in 40% ethanol in PBS, pH 10 for 20 min. The tissue was then washed with 40% ethanol in PBS and mounted with Fluoromount G mounting medium. Slides were imaged using Cytaion7 (BioTek) and quantified using NIH ImageJ software. A Cytaion7 cell imaging multi-modal imager was used to create high-resolution images of the X-34 scanned brain sections. Total plaque coverage, total plaque count, and average plaque size were analyzed using NIH ImageJ software. Total plaque coverage was expressed as a percentage of the total area for each section and averaged across three sections per animal. Plaque count was expressed as the plaque count per square millimeter averaged across the three sections per animal. Plaque size was expressed in square microns averaged across all three sections for each mouse. Both the hippocampus and cortex were analyzed separately for each section. Statistical difference for plaque size, percentage of total area, and plaque count per square millimeter was measured using an unpaired Student's t-test.

### *Immunofluorescence*

Coronal brain sections (50µm) were permeabilized in 0.25% Triton X-100 for 30 min at room temperature. Slices were then stained with X-34 (0.001 mM; Sigma SML1954) dissolved in 40% ethanol in PBS for 20 min and blocked in 3% BSA/3% Normal Donkey serum in 0.1% Triton X-100 in PBS. X-34-stained samples were immunostained with antibodies HJ3.4 (2.4ug/mL;  $\alpha$ -A $\beta$ 1-13) or Iba1 (Abcam ab5076) and CD68 (BioRad MCA1957) at 4°C overnight. Three slices per animal were stained. Secondary antibodies of Alexa Fluor 488-conjugated donkey anti-rat IgG, Alexa Fluor 647-conjugated donkey anti-goat, and Alexa Fluor 647 donkey anti-mouse (Invitrogen). Slides were mounted with Fluoromount G mounting media.

High resolution 40x images were obtained using the Zeiss LSM 880 Confocal microscope with Airyscan. Z-stacks were analyzed using NIH ImageJ software, where max projection images (those with the highest signal intensity) were selected for each fluorescent channel. The Iba1 and CD68 signals were quantified within 15 $\mu$ m of the X-34-positive plaques. Iba1 and CD68 colocalization was also quantified. An outlier analysis was run using the ROUT method with a Q-value of 1%. Three outliers were removed from the APP/PS1x*Pld3*-KO mice in the Iba1 analysis. Statistical difference was measured using an unpaired Student's t-test.

To quantify HJ3.4 and X-34 colocalization, Z-stacks were analyzed using NIH ImageJ software, where max projection images were selected for each fluorescent channel. Plaque composition was quantified by measuring the percentage of HJ3.4 staining within X-34-positive areas. Nonfibrillar plaque area was normalized to the total X-34 area. A ROUT outlier analysis with a Q-value of 1% was run for each of these quantifications. No outliers were removed from the analysis of percent area. Four outliers were excluded in the APP/PS1x*Pld3*-WT mice, and three outliers were excluded in the APP/PS1x*Pld3*-KO mice in the nonfibrillar plaque area analysis. Statistical difference was measured using an unpaired Student's t-test.

#### **4.4 Results**

*AD risk variant PLD3 p.A442A is sufficient to alter PLD3 splicing and A $\beta$  levels*

Three highly conserved, rare variants in *PLD3* increase AD risk: p.M6R, p.V232M, and p.A442A [4]. *PLD3* p.A442A (G>A) was associated with increased AD risk in four independent case-control datasets ( $p=3.78\times 10^{-7}$ ; OR=2.12) [4]. *PLD3* p.A442A was predicted to modify a splicing enhancer-binding site, SRSF1, *in silico* [4]. In the brains of *PLD3* p.A442A carriers,

total *PLD3* and exon 11-containing transcript expression were reduced compared to controls [4]. However, these association studies did not allow us to attribute the causality of the risk variant to the phenotype.

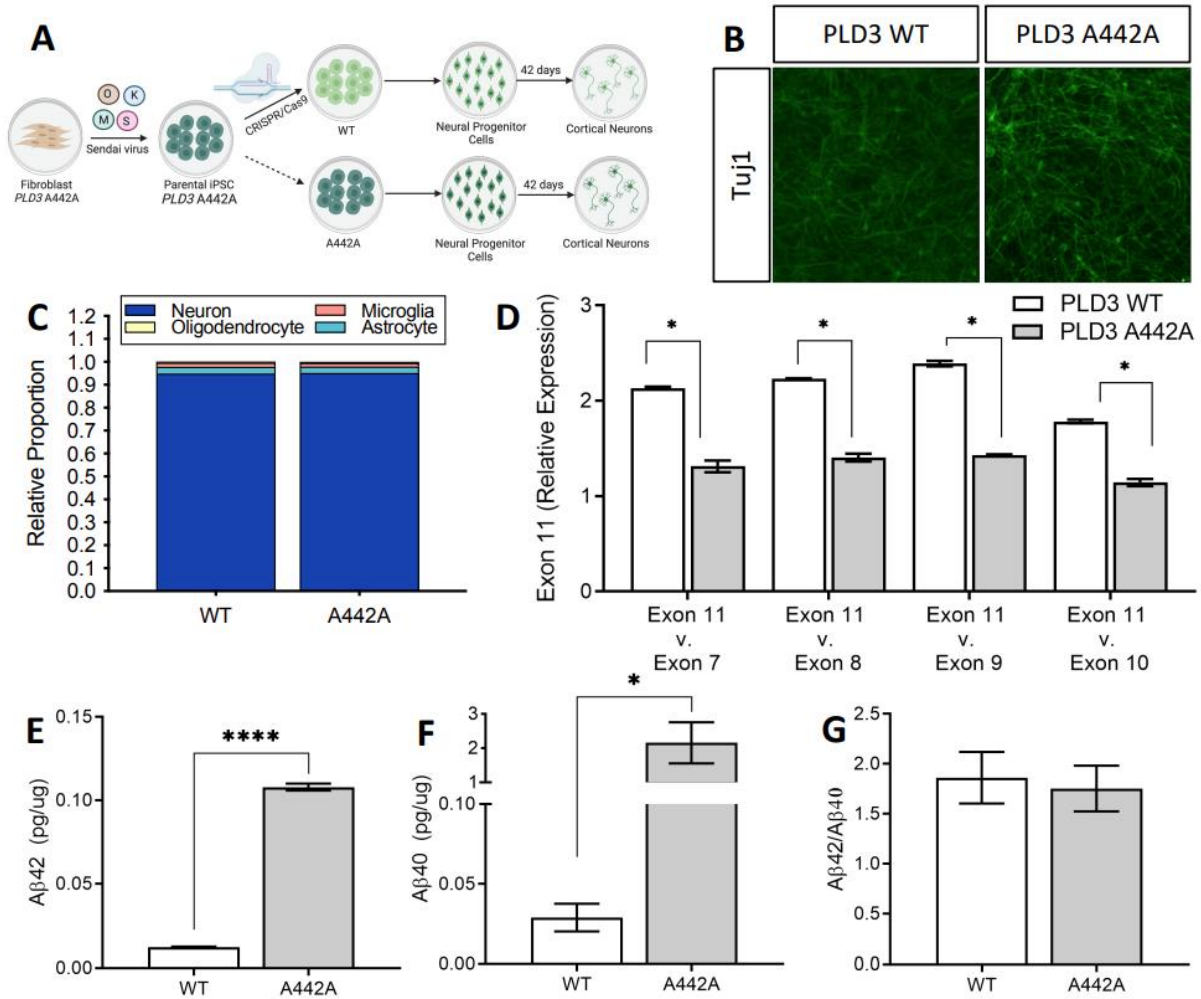


**Figure 4.1: iPSC-neurons expressing *PLD3* p.A442A phenocopy splicing defects observed in human brains A.**

Fibroblasts from a *PLD3* p.A442A variant carrier were reprogrammed into induced pluripotent stem cells (iPSCs). CRISPR-Cas9 technology was used to generate an isogenic control line. iPSCs were then differentiated into cortical neurons (see Methods). Downstream assays were performed after 42 days in culture. B. iPSC-derived neurons stained with Tuj1 illustrate a similar capacity of p.A442A and isogenic controls (*PLD3* WT) to form neurons. C.

Digital deconvolution of iPSC-derived neurons from transcriptomic data illustrates a similar enrichment of neurons in *PLD3* p.A442A and isogenic controls (*PLD3* WT). D. Expression of *PLD3* exon 11 compared to *PLD3* exons 7, 8, 9, and 10. E-G. Sandwich ELISA of media from iPSC-derived neurons (pg/mL) and corrected for total protein measured by BCA (pg/μg). Aβ42 (E), Aβ40 (F), Aβ42/40 (G). Graphs represent mean ± SEM. \* $<0.05$ , \*\*\* $<0.00005$ . Analyzed by two-tailed Student's *t* test.

Here, we coupled genome-editing with stem cell models to determine whether *PLD3* p.A442A is sufficient to alter *PLD3* splicing and phenocopy AD-related phenotypes. Primary dermal fibroblasts were obtained from a patient carrying a single copy of the *PLD3* p.A442A variant. Fibroblasts were de-differentiated into induced pluripotent stem cells using non-integrating Sendai virus. The resulting iPSC were characterized for pluripotency markers, the presence of the *PLD3* p.A442A variant, and chromosomal integrity (Supplemental Figure 4.1). To determine the causality of *PLD3* p.A442A on AD-related phenotypes, we used CRISPR/Cas9 to correct the A allele to G (wild-type) (Figure 4.1A) [13]. *PLD3* p.A442A and isogenic controls (*PLD3* WT) were then differentiated into cortical neurons using a growth factor-mediated approach as previously described (Figure 4.1A) [13], where they illustrated a similar capacity to form Tuj1-positive neurons (Figure 4.1B). To further verify the similarity between the cells in their capacity to form neurons, we estimated the relative proportion of neurons in the cultures using bulk transcriptomics and deconvolution methods that include all the major brain cell types [15]. We found that differentiated cultures from *PLD3* p.A442A and isogenic controls exhibited a similar enrichment of neurons (~95%; Figure 4.1C). These findings are consistent with a variant that impacts a late-onset disease, where we would not predict a significant developmental defect.

Having demonstrated that *PLD3* p.A442A and isogenic controls share a similar capacity to form neurons, we next asked whether the *PLD3* p.A442A variant was sufficient to alter *PLD3*

splicing in a manner consistent with our prior observations in human brains from *PLD3* p.A442A carriers [4]. RNA isolated from neurons expressing *PLD3* p.A442A and isogenic controls was converted to cDNA, and *PLD3* exons 7, 8, 9, 10, and 11 were amplified and quantified. We found that *PLD3* exons are significantly reduced in the *PLD3* p.A442A neurons, which is restored upon correction of the variant allele to WT (Figure 4.1D). To determine whether *PLD3* p.A442A neurons exhibit changes in A $\beta$ , which would be consistent with a variant that impacts amyloid plaque deposition, we measured extracellular A $\beta$  by sandwich ELISA in the media of *PLD3* p.A442A and isogenic control neurons. After correcting for total protein, we observed a significant increase in A $\beta$ 42 and A $\beta$ 40 in media from neurons expressing *PLD3* p.A442A (Figure 4.1E and 4.1F) without changing the A $\beta$ 42/40 ratio (Figure 4.1G) when compared to isogenic controls. Together, these findings illustrate that in nearly identical, isogenic neurons, the presence of the *PLD3* p.A442A is sufficient to alter *PLD3* transcripts and extracellular A $\beta$  levels.

### *PLD3 expression is altered in LOAD brains*

Having demonstrated that the AD risk variant in *PLD3* (*PLD3* p.A442A) was sufficient to alter *PLD3* transcripts and A $\beta$  levels, we sought to determine whether *PLD3* is altered in LOAD. We examined *PLD3* expression in laser-captured microdissected neurons across multiple brain regions from AD cases and neuropathology-free controls. *PLD3* expression was significantly lower in AD brains compared with control brains in the entorhinal cortex, hippocampus, medial temporal gyrus, and superior frontal gyrus (Figure 4.2), regions that exhibit amyloid and tau pathology. Interestingly, *PLD3* expression was unaltered in the primary visual cortex, which is largely spared of AD pathology (Figure 4.2) [30]. *PLD3* expression was also significantly reduced in an independent cohort of temporal cortices isolated from AD and control

brains ( $\beta=-0.36$ ;  $p=3.23\times10^{-4}$ ) [31]. These findings are consistent with prior reports of reduced *PLD3* expression in LOAD brains [4].

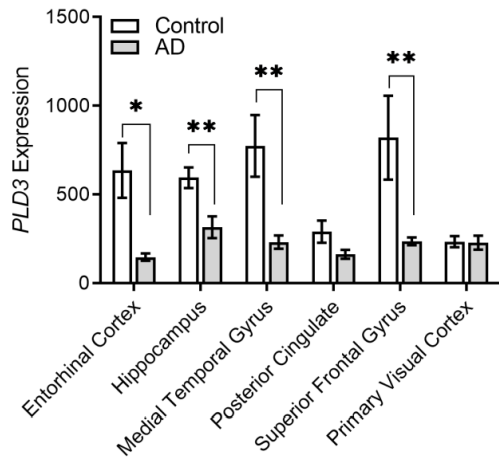


**Figure 4.2: *PLD3* expression is significantly reduced in brain regions vulnerable to AD pathology.** Laser capture of microdissected neurons from the brains of neuropathology confirmed control and AD brains [32]. Quantification of *PLD3* expression in laser microdissected neurons isolated from AD and control brains (AU). The graph represents mean  $\pm$  SEM. \* $p<0.05$ . Analyzed by two-tailed Student's *t* test.

### *Pld3 regulates A $\beta$ in APP/PS1 mice*

*PLD3* expression is reduced in brains from *PLD3* p.A442A carriers and in LOAD brains (Figure 4.2) [4], and overexpression or silencing of *PLD3* in mouse neuroblastoma cells leads to inverse changes in A $\beta$  levels [4]. Thus, we sought to determine whether modulating *PLD3* expression is sufficient to alter A $\beta$  *in vivo*. In mice, A $\beta$  is primarily generated in neurons and released into the ISF, where it can be cleared by extracellular proteolysis, transported into CSF or across the blood-brain barrier, or by cellular uptake and degradation. The steady-state level of ISF A $\beta$ , thus, reflects these production and degradation/clearance mechanisms. We hypothesized that reducing endogenous *Pld3* expression, as observed in human AD brains, would elevate ISF

$\text{A}\beta$  levels. To address this hypothesis, 3-month-old APP/PS1 mice were injected with AAV8 particles containing shPld3 or shScrambled (control) and evaluated at five months of age by *in vivo* microdialysis (Figure 4.3A). At five months of age, shPld3 was sufficient to significantly reduce endogenous *Pld3* transcript level in the hippocampus compared with scrambled controls by 28% (Figure 4.3B). This modest reduction of *Pld3* did not alter steady-state ISF  $\text{A}\beta$  levels (Figure 4.3C and 4.3D;  $p=0.27$ ). Next, to test the impact of *Pld3* silencing on the  $\text{A}\beta$  elimination rate (half-life),  $\text{A}\beta$  levels were monitored after treatment with a  $\gamma$ -secretase inhibitor (Figure 4.3C). The secretase inhibitor rapidly blocks  $\text{A}\beta$  generation within minutes, then ISF is sampled hourly to calculate the rate of elimination of existing  $\text{A}\beta$ . Silencing of *Pld3* resulted in a 135% increase in  $\text{A}\beta$  elimination half-life (Figure 4.3C and 4.3E;  $p=0.0025$ ). Thus, PLD3 is likely involved in  $\text{A}\beta$  clearance. The striking impact of a modest *Pld3* decrease in  $\text{A}\beta$  levels in the APP/PS1 mice led us to investigate the impact of a global knockout of *Pld3* on  $\text{A}\beta$  (Figure 4.3F). Global *Pld3* knockout mice were generated using CRISPR/Cas9. A guideRNA targeting an early, highly conserved exon was validated *in vitro* and injected into murine oocytes (see Methods; Supplemental Figure 4.2). Founders were established and backcrossed to C57Bl/6;C3B6 prior to breeding with APP/PS1 mice (Supplemental Figure 4.3C). Consistent with prior reports, *Pld3* KO mice were viable and did not exhibit gross defects [9, 33]. *Pld3*-deficient APP/PS1 mice exhibited a 35% increase in steady-state ISF  $\text{A}\beta$  at four months of age (Figure 4.3G-4.3I). In agreement with the AAV-mediated knockdown, *Pld3*-deficient APP/PS1 mice exhibited a 49% increase in  $\text{A}\beta$  elimination half-life following the administration of a  $\gamma$ -secretase inhibitor (Figure 4.3G and 4.3I). Thus, *Pld3* reduction in the brain is sufficient to reduce the turnover of ISF  $\text{A}\beta$ .

*In vitro* overexpression of *PLD3* was sufficient to reduce extracellular A $\beta$  [4]. Thus, we asked whether overexpression of *hPLD3* in APP/PS1 mice could rescue the ISF A $\beta$  phenotype (Figure 4.3A). The hippocampus of APP/PS1 mice was bilaterally injected with AAV8 particles containing hPLD3 or GFP (control) at three months of age, and two months later, ISF A $\beta$  was

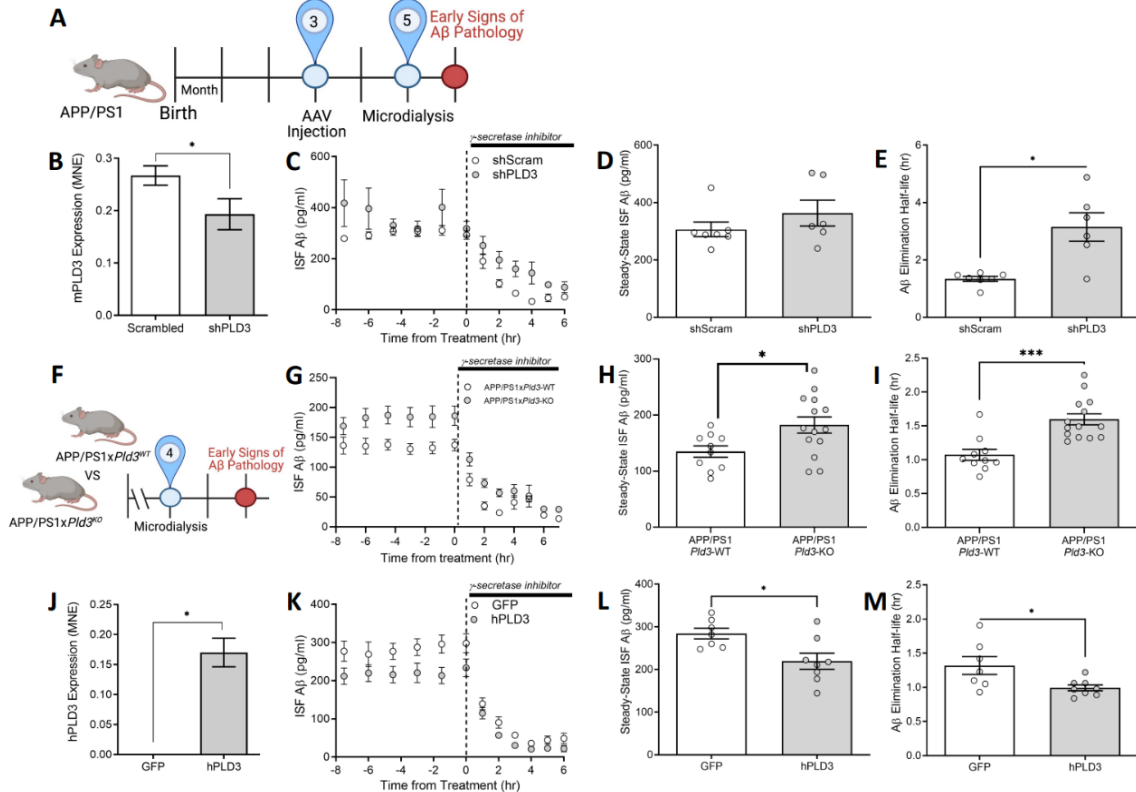


**Figure 4.3: Bi-directional expression of *Pld3* alters A $\beta$  turnover *in vivo*.** A-E. The impact of *Pld3* silencing on ISF A $\beta$ . A. Diagram of the experimental timeline: APP/PS1 mice were injected with shScramble sh*Pld3* (compared to *shScram* control)-containing AAV8 particles at three months of age and were evaluated by *in vivo* microdialysis at five months of age. *shScramble* (n=7) and *shPld3* (n=6). B. Knockdown of endogenous *Pld3*. C. A $\beta$  levels in ISF sampled over 14 hours in *shScram*, and *shPld3* injected APP/PS1 mice. D. Steady-state levels of ISF A $\beta$ . E. Elimination half-life of ISF A $\beta$ . F-I. The impact of *Pld3* KO on ISF A $\beta$ . F. Diagram outlining the experimental timeline: APP/PS1x*Pld3*-WT and APP/PS1x*Pld3*-KO mice were evaluated by *in vivo* microdialysis at four months of age. APP/PS1x*Pld3*-WT (n=10), APP/PS1x*Pld3*-KO (n=14). G. A $\beta$  levels in ISF sampled over 14 hours in APP/PS1x*Pld3*-WT and APP/PS1x*Pld3*-KO mice. H. Steady-state levels of ISF A $\beta$ . I. Elimination half-life of ISF A $\beta$ . J-M. APP/PS1 mice were injected with hPLD3 (compared to GFP control)-containing AAV8 particles at three months of age and were evaluated by *in vivo* microdialysis at five months of age. GFP (n=7), hPLD3 (n=8). J. Overexpression of *hPLD3*. K. A $\beta$  levels in ISF sampled over 14 hours in *GFP* and *hPLD3* injected APP/PS1 mice. L. Steady-state levels of ISF A $\beta$ . M. Elimination half-life of ISF A $\beta$ . Graphs represent mean  $\pm$  SEM. \*p < 0.05, \*\*\*p < 0.0005. Analyzed by two-tailed Student's *t* test.

measured by microdialysis (Figure 4.3A). Overexpression of *hPLD3* significantly reduced steady-state levels of ISF A $\beta$  and A $\beta$  elimination half-life by approximately 25% (Figure 4.3J-M). Taken together, our findings illustrate that PLD3 expression regulates A $\beta$  turnover in APP/PS1 mice.

### *Pld3-deficiency alters plaque composition*

Impairment in protein clearance has been implicated in amyloid plaque accumulation and AD pathogenesis [34, 35]. A $\beta$  aggregation in the extracellular space (ISF) into soluble oligomers or insoluble amyloid plaques is a critical driver of AD pathogenesis, and conversion of monomeric A $\beta$  into these aggregates is facilitated at higher concentrations [36]. Thus, we sought to determine whether increased ISF A $\beta$  in four months old APP/PS1x*Pld3*-KO mice could impact amyloid plaque pathology in older animals (Figure 4.4A). To assess plaque pathology, APP/PS1x*Pld3*-KO mice were sacrificed at nine months of age, and brain sections were co-stained with HJ3.4 (total A $\beta$ ) and X-34 ( $\beta$ -sheet rich dense cores; Figure 4.4B). Plaque composition was then analyzed as the percent of X-34 stain within HJ3.4-positive plaques (termed: fibrillar plaques) and the extent of HJ3.4-positivity outside X-34 plaques (termed: Non-fibrillar plaque area). In APP/PS1x*Pld3*-KO mice, the percentage of fibrillar plaques was significantly reduced compared with APP/PS1x*Pld3*-WT mice (Figure 4.4C). Conversely, the non-fibrillar plaque area was significantly increased compared with APP/PS1x*Pld3*-WT mice (Figure 4.4D). In complementary analyses, we found that A $\beta$  plaque size was significantly increased in the cortex of APP/PS1x*Pld3*-KO compared with APP/PS1x*Pld3*-WT mice (Supplemental Figure 4.3) without a change in the overall plaque burden as defined by the percentage area of HJ3.4-positive immunostaining (e.g., plaque density). X-34 staining remained

unchanged in the absence of *Pld3* (Supplemental Figure 4.4). Thus, *Pld3* KO impacts plaque composition, shifting the pathology to a less fibrillar structure [37].

### *Pld3* deficiency impact microglial recruitment to amyloid plaques

**Table 4.1:** Differential microglia gene expression in APP/PS1x*Pld3*-KO compared with APP/PS1x*Pld3*-WT brains

Gene	Log2FoldChange	p-value
<i>Trem2</i>	0.48	1.07E-03
<i>Tyrobp</i>	0.57	1.06E-03
<i>Ctsd</i>	0.25	4.18E-03
<i>Cst7</i>	0.56	2.91E-02
<i>Cd68</i>	0.35	6.27E-02
<i>Aifl</i>	0.33	1.08E-01
<i>Tmem119</i>	0.04	6.49E-01
<i>P2ry12</i>	0.05	5.99E-01

The absence of *Pld3* in the APP/PS1 mice resulted in more non-fibrillar plaques. This shift in plaque composition is similar with findings from *Trem2*- and *ApoE*-deficient APP/PS1 mice [38-41]. Loss of these AD risk genes also significantly reduced microglial recruitment to the amyloid plaques [38-41]. Thus, we hypothesized that the loss of *Pld3* may alter the microglial response in APP/PS1 mice. To test this hypothesis, fixed brain tissue from the APP/PS1x*Pld3*-KO and APP/PS1x*Pld3*-WT mice were stained for total microglia (Iba1), activated microglia (CD68), and dense core A $\beta$  plaques (X-34) (Figure 4.5A). The amount of activated microglia as a percentage of total microglia was similar between APP/PS1x*Pld3*-KO and APP/PS1x*Pld3*-WT mice (Figure 4.5D). However, APP/PS1x*Pld3*-KO mice exhibited a significant reduction in the recruitment of microglia around the X-34-positive plaques (Figure

4.5B). No significant change was observed in the amount of CD68-positive, activated microglia around the X-34-positive (Figure 4.5C and 4.5D). *Pld3* deficient APP/PS1 mice also exhibited a significant increase in expression of microglia genes associated with neurodegeneration including *Trem2*, *Tyrobp*, *Ctsd*, and *Cst7* (Table 4.1) without a corresponding change in homeostatic microglia genes (Table 4.1). Thus, loss of *Pld3* impacts microglia function in response to amyloid plaques.

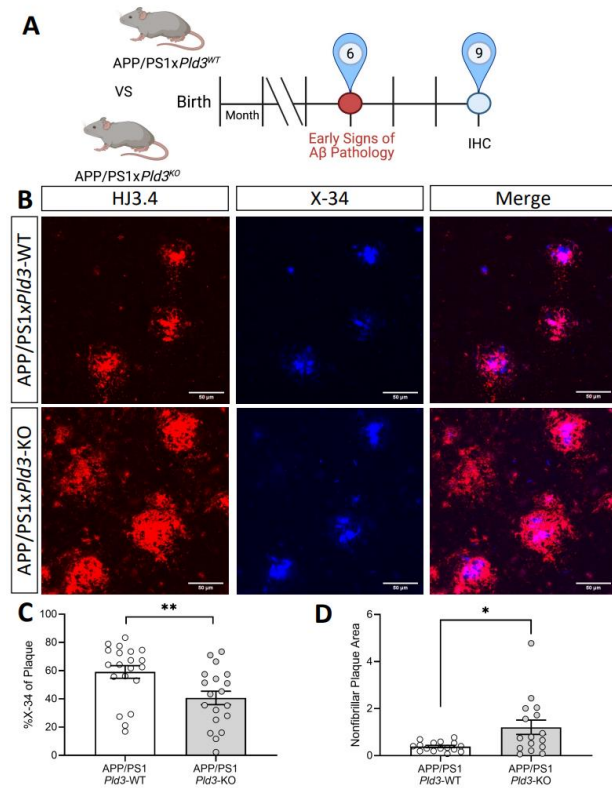


**Figure 4.4: Loss of *Pld3* alters plaque composition in APP/PS1 mouse cortex.** A. Experimental timeline. APP/PS1x*Pld3*-WT (n=20), APP/PS1x*Pld3*-KO (n=15). B. Representative confocal images of mouse cortex co-stained with HJ3.4 (total Aβ) and X-34 ( $\beta$ -sheet rich dense cores). C-D. Quantification of the plaque composition. C. Percent of X-34 within a HJ3.4-positive area. D. Area HJ3.4 outside of X-34-positive area (nonfibrillar area). The total area of X-34 normalized signal microns. Graphs represent mean  $\pm$  SEM. \*\*, p=0.0010; \*\*\*, p=0.0003. Analyzed by two-tailed Student's *t* test with a ROUT outlier analysis (Q=1%).

## *A role for PLD3 in microglia*

Given the association of *Pld3* loss with altered microglia function in mouse models, we sought to determine whether *PLD3* is altered in microglia in human brains. Nuclei were isolated and sequenced from frozen AD and age-matched control brains (Figure 4.6A)[17, 18]. AD brains were further classified based on the presence of *TREM2* risk variants (named: TREM2). Unsupervised clustering of the brain nuclei revealed 15 cell-type specific clusters that correspond to the major cell-types found in the brain [17]. We isolated microglia from other cells and reexamined the alternative transcriptional states that we further classified into nine subclusters (Figure 4.6B). *PLD3* expression was significantly overexpressed in Mic.1 and reduced Mic.2 microglia subclusters compared to all microglia clusters (Figure 4.6B;  $p=2.71\times10^{-5}$  and  $2.27\times10^{-6}$ , respectively; Supplemental Table 4.2). In contrast, homeostatic microglia (Mic.0) did not show differential expression of *PLD3* (Figure 4.6B;  $p=0.52$ ; Supplemental Table 4.2). Microglia in Mic.1 have an expression signature consistent with microglia associated with neurodegeneration (e.g. disease associated or activated response microglia) [33, 42, 43], while Mic.2 clusters are enriched among *TREM2* variant carriers and exhibit upregulated resting state microglia markers with minimal elevation of genes associated with activated microglia [17].

To understand how *PLD3* expression changes in microglia with disease, we examined control, sporadic AD and *TREM2* risk variant carriers. *PLD3* expression was significantly reduced in homeostatic microglia in sporadic AD brains and *TREM2* risk variants compared to controls (Figure 4.6C;  $p=1.04\times10^{-3}$  and  $p=2.46\times10^{-2}$ , respectively; Supplemental Table 4.3). *PLD3* expression was further dysregulated in disease associated Mic.1 cluster in *TREM2* risk variant carriers compared with controls (Figure 4.6D;  $p=4.13\times10^{-3}$ ; Supplemental Table 4.3).

To further clarify the relationship between PLD3 and microglia function, we analyzed *PLD3* expression in single cell RNAseq data obtained from human iPSC expressing inducible CRISPRi machinery that were transduced with 81 sgRNAs and differentiated into iTF-Microglia (Figure 4.6E) [44]. Unsupervised clustering analyses revealed nine distinct microglia subclusters (Figure 4.6E), representing distinct transcriptional states. Among these subclusters, *PLD3* was significantly overexpressed in clusters 1, 2, and 3 and significantly reduced in clusters 4, 5, 7, and 9 (Figure 4.6F and 4.6G; Supplemental Table 4.4). Clusters 1-3 correspond with interferon-induced gene activation states [44], while clusters 4-9 are enriched for genes associated with chemokine/cytokine activation states [44]. Cluster 3, where *PLD3* is significantly elevated, is enriched in *SPP1* expression, a marker of disease associated microglia [44]. Additionally, cluster 7, where *PLD3* is significantly reduced, is enriched in markers of microglia proliferation [44]. Together, these data support a role for *PLD3* in microglia activation in health and disease.

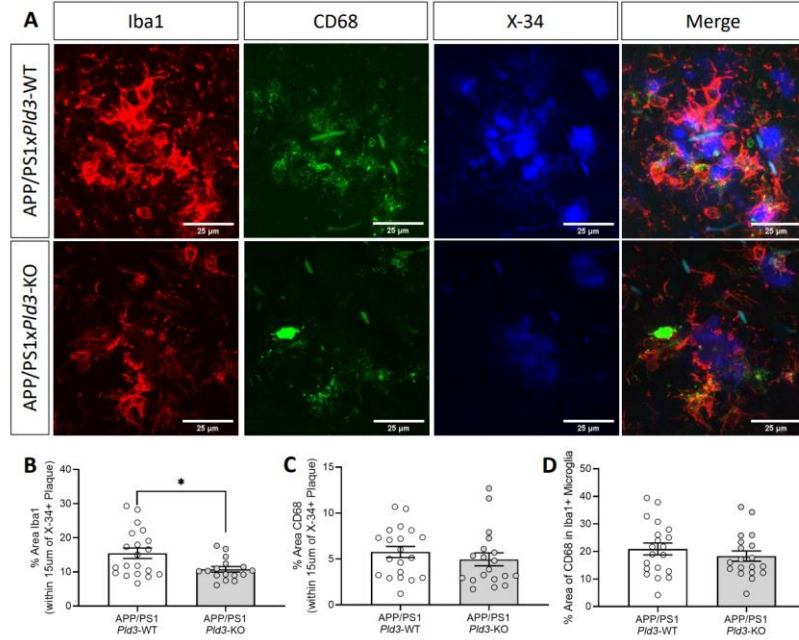


**Figure 4.5: Loss of *Pld3* alters the microglial response to Aβ pathology.** A. Representative images of APP/PS1x*Pld3*-WT and APP/PS1x*Pld3*-KO mice co-stained with Iba1 (total microglia), CD68 (activated

microglia), and X-34 ( $\beta$ -sheet-rich dense cores). APP/PS1x*Pld3*-WT (n=20), APP/PS1x*Pld3*-KO (n=19). B. Quantification of Iba1 localization within 15  $\mu$ m of the X-34+ dense core plaques (\*, p=0.03). C. Quantification of CD68 localization within 15  $\mu$ m of the dense plaques. D. Quantification of Iba1 and CD68 colocalization. Graphs represent mean  $\pm$  SEM. Analyzed by two-tailed Student's *t* test with a ROUT outlier analysis (Q=1%).

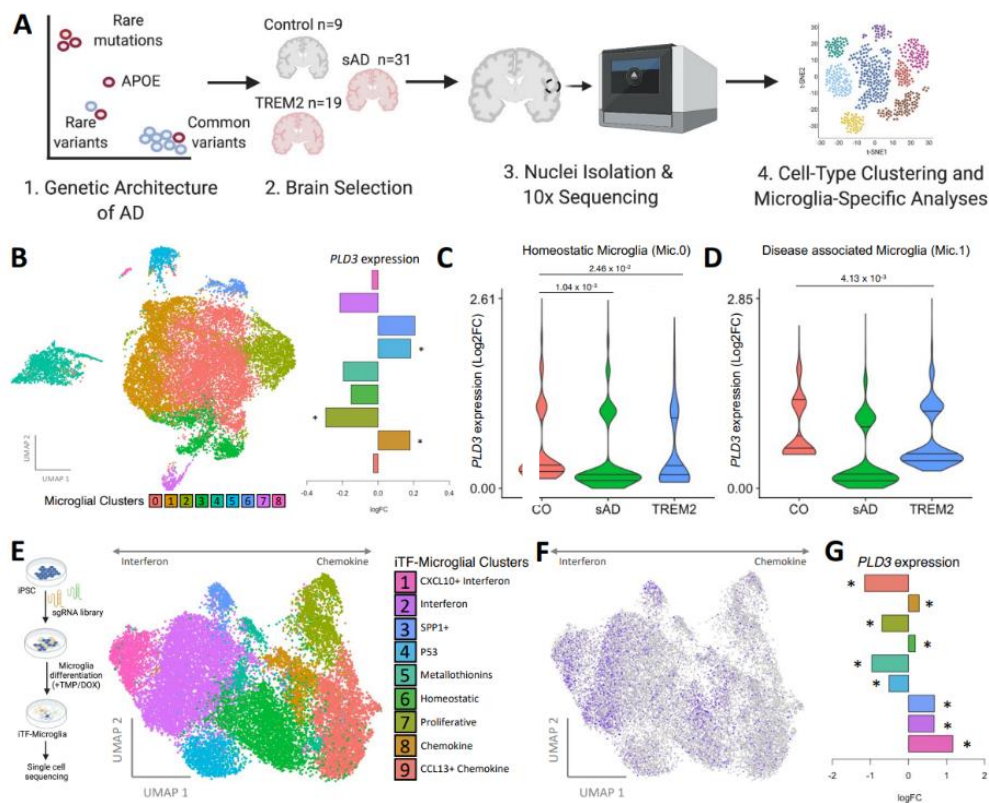


**Figure 4.6: *PLD3* is enriched in specific microglia states in human brains.** A. Diagram of the study design for human brain sequencing. B. UMAP plot depicting segregation of human brain microglia into nine major subclusters, left. Bar plot of the log<sub>2</sub> fold change of *PLD3* by microglia subcluster, right. \*, p<0.05. C-D. Violin plot of *PLD3* expression from control (CO), sporadic AD (sAD), and *TREM2* risk variant carriers in homeostatic (Mic.0; C) and disease associated (Mic.1; D). E-G. Single cell RNAseq data obtained iTF-Microglia CROP-seq described previously [44]. E. UMAP plot reveals 9 microglia clusters. F. Diagram of study design for iTF-Microglia, left. UMAP plot of *PLD3* expression, right. Cells are colored by the *PLD3* expression levels. G. Bar plot of the log<sub>2</sub> fold change of *PLD3* by microglia subcluster. \*, p<0.05.

## 4.5 Discussion

In this study, we sought to understand the contribution of PLD3 to pathways that promote AD pathology. We demonstrate that the AD risk variant, *PLD3* p.A442A, is sufficient to alter *PLD3* splicing and A $\beta$  levels in iPSC-derived neurons in a manner consistent with similar findings in AD brains [4]. Additionally, we describe a role for PLD3 in LOAD, whereby modifying *PLD3* expression in APP/PS1 mice is sufficient to regulate A $\beta$  turnover in the ISF. The observed reduced ISF A $\beta$  turnover, in turn, leads to a change in amyloid plaques in aged animals. We observed that loss of *Pld3* in APP/PS1 mice results in a shift in plaque composition to a more nonfibrillar structure. This altered plaque composition is accompanied by impaired microglial recruitment to the plaques, consistent with prior reports from *Trem2* deficient mice. In human brains, *PLD3* is enriched in disease associated microglia and expression is altered in AD brains. Together, these results suggest that *PLD3* plays cell-autonomous and non-cell autonomous roles in AD pathogenesis.

Deciphering the contribution of risk variants and pathogenic mutations to AD pathogenesis has led to groundbreaking discoveries of A $\beta$  metabolism, synaptic function, and immune function to AD and revealed novel therapeutic targets [45]. Emerging sequencing technologies in increasingly larger cohorts have revealed the contribution of rare variants to AD risk [45, 46]. Nevertheless, resolving the contribution of rare variants to disease can be challenging when relying on association studies and autopsy brain tissue that captures a snapshot of disease.

Here, patient-derived cell culture models represent a tractable, human platform that recapitulates disease-specific phenotypes and when coupled with genome engineering, allows for

the study of genotype x phenotype relationships. This study demonstrates that iPSC-derived neurons are highly informative and recapitulate early pathogenic events in AD.

In this study, we used genome editing technology to molecularly pinpoint the contribution of the A allele to PLD3 and AD-related phenotypes. While we cannot exclude the possibility that genomic factors beyond PLD3 p.A442A contribute to the risk profile in the iPSC donor line used in this study, we can attribute the defect in PLD3 splicing and the increase in A $\beta$  levels to this synonymous variant. The increase in both A $\beta$ 42 and A $\beta$ 40 is consistent with the effects of other known pathogenic mutations, including APP KM670/671NL [47, 48]. The absence of an effect of *PLD3* p.A442A on the A $\beta$ 42/40 ratio suggests that A $\beta$  recycling and trafficking. This is consistent with recently reported functions of PLD3 as a type II membrane protein functioning in endosomes and lysosomes, the primary site of APP cleavage [49, 50]. Together, these human stem cell findings suggest a role for PLD3 p.A442A in altering APP/A $\beta$  recycling and trafficking in a manner that elevates total A $\beta$  levels.

PLD3 p.A442A was predicted to disrupt a splicing enhancer-binding site [4]. We observe defective *PLD3* splicing in iPSC-derived neurons from a *PLD3* p.A442A carrier, which replicates the observations in brains from *PLD3* p.A442A carriers [4]. We go on to demonstrate that correcting the risk allele with CRISPR/Cas9 is sufficient to restore the splicing defect. The functional impact of distinct PLD3 isoforms remains unknown; however, as the functional roles of PLD3 are resolved, this will be an important area to explore.

We show that PLD3 is a major regulator of ISF A $\beta$  turnover *in vivo*. Hippocampal reduction of endogenous *Pld3* in adulthood via AAV8-mediated knockdown or global knockout of *Pld3* in the background of APP/PS1 mice resulted in a strong increase in ISF A $\beta$  half-life,

suggesting that A $\beta$  is turned over more slowly in the absence of *Pld3*. A $\beta$  clearance mechanisms have been proposed to drive LOAD [35]. Following secretion from presynaptic neurons, A $\beta$  is either taken up and degraded in the lysosomes of post-synaptic neurons, taken up and degraded in the lysosomes of glial cells, degraded by extracellular proteases, is transported to CSF, or transcytosed across the blood-brain barrier (BBB). Amyloid accumulation occurs in an A $\beta$  concentration-dependent manner [36]; thus, dysregulation of ISF A $\beta$  clearance drives amyloid accumulation and AD pathogenesis. Neurons from *Pld3* KO mice exhibit lysosomes with increased density and size [33]. PLD3 is enriched in lysosomes surrounding amyloid plaques in human AD brains and mouse models of amyloid accumulation [9]. Thus, *Pld3* may regulate ISF A $\beta$  through lysosome-mediated clearance mechanisms in neurons or other glial cells.

The absence of *Pld3* in APP/PS1 mice led to a shift in the composition of amyloid plaques to being more diffuse and less fibrillar. While amyloid plaques may adopt a series of morphologies and architecture, a major structure is characterized by a dense “fibrillar” core of A $\beta$  surrounded by more diffuse “non-fibrillar” of A $\beta$  deposits [51]. Non-fibrillar A $\beta$  is proposed to contribute to its higher toxicity, possible because either its structure is more toxic or they serve as a reservoir for more diffusible A $\beta$  oligomers [37, 52]. Thus, a PLD3-mediated shift to more non-fibrillar plaques is consistent with more toxic effects given the same amount of overall A $\beta$  deposition. Silencing AD risk genes, including *Trem2* and *ApoE*, result in a similar shift of plaque composition shift in APP/PS1 mice [38, 39, 41]. Thus, modeling the reduction of *PLD3* observed in *PLD3* p.A442A carriers, and LOAD brains in an animal model of amyloid accumulation leads to a phenotype consistent with a gene that exacerbates disease.

In prior studies where gene silencing in amyloid mice led to a change in plaque formation and composition, a role for an altered microglial response to amyloid plaques was implicated

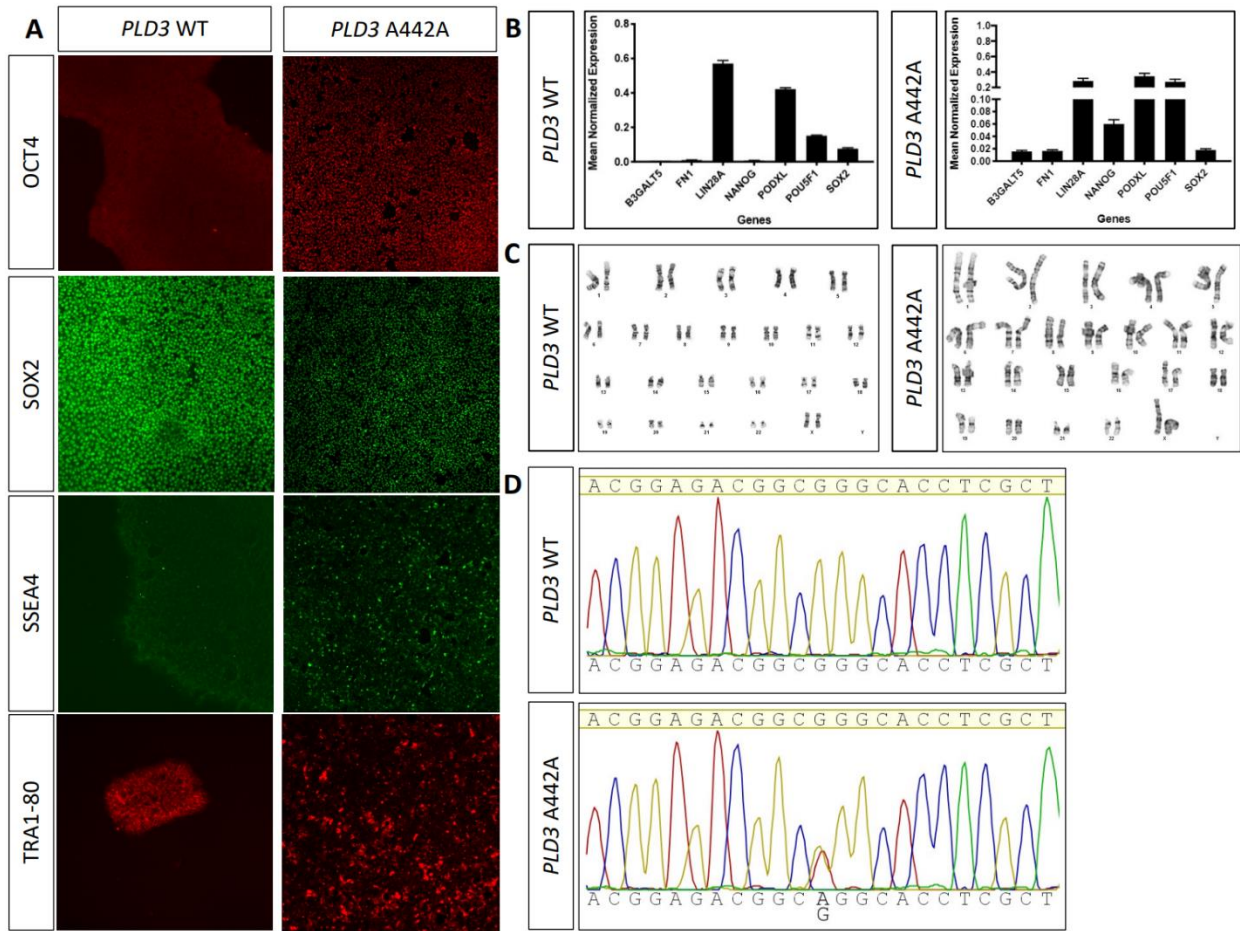
[38, 39, 41]. APP/PS1x*Pld3*-KO and APP/PS1x*Pld3*-WT mice exhibited a similar abundance of Iba1 positive microglia. Yet, recruitment of Iba1-positive microglia to X-34-positive plaques was significantly reduced in APP/PS1x*Pld3*-KO mice compared to APP/PS1x*Pld3*-WT mice. This could suggest a role for PLD3 in recruiting microglia to surround and alter A $\beta$  structure and limit A $\beta$ -induced toxicity similar to mechanisms described for TREM2 [38]. In mice, *Pld3* mRNA is expressed in microglia [53]. Microglia isolated from amyloid mouse models (APP<sup>NL-F-G</sup>) reveal an activation state enriched for MHC class II, tissue repair genes, and enrichment of AD risk genes, including *Pld3* [54]. Thus, loss of *Pld3* in the global knockout may impact the molecular identity of microglia, which impairs the recruitment and responsiveness of the glia to plaques.

In human microglia, PLD3 plays a role in microglia that is disrupted in AD. Microglia maintain distinct transcriptional states that likely reflect functional changes due to environmental stimuli [55]. We demonstrate that *PLD3* expression is enriched in disease associated microglia (Brain Mic.1 and iTF-Microglia cluster 3) and depleted in population of microglia that are found in *TREM2* risk variant carriers (Brain Mic.2). Mic.2 reflect a dampened activation state, distinct from homeostatic microglia (Mic.0) with an upregulation of resting state microglia markers (*TMEM119*, *P2RY13*, *MED12L*) and modest elevation of activated markers (*ABCA1*, *C5AR1*, and *CD83*) [17]. This finding along with the observation that *PLD3* expression is reduced in disease associated microglia (Mic.1) in *TREM2* risk variant carriers suggests a potential interaction between these AD risk genes. These results also support the parallels between our mouse model findings and those in *Trem2* deficient mice. In addition to association with disease associated microglia, PLD3 and TREM2 have also been implicated in lysosomal function [9, 33, 40, 49, 50].

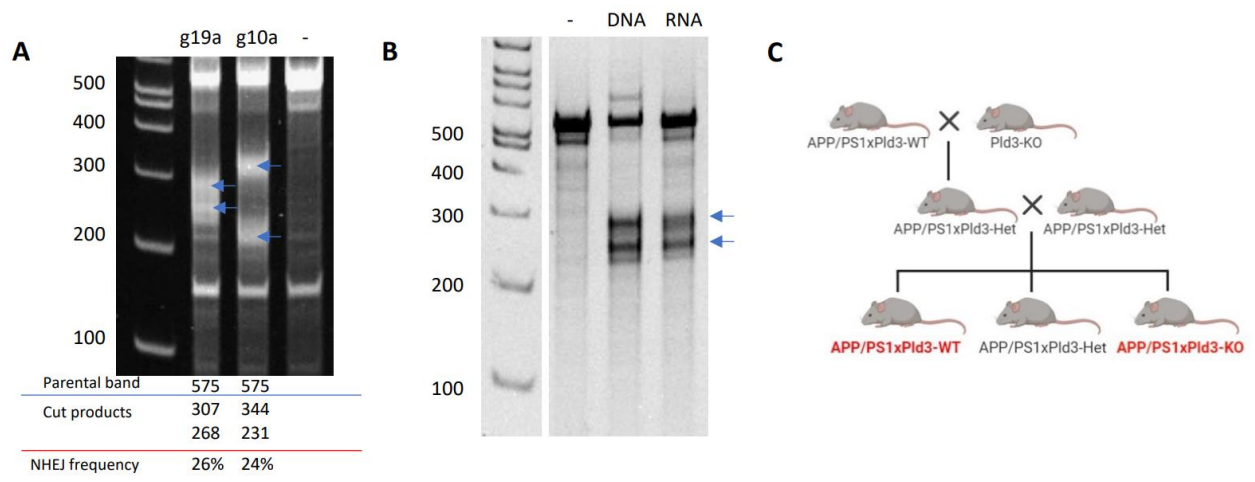
Overall, we observed a modest impact on amyloid plaque pathology in APP/PS1x*Pld3*-KO mice. The modest impact is highly consistent with PLD3 as a disease modifier rather than a fully penetrant, causative mutation. Alternatively, this could reflect redundant mechanisms for mouse *Pld3*.

Here, we demonstrate a therapeutic potential for PLD3. *hPLD3* overexpression by AAV8 in APP/PS1 mice resulted in a significant decrease in ISF A $\beta$  levels and accelerated A $\beta$  turnover. *PLD3* levels are significantly reduced in AD brains, and *PLD3* expression is positively correlated with cognition in humans and mouse models [9]. Thus, by promoting A $\beta$  turnover and facilitating the microglial response to amyloid plaques, *PLD3* occupies a crucial role in brain health.

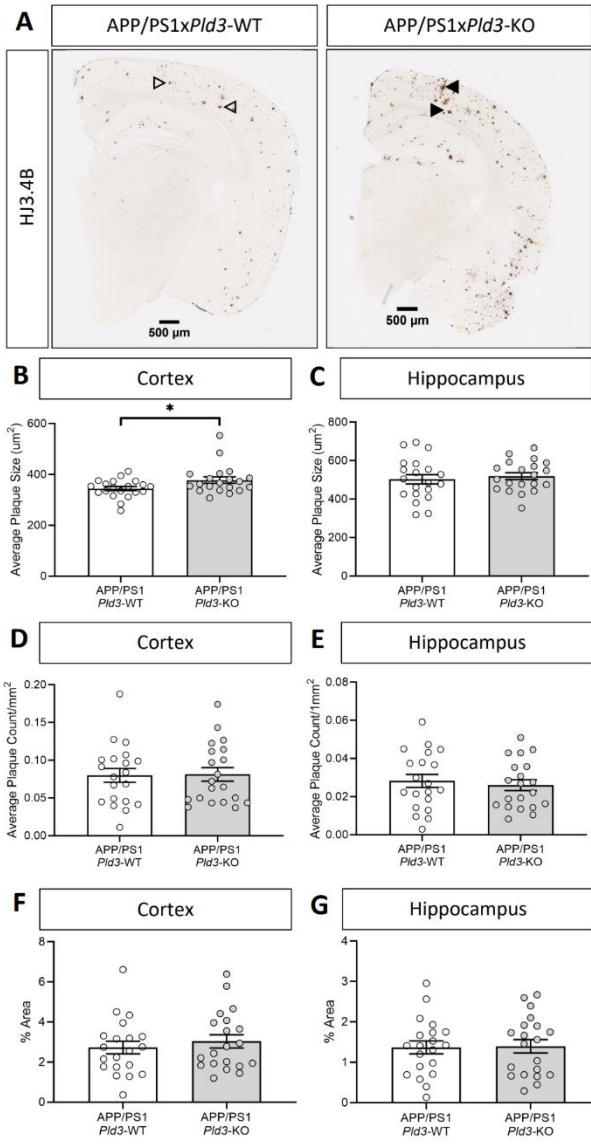
## 4.6 Supplemental Figures



**Supplemental Figure 4.1: Characterization of the *PLD3* p.A442A iPSC-derived neurons.** A. Representative images of *PLD3* p.A442A and the corrected WT iPSCs stained for NANOG, OCT4, SOX2, SSEA4, and TRA1-80. B. qPCR from known markers of pluripotency. C. Karyotype. D. Sanger sequencing.



**Supplemental Figure 4.2: Generation of a *Pld3*-deficient amyloid mouse model.** A. Mismatch detection assay. B. RNA activity validation. C. Breeding scheme for the *Pld3*-deficient mouse with APP/PS1 mutant mice to develop a transgenic APP/PS1x*Pld3*-KO mouse line along with APP/PS1x*Pld3*-WT littermate controls.



**Supplemental Figure 4.3: Loss of *Pld3* significantly increases plaque size without changing plaque area.** A.

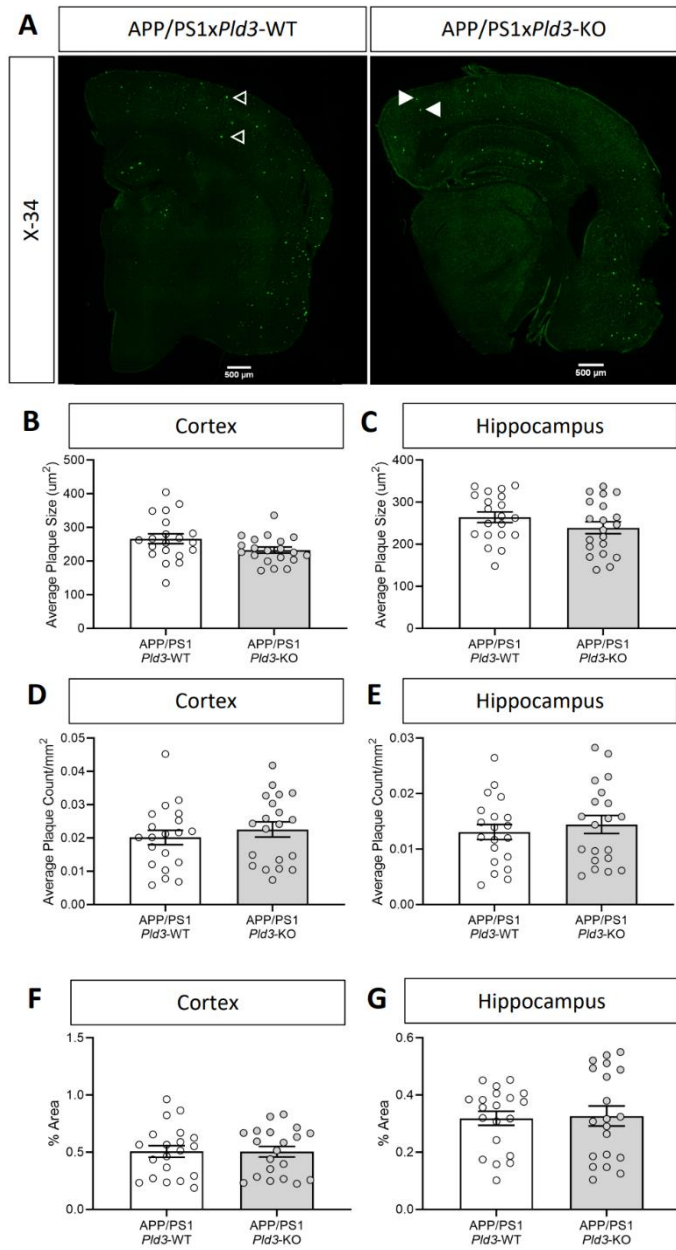
Representative images of mice brain cross-sections stained for total A $\beta$  (HJ3.4) with arrows specifying plaques

(open arrows for WT; closed arrows for KO). APP/PS1xPld3-WT (n=20), APP/PS1xPld3-KO (n=20). B-C.

Quantification of average plaque size in the cortex (B) and hippocampus (C). D-E. Quantification of average plaque

count per  $\text{mm}^2$  in the cortex (D) and the hippocampus (E). F-G. Quantification of the plaque burden by the

percentage of the total area for the cortex (F) and the hippocampus (G). Graphs represent mean  $\pm$  SEM. \*, p>0.05.



**Supplemental Figure 4.4: Loss of *Pld3* does not change dense core plaques.** A. Representative images of mice brain cross sections stained with X-34 with arrows specifying plaques (open arrows for WT; closed arrows for KO). APP/PS1x*Pld3*-WT (n=20), APP/PS1x*Pld3*-KO (n=20). B-C. Quantification of average plaque size in the cortex (B) and hippocampus (C). D-E. Quantification of average plaque count per  $\text{mm}^2$  in the cortex (D) and hippocampus (E). F-G. The quantification of the plaque burden by the percentage of the total area for the cortex (F) and hippocampus (G). Graphs represent mean  $\pm$  SEM.

## 4.7 Supplemental Tables

**Supplemental Table 4.1:** Human brain demographics for snRNAseq

	Total Number	Sex (% male)	Mean Age at Death (years)	APOE4	Mean Postmortem Interval (years)
Controls	9	33%	90	11%	10.9
sAD	31	45%	81	54%	11.9

**Supplemental Table 4.2:** PLD3 expression in human brain microglia

Cluster Name	LogFC	z-score	p-value	BH corrected p-value
Mic.0	-0.0262225	-0.6410652	5.21E-01	7.32E-01
Mic.1	0.1800801	4.19659881	2.71E-05	2.86E-04
Mic.2	-0.2949385	-4.7275062	2.27E-06	1.26E-04
Mic.3	-0.1519921	-1.274392	2.03E-01	5.14E-01
Mic.4	-0.1953743	-1.718988	8.56E-02	2.51E-01
Mic.5	0.1829342	1.98158159	4.75E-02	1.75E-01
Mic.6	0.20610645	1.89898926	5.76E-02	1.96E-01
Mic.7	-0.2146737	-1.3839443	1.66E-01	4.50E-01
Mic.8	-0.0345632	-0.1138777	9.09E-01	9.99E-01

**Supplemental Table 4.3:** PLD3 expression within microglia subclusters by disease status

Comparison	LogFC	z-score	p-value	BH corrected p-value	Subcluster
sAD vs CO	0.4017806	3.2799941	1.04E-03	1.43E-01	Mic.0
TREM2 vs CO	0.2766865	-2.247029	2.46E-02	3.91E-01	Mic.0
sAD vs CO	0.3455155	1.8251283	6.80E-02	1.00E+00	Mic.1
TREM2 vs CO	0.4217827	2.8679334	4.13E-03	3.21E-01	Mic.1

**Supplemental Table 4.4:** PLD3 expression in iTF-Microglia CROP-Seq

Cluster Name	Estimate	Std. Error	z value	Pr(> z )
cluster 1	1.163684751	0.079301251	14.67422936	9.43E-49
cluster 2	0.673908846	0.041847298	16.10399883	2.39E-58
cluster 3	0.679645559	0.12978185	5.236830561	1.63E-07
cluster 4	0.511168775	0.081414971	6.278559975	3.42E-10
cluster 5	0.966514606	0.105007855	9.204212437	3.44E-20
cluster 6	0.178261422	0.050290361	3.544643891	3.93E-04
cluster 7	0.696815579	0.075041761	9.285703981	1.61E-20
cluster 8	0.277388403	0.093662032	2.961588568	3.06E-03
cluster 9	1.155055839	0.051935689	22.24011787	1.41E-109

## 4.8 References

- [1] J. Hardy, D.J. Selkoe, The amyloid hypothesis of Alzheimer's disease: progress and problems on the road to therapeutics, *Science* 297(5580) (2002) 353-6.
- [2] C.M. Karch, A.M. Goate, Alzheimer's disease risk genes and mechanisms of disease pathogenesis, *Biol Psychiatry* 77(1) (2015) 43-51.
- [3] S.M. Neuner, J. Tcw, A.M. Goate, Genetic architecture of Alzheimer's disease, *Neurobiol Dis* 143 (2020) 104976.
- [4] C. Cruchaga, C.M. Karch, S.C. Jin, B.A. Benitez, Y. Cai, R. Guerreiro, O. Harari, J. Norton, J. Budde, S. Bertelsen, A.T. Jeng, B. Cooper, T. Skorupa, D. Carrell, D. Levitch, S. Hsu, J. Choi, M. Ryten, C. Sassi, J. Bras, R.J. Gibbs, D.G. Hernandez, M.K. Lupton, J. Powell, P. Forabosco, P.G. Ridge, C.D. Corcoran, J.T. Tschanz, M.C. Norton, R.G. Munger, C. Schmutz, M. Leary, F.Y. Demirci, M.N. Bamne, X. Wang, O.L. Lopez, M. Ganguli, C. Medway, J. Turton, J. Lord, A. Braae, I. Barber, K. Brown, U.K.C. Alzheimer's Research, P. Pastor, O. Lorenzo-Betancor, Z. Brkanac, E. Scott, E. Topol, K. Morgan, E. Rogaea, A. Singleton, J. Hardy, M.I. Kamboh, P.S. George-Hyslop, N. Cairns, J.C. Morris, J.S.K. Kauwe, A.M. Goate, Rare coding variants in the phospholipase D3 gene confer risk for Alzheimer's disease, *Nature* 505(7484) (2014) 550-554.
- [5] M. Osisami, W. Ali, M.A. Frohman, A role for phospholipase D3 in myotube formation, *PLoS One* 7(3) (2012) e33341.
- [6] A. Munck, C. Bohm, N.M. Seibel, Z. Hashemol Hosseini, W. Hampe, Hu-K4 is a ubiquitously expressed type 2 transmembrane protein associated with the endoplasmic reticulum, *The FEBS journal* 272(7) (2005) 1718-26.
- [7] K.M. Pedersen, B. Finsen, J.E. Celis, N.A. Jensen, Expression of a novel murine phospholipase D homolog coincides with late neuronal development in the forebrain, *The Journal of biological chemistry* 273(47) (1998) 31494-504.
- [8] J. Satoh, Y. Kino, Y. Yamamoto, N. Kawana, T. Ishida, Y. Saito, K. Arima, PLD3 is accumulated on neuritic plaques in Alzheimer's disease brains, *Alzheimers Res Ther* 6(9) (2014) 70.
- [9] A.G. Nackenoff, T.J. Hohman, S.M. Neuner, C.S. Akers, N.C. Weitzel, A. Shostak, S.M. Ferguson, B. Mobley, D.A. Bennett, J.A. Schneider, A.L. Jefferson, C.C. Kaczorowski, M.S. Schrag, PLD3 is a neuronal lysosomal phospholipase D associated with beta-amyloid plaques and cognitive function in Alzheimer's disease, *PLoS Genet* 17(4) (2021) e1009406.
- [10] C. Wang, H.F. Wang, M.S. Tan, Y. Liu, T. Jiang, D.Q. Zhang, L. Tan, J.T. Yu, I. Alzheimer's Disease Neuroimaging, Impact of Common Variations in PLD3 on Neuroimaging Phenotypes in Non-demented Elders, *Mol Neurobiol* 53(7) (2016) 4343-51.
- [11] K. Takahashi, S. Yamanaka, Induction of pluripotent stem cells from mouse embryonic and adult fibroblast cultures by defined factors, *Cell* 126(4) (2006) 663-76.
- [12] H. Ban, N. Nishishita, N. Fusaki, T. Tabata, K. Saeki, M. Shikamura, N. Takada, M. Inoue, M. Hasegawa, S. Kawamata, S. Nishikawa, Efficient generation of transgene-free human induced pluripotent stem cells (iPSCs) by temperature-sensitive Sendai virus vectors, *Proceedings of the National Academy of Sciences of the United States of America* 108(34) (2011) 14234-9.
- [13] C.M. Karch, A.W. Kao, A. Karydas, K. Onanuga, R. Martinez, A. Argouarch, C. Wang, C. Huang, P.D. Sohn, K.R. Bowles, S. Spina, M.C. Silva, J.A. Marsh, S. Hsu, D.A. Pugh, N. Ghoshal, J. Norton, Y. Huang, S.E. Lee, W.W. Seeley, P. Theofilas, L.T. Grinberg, F. Moreno,

- K. McIlroy, B.F. Boeve, N.J. Cairns, J.F. Crary, S.J. Haggarty, J.K. Ichida, K.S. Kosik, B.L. Miller, L. Gan, A.M. Goate, S. Temple, G. Tau Consortium Stem Cell, A Comprehensive Resource for Induced Pluripotent Stem Cells from Patients with Primary Tauopathies, *Stem Cell Reports* 13(5) (2019) 939-955.
- [14] S.W. Cho, S. Kim, J.M. Kim, J.S. Kim, Targeted genome engineering in human cells with the Cas9 RNA-guided endonuclease, *Nat Biotechnol* 31(3) (2013) 230-2.
- [15] Z. Li, J.L. Del-Aguila, U. Dube, J. Budde, R. Martinez, K. Black, Q. Xiao, N.J. Cairns, N. Dominantly Inherited Alzheimer, J.D. Dougherty, J.M. Lee, J.C. Morris, R.J. Bateman, C.M. Karch, C. Cruchaga, O. Harari, Genetic variants associated with Alzheimer's disease confer different cerebral cortex cell-type population structure, *Genome Med* 10(1) (2018) 43.
- [16] M. Allen, M.M. Carrasquillo, C. Funk, B.D. Heavner, F. Zou, C.S. Younkin, J.D. Burgess, H.S. Chai, J. Crook, J.A. Eddy, H. Li, B. Logsdon, M.A. Peters, K.K. Dang, X. Wang, D. Serie, C. Wang, T. Nguyen, S. Lincoln, K. Malphrus, G. Bisceglie, M. Li, T.E. Golde, L.M. Mangravite, Y. Asmann, N.D. Price, R.C. Petersen, N.R. Graff-Radford, D.W. Dickson, S.G. Younkin, N. Ertekin-Taner, Human whole genome genotype and transcriptome data for Alzheimer's and other neurodegenerative diseases, *Sci Data* 3 (2016) 160089.
- [17] L. Brase, S.-F. You, J. del Aguila, Y. Dai, B.C. Novotny, C. Soriano-Tarraga, T. Dykstra, M.V. Fernandez, J.P. Budde, K. Bergmann, J.C. Morris, R.J. Bateman, R.J. Perrin, E. McDade, C. Xiong, A. Goate, M. Farlow, J.P. Chhatwal, P. Schofield, H. Chui, D.I.A. Network, G.T. Sutherland, J. Kipnis, C.M. Karch, B.A. Benitez, C. Cruchaga, O. Harari, A landscape of the genetic and cellular heterogeneity in Alzheimer disease, *medRxiv* (2021) 2021.11.30.21267072.
- [18] S. Da Mesquita, Z. Papadopoulos, T. Dykstra, L. Brase, F.G. Farias, M. Wall, H. Jiang, C.D. Kodira, K.A. de Lima, J. Herz, A. Louveau, D.H. Goldman, A.F. Salvador, S. Onengut-Gumuscu, E. Farber, N. Dabhi, T. Kennedy, M.G. Milam, W. Baker, I. Smirnov, S.S. Rich, N. Dominantly Inherited Alzheimer, B.A. Benitez, C.M. Karch, R.J. Perrin, M. Farlow, J.P. Chhatwal, D.M. Holtzman, C. Cruchaga, O. Harari, J. Kipnis, Meningeal lymphatics affect microglia responses and anti-Abeta immunotherapy, *Nature* 593(7858) (2021) 255-260.
- [19] J.L. Jankowsky, D.J. Fadale, J. Anderson, G.M. Xu, V. Gonzales, N.A. Jenkins, N.G. Copeland, M.K. Lee, L.H. Younkin, S.L. Wagner, S.G. Younkin, D.R. Borchelt, Mutant presenilins specifically elevate the levels of the 42 residue beta-amyloid peptide in vivo: evidence for augmentation of a 42-specific gamma secretase, *Hum Mol Genet* 13(2) (2004) 159-70.
- [20] Q. Xiao, P. Yan, X. Ma, H. Liu, R. Perez, A. Zhu, E. Gonzales, D.L. Tripoli, L. Czerniewski, A. Ballabio, J.R. Cirrito, A. Diwan, J.M. Lee, Neuronal-Targeted TFEB Accelerates Lysosomal Degradation of APP, Reducing Abeta Generation and Amyloid Plaque Pathogenesis, *J Neurosci* 35(35) (2015) 12137-51.
- [21] Q. Xiao, S.C. Gil, P. Yan, Y. Wang, S. Han, E. Gonzales, R. Perez, J.R. Cirrito, J.M. Lee, Role of phosphatidylinositol clathrin assembly lymphoid-myeloid leukemia (PICALM) in intracellular amyloid precursor protein (APP) processing and amyloid plaque pathogenesis, *The Journal of biological chemistry* 287(25) (2012) 21279-89.
- [22] J. Riddoch-Contreras, S.-Y. Yang, J.R.T. Dick, G. Goldspink, R.W. Orrell, L. Greensmith, Mechano-growth factor, an IGF-I splice variant, rescues motoneurons and improves muscle function in SOD1(G93A) mice, *Experimental Neurology* 215(2) (2009) 281-9.
- [23] D.R. Borchelt, T. Ratovitski, J. van Lare, M.K. Lee, V. Gonzales, N.A. Jenkins, N.G. Copeland, D.L. Price, S.S. Sisodia, Accelerated amyloid deposition in the brains of transgenic

- mice coexpressing mutant presenilin 1 and amyloid precursor proteins, *Neuron* 19(4) (1997) 939-45.
- [24] Q. Xiao, P. Yan, X. Ma, H. Liu, R. Perez, A. Zhu, E. Gonzales, J.M. Burchett, D.R. Schuler, J.R. Cirrito, A. Diwan, J.M. Lee, Enhancing astrocytic lysosome biogenesis facilitates Abeta clearance and attenuates amyloid plaque pathogenesis, *J Neurosci* 34(29) (2014) 9607-20.
- [25] J.R. Cirrito, P.C. May, M.A. O'Dell, J.W. Taylor, M. Parsadanian, J.W. Cramer, J.E. Audia, J.S. Nissen, K.R. Bales, S.M. Paul, R.B. DeMattos, D.M. Holtzman, In vivo assessment of brain interstitial fluid with microdialysis reveals plaque-associated changes in amyloid-beta metabolism and half-life, *The Journal of neuroscience : the official journal of the Society for Neuroscience* 23(26) (2003) 8844-53.
- [26] J.R. Cirrito, K.A. Yamada, M.B. Finn, R.S. Sloviter, K.R. Bales, P.C. May, D.D. Schoepp, S.M. Paul, S. Mennerick, D.M. Holtzman, Synaptic activity regulates interstitial fluid amyloid-beta levels in vivo, *Neuron* 48(6) (2005) 913-22.
- [27] J.C. Hettinger, H. Lee, G. Bu, D.M. Holtzman, J.R. Cirrito, AMPA-ergic regulation of amyloid-beta levels in an Alzheimer's disease mouse model, *Mol Neurodegener* 13(1) (2018) 22.
- [28] W. Farris, S.G. Schutz, J.R. Cirrito, G.M. Shankar, X. Sun, A. George, M.A. Leissring, D.M. Walsh, W.Q. Qiu, D.M. Holtzman, D.J. Selkoe, Loss of neprilysin function promotes amyloid plaque formation and causes cerebral amyloid angiopathy, *The American journal of pathology* 171(1) (2007) 241-51.
- [29] J.H. Roh, Y. Huang, A.W. Bero, T. Kasten, F.R. Stewart, R.J. Bateman, D.M. Holtzman, Disruption of the sleep-wake cycle and diurnal fluctuation of beta-amyloid in mice with Alzheimer's disease pathology, *Sci Transl Med* 4(150) (2012) 150ra122.
- [30] H. Braak, E. Braak, Neuropathological stageing of Alzheimer-related changes, *Acta Neuropathol* 82(4) (1991) 239-59.
- [31] P.G. Ridge, C.M. Karch, S. Hsu, I. Arano, C.C. Teerlink, M.T.W. Ebbert, J.D. Gonzalez Murcia, J.M. Farnham, A.R. Damato, M. Allen, X. Wang, O. Harari, V.M. Fernandez, R. Guerreiro, J. Bras, J. Hardy, R. Munger, M. Norton, C. Sassi, A. Singleton, S.G. Younkin, D.W. Dickson, T.E. Golde, N.D. Price, N. Ertekin-Taner, C. Cruchaga, A.M. Goate, C. Corcoran, J. Tschanz, L.A. Cannon-Albright, J.S.K. Kauwe, I. Alzheimer's Disease Neuroimaging, Linkage, whole genome sequence, and biological data implicate variants in RAB10 in Alzheimer's disease resilience, *Genome Med* 9(1) (2017) 100.
- [32] W.S. Liang, T. Dunckley, T.G. Beach, A. Grover, D. Mastroeni, D.G. Walker, R.J. Caselli, W.A. Kukull, D. McKeel, J.C. Morris, C. Hulette, D. Schmechel, G.E. Alexander, E.M. Reiman, J. Rogers, D.A. Stephan, Gene expression profiles in anatomically and functionally distinct regions of the normal aged human brain, *Physiol Genomics* 28(3) (2007) 311-22.
- [33] P. Fazzari, K. Horre, A.M. Arranz, C.S. Frigerio, T. Saito, T.C. Saido, B. De Strooper, PLD3 gene and processing of APP, *Nature* 541(7638) (2017) E1-E2.
- [34] J.M. Tarasoff-Conway, R.O. Carare, R.S. Osorio, L. Glodzik, T. Butler, E. Fieremans, L. Axel, H. Rusinek, C. Nicholson, B.V. Zlokovic, B. Frangione, K. Blennow, J. Menard, H. Zetterberg, T. Wisniewski, M.J. de Leon, Clearance systems in the brain-implications for Alzheimer disease, *Nat Rev Neurol* 11(8) (2015) 457-70.
- [35] K.G. Mawuenyega, W. Sigurdson, V. Ovod, L. Munsell, T. Kasten, J.C. Morris, K.E. Yarasheski, R.J. Bateman, Decreased clearance of CNS beta-amyloid in Alzheimer's disease, *Science* 330(6012) (2010) 1774.

- [36] A.W. Bero, P. Yan, J.H. Roh, J.R. Cirrito, F.R. Stewart, M.E. Raichle, J.M. Lee, D.M. Holtzman, Neuronal activity regulates the regional vulnerability to amyloid-beta deposition, *Nat Neurosci* 14(6) (2011) 750-6.
- [37] C.M. Vander Zanden, L. Wampler, I. Bowers, E.B. Watkins, J. Majewski, E.Y. Chi, Fibrillar and Nonfibrillar Amyloid Beta Structures Drive Two Modes of Membrane-Mediated Toxicity, *Langmuir* 35(48) (2019) 16024-16036.
- [38] Y. Wang, T.K. Ulland, J.D. Ulrich, W. Song, J.A. Tzaferis, J.T. Hole, P. Yuan, T.E. Mahan, Y. Shi, S. Gilfillan, M. Cella, J. Grutzendler, R.B. DeMattos, J.R. Cirrito, D.M. Holtzman, M. Colonna, TREM2-mediated early microglial response limits diffusion and toxicity of amyloid plaques, *J Exp Med* 213(5) (2016) 667-75.
- [39] J.D. Ulrich, T.K. Ulland, T.E. Mahan, S. Nystrom, K.P. Nilsson, W.M. Song, Y. Zhou, M. Reinartz, S. Choi, H. Jiang, F.R. Stewart, E. Anderson, Y. Wang, M. Colonna, D.M. Holtzman, ApoE facilitates the microglial response to amyloid plaque pathology, *J Exp Med* 215(4) (2018) 1047-1058.
- [40] T.K. Ulland, W.M. Song, S.C. Huang, J.D. Ulrich, A. Sergushichev, W.L. Beatty, A.A. Loboda, Y. Zhou, N.J. Cairns, A. Kambal, E. Loginicheva, S. Gilfillan, M. Cella, H.W. Virgin, E.R. Unanue, Y. Wang, M.N. Artyomov, D.M. Holtzman, M. Colonna, TREM2 Maintains Microglial Metabolic Fitness in Alzheimer's Disease, *Cell* 170(4) (2017) 649-663 e13.
- [41] J.D. Ulrich, M.B. Finn, Y. Wang, A. Shen, T.E. Mahan, H. Jiang, F.R. Stewart, L. Piccio, M. Colonna, D.M. Holtzman, Altered microglial response to Abeta plaques in APPPS1-21 mice heterozygous for TREM2, *Mol Neurodegener* 9 (2014) 20.
- [42] S. Krasemann, C. Madore, R. Cialic, C. Baufeld, N. Calcagno, R. El Fatimy, L. Beckers, E. O'Loughlin, Y. Xu, Z. Fanek, D.J. Greco, S.T. Smith, G. Tweet, Z. Humulock, T. Zrzavy, P. Conde-Sanroman, M. Gacias, Z. Weng, H. Chen, E. Tjon, F. Mazaheri, K. Hartmann, A. Madi, J.D. Ulrich, M. Glatzel, A. Worthmann, J. Heeren, B. Budnik, C. Lemere, T. Ikezu, F.L. Heppner, V. Litvak, D.M. Holtzman, H. Lassmann, H.L. Weiner, J. Ochando, C. Haass, O. Butovsky, The TREM2-APOE Pathway Drives the Transcriptional Phenotype of Dysfunctional Microglia in Neurodegenerative Diseases, *Immunity* 47(3) (2017) 566-581 e9.
- [43] H. Keren-Shaul, A. Spinrad, A. Weiner, O. Matcovitch-Natan, R. Dvir-Szternfeld, T.K. Ulland, E. David, K. Baruch, D. Lara-Astaiso, B. Toth, S. Itzkovitz, M. Colonna, M. Schwartz, I. Amit, A Unique Microglia Type Associated with Restricting Development of Alzheimer's Disease, *Cell* 169(7) (2017) 1276-1290 e17.
- [44] N.M. Dräger, S.M. Sattler, C.T.-L. Huang, O.M. Teter, K. Leng, S.H. Hashemi, J. Hong, C.D. Clelland, L. Zhan, L. Kodama, A.B. Singleton, M.A. Nalls, J. Ichida, M.E. Ward, F. Faghri, L. Gan, M. Kampmann, A CRISPRi/a platform in iPSC-derived microglia uncovers regulators of disease states, *bioRxiv* (2021) 2021.06.16.448639.
- [45] C.M. Karch, A.M. Goate, Alzheimer's Disease Risk Genes and Mechanisms of Disease Pathogenesis, *Biol Psychiatry* (2014).
- [46] R. Sims, S.J. van der Lee, A.C. Naj, C. Bellenguez, N. Badarinarayan, J. Jakobsdottir, B.W. Kunkle, A. Boland, R. Raybould, J.C. Bis, E.R. Martin, B. Grenier-Boley, S. Heilmann-Heimbach, V. Chouraki, A.B. Kuzma, K. Sleegers, M. Vronskaya, A. Ruiz, R.R. Graham, R. Olaso, P. Hoffmann, M.L. Grove, B.N. Vardarajan, M. Hiltunen, M.M. Nothen, C.C. White, K.L. Hamilton-Nelson, J. Epelbaum, W. Maier, S.H. Choi, G.W. Beecham, C. Dulary, S. Herms, A.V. Smith, C.C. Funk, C. Derbois, A.J. Forstner, S. Ahmad, H. Li, D. Bacq, D. Harold, C.L. Satizabal, O. Valladares, A. Squassina, R. Thomas, J.A. Brody, L. Qu, P. Sanchez-Juan, T. Morgan, F.J. Wolters, Y. Zhao, F.S. Garcia, N. Denning, M. Fornage, J. Malamon, M.C.D.

Naranjo, E. Majounie, T.H. Mosley, B. Dombroski, D. Wallon, M.K. Lupton, J. Dupuis, P. Whitehead, L. Fratiglioni, C. Medway, X. Jian, S. Mukherjee, L. Keller, K. Brown, H. Lin, L.B. Cantwell, F. Panza, B. McGuinness, S. Moreno-Grau, J.D. Burgess, V. Solfrizzi, P. Proitsi, H.H. Adams, M. Allen, D. Seripa, P. Pastor, L.A. Cupples, N.D. Price, D. Hannequin, A. Frank-Garcia, D. Levy, P. Chakrabarty, P. Caffarra, I. Giegling, A.S. Beiser, V. Giedraitis, H. Hampel, M.E. Garcia, X. Wang, L. Lannfelt, P. Mecocci, G. Eiriksdottir, P.K. Crane, F. Pasquier, V. Boccardi, I. Henandez, R.C. Barber, M. Scherer, L. Tarraga, P.M. Adams, M. Leber, Y. Chen, M.S. Albert, S. Riedel-Heller, V. Emilsson, D. Beekly, A. Braae, R. Schmidt, D. Blacker, C. Masullo, H. Schmidt, R.S. Doody, G. Spalletta, W.T. Longstreth, Jr., T.J. Fairchild, P. Bossu, O.L. Lopez, M.P. Frosch, E. Sacchinelli, B. Ghetti, Q. Yang, R.M. Huebinger, F. Jessen, S. Li, M.I. Kamboh, J. Morris, O. Sotolongo-Grau, M.J. Katz, C. Corcoran, M. Dunstan, A. Braddel, C. Thomas, A. Meggy, R. Marshall, A. Gerrish, J. Chapman, M. Aguilar, S. Taylor, M. Hill, M.D. Fairen, A. Hodges, B. Vellas, H. Soininen, I. Kloszewska, M. Daniilidou, J. Uphill, Y. Patel, J.T. Hughes, J. Lord, J. Turton, A.M. Hartmann, R. Cecchetti, C. Fenoglio, M. Serpente, M. Arcaro, C. Caltagirone, M.D. Orfei, A. Ciaramella, S. Pichler, M. Mayhaus, W. Gu, A. Lleo, J. Fortea, R. Blesa, I.S. Barber, K. Brookes, C. Cupidi, R.G. Maletta, D. Carrell, S. Sorbi, S. Moebus, M. Urbano, A. Pilotto, J. Kornhuber, P. Bosco, S. Todd, D. Craig, J. Johnston, M. Gill, B. Lawlor, A. Lynch, N.C. Fox, J. Hardy, A. Consortium, R.L. Albin, L.G. Apostolova, S.E. Arnold, S. Asthana, C.S. Atwood, C.T. Baldwin, L.L. Barnes, S. Barral, T.G. Beach, J.T. Becker, E.H. Bigio, T.D. Bird, B.F. Boeve, J.D. Bowen, A. Boxer, J.R. Burke, J.M. Burns, J.D. Buxbaum, N.J. Cairns, C. Cao, C.S. Carlson, C.M. Carlsson, R.M. Carney, M.M. Carrasquillo, S.L. Carroll, C.C. Diaz, H.C. Chui, D.G. Clark, D.H. Cribbs, E.A. Crocco, C. DeCarli, M. Dick, R. Duara, D.A. Evans, K.M. Faber, K.B. Fallon, D.W. Fardo, M.R. Farlow, S. Ferris, T.M. Foroud, D.R. Galasko, M. Gearing, D.H. Geschwind, J.R. Gilbert, N.R. Graff-Radford, R.C. Green, J.H. Growdon, R.L. Hamilton, L.E. Harrell, L.S. Honig, M.J. Huentelman, C.M. Hulette, B.T. Hyman, G.P. Jarvik, E. Abner, L.W. Jin, G. Jun, A. Karydas, J.A. Kaye, R. Kim, N.W. Kowall, J.H. Kramer, F.M. LaFerla, J.J. Lah, J.B. Leverenz, A.I. Levey, G. Li, A.P. Lieberman, K.L. Lunetta, C.G. Lyketsos, D.C. Marson, F. Martiniuk, D.C. Mash, E. Masliah, W.C. McCormick, S.M. McCurry, A.N. McDavid, A.C. McKee, M. Mesulam, B.L. Miller, C.A. Miller, J.W. Miller, J.C. Morris, J.R. Murrell, A.J. Myers, S. O'Bryant, J.M. Olichney, V.S. Pankratz, J.E. Parisi, H.L. Paulson, W. Perry, E. Peskind, A. Pierce, W.W. Poon, H. Potter, J.F. Quinn, A. Raj, M. Raskind, B. Reisberg, C. Reitz, J.M. Ringman, E.D. Roberson, E. Rogaeva, H.J. Rosen, R.N. Rosenberg, M.A. Sager, A.J. Saykin, J.A. Schneider, L.S. Schneider, W.W. Seeley, A.G. Smith, J.A. Sonnen, S. Spina, R.A. Stern, R.H. Swerdlow, R.E. Tanzi, T.A. Thornton-Wells, J.Q. Trojanowski, J.C. Troncoso, V.M. Van Deerlin, L.J. Van Eldik, H.V. Vinters, J.P. Vonsattel, S. Weintraub, K.A. Welsh-Bohmer, K.C. Wilhelmsen, J. Williamson, T.S. Wingo, R.L. Woltjer, C.B. Wright, C.E. Yu, L. Yu, F. Garzia, F. Golamaully, G. Septier, S. Engelborghs, R. Vandenberghe, P.P. De Deyn, C.M. Fernandez, Y.A. Benito, H. Thonberg, C. Forsell, L. Lilius, A. Kinhult-Stahlbom, L. Kilander, R. Brundin, L. Concari, S. Helisalmi, A.M. Koivisto, A. Haapasalo, V. Dermecourt, N. Fievet, O. Hanon, C. Dufouil, A. Brice, K. Ritchie, B. Dubois, J.J. Himali, C.D. Keene, J. Tschanz, A.L. Fitzpatrick, W.A. Kukull, M. Norton, T. Aspelund, E.B. Larson, R. Munger, J.I. Rotter, R.B. Lipton, M.J. Bullido, A. Hofman, T.J. Montine, E. Coto, E. Boerwinkle, R.C. Petersen, V. Alvarez, F. Rivadeneira, E.M. Reiman, M. Gallo, C.J. O'Donnell, J.S. Reisch, A.C. Bruni, D.R. Royall, M. Dichgans, M. Sano, D. Galimberti, P. St George-Hyslop, E. Scarpini, D.W. Tsuang, M. Mancuso, U. Bonuccelli, A.R. Winslow, A. Daniele, C.K. Wu, C.A.E. Gerad/Perades, O. Peters, B. Nacmias, M.

- Riemenschneider, R. Heun, C. Brayne, D.C. Rubinsztein, J. Bras, R. Guerreiro, A. Al-Chalabi, C.E. Shaw, J. Collinge, D. Mann, M. Tsolaki, J. Clarimon, R. Sussams, S. Lovestone, M.C. O'Donovan, M.J. Owen, T.W. Behrens, S. Mead, A.M. Goate, A.G. Uitterlinden, C. Holmes, C. Cruchaga, M. Ingelsson, D.A. Bennett, J. Powell, T.E. Golde, C. Graff, P.L. De Jager, K. Morgan, N. Ertekin-Taner, O. Combarros, B.M. Psaty, P. Passmore, S.G. Younkin, C. Berr, V. Gudnason, D. Rujescu, D.W. Dickson, J.F. Dartigues, A.L. DeStefano, S. Ortega-Cubero, H. Hakonarson, D. Campion, M. Boada, J.K. Kauwe, L.A. Farrer, C. Van Broeckhoven, M.A. Ikram, L. Jones, J.L. Haines, C. Tzourio, L.J. Launer, V. Escott-Price, R. Mayeux, J.F. Deleuze, N. Amin, P.A. Holmans, M.A. Pericak-Vance, P. Amouyel, C.M. van Duijn, A. Ramirez, L.S. Wang, J.C. Lambert, S. Seshadri, J. Williams, G.D. Schellenberg, Rare coding variants in PLCG2, ABI3, and TREM2 implicate microglial-mediated innate immunity in Alzheimer's disease, *Nat Genet* 49(9) (2017) 1373-1384.
- [47] S. Hsu, A.A. Pimenova, K. Hayes, J.A. Villa, M.J. Rosene, M. Jere, A.M. Goate, C.M. Karch, Systematic validation of variants of unknown significance in APP, PSEN1 and PSEN2, *Neurobiol Dis* 139 (2020) 104817.
- [48] S. Hsu, B.A. Gordon, R. Hornbeck, J.B. Norton, D. Levitch, A. Louden, E. Ziegemeier, R. Laforce, Jr., J. Chhatwal, G.S. Day, E. McDade, J.C. Morris, A.M. Fagan, T.L.S. Benzinger, A.M. Goate, C. Cruchaga, R.J. Bateman, N. Dominantly Inherited Alzheimer, C.M. Karch, Discovery and validation of autosomal dominant Alzheimer's disease mutations, *Alzheimers Res Ther* 10(1) (2018) 67.
- [49] A.S. Mukadam, S.Y. Breusegem, M.N.J. Seaman, Analysis of novel endosome-to-Golgi retrieval genes reveals a role for PLD3 in regulating endosomal protein sorting and amyloid precursor protein processing, *Cell Mol Life Sci* 75(14) (2018) 2613-2625.
- [50] A.C. Gonzalez, M. Schweizer, S. Jagdmann, C. Bernreuther, T. Reinheckel, P. Saftig, M. Damme, Unconventional Trafficking of Mammalian Phospholipase D3 to Lysosomes, *Cell Rep* 22(4) (2018) 1040-1053.
- [51] L.C. Walker, Abeta Plaques, *Free Neuropathol* 1 (2020).
- [52] A.R. Ladiwala, J. Litt, R.S. Kane, D.S. Aucoin, S.O. Smith, S. Ranjan, J. Davis, W.E. Van Nostrand, P.M. Tessier, Conformational differences between two amyloid beta oligomers of similar size and dissimilar toxicity, *J Biol Chem* 287(29) (2012) 24765-73.
- [53] Y. Zhang, K. Chen, S.A. Sloan, M.L. Bennett, A.R. Scholze, S. O'Keeffe, H.P. Phatnani, P. Guarnieri, C. Caneda, N. Ruderisch, S. Deng, S.A. Liddelow, C. Zhang, R. Daneman, T. Maniatis, B.A. Barres, J.Q. Wu, An RNA-sequencing transcriptome and splicing database of glia, neurons, and vascular cells of the cerebral cortex, *J Neurosci* 34(36) (2014) 11929-47.
- [54] C. Sala Frigerio, L. Wolfs, N. Fattorelli, N. Thrupp, I. Voytyuk, I. Schmidt, R. Mancuso, W.T. Chen, M.E. Woodbury, G. Srivastava, T. Moller, E. Hudry, S. Das, T. Saido, E. Karran, B. Hyman, V.H. Perry, M. Fiers, B. De Strooper, The Major Risk Factors for Alzheimer's Disease: Age, Sex, and Genes Modulate the Microglia Response to Abeta Plaques, *Cell Rep* 27(4) (2019) 1293-1306 e6.
- [55] T.D. Troutman, E. Kofman, C.K. Glass, Exploiting dynamic enhancer landscapes to decode macrophage and microglia phenotypes in health and disease, *Mol Cell* 81(19) (2021) 3888-3903.

4.8



## **Chapter 5: Conclusions**

## **5.1 Introduction**

Since it was first observed and characterized by Aloysius Alzheimer back in 1908, Alzheimer disease (AD) has remained one of the biggest medical challenges to humanity. However, the lack of effective therapeutics should not be mistaken as a lack of understanding of the disease. Over decades of AD research, significant contributions have been made to the understanding of AD genetics and core disease mechanisms. Through these efforts, the research has been able to shed light on the breadth of genes that affect AD, the cellular pathways involved, and the mechanistic steps that drive disease. In this dissertation, I outlined our work in expanding our knowledge through three genes: *LMNA*, *RAB10*, and *PLD3*.

## **5.2 Dissertation work furthers research into genetics driving AD pathology**

### *LMNA and the role of nucleoskeletal integrity in AD*

When studying a particular disease, much can be gained from looking at similar diseases that share characteristics. A perfect example of this is the nucleoskeletal dysfunction observed in AD that occurs in more well-studied laminopathies. In **Chapter 2**, we demonstrate how mRNA expression from laser-captured microdissected neurons leads to dysregulation in the expression of *LMNA* and *ZMPSTE24*, causing an imbalance of mature lamin A protein in a manner that resembles what is observed in Hutchinson Guilford Progeria Syndrome (HGPS). As a result, the many of the same nucleoskeletal dysfunction observed in HGPS is also observed in AD [1, 2]. This can result in changes in the nucleoskeletal dysfunction, such as the formation of tubular

invaginations in the nuclear membrane [3]. These alterations to the nuclear shape can cause changes to chromatin structure, abnormal gene expression, and increased DNA damage [1, 2, 4]. Furthermore, when HGPS was induced in iPSC-derived neurons through forced progerin expression, many of the genes disrupted by progerin were found to match those disrupted in AD, notably lysosomal signaling. Irregularities in the structure of the nuclear lamina can also be caused by influences outside the nucleus, such as alterations to the cytoskeleton driven by tau accumulation can also alter the nuclear lamina through the linker of nucleoskeleton and cytoskeleton (LINC) complex [3]. Therefore, while nuclear defects are observed in AD, it is yet to be seen whether such changes occur as the result of AD pathology or vice versa.

*RAB10 variant rs142787485 may confer resilience to AD through a miRNA-centric pathway*

As we learn more about the genetics of AD, we must also dedicate our efforts to identifying variants that protect against AD, for understanding such variants could grant us invaluable insight for the development of therapeutics that emulate the mechanistic elements of these variants. In **Chapter 3**, we discuss an example of such a variant and how it may confer resilience to disease. A SNP in the 3'-UTR of *RAB10*, rs142787485, was identified when studying the genomes of individuals at least 75 years old and cognitively normal despite carrying at least a single copy of *APOE4*, which is associated with at least a 3-4 fold increase in disease risk. In the original study, silencing of *RAB10* resulted in a shift of the ratio of A $\beta$ 42/40 in a manner that was less prone to aggregation [5]. In agreement with this, RAB10 protein levels were elevated in AD brains, leading us to hypothesize that overexpression of *RAB10* was conducive to AD development and the rs142787485 SNP acted opposite to this by reducing

expression. However, unexpectedly, the SNP was found to have no effect on mRNA expression of *RAB10* and there was no significant allele specific expression between WT and SNP alleles. This leads us to consider post-transcriptional regulation of *RAB10* expression, such as miRNA. Rs142787485 is predicted to disrupt the binding of six miRNAs. However, further biochemical verification is required to investigate this possibility further.

As a member of the Rab family of GTPases, *RAB10* serves as a key regulator of subcellular vesicle and trafficking pathways, from the regulation of ER dynamics to the regulation of recycling endosome tubulization and endosomal function and recruitment of CNT-1 [6-8]. *RAB10* is also associated with lysosomal secretion during stress [9] and requires phosphorylation at threonine 73 (T73) by leucine rich repeat kinase 2 (*LRRK2*), a known risk gene in Parkinson's disease [10]. This is especially intriguing because APP processing occurs within many of these same compartments [11]. Additional protective factors associated with reduced AD risk are also function proximally to the process of APP metabolism, such as the *APP* A673T mutation [12] or the *APOE* R136S Christchurch mutation [13, 14].

### *PLD3 alters the microglial response and amyloid pathology as a response*

In **Chapter 4**, using both *in vitro* and *in vivo* systems, we investigated the role of *PLD3*, an enzyme with genetic variants that were associated with disease risk. Using iPSC-derived cortical neurons, we show that the silent mutation *PLD3* A442A was sufficient to both alter the splicing of *PLD3* and omit exon 11, in corroboration to what was observed in the brains of carriers [15], and increase overall secreted A $\beta$  levels. Furthermore, when *Pld3* expression was reduced in an amyloid mouse model, the overall turnover of A $\beta$  was significantly inhibited, implying that *Pld3* played an important role in the clearance of A $\beta$ . When *Pld3* was knocked out

in this same mouse model, we also observe a change in the microglial response, demonstrated by a significant decrease in microglial recruitment around amyloid plaques. This altered microglial response leads to a shift in the overall makeup of amyloid plaques, resulting in plaques that are less fibrillary and more diffuse in nature, which have been shown to be more toxic overall. This is found to mirror what is observed in amyloid mouse models deficient for *Trem2* [16], a gene found to play an important role in the activation of disease associated microglia (DAM) [17], and when we ran an RNAseq analysis on our amyloid mice deficient for *Pld3*, we observed a shift in expression of genes associated with the DAM response. Furthermore, when we looked at snRNAseq data from human brains, we find upregulation of *PLD3* in activated microglia, further establishing that *PLD3* plays an important role in the microglial response to disease. Conversely, microglia with mutant *TREM2* expressed reduced microglial levels, also establishing the link we are observing between *PLD3* and *TREM2*. Considering this, it may be possible that therapeutic strategies that have been developed for *TREM2*-mediated processes can be leveraged to target *PLD3* as well.

### **5.3 Future directions: linking AD genetics, intracellular and extracellular processes, and AD pathology**

The genetics of LOAD is incredibly complex. In the scope of the work outlined in this dissertation, we examine seemingly disparate genes and how they ultimately drive AD risk. From looking at the genetics, much can be learned about these disease-relevant pathways and how they relate to each other. For example, while we discuss the roles played by nucleoskeletal integrity (**Chapter 2**) and the endo-lysosomal network (**Chapter 3**), it must also be remembered how these pathways are interconnected. Nutrient sensing between the lysosome and the nucleus

control energy metabolism [18] and TFEB-mediated lysosomal biogenesis requires tightly controlled signaling between both the lysosome and the nucleus [19].

Additionally, we examine the contribution of AD risk genes to processes outside of the neuron, with our findings showing how *PLD3* drives the microglial response to A $\beta$  (**Chapter 4**). This provides compelling support for investigations into the contribution of glia cells to AD pathogenesis. Therapeutic approaches that target nuclear-endo-lysosomal networks and promote glia function build off key genetic findings and hold promise for the future.

## 5.4 References

- [1] B. Frost, F.H. Bardai, M.B. Feany, Lamin Dysfunction Mediates Neurodegeneration in Tauopathies, *Curr Biol* 26(1) (2016) 129-36.
- [2] B. Frost, M. Hemberg, J. Lewis, M.B. Feany, Tau promotes neurodegeneration through global chromatin relaxation, *Nat Neurosci* 17(3) (2014) 357-66.
- [3] B. Frost, Alzheimer's disease: An acquired neurodegenerative laminopathy, *Nucleus* 7(3) (2016) 275-83.
- [4] J.A. Mellad, D.T. Warren, C.M. Shanahan, Nesprins LINC the nucleus and cytoskeleton, *Curr Opin Cell Biol* 23(1) (2011) 47-54.
- [5] P.G. Ridge, C.M. Karch, S. Hsu, I. Arano, C.C. Teerlink, M.T.W. Ebbert, J.D. Gonzalez Murcia, J.M. Farnham, A.R. Damato, M. Allen, X. Wang, O. Harari, V.M. Fernandez, R. Guerreiro, J. Bras, J. Hardy, R. Munger, M. Norton, C. Sassi, A. Singleton, S.G. Younkin, D.W. Dickson, T.E. Golde, N.D. Price, N. Ertekin-Taner, C. Cruchaga, A.M. Goate, C. Corcoran, J. Tschanz, L.A. Cannon-Albright, J.S.K. Kauwe, I. Alzheimer's Disease Neuroimaging, Linkage, whole genome sequence, and biological data implicate variants in RAB10 in Alzheimer's disease resilience, *Genome Med* 9(1) (2017) 100.
- [6] C.C. Chen, P.J. Schweinsberg, S. Vashist, D.P. Mareiniss, E.J. Lambie, B.D. Grant, RAB-10 is required for endocytic recycling in the *Caenorhabditis elegans* intestine, *Mol Biol Cell* 17(3) (2006) 1286-97.
- [7] S. Pant, M. Sharma, K. Patel, S. Caplan, C.M. Carr, B.D. Grant, AMPH-1/Amphiphysin/Bin1 functions with RME-1/Ehd1 in endocytic recycling, *Nat Cell Biol* 11(12) (2009) 1399-410.
- [8] A. Shi, C.C. Chen, R. Banerjee, D. Glodowski, A. Audhya, C. Rongo, B.D. Grant, EHBP-1 functions with RAB-10 during endocytic recycling in *Caenorhabditis elegans*, *Mol Biol Cell* 21(16) (2010) 2930-43.
- [9] T. Eguchi, T. Kuwahara, M. Sakurai, T. Komori, T. Fujimoto, G. Ito, S.I. Yoshimura, A. Harada, M. Fukuda, M. Koike, T. Iwatsubo, LRRK2 and its substrate Rab GTPases are sequentially targeted onto stressed lysosomes and maintain their homeostasis, *Proc Natl Acad Sci U S A* 115(39) (2018) E9115-E9124.
- [10] M. Steger, F. Tonelli, G. Ito, P. Davies, M. Trost, M. Vetter, S. Wachter, E. Lorentzen, G. Duddy, S. Wilson, M.A. Baptista, B.K. Fiske, M.J. Fell, J.A. Morrow, A.D. Reith, D.R. Alessi, M. Mann, Phosphoproteomics reveals that Parkinson's disease kinase LRRK2 regulates a subset of Rab GTPases, *Elife* 5 (2016).
- [11] R.W. Choy, Z. Cheng, R. Schekman, Amyloid precursor protein (APP) traffics from the cell surface via endosomes for amyloid beta (Abeta) production in the trans-Golgi network, *Proc Natl Acad Sci U S A* 109(30) (2012) E2077-82.
- [12] T. Jonsson, J.K. Atwal, S. Steinberg, J. Snaedal, P.V. Jonsson, S. Bjornsson, H. Stefansson, P. Sulem, D. Gudbjartsson, J. Maloney, K. Hoyte, A. Gustafson, Y. Liu, Y. Lu, T. Bhangale, R.R. Graham, J. Huttenlocher, G. Bjornsdottir, O.A. Andreassen, E.G. Jonsson, A. Palotie, T.W. Behrens, O.T. Magnusson, A. Kong, U. Thorsteinsdottir, R.J. Watts, K. Stefansson, A mutation in APP protects against Alzheimer's disease and age-related cognitive decline, *Nature* 488(7409) (2012) 96-9.

- [13] J.F. Arboleda-Velasquez, F. Lopera, M. O'Hare, S. Delgado-Tirado, C. Marino, N. Chmielewska, K.L. Saez-Torres, D. Amarnani, A.P. Schultz, R.A. Sperling, D. Leyton-Cifuentes, K. Chen, A. Baena, D. Aguillon, S. Rios-Romenets, M. Giraldo, E. Guzman-Velez, D.J. Norton, E. Pardilla-Delgado, A. Artola, J.S. Sanchez, J. Acosta-Uribe, M. Lalli, K.S. Kosik, M.J. Huentelman, H. Zetterberg, K. Blennow, R.A. Reiman, J. Luo, Y. Chen, P. Thiyyagura, Y. Su, G.R. Jun, M. Naymik, X. Gai, M. Bootwalla, J. Ji, L. Shen, J.B. Miller, L.A. Kim, P.N. Tariot, K.A. Johnson, E.M. Reiman, Y.T. Quiroz, Resistance to autosomal dominant Alzheimer's disease in an APOE3 Christchurch homozygote: a case report, *Nat Med* 25(11) (2019) 1680-1683.
- [14] M.R. Wardell, S.O. Brennan, E.D. Janus, R. Fraser, R.W. Carrell, Apolipoprotein E2-Christchurch (136 Arg----Ser). New variant of human apolipoprotein E in a patient with type III hyperlipoproteinemia, *J Clin Invest* 80(2) (1987) 483-90.
- [15] C. Cruchaga, C.M. Karch, S.C. Jin, B.A. Benitez, Y. Cai, R. Guerreiro, O. Harari, J. Norton, J. Budde, S. Bertelsen, A.T. Jeng, B. Cooper, T. Skorupa, D. Carrell, D. Levitch, S. Hsu, J. Choi, M. Ryten, C. Sassi, J. Bras, R.J. Gibbs, D.G. Hernandez, M.K. Lupton, J. Powell, P. Forabosco, P.G. Ridge, C.D. Corcoran, J.T. Tschanz, M.C. Norton, R.G. Munger, C. Schmutz, M. Leary, F.Y. Demirci, M.N. Bamne, X. Wang, O.L. Lopez, M. Ganguli, C. Medway, J. Turton, J. Lord, A. Braae, I. Barber, K. Brown, U.K.C. Alzheimer's Research, P. Pastor, O. Lorenzo-Betancor, Z. Brkanac, E. Scott, E. Topol, K. Morgan, E. Rogaeva, A. Singleton, J. Hardy, M.I. Kamboh, P.S. George-Hyslop, N. Cairns, J.C. Morris, J.S.K. Kauwe, A.M. Goate, Rare coding variants in the phospholipase D3 gene confer risk for Alzheimer's disease, *Nature* 505(7484) (2014) 550-554.
- [16] Y. Wang, T.K. Ulland, J.D. Ulrich, W. Song, J.A. Tzaferis, J.T. Hole, P. Yuan, T.E. Mahan, Y. Shi, S. Gilfillan, M. Cella, J. Grutzendler, R.B. DeMattos, J.R. Cirrito, D.M. Holtzman, M. Colonna, TREM2-mediated early microglial response limits diffusion and toxicity of amyloid plaques, *J Exp Med* 213(5) (2016) 667-75.
- [17] T.K. Ulland, M. Colonna, TREM2 - a key player in microglial biology and Alzheimer disease, *Nat Rev Neurol* 14(11) (2018) 667-675.
- [18] C. Settembre, A. Fraldi, D.L. Medina, A. Ballabio, Signals from the lysosome: a control centre for cellular clearance and energy metabolism, *Nat Rev Mol Cell Biol* 14(5) (2013) 283-96.
- [19] D.L. Medina, S. Di Paola, I. Peluso, A. Armani, D. De Stefani, R. Venditti, S. Montefusco, A. Scotto-Rosato, C. Prezioso, A. Forrester, C. Settembre, W. Wang, Q. Gao, H. Xu, M. Sandri, R. Rizzuto, M.A. De Matteis, A. Ballabio, Lysosomal calcium signalling regulates autophagy through calcineurin and TFEB, *Nat Cell Biol* 17(3) (2015) 288-99.

## **Appendix 1: Genes dysregulated by forced progerin expression in iPSC-derived neurons**

Gene	Direction in Progerin Transduction	Progerin v. GFP (82yr iPSC-mDA)		Progerin v. GFP (11yr iPSC-mDA)	
		B	p value	$\beta$	p value
<i>LMNA</i>	Upregulated	9.375119138	1.32827E-05	10.0911755	8.48901E-06
<i>NOP10</i>	Upregulated	1.732412984	0.000340553	1.52061923	0.000705462
<i>SNHG15</i>	Upregulated	1.695953272	0.000785928	1.526546192	0.001386872
<i>ENHO</i>	Upregulated	1.662578754	0.000393343	1.407485256	0.000987834
<i>NDUFB6</i>	Upregulated	1.628882059	6.66956E-05	1.223009584	0.000351228
<i>ATP5L</i>	Upregulated	1.592370717	0.000117022	1.006282614	0.001526688
<i>NEDD8</i>	Upregulated	1.58923555	0.000376062	1.005728895	0.004272559
<i>PPIB</i>	Upregulated	1.581496767	0.001149768	1.035550459	0.009467005
<i>TMSB10</i>	Upregulated	1.539837612	0.000215936	1.336688033	0.000481771
<i>PRDX4</i>	Upregulated	1.523527472	0.001043477	1.092313821	0.005709165
<i>FTL</i>	Upregulated	1.493552581	0.000767656	1.062409476	0.004515924
<i>TMSB4X</i>	Upregulated	1.487630688	0.000914481	1.124181183	0.003927462
<i>ATOX1</i>	Upregulated	1.475715084	0.000776274	1.337181808	0.001322595
<i>CCDC126</i>	Upregulated	1.471548609	9.38036E-05	1.524986052	7.6036E-05
<i>PSMB3</i>	Upregulated	1.469479933	0.000363831	1.7662128	0.000126458
<i>LOC100128822</i>	Upregulated	1.440876824	0.003203627	1.288058638	0.00555505
<i>TSNAX</i>	Upregulated	1.432132242	0.000142155	1.811161622	3.55279E-05
<i>TCEAL7</i>	Upregulated	1.431234805	0.00054714	1.454932214	0.000499293
<i>UBC</i>	Upregulated	1.421052124	0.000633532	1.185017044	0.001688352
<i>ZNHIT3</i>	Upregulated	1.413750616	0.001009087	1.016970098	0.005454953
<i>PCNA</i>	Upregulated	1.412258184	0.000977948	1.395867244	0.001041677
<i>LOC401397</i>	Upregulated	1.407637811	0.00054046	1.149132939	0.001624053
<i>C4orf52</i>	Upregulated	1.407547781	0.000745946	1.417019042	0.000718971
<i>NDUFA5</i>	Upregulated	1.40568193	0.001312865	1.372483429	0.001490613
<i>EAPP</i>	Upregulated	1.394670142	8.50607E-05	1.031926692	0.000480897
<i>COX14</i>	Upregulated	1.394087166	0.000609251	1.093212166	0.002241283
<i>UBE2T</i>	Upregulated	1.388059153	0.003153204	1.115053251	0.009018116
<i>SVIP</i>	Upregulated	1.381316067	0.001146964	1.96065781	0.000161219
<i>CD164</i>	Upregulated	1.380010993	0.006825565	1.296015267	0.009121577

<i>RPL12</i>	Upregulated	1.36974694	0.001058001	1.217411003	0.001976442
<i>SCOC</i>	Upregulated	1.366874738	0.001005535	1.494146665	0.000617733
<i>ARL6IP5</i>	Upregulated	1.345878412	0.000755084	1.151784162	0.00174209
<i>UBL5</i>	Upregulated	1.344510357	0.000256643	1.014211479	0.001226031
<i>SEC11C</i>	Upregulated	1.339729314	0.001157796	1.20654946	0.002013272
<i>VPS25</i>	Upregulated	1.33720159	0.002481602	1.060228961	0.007711955
<i>ITM2C</i>	Upregulated	1.335797925	0.00070546	1.100869062	0.00198831
<i>TFAM</i>	Upregulated	1.333673096	0.000317022	1.095345791	0.000946755
<i>PRDX1</i>	Upregulated	1.329438264	0.001626438	1.046293861	0.005442053
<i>ABHD10</i>	Upregulated	1.323920811	0.000421969	1.115009335	0.001086651
<i>BUD31</i>	Upregulated	1.323767091	0.000555846	1.08717058	0.001615903
<i>TCEB2</i>	Upregulated	1.323167527	0.002504316	1.03072709	0.008434898
<i>WRB</i>	Upregulated	1.316572465	8.44045E-05	1.309185664	8.72461E-05
<i>PFN1</i>	Upregulated	1.29309319	0.000276098	1.008897825	0.001095648
<i>TCEAL8</i>	Upregulated	1.290579091	0.004530056	1.238193914	0.005535314
<i>RGS2</i>	Upregulated	1.285635194	0.000622585	1.375285198	0.000427553
<i>C5orf15</i>	Upregulated	1.283325922	0.000411436	1.069294428	0.001123676
<i>ATP6V1G1</i>	Upregulated	1.280549183	9.25203E-05	1.038930694	0.000310087
<i>YPEL5</i>	Upregulated	1.259226231	0.001732238	1.388273829	0.00103031
<i>MT3</i>	Upregulated	1.256254073	0.005099663	1.2850998	0.004567633
<i>UQCR10</i>	Upregulated	1.2543698	0.006234145	1.17398857	0.008487298
<i>TMEM14A</i>	Upregulated	1.25326206	0.000111712	1.225318664	0.000127437
<i>DNAJC8</i>	Upregulated	1.249310085	0.001039804	1.073928287	0.00231018
<i>SUMO2</i>	Upregulated	1.246660271	0.000239595	1.326501812	0.00016757
<i>BEX1</i>	Upregulated	1.246459042	0.000175198	1.054059451	0.000455319
<i>NDUFB11</i>	Upregulated	1.246282072	0.003690317	1.120932613	0.006174686
<i>LAMTOR1</i>	Upregulated	1.24261885	0.000224845	1.154551038	0.00034192
<i>ATP5G3</i>	Upregulated	1.227488948	0.000466262	1.109774694	0.000814496
<i>VBPI</i>	Upregulated	1.225197596	0.000246745	1.1676853	0.000324518
<i>QPCT</i>	Upregulated	1.218729435	0.005333479	1.174432155	0.006363023
<i>ZCCHC10</i>	Upregulated	1.216985968	0.001141391	1.216938558	0.00114163
<i>NDUFBI</i>	Upregulated	1.212647595	0.000123582	1.177928905	0.000146358

<i>MMADHC</i>	Upregulated	1.209472174	0.000213209	1.258632949	0.000169429
<i>HSBP1</i>	Upregulated	1.209050371	0.000408007	1.048451016	0.00089813
<i>CAPZA2</i>	Upregulated	1.204062211	0.000428945	1.192510664	0.000452782
<i>CNO</i>	Upregulated	1.201577919	0.000484943	1.12808019	0.000688341
<i>SELT</i>	Upregulated	1.194192075	0.000280393	1.214488025	0.000254671
<i>CCDC72</i>	Upregulated	1.189499315	0.002739677	1.082352271	0.004388627
<i>ATF4</i>	Upregulated	1.189477222	0.000165305	1.048484664	0.000340589
<i>GABARAPL2</i>	Upregulated	1.164210414	0.001013557	1.084828859	0.001479084
<i>AASDHPPT</i>	Upregulated	1.16059799	0.000603085	1.189145455	0.00052693
<i>BANF1</i>	Upregulated	1.157267236	0.005998755	1.135876447	0.006552495
<i>SUB1</i>	Upregulated	1.153842938	0.00037788	1.276906092	0.000212118
<i>EIDI</i>	Upregulated	1.148286664	0.000232526	1.229711983	0.000156625
<i>SLIRP</i>	Upregulated	1.13062867	0.011809836	1.309167838	0.00603561
<i>PFDN2</i>	Upregulated	1.123582749	0.000624993	1.002655021	0.001162718
<i>EIF3M</i>	Upregulated	1.119433556	0.013692631	1.187841738	0.01055505
<i>CYB5A</i>	Upregulated	1.108970483	0.006173215	1.30981704	0.002722356
<i>FDFT1</i>	Upregulated	1.106928803	0.000715114	1.197020725	0.000463215
<i>CDC42</i>	Upregulated	1.106027634	0.000264574	1.030596382	0.000394985
<i>DYNLT3</i>	Upregulated	1.103555116	0.000981515	1.364816583	0.000301278
<i>C12orf29</i>	Upregulated	1.100854237	0.007379645	1.042798325	0.009462164
<i>RG9MTD1</i>	Upregulated	1.097127636	0.00469358	1.234738755	0.002603568
<i>FOS</i>	Upregulated	1.096376775	0.005246573	1.019374129	0.007406276
<i>CCT3</i>	Upregulated	1.09583174	0.000291884	1.037716754	0.000397397
<i>ZCRB1</i>	Upregulated	1.093920722	0.000689234	1.022551006	0.000996213
<i>TMBIM6</i>	Upregulated	1.090975514	0.004624553	1.035425691	0.005947867
<i>GTF2B</i>	Upregulated	1.090514909	0.006157066	1.186724489	0.004091316
<i>ILF2</i>	Upregulated	1.087075934	0.000461588	1.008799048	0.000698997
<i>POMP</i>	Upregulated	1.080594528	0.00271545	1.015387046	0.00371312
<i>ZBTB6</i>	Upregulated	1.070254806	0.001627732	1.165439369	0.001033216
<i>IDII</i>	Upregulated	1.068224421	0.000342885	1.238444019	0.000146769
<i>ISCA1</i>	Upregulated	1.066384941	0.00116214	1.139730622	0.000810485
<i>PRDX6</i>	Upregulated	1.065824536	0.004671756	1.013303186	0.005958031

<i>TTC33</i>	Upregulated	1.065522372	0.000798038	1.016663557	0.001030033
<i>ANAPC13</i>	Upregulated	1.063288186	0.003362158	1.134089648	0.00242506
<i>DDX24</i>	Upregulated	1.063240738	0.000632372	1.047341234	0.000687196
<i>CCNG1</i>	Upregulated	1.061535446	0.000447783	1.034146364	0.000518246
<i>TIMM17B</i>	Upregulated	1.048926853	0.006406986	1.069214238	0.005850419
<i>MRPS35</i>	Upregulated	1.04670965	0.002659618	1.093203808	0.002127518
<i>PGRMC1</i>	Upregulated	1.046018795	0.002961709	1.101093416	0.002279303
<i>CHMP1B</i>	Upregulated	1.045660536	0.002075504	1.320630421	0.000591945
<i>RPS19BP1</i>	Upregulated	1.043381039	0.003391494	1.259895772	0.001277592
<i>SRP9</i>	Upregulated	1.039507762	0.000754306	1.283344584	0.000230944
<i>CCDC90B</i>	Upregulated	1.039162909	0.001232157	1.064962543	0.001080123
<i>MORF4L1</i>	Upregulated	1.03172995	0.000402781	1.088873945	0.000296865
<i>EEF1E1</i>	Upregulated	1.028896714	0.005683054	1.010328598	0.006197528
<i>PPP2RIA</i>	Upregulated	1.018359924	0.00640431	1.037001665	0.005876339
<i>PSMA7</i>	Upregulated	1.014828284	0.001396944	1.398309312	0.000236669
<i>PDRG1</i>	Upregulated	1.010457811	0.000413788	1.048670218	0.000335564
<i>PKIB</i>	Upregulated	1.007233859	0.001785411	1.172290071	0.000791822
<i>JKAMP</i>	Upregulated	1.002594302	0.007475103	1.050402029	0.006005318
<i>DPM1</i>	Upregulated	1.002553264	0.000777388	1.024962041	0.000688507
<i>TAF7</i>	Upregulated	1.000735631	0.000354799	1.031068229	0.000299523
<i>RMRP</i>	Downregulated	-8.851971839	4.30933E-07	-5.281991101	1.03775E-05
<i>RPPH1</i>	Downregulated	-8.619304961	1.595E-05	-5.496631131	0.000228353
<i>MIR3648</i>	Downregulated	-6.585701345	0.000131097	-5.064513293	0.000585255
<i>MIR3687</i>	Downregulated	-6.374819645	7.622E-06	-4.526781303	5.99655E-05
<i>C3orf72</i>	Downregulated	-6.044405494	0.000114288	-4.008067503	0.001156125
<i>TNIP3</i>	Downregulated	-5.827706142	0.000263675	-4.651290485	0.000927715
<i>NOSTRIN</i>	Downregulated	-5.651875552	1.20323E-05	-4.75135728	3.42856E-05
<i>MIR663A</i>	Downregulated	-5.641911575	0.000120688	-3.905852314	0.000963661
<i>GVINPI</i>	Downregulated	-5.615661316	9.87421E-05	-4.935292069	0.000209159
<i>PRDM1</i>	Downregulated	-5.59753266	3.53303E-07	-4.221939062	2.02903E-06
<i>C1orf129</i>	Downregulated	-5.596359896	2.76693E-05	-4.161838477	0.000159349
<i>MARCO</i>	Downregulated	-5.540452894	1.30404E-05	-3.983836365	9.375E-05

<i>TG</i>	Downregulated	-5.514495944	0.000149728	-3.450092491	0.002008437
<i>PEAR1</i>	Downregulated	-5.506832379	0.000225218	-2.957864199	0.006104584
<i>LAMC3</i>	Downregulated	-5.488530257	0.000215513	-3.232439026	0.00376113
<i>BCAS1</i>	Downregulated	-5.456480576	3.55782E-05	-4.201447975	0.000166081
<i>LOC285084</i>	Downregulated	-5.455054283	0.000248615	-4.902979756	0.000455009
<i>CDHR4</i>	Downregulated	-5.419948845	0.000142573	-2.87908578	0.004397591
<i>FLI1</i>	Downregulated	-5.377504396	0.000112121	-3.959509903	0.000641868
<i>SLC14A2</i>	Downregulated	-5.370557061	6.0004E-05	-4.869525804	0.000106867
<i>BHMT2</i>	Downregulated	-5.356535859	5.024E-05	-4.63939721	0.000117279
<i>SH3TC2</i>	Downregulated	-5.295859945	9.78101E-05	-4.139587761	0.00040382
<i>OLAH</i>	Downregulated	-5.259765054	1.60909E-05	-4.155763936	6.59873E-05
<i>STAB2</i>	Downregulated	-5.247178519	0.000108691	-3.757445641	0.000726726
<i>SLC5A1</i>	Downregulated	-5.174231377	0.000877214	-4.349661726	0.002205082
<i>SLFN11</i>	Downregulated	-5.174231377	0.001120685	-4.986952075	0.001364999
<i>VIT</i>	Downregulated	-5.169295031	0.002282804	-4.690799402	0.003731485
<i>KIAA1755</i>	Downregulated	-5.122768245	0.000913254	-3.646520793	0.005251622
<i>SEC14L4</i>	Downregulated	-5.122768245	0.001902222	-3.839248466	0.007887924
<i>LEP</i>	Downregulated	-5.106981704	0.000137876	-5.338755574	0.000106403
<i>SHE</i>	Downregulated	-5.089692078	4.48004E-05	-3.234547268	0.000613887
<i>DISCI</i>	Downregulated	-5.061800716	1.81558E-06	-3.113790338	3.50604E-05
<i>GJA5</i>	Downregulated	-5.047290363	0.001477877	-3.528807428	0.008704362
<i>SNORA53</i>	Downregulated	-5.036319087	3.43144E-06	-2.924236729	9.11993E-05
<i>LOC284801</i>	Downregulated	-5.009382814	0.000139815	-5.08491218	0.000128146
<i>APCDD1L</i>	Downregulated	-4.990037674	0.000324201	-3.089211664	0.004184548
<i>LOC100507156</i>	Downregulated	-4.957243503	0.000215936	-2.479235105	0.008233865
<i>TBXA2R</i>	Downregulated	-4.946797913	2.22189E-05	-3.895023617	9.22825E-05
<i>FOXD2</i>	Downregulated	-4.942787632	0.00360873	-4.113055228	0.008684239
<i>EMR2</i>	Downregulated	-4.912064424	0.000528967	-3.260856587	0.004553361
<i>LOC727710</i>	Downregulated	-4.910864391	4.77869E-05	-4.422427659	8.88356E-05
<i>HOXC8</i>	Downregulated	-4.904399799	0.000299955	-6.120135167	8.31279E-05
<i>TGM5</i>	Downregulated	-4.896462513	0.001352492	-3.623359788	0.006183233
<i>MYHI</i>	Downregulated	-4.874602959	1.67283E-05	-4.550104817	2.53487E-05

<i>LOC283547</i>	Downregulated	-4.830613323	1.73666E-05	-3.99525033	5.42247E-05
<i>SGOL1</i>	Downregulated	-4.815713822	0.000239673	-3.980121234	0.000699696
<i>LOC100216001</i>	Downregulated	-4.802092212	0.000559973	-4.985952113	0.000454053
<i>CMKLR1</i>	Downregulated	-4.773736794	0.003509115	-4.707822221	0.003760406
<i>PDGFRA</i>	Downregulated	-4.743552014	0.000255728	-3.704450935	0.001014026
<i>HMCN1</i>	Downregulated	-4.738559356	2.18124E-05	-3.993285146	6.06965E-05
<i>COL6A6</i>	Downregulated	-4.735745122	0.000113455	-3.284205669	0.000901358
<i>LIPJ</i>	Downregulated	-4.731292346	0.000801441	-3.807004102	0.002535992
<i>MFAP5</i>	Downregulated	-4.731014155	0.000126788	-4.072261461	0.000300831
<i>WWTR1-AS1</i>	Downregulated	-4.730859559	9.82736E-07	-3.905540716	3.20936E-06
<i>LOC100292680</i>	Downregulated	-4.730693033	1.96816E-05	-3.609039764	9.8721E-05
<i>GLII</i>	Downregulated	-4.725427699	0.000993369	-4.496259914	0.001297593
<i>GPRC5A</i>	Downregulated	-4.725427699	6.72416E-06	-2.759348559	0.000167387
<i>FLT1</i>	Downregulated	-4.718989748	0.000318855	-4.73257643	0.000313693
<i>RIPK3</i>	Downregulated	-4.705527195	0.000252245	-3.312751922	0.001739502
<i>MYOCD</i>	Downregulated	-4.696124722	0.000989698	-3.847626894	0.002817986
<i>MEFV</i>	Downregulated	-4.695765738	0.002679106	-4.334415638	0.004002985
<i>DNM3OS</i>	Downregulated	-4.677473854	0.00013033	-4.115252049	0.00027282
<i>MYH11</i>	Downregulated	-4.658134679	0.000795723	-3.906173956	0.002036115
<i>ATP6V0A4</i>	Downregulated	-4.651540862	0.000175181	-5.006876613	0.000114176
<i>MIR143HG</i>	Downregulated	-4.64688724	0.001262363	-5.427659804	0.000540778
<i>FXYD5</i>	Downregulated	-4.637884346	0.00046176	-3.331405094	0.002722541
<i>PIK3R5</i>	Downregulated	-4.637884346	0.003309274	-3.645159826	0.01039356
<i>KCNA7</i>	Downregulated	-4.600747965	0.00015605	-3.815201322	0.000454257
<i>LOC642236</i>	Downregulated	-4.600747965	2.92499E-05	-2.005986095	0.003101875
<i>ZNF662</i>	Downregulated	-4.594136944	9.32318E-06	-3.399601004	5.71249E-05
<i>C7orf58</i>	Downregulated	-4.593970581	0.000167656	-3.29732144	0.001076115
<i>TRPA1</i>	Downregulated	-4.591804371	0.000131366	-3.343782406	0.000791899
<i>LOC100505702</i>	Downregulated	-4.569260426	0.009482777	-4.762735765	0.007845048
<i>TMEM154</i>	Downregulated	-4.565689391	0.00045769	-3.257870139	0.002793336
<i>IL1R1</i>	Downregulated	-4.565112832	0.000103928	-3.534527394	0.000451527
<i>GLP2R</i>	Downregulated	-4.560773887	0.000179127	-3.272918351	0.001145539

<i>COL17A1</i>	Downregulated	-4.534698246	0.000441313	-2.658793492	0.00705955
<i>SNX29P2</i>	Downregulated	-4.520940316	0.001240574	-4.012114344	0.002321891
<i>MSRI</i>	Downregulated	-4.518789179	0.003898878	-4.004352628	0.006977497
<i>GSDMC</i>	Downregulated	-4.511572035	0.001411976	-4.599485353	0.001274069
<i>APOL1</i>	Downregulated	-4.498741019	9.67896E-05	-3.490753906	0.000416658
<i>TMC1</i>	Downregulated	-4.487868516	0.001529984	-4.646255737	0.001272484
<i>CYP19A1</i>	Downregulated	-4.476801568	0.002331215	-3.701758081	0.005980655
<i>CCBE1</i>	Downregulated	-4.471079396	5.13161E-06	-3.166138375	4.14868E-05
<i>ALPK2</i>	Downregulated	-4.470487764	0.000677571	-3.671353091	0.00194922
<i>LOC100507462</i>	Downregulated	-4.455994656	0.000124029	-4.727935784	8.76569E-05
<i>CCDC36</i>	Downregulated	-4.452095471	8.59507E-05	-3.910229541	0.000183211
<i>PSG5</i>	Downregulated	-4.446717679	0.004244973	-4.040233764	0.006728839
<i>MLLT10P1</i>	Downregulated	-4.440269837	0.00060114	-3.293767997	0.002940342
<i>P2RX7</i>	Downregulated	-4.435319191	5.94255E-06	-4.699760004	4.16732E-06
<i>DNAJC22</i>	Downregulated	-4.42719863	7.21429E-06	-3.825988027	1.75169E-05
<i>LOC100506874</i>	Downregulated	-4.422567169	0.000213712	-2.568614327	0.004000479
<i>MYPN</i>	Downregulated	-4.4193013	0.004847127	-5.216230418	0.00210866
<i>CASP10</i>	Downregulated	-4.405385734	0.000155777	-3.808941257	0.000358516
<i>EXO1</i>	Downregulated	-4.401401233	3.34051E-06	-4.424514117	3.23466E-06
<i>CSNKIA1P1</i>	Downregulated	-4.393019795	1.09649E-05	-3.271924845	6.43783E-05
<i>ADAMTS4</i>	Downregulated	-4.391428201	0.000166285	-3.564638767	0.000544119
<i>SKA1</i>	Downregulated	-4.391067985	9.04748E-06	-4.64027912	6.45956E-06
<i>DAND5</i>	Downregulated	-4.380405426	0.000533962	-5.059650687	0.000236381
<i>C4orf19</i>	Downregulated	-4.364047458	1.69401E-05	-3.45750523	6.82754E-05
<i>S1PR5</i>	Downregulated	-4.361772112	5.11215E-06	-4.081483928	7.67348E-06
<i>FLJ43879</i>	Downregulated	-4.347063275	0.001425124	-3.075951226	0.007982489
<i>ROS1</i>	Downregulated	-4.337960977	0.000773681	-4.540567108	0.000601641
<i>IGSF10</i>	Downregulated	-4.331325403	0.001607813	-3.188072187	0.007390983
<i>TPRG1</i>	Downregulated	-4.331314922	0.000149212	-4.371800556	0.000141359
<i>SLC2A5</i>	Downregulated	-4.330286995	0.000296255	-2.686125229	0.003831602
<i>LOC399715</i>	Downregulated	-4.327710751	0.000167938	-4.093185334	0.000231518
<i>GIPC3</i>	Downregulated	-4.315590103	2.18883E-05	-3.264895868	0.000114952

<i>E2F2</i>	Downregulated	-4.311148213	0.000653798	-4.815479137	0.000352248
<i>KCNQ1OT1</i>	Downregulated	-4.303848674	0.000333334	-2.412001004	0.006909367
<i>RAD51B</i>	Downregulated	-4.301268119	0.000103392	-4.508278575	7.84284E-05
<i>KDR</i>	Downregulated	-4.300641577	0.000999952	-3.7310997	0.002122245
<i>CPM</i>	Downregulated	-4.294258181	0.000158518	-3.831385962	0.000305174
<i>MRVII</i>	Downregulated	-4.292735426	3.63684E-05	-1.63487644	0.00714073
<i>SOAT2</i>	Downregulated	-4.292596089	0.000312149	-3.46106525	0.001030856
<i>NFATC2</i>	Downregulated	-4.291340844	4.20632E-06	-2.673538694	7.32109E-05
<i>TNFRSF1IA</i>	Downregulated	-4.288870473	0.001122579	-3.565571946	0.002945963
<i>ITGBL1</i>	Downregulated	-4.278885301	0.000777973	-4.27108773	0.000785782
<i>MKRN9P</i>	Downregulated	-4.27510631	2.23941E-05	-3.211081293	0.000122569
<i>LOC338817</i>	Downregulated	-4.267898741	1.27868E-05	-3.095236909	8.74628E-05
<i>AGTR1</i>	Downregulated	-4.258984797	0.000162658	-3.309942386	0.000677912
<i>ERG</i>	Downregulated	-4.254542567	0.001013562	-4.173836218	0.001123825
<i>MAPILC3C</i>	Downregulated	-4.240000872	0.000102664	-3.068510229	0.000649777
<i>SP7</i>	Downregulated	-4.240000872	0.000111635	-2.036514598	0.005841285
<i>NOX5</i>	Downregulated	-4.224258389	0.00123988	-3.535564831	0.003126723
<i>EGFLAM</i>	Downregulated	-4.212443197	0.003607475	-3.405727134	0.00989329
<i>RIBC2</i>	Downregulated	-4.21166636	3.99656E-05	-3.479605576	0.00012348
<i>C3</i>	Downregulated	-4.206622969	0.001469331	-2.923830794	0.008896198
<i>SEC1</i>	Downregulated	-4.20586341	0.000318916	-3.908874059	0.000481798
<i>PAPPA2</i>	Downregulated	-4.198061333	6.36008E-06	-4.01688942	8.32637E-06
<i>ABCA4</i>	Downregulated	-4.188156294	0.000674813	-2.474403976	0.009680024
<i>DNAH11</i>	Downregulated	-4.185287661	9.89679E-05	-3.740667719	0.000190252
<i>ACTL8</i>	Downregulated	-4.179853755	0.000386664	-3.293767997	0.00142723
<i>FLT3LG</i>	Downregulated	-4.179853755	3.09525E-06	-1.960621207	0.000284815
<i>PKP1</i>	Downregulated	-4.179853755	0.00087947	-2.911116204	0.005640592
<i>LOC100130581</i>	Downregulated	-4.160636394	2.30054E-05	-2.026898451	0.001420572
<i>LINC00311</i>	Downregulated	-4.159581997	0.000228549	-4.234049435	0.000206394
<i>ATAD3C</i>	Downregulated	-4.155759359	0.001678249	-3.779690224	0.002740935
<i>ITK</i>	Downregulated	-4.145778327	0.000124011	-2.603595606	0.001662553
<i>C1QTNF2</i>	Downregulated	-4.145261973	0.000523339	-4.105233172	0.000552382

<i>PAPL</i>	Downregulated	-4.141690938	1.47193E-05	-2.034843844	0.000912503
<i>KCNE3</i>	Downregulated	-4.138042623	2.62697E-05	-3.371370759	8.89181E-05
<i>ADCY10</i>	Downregulated	-4.130651903	2.72227E-05	-3.182692121	0.000127642
<i>ELTD1</i>	Downregulated	-4.130217684	7.20976E-05	-3.044189414	0.000419949
<i>RAET1E</i>	Downregulated	-4.122809242	0.000224934	-5.749169854	3.18389E-05
<i>NOX4</i>	Downregulated	-4.114231489	2.8081E-05	-2.411972607	0.000622857
<i>FKBPIAPI</i>	Downregulated	-4.105285689	0.00010563	-3.527758958	0.000254151
<i>TMEM106A</i>	Downregulated	-4.099934422	2.86529E-05	-1.630232754	0.004811439
<i>STX11</i>	Downregulated	-4.090440212	1.16625E-05	-2.492369776	0.000220534
<i>ADAMTSL3</i>	Downregulated	-4.088466338	0.001019031	-4.398703247	0.00068362
<i>EEF1DP3</i>	Downregulated	-4.087573581	0.000786773	-3.054441197	0.003621566
<i>EMCN</i>	Downregulated	-4.084024108	0.000333534	-4.054937229	0.000347313
<i>MRI</i>	Downregulated	-4.080576521	0.001387986	-2.998180947	0.006543738
<i>HOXD-AS1</i>	Downregulated	-4.076628317	0.000408768	-2.790793364	0.003111211
<i>FERIL5</i>	Downregulated	-4.072457593	5.33586E-05	-2.61943503	0.000675567
<i>ADAM20</i>	Downregulated	-4.061110101	0.000479115	-2.641408594	0.004613778
<i>GPR183</i>	Downregulated	-4.058715833	0.001437749	-3.033506777	0.006228518
<i>PYY</i>	Downregulated	-4.052090321	1.67958E-05	-2.399766622	0.000365351
<i>C10orf54</i>	Downregulated	-4.047080943	0.001054401	-3.251323548	0.003301067
<i>MIRLET7BHG</i>	Downregulated	-4.046196566	8.86969E-06	-3.119978689	4.25868E-05
<i>AURKB</i>	Downregulated	-4.042036534	0.001796073	-2.873322987	0.009550648
<i>GSDMA</i>	Downregulated	-4.042036534	0.003593069	-4.251613887	0.002786504
<i>SCIN</i>	Downregulated	-4.031236369	0.000128283	-3.853186111	0.000166786
<i>IQGAP3</i>	Downregulated	-4.023688904	1.53504E-05	-3.026382299	8.42844E-05
<i>C9orf84</i>	Downregulated	-4.015316905	0.00015398	-2.273571902	0.003423851
<i>NEIL3</i>	Downregulated	-4.010562451	3.25902E-05	-3.564290689	6.58057E-05
<i>MME</i>	Downregulated	-4.008599952	0.00071106	-4.024551678	0.00069569
<i>OPN1SW</i>	Downregulated	-3.992022125	0.000108479	-3.352726	0.000297244
<i>C6orf99</i>	Downregulated	-3.986520878	0.000473357	-3.066655864	0.00195749
<i>LCP1</i>	Downregulated	-3.98374802	3.57847E-05	-3.211276471	0.000127977
<i>NCKAP1L</i>	Downregulated	-3.980596422	0.000133772	-3.034569047	0.000626122
<i>ABRA</i>	Downregulated	-3.978580478	0.001131135	-3.010070075	0.004735541

<i>CHI3L2</i>	Downregulated	-3.968561601	0.000348714	-2.794530924	0.002335203
<i>LILRA6</i>	Downregulated	-3.966564377	8.44984E-05	-3.121585255	0.00033771
<i>CIITA</i>	Downregulated	-3.954432699	0.002345285	-3.064820782	0.008141584
<i>TIE1</i>	Downregulated	-3.946206887	0.007777177	-3.736023027	0.009982032
<i>UNQ6975</i>	Downregulated	-3.945383783	0.000207857	-4.926572171	5.66856E-05
<i>USH2A</i>	Downregulated	-3.942181884	0.000111488	-3.660993126	0.000171484
<i>TAF4B</i>	Downregulated	-3.935084568	0.000716727	-3.437887432	0.00148618
<i>POLQ</i>	Downregulated	-3.933969819	0.000856415	-4.041631953	0.000738807
<i>LSPI</i>	Downregulated	-3.92872803	0.004104615	-4.16385201	0.003072465
<i>ZYG11A</i>	Downregulated	-3.927212415	0.000205843	-4.556672305	8.662E-05
<i>CD14</i>	Downregulated	-3.919227858	0.00020558	-3.546588021	0.000363492
<i>GDNF</i>	Downregulated	-3.919110837	3.81238E-05	-2.08106252	0.001405487
<i>BDKRB1</i>	Downregulated	-3.9174062	1.37704E-05	-2.947372306	7.56939E-05
<i>ALOX5AP</i>	Downregulated	-3.913962524	0.000503585	-4.127777117	0.000373602
<i>GPR156</i>	Downregulated	-3.913962524	0.00078807	-2.895067273	0.003815144
<i>ZP1</i>	Downregulated	-3.913045945	0.000208855	-1.901317961	0.009149138
<i>SYCP3</i>	Downregulated	-3.911603249	0.000143698	-2.415987538	0.002069657
<i>TMEM217</i>	Downregulated	-3.908999104	0.000154767	-4.03812822	0.000128111
<i>UHRF1</i>	Downregulated	-3.905579436	0.008024174	-3.990896711	0.007259346
<i>GABRR2</i>	Downregulated	-3.900375824	0.000788041	-2.656806636	0.005697554
<i>FGF18</i>	Downregulated	-3.896426608	0.00074502	-3.879896485	0.000762597
<i>ADAMTS14</i>	Downregulated	-3.89406202	0.010020515	-4.116843635	0.007775584
<i>SLC15A3</i>	Downregulated	-3.89406202	5.515E-06	-2.50655208	7.83711E-05
<i>CAVI</i>	Downregulated	-3.883233954	0.000190395	-2.844614721	0.001085521
<i>COL11AI</i>	Downregulated	-3.871385401	0.000761796	-2.344446889	0.009565199
<i>COL13AI</i>	Downregulated	-3.867324182	0.000206723	-4.029120019	0.000163157
<i>PTPRC</i>	Downregulated	-3.866644087	0.000918988	-3.461816085	0.001660307
<i>LRRC19</i>	Downregulated	-3.85770094	0.00042905	-3.981874688	0.000358908
<i>ACSM5</i>	Downregulated	-3.847370297	0.000196227	-3.717309612	0.000239105
<i>LOC648987</i>	Downregulated	-3.841300148	2.43116E-05	-2.344461778	0.000435461
<i>C8orf46</i>	Downregulated	-3.839971236	0.000417002	-3.828864791	0.000423846
<i>ANKRD26P1</i>	Downregulated	-3.838723904	0.005101438	-4.033038217	0.004008726

<i>GTF2IRD2P1</i>	Downregulated	-3.838723904	0.000101064	-4.121219367	6.65168E-05
<i>SLC2A4</i>	Downregulated	-3.838723904	0.000893345	-4.280400107	0.000489926
<i>TXNRD3NB</i>	Downregulated	-3.833914903	0.001050272	-2.888753469	0.004517581
<i>LOC100506810</i>	Downregulated	-3.825702837	0.001015569	-3.520999957	0.001582127
<i>HGF</i>	Downregulated	-3.816636292	0.000108121	-2.21541609	0.002217432
<i>HNRNPA3P1</i>	Downregulated	-3.816002419	4.9053E-06	-2.282822592	0.000107713
<i>SKA3</i>	Downregulated	-3.81259983	1.0196E-05	-3.609039764	1.42289E-05
<i>BRIP1</i>	Downregulated	-3.809879614	4.33079E-06	-3.882507996	3.85683E-06
<i>SVEP1</i>	Downregulated	-3.798299751	0.00094057	-4.036343367	0.000674493
<i>CCDC168</i>	Downregulated	-3.789824227	0.000214392	-2.534184979	0.001962956
<i>GIPC2</i>	Downregulated	-3.786239125	4.92916E-05	-3.25457981	0.000120314
<i>TNS4</i>	Downregulated	-3.7767779176	0.000212636	-2.524980642	0.00195033
<i>PTPRB</i>	Downregulated	-3.772580004	6.96344E-05	-3.229890339	0.000172764
<i>CD40</i>	Downregulated	-3.765604685	0.000919608	-3.326790565	0.001781545
<i>LOC100134368</i>	Downregulated	-3.761535233	0.000195931	-3.016624631	0.000680884
<i>EN1</i>	Downregulated	-3.758688008	0.000426048	-3.516580906	0.000617593
<i>LOC148696</i>	Downregulated	-3.758065766	4.51579E-05	-3.153363443	0.00012711
<i>FERMT1</i>	Downregulated	-3.751516357	9.10089E-05	-3.470946877	0.000143366
<i>ITGB2</i>	Downregulated	-3.745748692	0.005274124	-3.442074749	0.007859499
<i>COL6A3</i>	Downregulated	-3.742227769	0.000129561	-3.263704367	0.000285139
<i>ATP8B5P</i>	Downregulated	-3.73607176	0.000690127	-2.696681723	0.003820806
<i>OTOA</i>	Downregulated	-3.732677484	0.000250757	-3.551351373	0.000332976
<i>PCDHGA12</i>	Downregulated	-3.73031821	4.86539E-05	-1.885482046	0.002253847
<i>TBX15</i>	Downregulated	-3.726764767	4.14051E-05	-4.98415324	7.14298E-06
<i>PTPN22</i>	Downregulated	-3.725848188	2.67095E-06	-2.336626357	4.54129E-05
<i>INHBA</i>	Downregulated	-3.725100483	0.001898244	-3.421311964	0.002938811
<i>BIRC3</i>	Downregulated	-3.721084835	0.00014277	-3.083625208	0.000418443
<i>BCL11B</i>	Downregulated	-3.717187617	0.000443633	-4.357626363	0.000179358
<i>CASC5</i>	Downregulated	-3.711779767	0.000148254	-4.085702409	8.4567E-05
<i>AXDND1</i>	Downregulated	-3.700199999	0.000701419	-4.345548484	0.000284898
<i>CYP27B1</i>	Downregulated	-3.692371155	0.000373353	-2.50484019	0.003003584
<i>LOC440028</i>	Downregulated	-3.692371155	0.00047646	-3.915873262	0.000342274

<i>PIP5K1P1</i>	Downregulated	-3.690233035	0.000591633	-3.825988027	0.000483843
<i>CYP11A1</i>	Downregulated	-3.683090922	0.000401265	-2.673510519	0.002269884
<i>ANKRD20A9P</i>	Downregulated	-3.680136929	7.67137E-05	-3.711348624	7.29834E-05
<i>BCL11A</i>	Downregulated	-3.670413511	0.000391188	-2.487392506	0.003147727
<i>DQXI</i>	Downregulated	-3.665516356	0.000652924	-2.672949566	0.003454241
<i>DPT</i>	Downregulated	-3.665067198	0.000817952	-2.320001707	0.008294662
<i>ROR1</i>	Downregulated	-3.651319323	0.001974871	-4.379750475	0.000746214
<i>SH2D4A</i>	Downregulated	-3.65066535	0.000884634	-3.830139679	0.000680142
<i>MOCOS</i>	Downregulated	-3.647788587	0.000204242	-3.780523736	0.000166158
<i>PLIN1</i>	Downregulated	-3.637628594	0.002027299	-2.900864519	0.006247356
<i>TPTE2</i>	Downregulated	-3.637450627	0.000242331	-3.883509912	0.00016622
<i>SLC38A4</i>	Downregulated	-3.630085919	0.000133684	-2.747092759	0.000651673
<i>COL24A1</i>	Downregulated	-3.62876615	0.000179596	-4.266244571	6.97077E-05
<i>TRIM29</i>	Downregulated	-3.618038081	1.57174E-05	-2.525536005	0.000133516
<i>CD101</i>	Downregulated	-3.615127016	0.000191535	-4.241286707	7.53823E-05
<i>HYMA1</i>	Downregulated	-3.61373826	0.002076738	-3.104070646	0.004468371
<i>SP110</i>	Downregulated	-3.608939819	0.00014956	-4.148655587	6.60464E-05
<i>CAGE1</i>	Downregulated	-3.602689682	4.53045E-05	-2.377211662	0.000503399
<i>HHIP</i>	Downregulated	-3.593321401	0.000672223	-3.350977952	0.000984536
<i>CYP2B7P1</i>	Downregulated	-3.587007597	0.000297741	-3.500484803	0.000342001
<i>CLCF1</i>	Downregulated	-3.584053961	0.000823537	-3.526510141	0.000899494
<i>ODF3L2</i>	Downregulated	-3.580347175	9.08217E-05	-3.467839899	0.000109526
<i>TMC2</i>	Downregulated	-3.577292332	0.001088945	-2.830233758	0.003671241
<i>MKX</i>	Downregulated	-3.57375052	0.000134126	-4.095254563	6.02271E-05
<i>LOC153684</i>	Downregulated	-3.568657545	0.000150123	-1.853558805	0.005121426
<i>BIRC5</i>	Downregulated	-3.566491334	0.00010816	-4.18130425	4.2231E-05
<i>FHAD1</i>	Downregulated	-3.561226001	5.73493E-06	-2.115461156	0.000130275
<i>PSTPIP1</i>	Downregulated	-3.558550934	0.004025646	-3.059271927	0.008275623
<i>EGF</i>	Downregulated	-3.558240793	0.000269931	-4.019602448	0.000133617
<i>C20orf152</i>	Downregulated	-3.555346974	8.2465E-05	-2.10042387	0.001590031
<i>LOC100133985</i>	Downregulated	-3.553918411	8.33703E-05	-2.44221107	0.000711021
<i>KLHL10</i>	Downregulated	-3.553049687	0.003423626	-3.099129044	0.006647607

<i>FAM129C</i>	Downregulated	-3.551793531	4.06801E-05	-2.286574219	0.000522265
<i>FMO4</i>	Downregulated	-3.548874002	0.000452314	-2.966813069	0.001208479
<i>EVC2</i>	Downregulated	-3.543246019	0.000143195	-2.41867504	0.001217684
<i>LYG2</i>	Downregulated	-3.537805745	0.000145377	-3.278337515	0.000225724
<i>COL5A3</i>	Downregulated	-3.533415758	0.000374853	-2.754360805	0.001468187
<i>SP100</i>	Downregulated	-3.526028381	0.003374814	-3.673274941	0.002745519
<i>C4orf22</i>	Downregulated	-3.525579223	0.002260737	-3.606867029	0.002009169
<i>CDC25C</i>	Downregulated	-3.525579223	0.001172542	-3.169692912	0.002056209
<i>IL15</i>	Downregulated	-3.525579223	8.54526E-05	-3.874297123	4.88925E-05
<i>LOC100288637</i>	Downregulated	-3.521339108	0.0001678	-3.229333512	0.000275971
<i>FLJ42289</i>	Downregulated	-3.521126446	0.003045333	-3.625719063	0.002625113
<i>ITGB4</i>	Downregulated	-3.516923892	0.000838192	-3.195779224	0.001403903
<i>LOC100130872</i>	Downregulated	-3.514670168	7.4607E-05	-2.073040673	0.00146599
<i>PLCG2</i>	Downregulated	-3.512137576	0.001836355	-2.736326178	0.006375594
<i>VEPH1</i>	Downregulated	-3.511232497	6.37338E-05	-2.927656106	0.000184624
<i>LILRB3</i>	Downregulated	-3.506082157	0.003061886	-2.979197022	0.006771123
<i>ANO3</i>	Downregulated	-3.503035278	0.001304303	-3.487637224	0.001335293
<i>FLJ14107</i>	Downregulated	-3.503035278	0.002547597	-3.054947005	0.005034303
<i>STAB1</i>	Downregulated	-3.49726262	0.000672353	-2.559921762	0.003480767
<i>ADH6</i>	Downregulated	-3.495278778	8.6128E-06	-2.384522679	8.55281E-05
<i>FBXW10</i>	Downregulated	-3.485417946	0.000403732	-3.180459493	0.000672478
<i>FLJ38109</i>	Downregulated	-3.480480318	0.00120462	-2.687480191	0.004539785
<i>NLRP14</i>	Downregulated	-3.477658628	2.15634E-05	-2.134498248	0.000377163
<i>PCDHGA9</i>	Downregulated	-3.474560566	3.24998E-05	-1.97991982	0.000832392
<i>ABCG2</i>	Downregulated	-3.470241107	0.005840803	-3.832769253	0.003598698
<i>LRRK1</i>	Downregulated	-3.465060851	0.000587845	-3.116887818	0.001049465
<i>SOX7</i>	Downregulated	-3.465060851	0.000279407	-2.92560653	0.000721166
<i>KIF6</i>	Downregulated	-3.460816727	2.6222E-05	-2.712349053	0.000111435
<i>LOC149773</i>	Downregulated	-3.460590829	0.003504598	-3.767780859	0.0022767
<i>FAM176A</i>	Downregulated	-3.457936374	0.000115681	-2.616923422	0.000567957
<i>KIAA1875</i>	Downregulated	-3.452920542	0.000557649	-2.635634037	0.00237215
<i>SLC26A8</i>	Downregulated	-3.450550498	0.000494184	-1.988235968	0.00840271

<i>CDK15</i>	Downregulated	-3.447519622	0.003430193	-4.188558107	0.001251447
<i>TM4SF18</i>	Downregulated	-3.440145392	0.004008354	-3.468553354	0.003848707
<i>KIF4B</i>	Downregulated	-3.435884732	6.00109E-05	-2.239954086	0.00069952
<i>ASB2</i>	Downregulated	-3.434580306	6.21863E-06	-1.727789421	0.000365122
<i>KCNJ14</i>	Downregulated	-3.430957344	0.000113105	-3.256705986	0.000153237
<i>LRRKQ4</i>	Downregulated	-3.430840323	4.54148E-05	-3.067118069	8.81893E-05
<i>LOC152742</i>	Downregulated	-3.427718447	0.004771611	-3.806510705	0.002834987
<i>PAQR5</i>	Downregulated	-3.424706216	2.42139E-05	-2.73166102	9.30117E-05
<i>LOC100506655</i>	Downregulated	-3.414141718	0.001738783	-2.72936499	0.005365908
<i>SND1-IT1</i>	Downregulated	-3.411431711	0.000147331	-4.043696844	5.42313E-05
<i>NLRC5</i>	Downregulated	-3.409728663	0.000343233	-2.178801841	0.003761134
<i>GLI2</i>	Downregulated	-3.408555262	0.00037544	-3.562466031	0.000292291
<i>DYSF</i>	Downregulated	-3.406981949	0.005333165	-3.404037479	0.005355379
<i>EPST11</i>	Downregulated	-3.405722557	0.002423162	-3.925148878	0.001149435
<i>BARD1</i>	Downregulated	-3.398506886	8.20691E-05	-3.837927381	3.98882E-05
<i>DENND2D</i>	Downregulated	-3.396605879	0.001761216	-3.241887867	0.002244276
<i>CDC45</i>	Downregulated	-3.392865897	0.00105015	-3.778224863	0.00058277
<i>FUT2</i>	Downregulated	-3.390860969	1.77319E-05	-2.771013029	5.94308E-05
<i>OSCAR</i>	Downregulated	-3.387372505	0.000265639	-2.869769543	0.000674099
<i>TINAGLI</i>	Downregulated	-3.38700125	0.000649953	-3.063035079	0.001124346
<i>INMT</i>	Downregulated	-3.379954984	0.004419813	-3.100057982	0.006691437
<i>HNMT</i>	Downregulated	-3.375484505	0.002227964	-5.832786829	0.000106794
<i>C19orf35</i>	Downregulated	-3.371203694	9.09787E-06	-2.301921707	8.97028E-05
<i>DTL</i>	Downregulated	-3.371203694	1.55384E-05	-3.065481243	2.75724E-05
<i>LOC100129931</i>	Downregulated	-3.368591712	0.001463421	-2.892807132	0.0032133
<i>SATB2</i>	Downregulated	-3.367015668	0.000224433	-3.596749142	0.000153326
<i>PRAMI</i>	Downregulated	-3.362741628	7.62635E-05	-2.704509032	0.000270353
<i>SLC12AI</i>	Downregulated	-3.361607355	0.000764028	-3.630777621	0.000498892
<i>ALPK1</i>	Downregulated	-3.359441144	0.000194908	-3.358288969	0.000195294
<i>EMX2OS</i>	Downregulated	-3.355694637	3.35116E-05	-2.472672668	0.0002021
<i>PRRG4</i>	Downregulated	-3.35548455	0.007491296	-4.416977949	0.00192637
<i>SPDY5</i>	Downregulated	-3.354078913	4.7816E-05	-1.764161086	0.001805282

<i>S1PRI</i>	Downregulated	-3.349790866	0.001414524	-3.713660291	0.000811411
<i>SP140L</i>	Downregulated	-3.347515389	0.0011055	-2.999174453	0.001977798
<i>TDRD9</i>	Downregulated	-3.346456335	0.000348868	-2.085485512	0.004316304
<i>ZMYND15</i>	Downregulated	-3.340734163	0.001176193	-2.39652897	0.006328979
<i>C14orf182</i>	Downregulated	-3.339841406	0.000189899	-3.265433485	0.000216205
<i>MIP</i>	Downregulated	-3.339784866	0.000666584	-4.399062484	0.000139509
<i>DLGAP5</i>	Downregulated	-3.331769115	0.00106028	-3.96948518	0.000403505
<i>APOBEC3D</i>	Downregulated	-3.329623141	0.002808266	-3.65985537	0.001723492
<i>PSMB9</i>	Downregulated	-3.328945784	0.000211359	-4.355060049	4.37124E-05
<i>LOC440600</i>	Downregulated	-3.327614885	0.000107142	-2.673787611	0.000377362
<i>CDRT1</i>	Downregulated	-3.321750238	0.003184612	-2.975299609	0.005471727
<i>LOC400891</i>	Downregulated	-3.316908962	1.36584E-05	-3.273870313	1.47838E-05
<i>MEII</i>	Downregulated	-3.314774324	0.000293265	-2.113035784	0.003315281
<i>GPR39</i>	Downregulated	-3.314076256	4.80792E-05	-2.034843844	0.000792022
<i>IGSF6</i>	Downregulated	-3.310336274	0.000311096	-2.351032191	0.002013474
<i>HOGA1</i>	Downregulated	-3.303681729	0.000242964	-4.391229447	4.5955E-05
<i>LOC285540</i>	Downregulated	-3.303400186	0.000310112	-3.914066505	0.000116607
<i>ZBTB20</i>	Downregulated	-3.296194048	3.20287E-06	-2.723278192	1.03022E-05
<i>ZNF850</i>	Downregulated	-3.29339613	0.000231227	-2.7484298	0.000640816
<i>CCDC158</i>	Downregulated	-3.291689742	0.000138857	-2.492686376	0.000673045
<i>ERAP2</i>	Downregulated	-3.291689742	1.57589E-06	-1.773387192	6.73558E-05
<i>KCTD19</i>	Downregulated	-3.288995678	0.000411095	-1.835557272	0.008368353
<i>ITGA11</i>	Downregulated	-3.285753632	0.008720193	-3.785708164	0.004462094
<i>TMPRSS5</i>	Downregulated	-3.285753632	0.000148067	-2.044725472	0.00204455
<i>ARHGAP6</i>	Downregulated	-3.284502001	7.10397E-06	-1.081479374	0.003926396
<i>NKX3-1</i>	Downregulated	-3.277261312	0.001134212	-3.735361164	0.000554484
<i>GREM1</i>	Downregulated	-3.275816441	0.001380847	-3.60328945	0.000826196
<i>DIAPH3</i>	Downregulated	-3.273441143	0.000311749	-3.717241217	0.000150159
<i>FRRS1</i>	Downregulated	-3.272548386	0.001138047	-3.015827278	0.001755916
<i>TLR5</i>	Downregulated	-3.272548386	0.000453857	-2.127302702	0.004413161
<i>LRTM1</i>	Downregulated	-3.27154929	0.001280742	-3.236242315	0.001357007
<i>ALS2CR11</i>	Downregulated	-3.270157388	2.98397E-05	-2.926848084	5.7846E-05

<i>KIF20A</i>	Downregulated	-3.262831993	0.000773248	-3.66651283	0.000404466
<i>BTBD18</i>	Downregulated	-3.261380918	0.001997147	-2.848606307	0.003966807
<i>PRR5L</i>	Downregulated	-3.256874691	0.000262574	-2.689377261	0.000767486
<i>RPGRIP1</i>	Downregulated	-3.256127972	0.000313249	-2.739329294	0.000821124
<i>MALAT1</i>	Downregulated	-3.25075196	2.11811E-06	-2.19163182	2.34951E-05
<i>GOLGA6L10</i>	Downregulated	-3.249555284	0.000103345	-2.477826223	0.00048918
<i>RERGL</i>	Downregulated	-3.249555284	0.000444848	-3.807004102	0.000180526
<i>GALM</i>	Downregulated	-3.247909873	0.002803194	-3.500478623	0.001906753
<i>PPP1R36</i>	Downregulated	-3.247250657	0.001982056	-2.917611217	0.003421981
<i>COLEC11</i>	Downregulated	-3.242619196	2.33497E-05	-1.133956899	0.007533315
<i>COX7A1</i>	Downregulated	-3.242619196	2.14104E-05	-1.600738781	0.001242303
<i>RAD21-AS1</i>	Downregulated	-3.23777792	0.001065064	-2.360518793	0.00536623
<i>PRR11</i>	Downregulated	-3.235418555	0.000197028	-3.031334042	0.000286207
<i>VDR</i>	Downregulated	-3.23504493	0.00017895	-2.82257937	0.000389901
<i>SPTBN5</i>	Downregulated	-3.231878207	0.002485376	-2.632041362	0.006816044
<i>HAS2</i>	Downregulated	-3.231464116	9.53576E-05	-3.027594059	0.000139566
<i>NCAPH</i>	Downregulated	-3.219526715	0.000612625	-2.694798308	0.001603534
<i>LOC158376</i>	Downregulated	-3.2185248	0.00032828	-2.868852964	0.000625309
<i>SERPINE3</i>	Downregulated	-3.2185248	5.01324E-05	-2.422310566	0.000263585
<i>CPS1</i>	Downregulated	-3.216421324	0.002397256	-4.034995627	0.000716776
<i>CAPN12</i>	Downregulated	-3.216115717	0.002228145	-2.62349611	0.006118223
<i>ACTR3C</i>	Downregulated	-3.216033634	6.43579E-06	-1.677775012	0.000306721
<i>NCF2</i>	Downregulated	-3.212401269	0.00111925	-3.072409414	0.001420142
<i>CX3CR1</i>	Downregulated	-3.209559751	0.000276281	-4.081085394	6.83318E-05
<i>ENDOU</i>	Downregulated	-3.207110835	0.000137013	-2.338338248	0.000818255
<i>IGFN1</i>	Downregulated	-3.206120177	0.001802973	-2.85981937	0.003240227
<i>ADAMTS9-AS2</i>	Downregulated	-3.206087465	0.000363915	-2.288784683	0.002262264
<i>HJURP</i>	Downregulated	-3.201873447	0.000786744	-4.183292773	0.000174199
<i>SGCG</i>	Downregulated	-3.194699598	0.000249665	-3.248219304	0.000226992
<i>LOC646626</i>	Downregulated	-3.193171319	0.004672503	-2.878593476	0.007649415
<i>C6orf97</i>	Downregulated	-3.182449907	0.000385818	-2.649102058	0.001062233
<i>TAT</i>	Downregulated	-3.182262263	0.001105984	-3.092582453	0.00128911

<i>WNK4</i>	Downregulated	-3.176903455	0.001003701	-2.269519876	0.005612193
<i>GLIS1</i>	Downregulated	-3.171328781	0.000549473	-3.233964973	0.000492724
<i>LOC100505826</i>	Downregulated	-3.169322948	0.000106943	-1.629829316	0.004048295
<i>RGS20</i>	Downregulated	-3.169322948	3.06917E-05	-2.360882193	0.000174404
<i>TMEM204</i>	Downregulated	-3.169322948	0.000664591	-2.084045696	0.005814409
<i>CPNE6</i>	Downregulated	-3.167369399	0.000219247	-1.8863869	0.003611053
<i>FGF7</i>	Downregulated	-3.161905427	0.00069888	-2.245131686	0.004189871
<i>POTEKP</i>	Downregulated	-3.153974549	0.002767163	-2.760864174	0.005346331
<i>RUNX2</i>	Downregulated	-3.153974549	4.42794E-05	-3.781335933	1.48743E-05
<i>NAT1</i>	Downregulated	-3.145073689	0.004279936	-3.197089149	0.003947904
<i>CFB</i>	Downregulated	-3.142726478	0.000484302	-1.824552901	0.007982852
<i>ROCKIP1</i>	Downregulated	-3.142252912	0.000192191	-2.927364012	0.00028845
<i>LOC100507178</i>	Downregulated	-3.137556535	0.000687777	-2.424479627	0.002704436
<i>RSPO1</i>	Downregulated	-3.134552481	0.000313137	-1.991765522	0.003568523
<i>TROAP</i>	Downregulated	-3.127795078	0.008283443	-3.932619582	0.002728972
<i>MCTP2</i>	Downregulated	-3.127144482	5.5261E-05	-2.902171185	8.59254E-05
<i>KIF14</i>	Downregulated	-3.124135729	0.000208337	-2.706187172	0.00047086
<i>TWIST1</i>	Downregulated	-3.123500551	0.001247642	-4.280451598	0.000216195
<i>CRISPLD2</i>	Downregulated	-3.122409574	0.000620705	-2.381928537	0.002626755
<i>MYLK2</i>	Downregulated	-3.120976364	0.002157694	-3.044661858	0.002451003
<i>PXDNL</i>	Downregulated	-3.118078685	0.000146551	-2.63687026	0.000382852
<i>C21orf7</i>	Downregulated	-3.107099262	0.000899383	-2.684942692	0.001957465
<i>LOC100499405</i>	Downregulated	-3.106851259	0.000128939	-3.09056187	0.00013295
<i>ACRV1</i>	Downregulated	-3.104801975	0.000571542	-1.806765601	0.00904957
<i>E2F8</i>	Downregulated	-3.104801975	0.01052354	-3.63103377	0.005080176
<i>NUF2</i>	Downregulated	-3.104801975	0.002281929	-5.25024666	0.000124521
<i>CD163</i>	Downregulated	-3.104080519	0.001097137	-2.673787611	0.002406004
<i>FGF5</i>	Downregulated	-3.103913342	0.00334149	-3.793983688	0.001178038
<i>DNAH5</i>	Downregulated	-3.103224212	0.00057709	-2.117914267	0.004293053
<i>ANKRD31</i>	Downregulated	-3.102872061	5.81392E-06	-1.949321074	9.51262E-05
<i>CC2D2B</i>	Downregulated	-3.09802075	0.001513489	-3.891838352	0.000435646
<i>MFSD7</i>	Downregulated	-3.09802075	4.11983E-05	-2.976831946	5.22538E-05

<i>PTGS1</i>	Downregulated	-3.097127993	0.002406217	-2.713054885	0.004667031
<i>RAD54L</i>	Downregulated	-3.096158328	4.53691E-05	-2.655633039	0.000112326
<i>NDE1</i>	Downregulated	-3.096060565	0.000472025	-3.90734648	0.000124627
<i>ADAM32</i>	Downregulated	-3.094504908	0.000302679	-2.949221916	0.000397349
<i>C8orf31</i>	Downregulated	-3.092892665	4.65871E-05	-1.472420463	0.002948375
<i>ANP32A-IT1</i>	Downregulated	-3.091474159	0.000207032	-2.125791375	0.001642848
<i>ATP10A</i>	Downregulated	-3.090718821	0.012051267	-3.804817252	0.00459535
<i>HKDC1</i>	Downregulated	-3.087523364	0.004622864	-2.597932397	0.010366816
<i>MSTIP2</i>	Downregulated	-3.083915964	0.000548795	-1.75656866	0.009647152
<i>IMPG1</i>	Downregulated	-3.083496484	0.000326487	-2.844958813	0.000513524
<i>PLAC8</i>	Downregulated	-3.079036825	0.005897336	-3.783543579	0.002114651
<i>LINC00315</i>	Downregulated	-3.07546579	0.005062936	-2.736326178	0.008767955
<i>TBX3</i>	Downregulated	-3.072100737	4.31785E-05	-3.609039764	1.63987E-05
<i>COL11A2</i>	Downregulated	-3.070285182	0.000464225	-2.376659169	0.001860607
<i>CDCP1</i>	Downregulated	-3.063354739	2.81736E-05	-2.545141948	8.48616E-05
<i>CCNB2</i>	Downregulated	-3.060644532	0.004251252	-3.357156555	0.002676819
<i>EDNRA</i>	Downregulated	-3.060644532	0.002410206	-2.646040055	0.004982696
<i>LOC100132215</i>	Downregulated	-3.057935576	0.000213496	-2.569963668	0.000570657
<i>DIO2</i>	Downregulated	-3.057203707	2.48931E-05	-3.713966004	7.65015E-06
<i>MPL</i>	Downregulated	-3.05649288	7.40504E-06	-2.044725472	8.29617E-05
<i>FBXO43</i>	Downregulated	-3.052921845	9.616E-05	-1.460277244	0.005274364
<i>ASPM</i>	Downregulated	-3.052492791	0.000382936	-3.677110311	0.000131592
<i>CAPN14</i>	Downregulated	-3.048662035	9.76445E-05	-3.302690514	6.09016E-05
<i>EYS</i>	Downregulated	-3.044999998	0.000725617	-2.392070015	0.002612992
<i>CCDC38</i>	Downregulated	-3.043553564	2.8071E-05	-2.204261009	0.000188312
<i>CDCA2</i>	Downregulated	-3.036592376	0.005498407	-3.550520054	0.002532346
<i>TLR1</i>	Downregulated	-3.036592376	0.01113836	-3.312751922	0.007502737
<i>MSTIR</i>	Downregulated	-3.030398742	0.003626366	-2.94641854	0.004167182
<i>TNFSF13B</i>	Downregulated	-3.027258729	0.000628395	-2.663581285	0.001260635
<i>HLA-F-AS1</i>	Downregulated	-3.026742374	0.003803728	-4.166661546	0.000711258
<i>GSG2</i>	Downregulated	-3.018889708	0.002955819	-3.117748291	0.002508963
<i>HOXC4</i>	Downregulated	-3.018889708	0.008332246	-3.014522852	0.008387774

<i>CCDC147</i>	Downregulated	-3.016723497	0.001415431	-2.66502398	0.002697543
<i>PLAUR</i>	Downregulated	-3.016659309	0.001370459	-2.387644556	0.004527347
<i>C9orf47</i>	Downregulated	-3.015665803	0.00257079	-3.83837198	0.000713455
<i>APOBEC3F</i>	Downregulated	-3.013218476	0.000638826	-3.227900486	0.000435409
<i>CLDN11</i>	Downregulated	-3.012343117	0.000338497	-2.427700717	0.001116135
<i>LOC401074</i>	Downregulated	-3.007045002	0.001377614	-2.481386242	0.003704719
<i>SSPO</i>	Downregulated	-3.006675881	0.001448975	-2.949156121	0.001604737
<i>TBX1</i>	Downregulated	-3.006640433	3.66805E-05	-2.869769543	4.84372E-05
<i>CCDC150</i>	Downregulated	-3.001724928	4.0027E-05	-1.893290065	0.000576492
<i>SLC11A1</i>	Downregulated	-3.000977224	0.000313369	-2.495104834	0.000875948
<i>IL21R</i>	Downregulated	-2.997426995	0.000641456	-3.425595791	0.000303369
<i>PODN</i>	Downregulated	-2.993352616	0.006853476	-3.209526483	0.004914922
<i>PRG4</i>	Downregulated	-2.991622376	0.008531613	-2.90418395	0.009762109
<i>FLJ12825</i>	Downregulated	-2.989900653	0.007975465	-3.227229151	0.005569116
<i>MEIS1</i>	Downregulated	-2.9873642	0.002358927	-2.501146488	0.005697918
<i>LOC100134713</i>	Downregulated	-2.981480158	0.001022689	-2.563555852	0.00227106
<i>XRCC2</i>	Downregulated	-2.981267464	0.000162155	-1.854323754	0.00222292
<i>ENAM</i>	Downregulated	-2.980620387	0.000160385	-2.582356491	0.000364606
<i>ABCA6</i>	Downregulated	-2.980150332	0.000487841	-3.33084309	0.000260102
<i>ITGA1</i>	Downregulated	-2.977417951	0.009671836	-3.540957674	0.004272148
<i>BRCA2</i>	Downregulated	-2.967813688	3.71477E-05	-1.504687191	0.0017534
<i>TRPV4</i>	Downregulated	-2.965651394	0.00066351	-2.01579097	0.00495184
<i>TLCD2</i>	Downregulated	-2.958673891	9.94549E-05	-2.608939488	0.000206619
<i>KIF2C</i>	Downregulated	-2.958324789	3.18354E-05	-2.336018539	0.000128797
<i>ANKRD1</i>	Downregulated	-2.957239083	0.010058085	-3.254095766	0.006474663
<i>PRH2</i>	Downregulated	-2.953844519	1.43876E-05	-1.803989878	0.000265332
<i>BHMT</i>	Downregulated	-2.953267441	0.000519179	-1.695451583	0.008897603
<i>NOTUM</i>	Downregulated	-2.953267441	0.004503562	-3.564882321	0.001734024
<i>C6orf132</i>	Downregulated	-2.951450444	4.45699E-05	-2.86745753	5.29268E-05
<i>PKD1L1</i>	Downregulated	-2.949984386	0.000222405	-1.738792473	0.003849092
<i>BDKRB2</i>	Downregulated	-2.943385814	0.000283226	-2.778332484	0.000392796
<i>CEP55</i>	Downregulated	-2.943385814	0.009580689	-3.41782549	0.004752029

<i>C2orf65</i>	Downregulated	-2.937836959	0.010597936	-3.57800928	0.004201275
<i>CCDC144A</i>	Downregulated	-2.937836959	0.002295126	-2.764073734	0.003130677
<i>MOVIOL1</i>	Downregulated	-2.937018077	0.001299919	-2.36337605	0.003975849
<i>PIWIL2</i>	Downregulated	-2.936418951	0.000362828	-1.732576223	0.005814697
<i>LOC100505806</i>	Downregulated	-2.934283516	0.000499365	-2.527051897	0.00113287
<i>TGFBI</i>	Downregulated	-2.929718667	0.007773758	-3.107757121	0.005893164
<i>MCM10</i>	Downregulated	-2.92964041	1.22285E-05	-1.689218949	0.000316032
<i>LOC100132774</i>	Downregulated	-2.925871205	1.74352E-05	-2.147582312	0.000110063
<i>PTPN14</i>	Downregulated	-2.918966697	0.000242371	-3.390602246	0.000101707
<i>CAV2</i>	Downregulated	-2.917147379	0.001510719	-3.002887962	0.001295231
<i>LOC388692</i>	Downregulated	-2.913733572	0.000170369	-3.190670165	0.000100377
<i>FLJ35024</i>	Downregulated	-2.911362519	0.000276567	-4.010288738	4.25266E-05
<i>FLJ12334</i>	Downregulated	-2.908746424	0.00029672	-2.821602923	0.000352607
<i>PLIN4</i>	Downregulated	-2.908687247	0.000204412	-2.171086487	0.001048475
<i>CTSW</i>	Downregulated	-2.903616431	0.001440808	-2.495785499	0.003151681
<i>ABCA17P</i>	Downregulated	-2.901489345	2.45841E-05	-2.018097146	0.000209343
<i>KIAA0101</i>	Downregulated	-2.891839067	1.88566E-05	-2.244763087	8.552E-05
<i>LDHAL6A</i>	Downregulated	-2.888101507	0.000249409	-2.304621535	0.000880885
<i>FKBP9L</i>	Downregulated	-2.885247073	0.001487659	-2.256633384	0.005170041
<i>HTR4</i>	Downregulated	-2.881588841	0.000689192	-3.714062815	0.000163898
<i>LINC00482</i>	Downregulated	-2.881072487	0.000418317	-1.751883818	0.005681335
<i>ANKFNI</i>	Downregulated	-2.879501449	5.91608E-05	-3.849448551	1.03217E-05
<i>MYH15</i>	Downregulated	-2.878767786	9.55487E-05	-2.82680874	0.000106319
<i>TOB2P1</i>	Downregulated	-2.87520784	2.1895E-05	-2.816558514	2.47887E-05
<i>EXPH5</i>	Downregulated	-2.871412684	0.000791657	-2.76939245	0.000964072
<i>AGAP11</i>	Downregulated	-2.865278605	0.000248026	-1.86446786	0.002575175
<i>ESPL1</i>	Downregulated	-2.865050547	0.011865114	-3.560730669	0.004311107
<i>METTL7A</i>	Downregulated	-2.862298039	0.000346969	-4.503805265	2.4334E-05
<i>IFI44L</i>	Downregulated	-2.862203166	0.006764214	-4.316882266	0.000828843
<i>NFIB</i>	Downregulated	-2.861227047	0.001860233	-4.49279483	0.000152393
<i>COL8A1</i>	Downregulated	-2.855307336	0.001207296	-2.770805126	0.001417072
<i>PII6</i>	Downregulated	-2.853099691	0.000242199	-2.236645146	0.000943444

<i>NR5A2</i>	Downregulated	-2.848847718	0.013832095	-3.171192596	0.008592467
<i>KIF23</i>	Downregulated	-2.848371249	0.002239119	-3.595100248	0.000644278
<i>MYO15A</i>	Downregulated	-2.843027433	7.51719E-05	-1.577495128	0.002033492
<i>RFX8</i>	Downregulated	-2.840160375	0.000905629	-2.537313369	0.001655659
<i>BLM</i>	Downregulated	-2.837955988	0.000133976	-1.486863181	0.00446509
<i>ABI3BP</i>	Downregulated	-2.83775629	0.000222918	-2.751944596	0.000265772
<i>RAC2</i>	Downregulated	-2.836323411	0.001714351	-2.372296157	0.004251921
<i>LOC729020</i>	Downregulated	-2.835233762	0.000777313	-2.282760869	0.00245674
<i>FLJ41484</i>	Downregulated	-2.834611521	0.002064878	-2.765673175	0.002344837
<i>COLEC10</i>	Downregulated	-2.831058077	0.000152199	-2.132803949	0.000755267
<i>ANGPT1</i>	Downregulated	-2.826019421	0.010781747	-4.249986481	0.001456952
<i>PRDM6</i>	Downregulated	-2.82555683	0.00034422	-3.251323548	0.000153915
<i>PRELID2</i>	Downregulated	-2.820975013	0.001380379	-1.874828098	0.010327228
<i>ACSL5</i>	Downregulated	-2.820623693	0.001136108	-2.596598546	0.001762772
<i>FRK</i>	Downregulated	-2.817882414	0.00348485	-2.671805205	0.004532206
<i>HCG25</i>	Downregulated	-2.813779466	0.000432072	-3.350977952	0.000159319
<i>LRRC2</i>	Downregulated	-2.813052118	0.004202099	-4.338064958	0.000423258
<i>PARPBP</i>	Downregulated	-2.807597554	0.001842092	-2.234089439	0.005783858
<i>ACYI</i>	Downregulated	-2.803012886	0.001455227	-2.269883276	0.004278058
<i>GRB7</i>	Downregulated	-2.801953832	0.000115496	-3.087679327	6.5233E-05
<i>AOXI</i>	Downregulated	-2.801477947	0.002242242	-2.904739663	0.001858209
<i>FANCD2</i>	Downregulated	-2.801209793	2.64587E-05	-2.971135554	1.85528E-05
<i>COL12A1</i>	Downregulated	-2.795186317	0.00306215	-3.404482577	0.001093745
<i>MGC23270</i>	Downregulated	-2.789631688	0.000146273	-2.821831703	0.000136829
<i>CHEK2</i>	Downregulated	-2.784754047	0.000323357	-2.338826464	0.000854403
<i>BMPER</i>	Downregulated	-2.780746033	2.68655E-05	-3.17957454	1.19506E-05
<i>ACRC</i>	Downregulated	-2.776950671	7.57084E-06	-2.290732921	2.43265E-05
<i>PKN3</i>	Downregulated	-2.774120521	0.003286592	-2.336116579	0.007541532
<i>CLEC14A</i>	Downregulated	-2.771982402	0.000100455	-3.059271927	5.61341E-05
<i>LOC100128788</i>	Downregulated	-2.767515071	0.00486067	-4.030733591	0.000686775
<i>JPH2</i>	Downregulated	-2.766069684	0.001571911	-2.231923229	0.004675559
<i>IGF1</i>	Downregulated	-2.765780558	0.000850963	-4.019501909	0.000101876

<i>IGFBP3</i>	Downregulated	-2.765655624	0.004589322	-3.146209949	0.00240662
<i>MBOAT1</i>	Downregulated	-2.765021213	0.00177945	-3.644702988	0.000395161
<i>EFCAB5</i>	Downregulated	-2.763700548	0.000252651	-1.553362534	0.005409728
<i>FAM160A1</i>	Downregulated	-2.76352075	0.001591099	-3.071463569	0.000903432
<i>KLHL30</i>	Downregulated	-2.757950219	0.010020099	-3.541746744	0.003031391
<i>ARHGAP9</i>	Downregulated	-2.752998476	0.006104807	-3.584878797	0.001622578
<i>ANPEP</i>	Downregulated	-2.748716845	0.000680244	-2.648787177	0.000833453
<i>DENND2C</i>	Downregulated	-2.745486123	0.000190076	-2.915722872	0.000134115
<i>TRPC4</i>	Downregulated	-2.740143935	0.000364713	-2.555204125	0.000539694
<i>FLJ31813</i>	Downregulated	-2.733097972	0.000116882	-1.617602794	0.002148434
<i>LOC100129845</i>	Downregulated	-2.733097972	0.000376199	-1.855552856	0.003012011
<i>LINC00312</i>	Downregulated	-2.726236113	0.000283946	-3.364199265	8.38895E-05
<i>RAD51</i>	Downregulated	-2.725933105	0.000271343	-2.688222102	0.000293765
<i>PABPC4L</i>	Downregulated	-2.72278055	0.003477784	-2.448075717	0.005844479
<i>CNTD2</i>	Downregulated	-2.710554028	6.54316E-05	-1.452650435	0.002155581
<i>MARK2P9</i>	Downregulated	-2.710554028	0.001557587	-2.334767213	0.003357673
<i>HERC2P3</i>	Downregulated	-2.710554028	0.000334902	-3.628461832	6.15779E-05
<i>CYP2A6</i>	Downregulated	-2.707811258	0.000504805	-1.923990073	0.003118345
<i>STARD13</i>	Downregulated	-2.705604797	0.001613182	-1.859671956	0.010135023
<i>GHRLOS</i>	Downregulated	-2.702141716	0.000732878	-2.217021641	0.002109347
<i>GSG1</i>	Downregulated	-2.697614712	0.000712945	-1.878724642	0.004688373
<i>SLC26A4</i>	Downregulated	-2.697164362	0.003586767	-3.054608026	0.001901382
<i>SHCBPI</i>	Downregulated	-2.688848128	0.000740687	-1.984275844	0.003648556
<i>CXorf69</i>	Downregulated	-2.688097817	0.000242594	-1.799091619	0.002184721
<i>COL7A1</i>	Downregulated	-2.683612826	0.000459828	-1.578223695	0.007203059
<i>MYLK3</i>	Downregulated	-2.68008293	0.001112055	-2.942960971	0.000667866
<i>LOC731275</i>	Downregulated	-2.67944146	0.002434202	-3.002059541	0.001343306
<i>C19orf40</i>	Downregulated	-2.675944003	0.001121432	-3.199811218	0.000419129
<i>ALS2CL</i>	Downregulated	-2.675649871	0.00018272	-1.633447148	0.002719008
<i>ENTPD3-AS1</i>	Downregulated	-2.67342144	0.002132228	-3.187695767	0.000835912
<i>CLCNKB</i>	Downregulated	-2.667475706	0.000785598	-2.720486254	0.000705177
<i>FAM53A</i>	Downregulated	-2.667475706	0.002423307	-2.041805032	0.008874545

<i>LOC100133315</i>	Downregulated	-2.665455123	1.32422E-06	-1.059545217	0.00033371
<i>SLC35F2</i>	Downregulated	-2.661732783	0.003264144	-3.01287217	0.001727626
<i>CLDN2</i>	Downregulated	-2.658424986	0.000377779	-1.391869445	0.010440452
<i>TNFAIP8</i>	Downregulated	-2.657781141	0.001594359	-2.119476133	0.005015062
<i>FLJ32224</i>	Downregulated	-2.655038371	0.000500002	-1.540886001	0.008208651
<i>VTCN1</i>	Downregulated	-2.649125654	0.000121987	-2.798467346	8.84608E-05
<i>LYN</i>	Downregulated	-2.64841286	0.010881955	-3.513370716	0.002823832
<i>TSHZ2</i>	Downregulated	-2.648358019	0.00020315	-3.310652468	5.49988E-05
<i>TM6SF2</i>	Downregulated	-2.644931761	3.21156E-05	-1.530174912	0.000757907
<i>ETS1</i>	Downregulated	-2.638529494	0.003036625	-3.364298668	0.000845629
<i>LOC100101266</i>	Downregulated	-2.638359073	0.000281976	-1.607285371	0.004013864
<i>ZNF90</i>	Downregulated	-2.637257779	0.002037371	-1.946765367	0.008982591
<i>NME9</i>	Downregulated	-2.636713663	8.6211E-05	-3.001762364	3.99579E-05
<i>UNC13D</i>	Downregulated	-2.636698286	0.00013664	-1.152049586	0.010609524
<i>ANKRD18B</i>	Downregulated	-2.630615571	0.001452388	-3.64485004	0.000239097
<i>EBLN2</i>	Downregulated	-2.630321692	0.000180978	-2.308413893	0.000381431
<i>TP53TG5</i>	Downregulated	-2.629872534	0.000982659	-1.811114356	0.006556084
<i>DAPK2</i>	Downregulated	-2.629353927	0.000446129	-2.195497568	0.001200293
<i>HELB</i>	Downregulated	-2.622244201	0.001651994	-2.495254584	0.002140389
<i>ORC1</i>	Downregulated	-2.619555111	0.00299072	-2.092718775	0.008816738
<i>SEPT7L</i>	Downregulated	-2.619555111	0.008925368	-3.914066505	0.001205888
<i>DLEU2</i>	Downregulated	-2.617347466	0.000233516	-1.307246531	0.008818116
<i>PPP1R13L</i>	Downregulated	-2.612230523	0.002497108	-2.19117032	0.005954099
<i>NUDT13</i>	Downregulated	-2.610546093	0.000195994	-1.565151379	0.003168299
<i>MMP12</i>	Downregulated	-2.607328589	0.003289814	-2.151787874	0.00828563
<i>NOS3</i>	Downregulated	-2.601779734	0.000806943	-1.887070924	0.004293309
<i>CEP128</i>	Downregulated	-2.600571186	8.93221E-06	-2.25166675	2.13955E-05
<i>BCL2L15</i>	Downregulated	-2.600384646	0.000518231	-3.124505694	0.000182639
<i>RPS10P7</i>	Downregulated	-2.597828416	0.001183461	-1.893392375	0.005902175
<i>LOC100506068</i>	Downregulated	-2.587745351	0.001274456	-2.849921571	0.000755805
<i>GYPC</i>	Downregulated	-2.587473734	0.002210519	-3.448171583	0.000469717
<i>AGMAT</i>	Downregulated	-2.586270454	0.00209684	-2.593837028	0.002065326

<i>CCRL1</i>	Downregulated	-2.586064622	0.005096097	-2.464755015	0.006410461
<i>TDRD6</i>	Downregulated	-2.580260485	0.00017202	-1.812724614	0.001236464
<i>SLC19A3</i>	Downregulated	-2.579419401	0.000479675	-2.190752234	0.001174432
<i>WDR65</i>	Downregulated	-2.575694668	5.01481E-05	-2.628494577	4.44397E-05
<i>MYOM3</i>	Downregulated	-2.569354162	0.012914417	-3.420401734	0.003376321
<i>SLC17A9</i>	Downregulated	-2.568589213	0.001075929	-2.891496238	0.000562611
<i>DHRS3</i>	Downregulated	-2.566890368	0.001815535	-2.961356223	0.000845465
<i>MATN1</i>	Downregulated	-2.562696475	0.000131069	-1.421929942	0.003298942
<i>BTN3A2</i>	Downregulated	-2.561654795	0.004507258	-2.602774143	0.004168912
<i>TBX2</i>	Downregulated	-2.560299472	0.001981405	-3.538175709	0.000339917
<i>CD37</i>	Downregulated	-2.558126737	0.000312073	-1.909074461	0.001557822
<i>PCDHGB3</i>	Downregulated	-2.558126737	0.000271215	-2.316877482	0.000474735
<i>MKI67</i>	Downregulated	-2.557741762	0.013518822	-3.997760459	0.001560858
<i>FAIM3</i>	Downregulated	-2.556990533	0.000194114	-2.31548524	0.000342224
<i>LOC100128881</i>	Downregulated	-2.553975085	0.001083596	-1.631674196	0.010064675
<i>DNAH12</i>	Downregulated	-2.543042151	0.000290258	-2.297233445	0.000514793
<i>SYPL2</i>	Downregulated	-2.542286814	0.000443523	-2.260445173	0.000849772
<i>HLA-DPA1</i>	Downregulated	-2.538704669	0.001058876	-2.635273474	0.000864834
<i>ABCA10</i>	Downregulated	-2.537688149	9.28893E-05	-2.501974645	0.000100947
<i>MSH5-SAPCD1</i>	Downregulated	-2.529268988	0.000594547	-1.853558805	0.003094925
<i>PCOLCE2</i>	Downregulated	-2.529268988	3.37766E-05	-1.555639876	0.000566294
<i>SNORA48</i>	Downregulated	-2.529268988	0.002373172	-2.542814616	0.002308876
<i>EFCAB6</i>	Downregulated	-2.527698901	0.000274368	-1.925220749	0.001239519
<i>SYNPO2</i>	Downregulated	-2.527308803	1.51754E-05	-2.493691327	1.6457E-05
<i>PRO0611</i>	Downregulated	-2.527096253	0.000119542	-2.174331819	0.000284711
<i>MPP4</i>	Downregulated	-2.524224579	3.44011E-05	-3.163013721	8.79688E-06
<i>MELK</i>	Downregulated	-2.521957971	0.002038089	-1.999803079	0.006447945
<i>CASS4</i>	Downregulated	-2.520252027	0.013098464	-2.937265696	0.006547429
<i>C3orf35</i>	Downregulated	-2.519387361	6.59061E-05	-1.950470439	0.000291825
<i>ITIH2</i>	Downregulated	-2.519090296	0.001121198	-2.391824273	0.001478598
<i>SLC2A9</i>	Downregulated	-2.517855023	0.006924178	-2.791841834	0.004217327
<i>LOC641298</i>	Downregulated	-2.517042466	0.002954428	-2.008728865	0.008761651

<i>KCNAB3</i>	Downregulated	-2.516093325	0.001785853	-2.319124155	0.002720275
<i>INPP4B</i>	Downregulated	-2.515596952	0.002550965	-2.630312246	0.002027329
<i>SYT15</i>	Downregulated	-2.514092814	0.000111876	-1.562480582	0.001600832
<i>ITGB3</i>	Downregulated	-2.512682623	0.002306365	-1.92070935	0.008545728
<i>CCDC33</i>	Downregulated	-2.510319514	0.000161819	-1.629829316	0.001775254
<i>ENPP3</i>	Downregulated	-2.507327201	0.009327541	-3.450298669	0.001960766
<i>PVRL4</i>	Downregulated	-2.505997695	0.000227307	-3.060704861	7.08686E-05
<i>NOXRED1</i>	Downregulated	-2.503915507	0.000133459	-1.271365396	0.005182303
<i>SIX1</i>	Downregulated	-2.503329969	0.004211264	-3.916355409	0.000391331
<i>LOC100268168</i>	Downregulated	-2.501521432	0.000256221	-2.560345658	0.000224276
<i>LOC389641</i>	Downregulated	-2.496843416	0.009282462	-2.706863779	0.006386819
<i>COL4A3</i>	Downregulated	-2.494612442	0.000601885	-3.004322766	0.000210492
<i>SLC7A5P2</i>	Downregulated	-2.494188738	0.000835563	-1.788860776	0.004678704
<i>SHOX2</i>	Downregulated	-2.491688985	0.000282276	-2.321436511	0.00042136
<i>MSLN</i>	Downregulated	-2.488356877	0.011664386	-2.926263166	0.005530951
<i>FOXH1</i>	Downregulated	-2.486824539	0.009205932	-2.911297413	0.004374623
<i>C1orf38</i>	Downregulated	-2.4839041	0.004090359	-2.465778385	0.00424036
<i>ADAP2</i>	Downregulated	-2.483699142	0.000246031	-2.504099928	0.000234767
<i>EMP2</i>	Downregulated	-2.479221577	0.000292727	-3.011041994	9.50681E-05
<i>BMP3</i>	Downregulated	-2.477722241	0.004389342	-3.674121606	0.000553735
<i>DUOXI</i>	Downregulated	-2.474984556	0.000151196	-1.595561181	0.00173267
<i>MYBL2</i>	Downregulated	-2.471394057	0.002429249	-3.602103677	0.000314336
<i>FERMT3</i>	Downregulated	-2.469402818	1.39989E-05	-1.572697647	0.000203296
<i>RANBP3L</i>	Downregulated	-2.467840614	0.000478703	-2.911931286	0.000186835
<i>USP18</i>	Downregulated	-2.466202428	0.001808297	-3.546131688	0.000245391
<i>LRRC8E</i>	Downregulated	-2.464269579	0.000924365	-3.445337705	0.000139576
<i>FOXM1</i>	Downregulated	-2.454901298	0.000553432	-2.250289256	0.000893297
<i>KANK4</i>	Downregulated	-2.454491101	0.001587504	-3.735996228	0.000153207
<i>ZNF587B</i>	Downregulated	-2.454381179	0.000129167	-1.13813843	0.007748159
<i>RGPD3</i>	Downregulated	-2.453765094	0.000142083	-2.384241967	0.000167868
<i>PTH1R</i>	Downregulated	-2.451957091	0.002091864	-2.156813945	0.00400343
<i>SLC28A3</i>	Downregulated	-2.451702995	0.002274326	-2.611518	0.00163682

<i>MTMRII</i>	Downregulated	-2.451320483	5.3829E-05	-1.723282096	0.000415202
<i>ANKRD19P</i>	Downregulated	-2.451183537	0.000139521	-1.492051219	0.002174075
<i>WFIKKN1</i>	Downregulated	-2.451064334	0.000489231	-1.660697838	0.003844684
<i>LOC729799</i>	Downregulated	-2.450137946	4.9276E-05	-1.981269415	0.000171561
<i>CDH15</i>	Downregulated	-2.445799	0.000545505	-2.798467346	0.000255081
<i>ADAM12</i>	Downregulated	-2.443160796	0.000701827	-2.845574704	0.000298851
<i>CCDC88B</i>	Downregulated	-2.43991944	7.03766E-05	-1.125454922	0.004865781
<i>HR</i>	Downregulated	-2.43795231	0.008718709	-3.134559481	0.002577938
<i>FAM194A</i>	Downregulated	-2.436988814	1.0475E-05	-1.698786619	9.10172E-05
<i>NPEPL1</i>	Downregulated	-2.436062426	0.006438797	-2.216776268	0.009945456
<i>ATP8B4</i>	Downregulated	-2.433586225	0.000194561	-1.506904605	0.002673589
<i>RNF125</i>	Downregulated	-2.432923765	0.002536784	-2.787872924	0.001243718
<i>CASQ1</i>	Downregulated	-2.430237442	0.000827479	-2.24079274	0.001282713
<i>FAM65C</i>	Downregulated	-2.424458599	0.011477455	-2.515226263	0.009741673
<i>CLSPN</i>	Downregulated	-2.421590773	0.000165571	-2.278459154	0.000235208
<i>DMCI</i>	Downregulated	-2.419383127	3.51347E-05	-3.268391346	5.67821E-06
<i>POLN</i>	Downregulated	-2.417597425	0.000384985	-3.468898321	4.72021E-05
<i>C8orf73</i>	Downregulated	-2.416328284	4.68663E-06	-2.467785892	4.11836E-06
<i>IL17RA</i>	Downregulated	-2.412995896	0.000601549	-3.404018833	8.37495E-05
<i>NEB</i>	Downregulated	-2.412363834	0.000182418	-2.830264666	7.17035E-05
<i>CASP8</i>	Downregulated	-2.41092561	0.000367145	-2.882745657	0.000131572
<i>C2</i>	Downregulated	-2.406870393	0.002355583	-2.210619939	0.003622228
<i>SOX6</i>	Downregulated	-2.405837778	0.000168374	-3.338730124	2.4237E-05
<i>RBL1</i>	Downregulated	-2.403672922	1.77975E-05	-1.651880957	0.000164709
<i>SECTM1</i>	Downregulated	-2.402606848	0.002802747	-3.729543814	0.000257552
<i>RRN3P2</i>	Downregulated	-2.399864078	0.002563126	-2.329104004	0.00298409
<i>FOXP3</i>	Downregulated	-2.396899632	0.003603757	-2.096272218	0.006889449
<i>GINS4</i>	Downregulated	-2.395645659	0.000189238	-2.440463023	0.000170018
<i>CNTD1</i>	Downregulated	-2.389781013	0.008514794	-2.300101203	0.010126616
<i>LINC00471</i>	Downregulated	-2.388497952	0.001892946	-1.872825875	0.006358176
<i>ZNF69</i>	Downregulated	-2.385679143	7.63852E-05	-1.444315967	0.001303555
<i>C22orf43</i>	Downregulated	-2.384515679	0.000278722	-1.921535341	0.000928306

<i>CD4</i>	Downregulated	-2.384515679	0.000796966	-2.017141176	0.00194854
<i>LOC100287036</i>	Downregulated	-2.384515679	0.000383418	-1.459310857	0.005113771
<i>IFI16</i>	Downregulated	-2.381294474	0.005619635	-3.643631547	0.00061763
<i>ARHGAP10</i>	Downregulated	-2.373439108	0.001386702	-3.315855103	0.000216879
<i>TBC1D3P1-DHX40P1</i>	Downregulated	-2.366474319	0.000802938	-2.506616268	0.000584858
<i>MYBPHL</i>	Downregulated	-2.364615175	0.000730106	-3.117890765	0.00015264
<i>ECT2L</i>	Downregulated	-2.363963819	0.000335633	-1.624946889	0.00255275
<i>FGF1</i>	Downregulated	-2.36341443	0.000261572	-1.644814315	0.001909889
<i>3-Mar</i>	Downregulated	-2.360648761	0.002181278	-2.468210579	0.001729634
<i>PPARG</i>	Downregulated	-2.359066321	0.00291402	-2.791841834	0.001210879
<i>NLRP1</i>	Downregulated	-2.354870993	0.009777808	-2.396380007	0.00903428
<i>LOC284454</i>	Downregulated	-2.353156313	0.004802309	-2.954897718	0.001509725
<i>ALDH3B1</i>	Downregulated	-2.352764083	0.001675801	-2.484510466	0.001255407
<i>KL</i>	Downregulated	-2.347983948	0.012733977	-3.631194212	0.001534822
<i>SUSD2</i>	Downregulated	-2.347983948	0.003434392	-2.113813448	0.005739445
<i>IRF7</i>	Downregulated	-2.345671008	0.000158982	-1.5310739	0.001698893
<i>MXRA5</i>	Downregulated	-2.336113136	0.002527565	-2.601954792	0.001441417
<i>KCNJ2</i>	Downregulated	-2.335608948	0.000240058	-3.112816677	4.46631E-05
<i>LOC100130093</i>	Downregulated	-2.33399374	0.001720054	-2.167774069	0.002522451
<i>PGM5P2</i>	Downregulated	-2.33263555	0.000831508	-1.789396756	0.003341573
<i>TMOD4</i>	Downregulated	-2.331654479	0.000123927	-2.113974886	0.000218611
<i>PKDREJ</i>	Downregulated	-2.326871774	0.000247017	-1.208541425	0.007706642
<i>DKFZP564C196</i>	Downregulated	-2.324081334	0.000302191	-1.602411383	0.002285651
<i>HLA-DMA</i>	Downregulated	-2.319256812	1.41184E-05	-1.291564446	0.000439596
<i>LRRK70</i>	Downregulated	-2.315874168	0.000876147	-1.698786619	0.004373617
<i>TMPRSS9</i>	Downregulated	-2.313465085	0.000535848	-2.79879296	0.000181772
<i>MICALCL</i>	Downregulated	-2.313213482	0.003610098	-1.967693298	0.007852486
<i>DEPDC1</i>	Downregulated	-2.313068429	0.004195298	-2.47935856	0.002967932
<i>COL15AI</i>	Downregulated	-2.309910959	0.000305018	-2.044970145	0.000604449
<i>MUC5B</i>	Downregulated	-2.309379773	0.000538997	-2.646040055	0.000249965
<i>FAM18B2</i>	Downregulated	-2.307677619	0.000476086	-1.68370092	0.002585183
<i>WDR76</i>	Downregulated	-2.298954732	0.000197424	-2.219696707	0.000241513

<i>ITGAS</i>	Downregulated	-2.297721216	0.008138896	-3.291025869	0.001357238
<i>IRF1</i>	Downregulated	-2.297489056	0.000316532	-2.256704494	0.000350352
<i>DGKH</i>	Downregulated	-2.292232153	0.000397039	-2.305281458	0.000384538
<i>NUDT4</i>	Downregulated	-2.289864514	0.002724164	-2.816195115	0.000915949
<i>GBP1</i>	Downregulated	-2.286555574	0.008508701	-2.53644506	0.005225683
<i>SLC28A2</i>	Downregulated	-2.286555574	0.00100152	-4.226053325	2.92129E-05
<i>TNFRSF10A</i>	Downregulated	-2.286555574	0.004901057	-4.418949376	0.000139306
<i>BMP6</i>	Downregulated	-2.285023237	0.002141806	-2.876526947	0.000623314
<i>HLA-L</i>	Downregulated	-2.284274347	0.00029011	-1.376349322	0.00434225
<i>CSGALNACT1</i>	Downregulated	-2.280690928	0.002402011	-2.722689052	0.000941792
<i>ESCO2</i>	Downregulated	-2.277187293	0.000138276	-2.053827769	0.000250901
<i>HEATR4</i>	Downregulated	-2.273489819	0.003272366	-2.036573594	0.005612794
<i>LOC729177</i>	Downregulated	-2.271245352	0.000367459	-1.854446491	0.001125069
<i>KIF15</i>	Downregulated	-2.268938243	0.003014619	-2.183225568	0.00365616
<i>DNAH17</i>	Downregulated	-2.267642364	0.000547362	-1.993291584	0.001108832
<i>APOL6</i>	Downregulated	-2.265396293	0.000125896	-2.51875478	6.75322E-05
<i>LOC387723</i>	Downregulated	-2.265047968	0.002884111	-3.076384013	0.000564641
<i>FAM54A</i>	Downregulated	-2.263562472	0.002789335	-2.979752385	0.000647317
<i>LOC100129858</i>	Downregulated	-2.26317427	0.000600726	-1.381850569	0.007562193
<i>CHRNA10</i>	Downregulated	-2.261178924	0.00036505	-1.287111669	0.006925406
<i>EMX2</i>	Downregulated	-2.261134866	0.001006927	-1.601399355	0.005865428
<i>LRRK2</i>	Downregulated	-2.256767002	0.000872264	-3.171091212	0.000127393
<i>PCDHB19P</i>	Downregulated	-2.255231331	0.001179169	-2.471068819	0.000717735
<i>LINC00173</i>	Downregulated	-2.252252776	0.002110968	-1.749052612	0.007340058
<i>RELL1</i>	Downregulated	-2.250102419	0.000114729	-2.277873694	0.000106783
<i>ASB3</i>	Downregulated	-2.246686603	7.80534E-05	-1.457491712	0.000916386
<i>GALNTL2</i>	Downregulated	-2.243138238	0.002572384	-2.382030703	0.001886341
<i>AGPAT9</i>	Downregulated	-2.240611555	0.000173285	-2.275560341	0.000158429
<i>WDR62</i>	Downregulated	-2.240340597	0.001701837	-2.306016472	0.001461241
<i>GRAMD2</i>	Downregulated	-2.234494487	0.000691305	-2.748828925	0.000215187
<i>OTOGL</i>	Downregulated	-2.233662039	0.006817504	-3.470260982	0.000711039
<i>ANGPTL4</i>	Downregulated	-2.233344545	0.001407599	-1.617806579	0.007081736

<i>LCNL1</i>	Downregulated	-2.232088389	0.002767566	-3.396076857	0.000284702
<i>SNORD116-20</i>	Downregulated	-2.231039918	0.000171461	-1.303790968	0.003207683
<i>BUB1</i>	Downregulated	-2.230273595	4.09944E-05	-3.306955607	3.758E-06
<i>DKK1</i>	Downregulated	-2.229729114	0.00236449	-1.95248447	0.004598675
<i>DPF3</i>	Downregulated	-2.225127201	0.004818421	-1.918442742	0.009655051
<i>RGS5</i>	Downregulated	-2.224165773	0.001007922	-2.281756491	0.000877356
<i>EBF2</i>	Downregulated	-2.220676949	0.000630471	-2.476459629	0.000342493
<i>CENPF</i>	Downregulated	-2.219861867	0.003906229	-3.001961874	0.000807658
<i>PHACTR3</i>	Downregulated	-2.218165007	0.000450415	-1.688182832	0.001976165
<i>ITIH4</i>	Downregulated	-2.21622949	2.64334E-05	-1.896180855	6.70306E-05
<i>RHBDL2</i>	Downregulated	-2.21436062	0.000975569	-2.33504921	0.000730334
<i>HSF4</i>	Downregulated	-2.211987508	0.001050578	-1.945899318	0.002070612
<i>C21orf49</i>	Downregulated	-2.211316955	0.000565336	-2.343547324	0.00040859
<i>GTSE1</i>	Downregulated	-2.210958031	0.000832143	-3.306521434	8.40516E-05
<i>KIAA1656</i>	Downregulated	-2.20994575	0.001014211	-1.675035214	0.004251583
<i>PRIMA1</i>	Downregulated	-2.204254009	0.001013416	-2.567980454	0.000436615
<i>SLC25A34</i>	Downregulated	-2.201230027	0.000135309	-1.379689897	0.001816811
<i>COL4A4</i>	Downregulated	-2.200029929	0.001456355	-3.195862367	0.000182689
<i>C6orf163</i>	Downregulated	-2.199012221	0.00047565	-1.527598668	0.003310843
<i>MCM9</i>	Downregulated	-2.194164094	0.00038812	-1.955027593	0.000737736
<i>TOMM20L</i>	Downregulated	-2.194096716	1.45193E-05	-1.683040346	7.10963E-05
<i>ZNF490</i>	Downregulated	-2.190725927	0.001402808	-1.51561053	0.008732
<i>CACNA2D3</i>	Downregulated	-2.184010436	0.000123918	-1.467937824	0.001158183
<i>IMPA2</i>	Downregulated	-2.183980731	0.002949115	-2.253485034	0.002514671
<i>RPL19P12</i>	Downregulated	-2.181221239	0.000722377	-2.262465755	0.000590321
<i>LMOD1</i>	Downregulated	-2.179891047	0.001995797	-1.712820428	0.006605121
<i>CCDC163P</i>	Downregulated	-2.178488859	0.002629969	-3.506463019	0.000194679
<i>PHEX</i>	Downregulated	-2.171552772	0.003051031	-2.919605269	0.000635319
<i>KLRG1</i>	Downregulated	-2.168627002	1.51012E-05	-1.759170812	5.30427E-05
<i>KIAA1462</i>	Downregulated	-2.167216398	0.000340039	-2.602961733	0.000118433
<i>ERBB3</i>	Downregulated	-2.16530382	0.000207902	-2.558145382	7.86766E-05
<i>NFATC1</i>	Downregulated	-2.164980084	0.004898281	-3.66627671	0.00029776

<i>MLN</i>	Downregulated	-2.160786191	0.000729171	-2.118816163	0.000811911
<i>OXT</i>	Downregulated	-2.160786191	0.002595545	-1.909074461	0.004811026
<i>TAGAP</i>	Downregulated	-2.160557916	8.13802E-05	-1.77485051	0.00025509
<i>LY6G5C</i>	Downregulated	-2.157011964	8.98648E-05	-1.294818136	0.001578689
<i>GP1BA</i>	Downregulated	-2.153050487	7.2795E-05	-1.043679872	0.003924126
<i>SYCP2</i>	Downregulated	-2.152763708	0.001039067	-2.850779042	0.00021647
<i>C15orf42</i>	Downregulated	-2.151962258	0.000214657	-2.239965941	0.000170352
<i>ZNF469</i>	Downregulated	-2.149664442	0.00069007	-2.884584822	0.000129866
<i>C3orf49</i>	Downregulated	-2.148738353	0.004772039	-1.96228549	0.007349654
<i>CCDC7</i>	Downregulated	-2.148539488	5.24294E-05	-1.465653939	0.000479449
<i>KCNK6</i>	Downregulated	-2.141802266	0.003806917	-2.325409515	0.002515669
<i>PKD1L3</i>	Downregulated	-2.140223824	0.001707014	-2.301477529	0.001160697
<i>CEP152</i>	Downregulated	-2.137894222	7.1686E-06	-1.396303973	9.25943E-05
<i>KRT15</i>	Downregulated	-2.135021041	0.005741993	-2.994534614	0.00101907
<i>PLCB3</i>	Downregulated	-2.134867597	0.001262781	-1.68126425	0.004304165
<i>TAS2R20</i>	Downregulated	-2.134225265	0.005195091	-2.782157241	0.00134933
<i>KIAA1614</i>	Downregulated	-2.133389954	6.19383E-05	-1.182215477	0.001725629
<i>MYO15B</i>	Downregulated	-2.129462868	0.004569936	-1.943352624	0.007073685
<i>ARHGAP31</i>	Downregulated	-2.125791651	0.010340162	-2.93539181	0.002168759
<i>IZUMO4</i>	Downregulated	-2.12364981	2.53527E-05	-1.661236221	0.000109035
<i>LOC221442</i>	Downregulated	-2.120701017	0.00798816	-2.274981014	0.005745008
<i>USP43</i>	Downregulated	-2.120584633	0.000347466	-2.017031187	0.000460609
<i>PDE1A</i>	Downregulated	-2.11444932	0.000162766	-1.684858151	0.000590827
<i>ATP8B3</i>	Downregulated	-2.112678533	0.000128766	-1.060920978	0.005306365
<i>BAIAP2L2</i>	Downregulated	-2.112541079	0.00050688	-1.699155218	0.001652884
<i>ABCC3</i>	Downregulated	-2.112060737	0.000570998	-2.236060596	0.000415123
<i>SPATA5</i>	Downregulated	-2.110078387	9.8166E-05	-1.363386267	0.001155929
<i>AGBL2</i>	Downregulated	-2.104166818	0.001300068	-3.061321212	0.000160029
<i>FAM71F2</i>	Downregulated	-2.103653163	2.63787E-05	-2.533099351	8.56246E-06
<i>CAPN3</i>	Downregulated	-2.101867946	0.000521502	-1.925596291	0.000845411
<i>RARB</i>	Downregulated	-2.100703615	5.1529E-05	-1.381727114	0.00057794
<i>PDGFRB</i>	Downregulated	-2.09654005	0.011044172	-2.838061797	0.002591288

<i>C10orf140</i>	Downregulated	-2.089240813	0.001325781	-2.092694676	0.001314159
<i>GPR126</i>	Downregulated	-2.083741747	0.003155488	-4.137795994	7.04344E-05
<i>KRTAP5-7</i>	Downregulated	-2.08272659	0.001632957	-2.403326641	0.0007561
<i>RHOJ</i>	Downregulated	-2.077497128	0.003102802	-2.978716617	0.000452444
<i>HERC2P7</i>	Downregulated	-2.076153902	0.000399447	-2.377862257	0.000184194
<i>SNX22</i>	Downregulated	-2.075341345	0.003055648	-2.182187813	0.002366471
<i>RBMS3</i>	Downregulated	-2.072380996	0.002271681	-2.883234447	0.000379916
<i>NLRC3</i>	Downregulated	-2.071090803	0.001395801	-1.704397464	0.003801358
<i>GRIN2C</i>	Downregulated	-2.067810978	0.000996847	-1.740173374	0.002475135
<i>FAM129A</i>	Downregulated	-2.065775973	0.00022114	-4.027426732	4.08514E-06
<i>SH3D21</i>	Downregulated	-2.064147437	7.70932E-05	-1.004960907	0.004029259
<i>TPTE2P1</i>	Downregulated	-2.063109607	0.000489356	-1.304891606	0.005379575
<i>NMI</i>	Downregulated	-2.062826086	0.004581705	-2.223090072	0.00316263
<i>UCP3</i>	Downregulated	-2.06123829	0.000265106	-1.806240368	0.0005581
<i>ADAMTS6</i>	Downregulated	-2.053609302	0.004724055	-2.342271636	0.002448217
<i>CFD</i>	Downregulated	-2.051875067	0.000874704	-2.314899663	0.000449017
<i>ARAP3</i>	Downregulated	-2.050976217	0.002271809	-2.263693095	0.001354637
<i>LOC439949</i>	Downregulated	-2.049095059	0.00195113	-1.846879613	0.003318008
<i>CLMP</i>	Downregulated	-2.042887682	0.003282942	-2.469921358	0.00122571
<i>AFAP1L1</i>	Downregulated	-2.041153071	0.013089521	-2.84630902	0.002713551
<i>ABCA9</i>	Downregulated	-2.0392107	0.000333413	-1.9899999	0.000382792
<i>LOC100506746</i>	Downregulated	-2.038605495	0.000936647	-1.831704485	0.001659697
<i>THSD4</i>	Downregulated	-2.038113362	0.006404268	-3.173714297	0.000652564
<i>RAB41</i>	Downregulated	-2.037773229	0.000220411	-1.562113824	0.000974395
<i>DUSP19</i>	Downregulated	-2.036003145	0.001509586	-2.332787119	0.000724462
<i>DLC1</i>	Downregulated	-2.034696586	0.000243419	-1.959482018	0.000301793
<i>LDB3</i>	Downregulated	-2.033627597	0.000743543	-2.815144453	0.000117225
<i>LOC648809</i>	Downregulated	-2.033507492	4.25879E-05	-1.163762835	0.001039379
<i>GSTM2P1</i>	Downregulated	-2.030902845	0.000290465	-2.945963424	3.28634E-05
<i>PCDHB11</i>	Downregulated	-2.028356467	0.00033551	-1.391376539	0.002579005
<i>LOC728377</i>	Downregulated	-2.02513518	0.005059728	-3.27978021	0.000398154
<i>RASA4</i>	Downregulated	-2.021001944	0.001640511	-1.753190251	0.00340429

<i>NPHP3</i>	Downregulated	-2.019875829	0.000370796	-2.208157186	0.000223205
<i>LOC388849</i>	Downregulated	-2.018817606	0.000495036	-1.117095192	0.010111295
<i>E2F7</i>	Downregulated	-2.017902777	0.006314088	-2.097605578	0.005248273
<i>LOC619207</i>	Downregulated	-2.017280661	4.42128E-05	-1.325123242	0.000504526
<i>EHBP1L1</i>	Downregulated	-2.016359686	0.000115804	-2.302959443	5.28969E-05
<i>ABCA1</i>	Downregulated	-2.012862014	0.006803257	-2.73175307	0.001472326
<i>MUC1</i>	Downregulated	-2.012646268	0.005894447	-2.194242114	0.003874833
<i>PHACTR2</i>	Downregulated	-2.009318884	0.00055384	-2.169396914	0.000360363
<i>FMNI</i>	Downregulated	-2.007627708	0.001217556	-2.450245262	0.000407234
<i>CARNIS1</i>	Downregulated	-2.00596745	0.002823254	-1.931618406	0.003414789
<i>ATP2C2</i>	Downregulated	-2.001250056	0.000897979	-1.522107963	0.003741345
<i>STL</i>	Downregulated	-2.000763839	0.001722883	-1.592725819	0.00543004
<i>COL16A1</i>	Downregulated	-2.000132467	0.001263919	-2.656447642	0.000262327
<i>LAMA4</i>	Downregulated	-1.999437527	0.000355517	-1.527359894	0.001555073
<i>MND1</i>	Downregulated	-1.996132378	0.002751842	-2.571817418	0.000718107
<i>GLI3</i>	Downregulated	-1.993743694	0.001821066	-2.522065069	0.000510206
<i>NFKBIZ</i>	Downregulated	-1.992894	0.00074577	-2.826487266	0.000102037
<i>LOC100505894</i>	Downregulated	-1.990784087	0.003791143	-2.468726657	0.001248968
<i>LMOD3</i>	Downregulated	-1.988936832	0.000206538	-2.984691118	1.87223E-05
<i>CATSPER3</i>	Downregulated	-1.985365797	0.000725603	-2.479235105	0.000207668
<i>LINC00174</i>	Downregulated	-1.982206493	0.000603573	-1.342109205	0.004643398
<i>DOCK5</i>	Downregulated	-1.980968997	0.004656934	-1.921340796	0.00539873
<i>NRXN3</i>	Downregulated	-1.980730732	0.006676796	-2.24764344	0.003620299
<i>ITGA10</i>	Downregulated	-1.979723403	0.000677049	-1.590291829	0.002184391
<i>TTN</i>	Downregulated	-1.979547878	1.7516E-05	-1.684778169	4.61191E-05
<i>MYOZ3</i>	Downregulated	-1.976897373	0.001125209	-2.39495762	0.000390828
<i>TAS2R31</i>	Downregulated	-1.976499498	0.000225993	-1.003867599	0.007954072
<i>IL27RA</i>	Downregulated	-1.973945792	0.001295365	-1.469512914	0.005782104
<i>SCARNA12</i>	Downregulated	-1.973588434	0.002943965	-1.888150587	0.003675355
<i>PDE6C</i>	Downregulated	-1.973357084	0.009813025	-2.790188713	0.001804696
<i>OPLAH</i>	Downregulated	-1.972463306	0.000340812	-3.13726734	2.23752E-05
<i>NPR3</i>	Downregulated	-1.971975144	0.001843602	-2.180352491	0.00108166

<i>PRSS36</i>	Downregulated	-1.965914451	0.005180865	-2.449608054	0.001708004
<i>DPH3P1</i>	Downregulated	-1.96457744	0.001575278	-1.402029438	0.008373708
<i>TAF1L</i>	Downregulated	-1.964564067	0.000266827	-1.688757336	0.000624764
<i>KIAA1530</i>	Downregulated	-1.963694939	7.18782E-05	-1.158352321	0.001416991
<i>DOK3</i>	Downregulated	-1.960826729	0.000177314	-1.48005952	0.000863232
<i>LOC387646</i>	Downregulated	-1.960748576	0.000209945	-2.191850297	0.00010997
<i>MIR940</i>	Downregulated	-1.960517226	0.000228258	-1.261346519	0.002533973
<i>HSPB6</i>	Downregulated	-1.957984634	0.003355253	-2.655690333	0.000671865
<i>P2RX5-TAX1BP3</i>	Downregulated	-1.956520464	0.000453187	-2.307614558	0.000177003
<i>CENPN</i>	Downregulated	-1.954902035	3.96595E-05	-1.997927112	3.48183E-05
<i>FBXO32</i>	Downregulated	-1.953750742	0.002698832	-3.32889482	0.000144206
<i>LOC285593</i>	Downregulated	-1.949103261	0.000627748	-1.454321189	0.002969806
<i>APOLD1</i>	Downregulated	-1.94655072	0.000734016	-1.738118936	0.001354471
<i>LRGUK</i>	Downregulated	-1.945469014	0.007059271	-1.929105343	0.007342979
<i>CDCA7</i>	Downregulated	-1.943837928	0.00018138	-1.799091619	0.000282779
<i>ILIRAP</i>	Downregulated	-1.936914364	0.00323878	-1.742251438	0.00544889
<i>NIDI</i>	Downregulated	-1.933124453	0.007342904	-2.607559064	0.001657468
<i>ATP2A1</i>	Downregulated	-1.932818015	0.000180115	-1.200533629	0.002457888
<i>PCDH12</i>	Downregulated	-1.932676322	0.000817825	-1.993321722	0.000690323
<i>EFNA4</i>	Downregulated	-1.928126564	0.001602852	-1.459310857	0.006468451
<i>SAMD9</i>	Downregulated	-1.928126564	0.010108858	-2.316676045	0.004263349
<i>ASF1B</i>	Downregulated	-1.927954405	0.010973064	-2.414043579	0.003808435
<i>ULK4</i>	Downregulated	-1.927260848	1.54605E-05	-1.813482628	2.23299E-05
<i>CDC6</i>	Downregulated	-1.921065925	0.00596738	-2.200339791	0.003067692
<i>HSF2BP</i>	Downregulated	-1.920815547	0.001218168	-1.461615484	0.004924512
<i>RFTN2</i>	Downregulated	-1.92010046	0.000582345	-2.431736456	0.000152068
<i>MCC</i>	Downregulated	-1.919346834	0.006673272	-2.608104043	0.001431084
<i>C3orf32</i>	Downregulated	-1.918072777	0.006265542	-1.969610078	0.00522232
<i>HARIA</i>	Downregulated	-1.918072777	0.000603643	-1.703125565	0.001154666
<i>TNFRSF25</i>	Downregulated	-1.916660908	0.000660286	-1.298441354	0.005010949
<i>LOC100506649</i>	Downregulated	-1.91507963	0.001948827	-1.870743857	0.002200494
<i>FLJ39653</i>	Downregulated	-1.911749749	0.000427143	-1.585725202	0.001193231

<i>ADM2</i>	Downregulated	-1.909007249	0.013390455	-2.992928049	0.001518027
<i>KLHL34</i>	Downregulated	-1.908549899	0.006736247	-1.98974494	0.005527897
<i>MGC16275</i>	Downregulated	-1.907516284	0.004225123	-2.271352782	0.001739619
<i>LTBR</i>	Downregulated	-1.904500457	0.005712943	-1.943844927	0.00517893
<i>LAMA3</i>	Downregulated	-1.904298467	0.006537129	-1.839250095	0.007689725
<i>CORO6</i>	Downregulated	-1.903690766	9.57613E-05	-1.059255897	0.002477807
<i>LOC100288846</i>	Downregulated	-1.901393479	0.001389639	-2.25985459	0.000542653
<i>C9orf100</i>	Downregulated	-1.896151691	6.39173E-05	-1.821085625	8.11419E-05
<i>JAK3</i>	Downregulated	-1.895940147	0.00147303	-1.402430948	0.006683276
<i>ANGPTL6</i>	Downregulated	-1.895528833	0.000112558	-1.381850569	0.00068066
<i>HSD17B11</i>	Downregulated	-1.894381837	0.004901334	-2.607753627	0.000943686
<i>C16orf74</i>	Downregulated	-1.893534781	0.000271429	-1.708805496	0.000484751
<i>CHDH</i>	Downregulated	-1.892676182	0.006572372	-3.638000185	0.000205072
<i>ZHX2</i>	Downregulated	-1.891486999	0.000584634	-2.022784478	0.000401778
<i>ENPEP</i>	Downregulated	-1.888961007	0.000532949	-2.199497657	0.000225279
<i>LOC100507501</i>	Downregulated	-1.884207389	0.003819014	-3.239212119	0.000204265
<i>MAK</i>	Downregulated	-1.882574962	0.003356107	-2.20821034	0.001474286
<i>SLC39A11</i>	Downregulated	-1.881267472	0.001209331	-2.142092424	0.000595813
<i>LOC100506451</i>	Downregulated	-1.87809271	0.00136153	-1.650640785	0.002667898
<i>ATG9B</i>	Downregulated	-1.876909881	0.000106954	-1.423369719	0.00052109
<i>UCKLI-ASI</i>	Downregulated	-1.876729623	0.011843518	-1.985656569	0.009204645
<i>MMS22L</i>	Downregulated	-1.872820061	0.001843808	-1.496399076	0.005676234
<i>TMC3</i>	Downregulated	-1.872074885	0.001891331	-1.533260818	0.00516
<i>GPR179</i>	Downregulated	-1.86956055	0.009755922	-1.956243097	0.007933942
<i>CCNE1</i>	Downregulated	-1.86903616	0.004984652	-1.907229581	0.004517847
<i>SARDH</i>	Downregulated	-1.868405765	0.000187621	-1.329112146	0.001253369
<i>ATHL1</i>	Downregulated	-1.864826964	0.007709493	-2.460123555	0.001966981
<i>PLEKHG4B</i>	Downregulated	-1.86090644	0.000193736	-1.947168805	0.000149049
<i>ARHGEF26</i>	Downregulated	-1.856743377	0.000861909	-3.504959057	2.17834E-05
<i>ALDH8A1</i>	Downregulated	-1.852390113	0.002783974	-1.548861052	0.006686054
<i>AMH</i>	Downregulated	-1.847299933	0.000946631	-1.179834953	0.009002134
<i>MIR137HG</i>	Downregulated	-1.844962407	5.5646E-05	-1.172308403	0.000751058

<i>PIWIL4</i>	Downregulated	-1.843135053	0.000892885	-2.431092536	0.000188522
<i>C5</i>	Downregulated	-1.842860352	0.002649129	-1.846007156	0.002626183
<i>CATSPER2</i>	Downregulated	-1.841445488	0.000888466	-1.613150018	0.001801482
<i>RNF144B</i>	Downregulated	-1.839657466	0.003967366	-2.450689298	0.000891822
<i>AIFM3</i>	Downregulated	-1.837840441	0.011120415	-1.978262026	0.007969984
<i>FAM186B</i>	Downregulated	-1.837840441	0.003892876	-1.488458652	0.010515593
<i>RAPGEF3</i>	Downregulated	-1.836736373	0.000950947	-1.166460648	0.009272018
<i>TUBD1</i>	Downregulated	-1.832806076	0.001194041	-2.739297747	0.000124741
<i>GALNT6</i>	Downregulated	-1.832273349	0.012615001	-1.952766916	0.009507181
<i>LOC389791</i>	Downregulated	-1.82707386	0.003825409	-1.54504444	0.008512913
<i>ERBB4</i>	Downregulated	-1.826808732	0.000185018	-2.374703752	3.95609E-05
<i>LRP5L</i>	Downregulated	-1.826690456	0.000126971	-1.121699456	0.001910073
<i>C7orf10</i>	Downregulated	-1.826482228	0.008860231	-2.285869471	0.003009889
<i>TPX2</i>	Downregulated	-1.824866215	0.000609161	-2.142677123	0.000246526
<i>C8orf51</i>	Downregulated	-1.82325965	0.000709603	-2.700895741	7.48994E-05
<i>PFNIP2</i>	Downregulated	-1.821161143	0.001757753	-2.168856669	0.000686654
<i>CCDC102B</i>	Downregulated	-1.821006546	0.001071126	-1.485370555	0.003103361
<i>PLB1</i>	Downregulated	-1.817861241	0.004237246	-1.8599014	0.003785248
<i>SNORD22</i>	Downregulated	-1.814847339	0.003692297	-1.528154329	0.008401986
<i>SPHK1</i>	Downregulated	-1.814847339	0.005208807	-2.972078403	0.000386869
<i>LGALS3</i>	Downregulated	-1.814704864	0.000132965	-2.258060192	3.6549E-05
<i>CYP20A1</i>	Downregulated	-1.814171336	0.000128334	-1.484016076	0.00040606
<i>FBXO36</i>	Downregulated	-1.810607415	0.002400759	-1.679388296	0.003513402
<i>ANO9</i>	Downregulated	-1.804687346	0.004428344	-2.677407933	0.000557814
<i>GNN</i>	Downregulated	-1.804687346	0.01166132	-2.448075717	0.00272975
<i>AIM1</i>	Downregulated	-1.803147578	0.000234233	-2.105830428	9.51496E-05
<i>CD27</i>	Downregulated	-1.802410004	0.002124547	-1.620727018	0.003643613
<i>RPL23AP64</i>	Downregulated	-1.793649192	0.000241461	-1.676800993	0.000354307
<i>PNPLA7</i>	Downregulated	-1.79305736	0.000757967	-2.278809163	0.00019646
<i>SERPINF2</i>	Downregulated	-1.788667867	1.65497E-05	-1.017807115	0.000451237
<i>ZNF563</i>	Downregulated	-1.787247937	0.000945378	-1.516991472	0.002252486
<i>MDM4</i>	Downregulated	-1.781225596	0.000617734	-1.225283996	0.004386618

<i>CDH23</i>	Downregulated	-1.778424835	0.001497628	-2.351643891	0.000322546
<i>TAF8</i>	Downregulated	-1.777541517	0.000578287	-2.260082891	0.000147543
<i>DCHS2</i>	Downregulated	-1.776912739	0.000997389	-2.240398813	0.00027452
<i>LOC100132247</i>	Downregulated	-1.771042127	0.000107571	-1.361995714	0.000484617
<i>LOC646214</i>	Downregulated	-1.766155003	0.003077601	-1.583491613	0.005271332
<i>HAPLN3</i>	Downregulated	-1.765645487	0.00222738	-1.605077726	0.003611852
<i>ISPD</i>	Downregulated	-1.761592962	7.1038E-05	-1.226579405	0.000569074
<i>FBLN2</i>	Downregulated	-1.760935516	0.002081579	-2.020121955	0.00100545
<i>DHRS4L1</i>	Downregulated	-1.756412112	0.000243642	-1.789391112	0.000218985
<i>P2RX5</i>	Downregulated	-1.753418965	0.000493536	-1.229423278	0.003266566
<i>ATG16L2</i>	Downregulated	-1.752990269	5.95091E-05	-1.208290873	0.000509724
<i>SH2D3A</i>	Downregulated	-1.752452955	0.000199745	-1.718965488	0.000223186
<i>ARRDC2</i>	Downregulated	-1.750863258	0.00034868	-1.550698274	0.000686959
<i>GHR</i>	Downregulated	-1.748988409	0.002086171	-2.433015298	0.000346363
<i>BRCA1</i>	Downregulated	-1.743962338	0.003635913	-2.485137955	0.000558818
<i>NRG4</i>	Downregulated	-1.743434757	0.000419572	-1.330588153	0.001823394
<i>LPIN3</i>	Downregulated	-1.742976085	0.000447443	-1.785543746	0.000390689
<i>LOC645166</i>	Downregulated	-1.73951993	8.4608E-05	-1.468118519	0.000226932
<i>B3GNT7</i>	Downregulated	-1.737675316	0.002080879	-1.889866176	0.001338425
<i>SLCO2A1</i>	Downregulated	-1.736787738	0.001221684	-2.09447782	0.000437113
<i>MYLK4</i>	Downregulated	-1.736140354	0.002743116	-2.190013905	0.00080368
<i>LOC400680</i>	Downregulated	-1.735684021	0.000321448	-2.239331228	7.33832E-05
<i>MYLK</i>	Downregulated	-1.734371868	0.010869404	-2.378269288	0.002381506
<i>SCNN1D</i>	Downregulated	-1.73304078	0.003386554	-1.42356136	0.008692898
<i>CA13</i>	Downregulated	-1.732707819	0.001262421	-1.322808039	0.005006044
<i>CENPL</i>	Downregulated	-1.727247471	0.002978693	-2.131506561	0.000989346
<i>FST</i>	Downregulated	-1.716381912	0.01025163	-3.720407228	0.000179139
<i>PCSK5</i>	Downregulated	-1.707166702	0.00026894	-2.524925354	2.6971E-05
<i>VWCE</i>	Downregulated	-1.706855544	0.000530595	-1.194989936	0.003511865
<i>NR6A1</i>	Downregulated	-1.703634913	0.00137353	-1.485076007	0.002805003
<i>FHOD1</i>	Downregulated	-1.697207319	0.001648674	-2.271692612	0.000333816
<i>XPNPEP3</i>	Downregulated	-1.695935656	0.002497076	-1.726810743	0.002276101

<i>MAP7D3</i>	Downregulated	-1.693312277	0.002574326	-1.82870907	0.001728546
<i>TMOD1</i>	Downregulated	-1.690789846	0.010838185	-2.475617053	0.001688285
<i>NEK8</i>	Downregulated	-1.683421244	2.70749E-05	-1.687453658	2.66883E-05
<i>ESR2</i>	Downregulated	-1.683200175	0.001351677	-1.294307215	0.005143361
<i>DMKN</i>	Downregulated	-1.680112907	0.000302685	-1.921139932	0.000139955
<i>PLCE1</i>	Downregulated	-1.67861847	0.000121426	-1.161251196	0.000972952
<i>C18orf56</i>	Downregulated	-1.675359364	0.001817989	-1.387115903	0.004719531
<i>SLC25A35</i>	Downregulated	-1.675359364	0.0046294	-2.017141176	0.001810266
<i>FANCI</i>	Downregulated	-1.6671913	0.000336367	-2.2518789	5.86565E-05
<i>CCDC154</i>	Downregulated	-1.662828732	0.00455202	-1.401360997	0.010148865
<i>LOC100506023</i>	Downregulated	-1.661601613	0.00015643	-1.518585545	0.000262643
<i>PTGIS</i>	Downregulated	-1.657680523	0.001044099	-1.178906538	0.005937134
<i>PRRX1</i>	Downregulated	-1.651510993	0.013293921	-2.56271512	0.001588719
<i>C9orf3</i>	Downregulated	-1.651147982	0.001687334	-1.660431252	0.001638314
<i>DNAH7</i>	Downregulated	-1.645168621	7.54247E-05	-1.201746367	0.000460973
<i>FBXO17</i>	Downregulated	-1.643834828	0.000706322	-1.234971373	0.003195528
<i>MIR149</i>	Downregulated	-1.642796542	0.003491517	-1.331722329	0.009490661
<i>CD44</i>	Downregulated	-1.641947425	0.01253907	-3.577822978	0.000225931
<i>FGFR4</i>	Downregulated	-1.639876103	0.002467514	-1.291564446	0.007912809
<i>TEP1</i>	Downregulated	-1.630367957	0.000166232	-1.1893417	0.000977963
<i>GNL3L</i>	Downregulated	-1.630072583	0.001277995	-1.169065268	0.006816668
<i>TRIM38</i>	Downregulated	-1.629736513	0.005366689	-2.840444373	0.000281512
<i>CLMN</i>	Downregulated	-1.629221573	0.000285159	-1.761858998	0.000181995
<i>CHST5</i>	Downregulated	-1.623680671	0.003541103	-1.724836101	0.002610583
<i>LTB4R</i>	Downregulated	-1.620976006	0.001434162	-1.264878245	0.005056625
<i>HMBOXI</i>	Downregulated	-1.616230947	0.000363284	-1.236896591	0.001571486
<i>ZNF573</i>	Downregulated	-1.616095169	0.005060477	-1.622295592	0.00496762
<i>PLEKHG6</i>	Downregulated	-1.614781506	0.009987802	-1.833141946	0.00554154
<i>MACROD2</i>	Downregulated	-1.613432533	0.000664126	-1.44486795	0.001210231
<i>LOC344967</i>	Downregulated	-1.611903307	0.002409617	-1.208361597	0.009705619
<i>GMEB1</i>	Downregulated	-1.607857058	0.00048519	-1.298792511	0.001550566
<i>GATSL2</i>	Downregulated	-1.605973945	0.002915939	-1.359306624	0.00659028

<i>ZNF221</i>	Downregulated	-1.605646246	0.002898116	-1.341782699	0.006957878
<i>C10orf103</i>	Downregulated	-1.603098156	0.004465291	-1.399327052	0.008501899
<i>SGK494</i>	Downregulated	-1.600797648	0.001112854	-1.326730301	0.00296791
<i>HYAL1</i>	Downregulated	-1.600751726	0.007133338	-2.828014719	0.000366516
<i>LOC100507053</i>	Downregulated	-1.594638575	0.000186984	-1.607940986	0.000178224
<i>LOC283440</i>	Downregulated	-1.592034429	0.006655742	-3.001583536	0.000232693
<i>ITGB1BP2</i>	Downregulated	-1.59111785	0.001881841	-1.467373339	0.00285418
<i>LOC100131067</i>	Downregulated	-1.589947834	0.002171875	-1.242891693	0.007302612
<i>DNAH1</i>	Downregulated	-1.589362768	0.001658446	-1.467420604	0.002509631
<i>C20orf132</i>	Downregulated	-1.589105467	0.000465711	-2.159032072	7.97268E-05
<i>MMP25</i>	Downregulated	-1.588679855	0.000723143	-1.088749304	0.005132657
<i>CDCA8</i>	Downregulated	-1.588242843	0.000179764	-1.556544712	0.000201933
<i>EDARADD</i>	Downregulated	-1.587853912	0.003110587	-1.90785707	0.001196483
<i>EFNA5</i>	Downregulated	-1.576622344	0.000737799	-1.861127624	0.000291574
<i>BNC2</i>	Downregulated	-1.573215576	0.000311215	-2.695037215	1.29638E-05
<i>NEK2</i>	Downregulated	-1.572133925	0.009269537	-2.288230905	0.001449728
<i>PDE11A</i>	Downregulated	-1.567645524	0.007855016	-1.593275522	0.007285649
<i>RYR3</i>	Downregulated	-1.567400468	0.001150473	-1.329579641	0.00272217
<i>DDR2</i>	Downregulated	-1.563013016	0.004953302	-1.780657166	0.002588896
<i>JMJD7</i>	Downregulated	-1.559783104	0.0006184	-1.299732043	0.001656504
<i>ZAK</i>	Downregulated	-1.559280087	0.006607657	-2.760363623	0.000330339
<i>CCDC18</i>	Downregulated	-1.557763977	0.000860255	-1.147317702	0.004217568
<i>COL9A2</i>	Downregulated	-1.55707087	0.014365544	-1.868103842	0.006317439
<i>MYL3</i>	Downregulated	-1.554855314	0.009906519	-2.129582744	0.002153145
<i>LOC100131655</i>	Downregulated	-1.551557181	0.010545513	-2.223859407	0.001827931
<i>SRCRB4D</i>	Downregulated	-1.54958998	0.000479399	-1.183743756	0.002053822
<i>DDX60L</i>	Downregulated	-1.549037964	0.008005927	-3.694743494	7.45377E-05
<i>MTL5</i>	Downregulated	-1.548904736	0.011034527	-1.582569937	0.010024516
<i>MOB3B</i>	Downregulated	-1.547577486	0.000300997	-1.179002698	0.00135011
<i>C4orf47</i>	Downregulated	-1.54742377	0.006964957	-1.902071032	0.002531112
<i>DSCR6</i>	Downregulated	-1.547419937	0.011616283	-1.874946833	0.004766507
<i>YJEFN3</i>	Downregulated	-1.546884485	0.000359007	-1.153201876	0.001783841

<i>KIFC1</i>	Downregulated	-1.542628792	0.012559979	-2.114220912	0.00282351
<i>PILRB</i>	Downregulated	-1.538056661	0.000608912	-1.214001479	0.002165938
<i>LOC100288198</i>	Downregulated	-1.537456339	0.009216601	-1.57536213	0.008246497
<i>PROC</i>	Downregulated	-1.536650664	0.00834871	-2.422310566	0.000834087
<i>ACACB</i>	Downregulated	-1.533551275	0.005282365	-2.247350685	0.000729823
<i>SSPN</i>	Downregulated	-1.533173632	0.013136722	-2.423181496	0.001420832
<i>SLC26A1</i>	Downregulated	-1.532930233	0.0023279	-1.176576702	0.008457021
<i>IBA57</i>	Downregulated	-1.530418922	0.001520766	-1.354061639	0.002867403
<i>C17orf53</i>	Downregulated	-1.527784365	0.002935046	-1.625568853	0.002136676
<i>LOC728989</i>	Downregulated	-1.525741609	0.006304651	-1.482333238	0.007219988
<i>GRHL1</i>	Downregulated	-1.521297095	0.00088719	-1.304404506	0.002011929
<i>CYP2D6</i>	Downregulated	-1.519706773	0.012840334	-1.634457063	0.009292826
<i>TTLL3</i>	Downregulated	-1.515557843	0.001084542	-1.094440611	0.005708276
<i>FAM46C</i>	Downregulated	-1.51552862	0.004035056	-2.402299995	0.000345984
<i>CPT1A</i>	Downregulated	-1.515427028	0.005363216	-2.618870018	0.000295243
<i>ZSCAN22</i>	Downregulated	-1.515378709	0.000212928	-1.218106539	0.000727877
<i>PIEZ01</i>	Downregulated	-1.51306633	0.002172659	-1.808316597	0.000841924
<i>AKR7A3</i>	Downregulated	-1.511986808	0.012411964	-1.613150018	0.009303225
<i>C1orf101</i>	Downregulated	-1.5108823	0.000912252	-1.746779923	0.00040872
<i>TONSL</i>	Downregulated	-1.510807387	0.002320495	-1.606660323	0.001685194
<i>LOC285456</i>	Downregulated	-1.509504806	0.002327379	-1.338025412	0.00426779
<i>CILP2</i>	Downregulated	-1.508223937	0.001009028	-1.006973333	0.007752018
<i>ASB14</i>	Downregulated	-1.505282787	0.008134398	-1.42276268	0.010504044
<i>RTDR1</i>	Downregulated	-1.50403523	0.005657251	-1.507318425	0.005598548
<i>TIAM2</i>	Downregulated	-1.502389418	0.000408852	-1.269020501	0.001037735
<i>POLR2J3</i>	Downregulated	-1.49939304	8.35383E-05	-1.355980733	0.0001504
<i>CCDC77</i>	Downregulated	-1.497063641	0.002753672	-1.570760217	0.002152269
<i>LOC728758</i>	Downregulated	-1.495870118	0.001066512	-2.273747315	9.99499E-05
<i>ARHGEF1</i>	Downregulated	-1.495740254	0.005365563	-1.359599647	0.008400372
<i>PRR16</i>	Downregulated	-1.494074324	0.001421486	-1.63093061	0.000887345
<i>TENI-CDK3</i>	Downregulated	-1.494074324	0.003436927	-1.610845391	0.002346766
<i>LOC100131208</i>	Downregulated	-1.488161606	0.002720513	-1.334642768	0.004678457

<i>FAM13A-AS1</i>	Downregulated	-1.488119365	0.000723156	-1.142358361	0.002928839
<i>NPAS2</i>	Downregulated	-1.485567907	0.00044263	-1.206023117	0.001384393
<i>PION</i>	Downregulated	-1.477335539	0.004753826	-2.000622632	0.000996675
<i>FMNL3</i>	Downregulated	-1.476549914	0.000669719	-1.071519405	0.003620809
<i>NOXO1</i>	Downregulated	-1.473867562	0.00373057	-1.282447768	0.007288898
<i>ASPRV1</i>	Downregulated	-1.473578936	0.002027505	-1.109589781	0.008167028
<i>SIRT4</i>	Downregulated	-1.466721378	0.00223401	-1.724568216	0.000947452
<i>DCDC2B</i>	Downregulated	-1.466675356	0.005710333	-1.367739424	0.007927433
<i>MYO7A</i>	Downregulated	-1.462644436	0.000388225	-1.644515618	0.000199026
<i>C10orf68</i>	Downregulated	-1.46171294	0.004126802	-1.485076007	0.003816007
<i>RRM2</i>	Downregulated	-1.460821409	0.004946018	-4.138726352	1.445E-05
<i>OBSCN</i>	Downregulated	-1.451649981	0.001267415	-1.148041655	0.004230253
<i>RGS11</i>	Downregulated	-1.450494108	0.003527396	-1.475123941	0.003242413
<i>LOC440300</i>	Downregulated	-1.447401566	0.001312443	-1.2856998	0.002439382
<i>FAM70B</i>	Downregulated	-1.446364541	0.001049994	-1.827793654	0.000286074
<i>ATAD5</i>	Downregulated	-1.445167641	0.000399486	-1.597149099	0.00022623
<i>LENG8</i>	Downregulated	-1.445142124	0.002462303	-1.084989473	0.009824629
<i>NBEAL2</i>	Downregulated	-1.442992663	0.001274611	-1.233499151	0.002884942
<i>C8orf77</i>	Downregulated	-1.441662912	0.000901569	1.037121052	0.004933435
<i>POLE</i>	Downregulated	-1.435910321	0.000157449	-1.207141205	0.000424338
<i>LINC00085</i>	Downregulated	-1.435120997	0.001159483	-1.563271735	0.00072858
<i>C15orf52</i>	Downregulated	-1.434342491	0.008598688	-2.618277561	0.000382827
<i>LOC401010</i>	Downregulated	-1.433927207	0.001150912	-1.154196383	0.003546523
<i>LOC642846</i>	Downregulated	-1.433750172	0.006480451	-1.821469038	0.001972477
<i>CYP27C1</i>	Downregulated	-1.430494813	0.009025259	-1.720685408	0.003745971
<i>ANKRD36</i>	Downregulated	-1.42597882	0.000338743	-1.071453865	0.001621881
<i>TMC7</i>	Downregulated	-1.425459949	0.001704097	-1.115881758	0.005825045
<i>PDZD2</i>	Downregulated	-1.42461756	0.000223889	-1.262895112	0.000443728
<i>GAL3ST4</i>	Downregulated	-1.423030512	0.000544028	-1.309428138	0.000860301
<i>HYDIN</i>	Downregulated	-1.419188716	0.005647135	-1.402849005	0.005967781
<i>CSMD2</i>	Downregulated	-1.417412789	0.00013386	-1.322413204	0.000200068
<i>RNF112</i>	Downregulated	-1.412344785	0.001209238	-1.006933791	0.00667664

<i>LAMP3</i>	Downregulated	-1.407625165	0.007987927	-1.839052241	0.002152498
<i>LOC100130987</i>	Downregulated	-1.406530971	0.000674828	-1.352266266	0.000837383
<i>LOC100289019</i>	Downregulated	-1.406146657	0.000573184	-1.052980438	0.002683071
<i>OAF</i>	Downregulated	-1.403788201	0.008569316	-2.582583999	0.000364782
<i>LEPRELI</i>	Downregulated	-1.400704501	0.012196641	-1.923079291	0.002704579
<i>AGER</i>	Downregulated	-1.394172763	0.001435433	-1.58075294	0.000728318
<i>ROBO3</i>	Downregulated	-1.392078281	0.007196106	-1.398070607	0.007053192
<i>FDXACB1</i>	Downregulated	-1.39188591	0.003384708	-1.142554398	0.008715491
<i>CDKN3</i>	Downregulated	-1.390848885	0.003824573	-1.579814907	0.002002803
<i>LOC100132832</i>	Downregulated	-1.388060392	0.010323819	-1.411601075	0.009572055
<i>RREB1</i>	Downregulated	-1.38761776	0.009985799	-2.183751072	0.001042532
<i>LOC100507577</i>	Downregulated	-1.384681297	0.000442455	-1.119268835	0.001416042
<i>EML3</i>	Downregulated	-1.383580839	0.00088801	-1.654378471	0.000328611
<i>TRPC3</i>	Downregulated	-1.37993983	0.001645318	-3.548682831	6.93453E-06
<i>LOC646851</i>	Downregulated	-1.376074405	0.000242137	-1.277585095	0.000369411
<i>FZD4</i>	Downregulated	-1.374515318	0.002399072	-1.856551072	0.00047618
<i>NPIPL3</i>	Downregulated	-1.373617072	0.010533832	-1.391869445	0.009928934
<i>TMEM30B</i>	Downregulated	-1.373169386	0.004687014	-2.613477234	0.000144336
<i>MEGF6</i>	Downregulated	-1.372998212	0.00305903	-1.352304211	0.003301755
<i>HIF3A</i>	Downregulated	-1.37200445	0.000832503	-1.579611716	0.000380672
<i>PCSK4</i>	Downregulated	-1.371412956	0.000801335	-1.131151677	0.002232973
<i>CENPE</i>	Downregulated	-1.370817661	0.0016526	-1.894781487	0.000278765
<i>SSC5D</i>	Downregulated	-1.370126526	0.006582025	-1.322126871	0.007774137
<i>DEPDC4</i>	Downregulated	-1.368304941	0.011538644	-2.008152306	0.001795934
<i>FRMPD4</i>	Downregulated	-1.367972981	0.00013853	-1.461315112	9.41779E-05
<i>B3GALT5</i>	Downregulated	-1.366914265	0.003830165	-1.860562234	0.000762641
<i>TMEM51</i>	Downregulated	-1.361625749	0.001998671	-1.330942801	0.002248984
<i>SLC12A8</i>	Downregulated	-1.361476807	0.001455694	-2.01611488	0.00016339
<i>ETV6</i>	Downregulated	-1.36052377	0.002502138	-1.604620455	0.001049969
<i>LOC283922</i>	Downregulated	-1.36034168	0.001208406	-1.042700467	0.004718868
<i>NTN3</i>	Downregulated	-1.359117584	0.0018236	-1.304509352	0.002256322
<i>ARID3A</i>	Downregulated	-1.354833911	0.002199531	-1.488895086	0.001340709

<i>FES</i>	Downregulated	-1.351397584	0.011158441	-2.720728867	0.000305095
<i>LRRC16A</i>	Downregulated	-1.349495769	0.008033814	-1.61342541	0.003401908
<i>CLCNKA</i>	Downregulated	-1.347716832	0.00369419	-1.271479227	0.004916013
<i>UTRN</i>	Downregulated	-1.347249664	0.008680455	-1.404508055	0.007162414
<i>MACC1</i>	Downregulated	-1.345860123	0.003385858	-1.455262972	0.002276631
<i>ARHGAP25</i>	Downregulated	-1.341791693	0.00766137	-2.218639013	0.000578711
<i>NRIP2</i>	Downregulated	-1.341486181	0.000123945	-1.414038476	9.10455E-05
<i>GPLD1</i>	Downregulated	-1.340046657	6.43572E-05	-1.112547232	0.000191052
<i>BMP8A</i>	Downregulated	-1.33908156	0.006828625	-1.827008387	0.001437495
<i>MAF</i>	Downregulated	-1.337056798	0.005616027	-3.122523288	5.40239E-05
<i>TTF2</i>	Downregulated	-1.335243374	0.002504373	-1.144006599	0.005395105
<i>SGK1</i>	Downregulated	-1.333950181	0.002660772	-1.027178521	0.009385083
<i>TRMT2B</i>	Downregulated	-1.333334821	0.00226813	-1.74151895	0.000540272
<i>MCM8</i>	Downregulated	-1.332309758	0.000360613	-1.575725164	0.000137649
<i>ZNF276</i>	Downregulated	-1.330350052	0.000748425	-1.068784596	0.002397885
<i>PDE7B</i>	Downregulated	-1.330101646	0.004143833	-2.048808348	0.00041927
<i>MAP3K5</i>	Downregulated	-1.325349984	0.000386641	-1.236623929	0.00056978
<i>LIPT1</i>	Downregulated	-1.319411508	0.004225862	-1.863809031	0.000693954
<i>TENC1</i>	Downregulated	-1.316465701	0.001060351	-1.080202164	0.002983653
<i>BCO2</i>	Downregulated	-1.316112404	0.002410948	-1.22608471	0.003451671
<i>KCNMB3</i>	Downregulated	-1.314774611	0.004862645	-1.485076007	0.002652457
<i>CNIH3</i>	Downregulated	-1.312896245	0.010395176	-1.863544223	0.001891298
<i>RTKN2</i>	Downregulated	-1.310846914	0.001104009	-1.413213012	0.000733475
<i>KNTC1</i>	Downregulated	-1.309368235	0.000622698	-1.059475957	0.001944542
<i>HRC</i>	Downregulated	-1.306876567	0.009843336	-1.476936598	0.005575133
<i>SLC16A4</i>	Downregulated	-1.305272383	0.00093818	-2.058192685	7.00396E-05
<i>SYTL2</i>	Downregulated	-1.299133987	0.002146022	-1.165774188	0.003716873
<i>CCDC84</i>	Downregulated	-1.299097063	0.005973494	-1.301620513	0.005918595
<i>PLAGL1</i>	Downregulated	-1.295001764	0.005866236	-2.065510568	0.000515516
<i>PPFIBP2</i>	Downregulated	-1.294439232	0.000474569	-1.335641864	0.00039803
<i>NFIA</i>	Downregulated	-1.291371385	0.011671483	-3.183359238	0.000100411
<i>HSPG2</i>	Downregulated	-1.287869472	0.005207575	-2.087129425	0.000410229

<i>SERINC4</i>	Downregulated	-1.284636731	0.00448385	-1.235804844	0.005409767
<i>ADAMTS16</i>	Downregulated	-1.283093381	0.013689583	-2.013403616	0.001552355
<i>VAMP8</i>	Downregulated	-1.283028196	0.001260859	-1.734984967	0.000236038
<i>MGC27345</i>	Downregulated	-1.281731427	0.000510767	-1.283585009	0.000506666
<i>PPIEL</i>	Downregulated	-1.277294422	0.00214123	-1.339253159	0.001672516
<i>CNKSRI</i>	Downregulated	-1.277281243	0.003729803	-1.115173235	0.007173027
<i>OIPS</i>	Downregulated	-1.276845179	0.008593129	-1.681359617	0.002243713
<i>CROCC</i>	Downregulated	-1.275416205	0.002050681	-1.038804568	0.005710006
<i>MYOM1</i>	Downregulated	-1.274879757	0.012508185	-1.624516721	0.004045582
<i>LOC146880</i>	Downregulated	-1.274838827	0.000316009	-1.349150686	0.000228691
<i>BDNF-AS1</i>	Downregulated	-1.274366972	0.008818646	-1.88069573	0.001270389
<i>BUB1B</i>	Downregulated	-1.270713434	0.00426056	-1.974279626	0.00041233
<i>LOC441454</i>	Downregulated	-1.269273395	0.002066687	-2.320001707	7.04555E-05
<i>ZNF530</i>	Downregulated	-1.267736448	0.00268143	-1.468499381	0.00124401
<i>RCN3</i>	Downregulated	-1.26321572	0.00573058	-1.189494372	0.007605327
<i>CCDC142</i>	Downregulated	-1.259698849	0.001153147	-1.342415735	0.000817034
<i>DDX58</i>	Downregulated	-1.258695854	0.005264548	-1.803022147	0.000823636
<i>LOC286437</i>	Downregulated	-1.255098471	0.012814022	-1.763754172	0.002544418
<i>APIG2</i>	Downregulated	-1.253725604	0.00056346	-1.118353075	0.001053632
<i>IKBKB</i>	Downregulated	-1.252379946	0.000556155	-1.701985799	9.59885E-05
<i>CTAGE1</i>	Downregulated	-1.249016016	0.003975471	-2.954375735	3.27612E-05
<i>HSPBAPI</i>	Downregulated	-1.244200357	0.005293637	-1.102560656	0.009312854
<i>KCND1</i>	Downregulated	-1.243003215	0.000765396	-1.125828046	0.001307574
<i>PPARGC1B</i>	Downregulated	-1.240881881	0.006353234	-1.57419844	0.001944213
<i>NEXN</i>	Downregulated	-1.240839703	0.006469575	-2.629408828	0.000114208
<i>MSS51</i>	Downregulated	-1.2406426	0.003532573	-1.374325266	0.002099403
<i>RTTN</i>	Downregulated	-1.239377135	0.000243729	-1.258873986	0.000222863
<i>GSDMB</i>	Downregulated	-1.235521214	0.000159581	-1.450527722	6.22911E-05
<i>FBLN1</i>	Downregulated	-1.233790305	0.0019805	-1.947846543	0.000158353
<i>FBXL13</i>	Downregulated	-1.229448988	0.001094139	-1.199416829	0.001249411
<i>CCDC69</i>	Downregulated	-1.228816966	0.012644359	-1.764669653	0.002240842
<i>FAM72B</i>	Downregulated	-1.228816966	0.005669645	-1.485076007	0.00220826

<i>SLC25A45</i>	Downregulated	-1.227408083	0.005878212	-1.788796309	0.000850005
<i>FRZB</i>	Downregulated	-1.222875025	0.012367215	-2.193584939	0.000664051
<i>POLE2</i>	Downregulated	-1.221382244	0.010883807	-1.254589116	0.009651691
<i>LOC100131691</i>	Downregulated	-1.220844181	0.002060876	-1.313539056	0.001403401
<i>PLK4</i>	Downregulated	-1.208460129	0.000368368	-1.634670593	6.39564E-05
<i>LOC401321</i>	Downregulated	-1.201066725	0.001372403	-1.495419144	0.000412936
<i>RAD9A</i>	Downregulated	-1.1990649	0.001173688	-1.452438754	0.000408809
<i>CASP6</i>	Downregulated	-1.193732346	0.000724322	-1.983655752	3.86978E-05
<i>TPK1</i>	Downregulated	-1.19251822	0.012617438	-1.501079254	0.004338753
<i>LRRC37A4</i>	Downregulated	-1.191228054	0.001406082	-1.338243261	0.000749965
<i>GLDC</i>	Downregulated	-1.187524656	0.00027414	-1.801480189	2.36266E-05
<i>MTBP</i>	Downregulated	-1.187019901	0.012305729	-1.464247203	0.004657069
<i>CHRD</i>	Downregulated	-1.181606171	0.001803957	-1.538692456	0.000429418
<i>C9orf169</i>	Downregulated	-1.181107183	0.003273586	-1.25338712	0.002421814
<i>B3GNTL1</i>	Downregulated	-1.176379602	0.004479793	-1.000770953	0.009585927
<i>TOM1L1</i>	Downregulated	-1.171940872	0.002854469	-1.147776675	0.003171105
<i>SLC26A5</i>	Downregulated	-1.17120465	0.008191245	-1.738556002	0.001129441
<i>IFIT3</i>	Downregulated	-1.168787294	0.006751449	-1.731780289	0.000911043
<i>DNAH10</i>	Downregulated	-1.151048674	0.004393442	-1.177299972	0.00393223
<i>SCUBE3</i>	Downregulated	-1.15015705	0.00026009	-1.458528922	6.52198E-05
<i>PROM2</i>	Downregulated	-1.149855503	0.0015539	-1.3486536	0.000656379
<i>ERNI</i>	Downregulated	-1.148180582	0.000960329	-1.548579347	0.0001791
<i>MIR210HG</i>	Downregulated	-1.146239735	0.002790574	-1.925753759	0.000162551
<i>HEATR7A</i>	Downregulated	-1.145710824	0.004774034	-1.137265639	0.004948457
<i>BAHCCI</i>	Downregulated	-1.138789019	0.001323982	-1.035261813	0.002183672
<i>H1FX-AS1</i>	Downregulated	-1.13696826	0.005928383	-1.719396336	0.000700975
<i>CLEC16A</i>	Downregulated	-1.135300929	0.000937095	-1.234690729	0.000591273
<i>ATP8B1</i>	Downregulated	-1.131208277	0.013033617	-1.775547168	0.001459813
<i>SNTB2</i>	Downregulated	-1.129168421	0.00770111	-1.624337826	0.00124411
<i>FAM26F</i>	Downregulated	-1.125591527	0.006991752	-1.5580912	0.001367347
<i>EDA</i>	Downregulated	-1.120211448	0.001993804	-1.098998496	0.002201415
<i>TRPS1</i>	Downregulated	-1.109773772	0.012692042	-2.026400763	0.000622034

<i>STC2</i>	Downregulated	-1.109318164	0.00816491	-1.321825595	0.003520739
<i>C19orf57</i>	Downregulated	-1.10850964	0.000448154	-1.530365865	6.96622E-05
<i>FUT4</i>	Downregulated	-1.098173594	0.009586556	-1.470001934	0.002334066
<i>SLC13A3</i>	Downregulated	-1.096363732	0.00768214	-1.567135697	0.001283515
<i>PRKD3</i>	Downregulated	-1.09230581	0.001740776	-1.826885715	9.79199E-05
<i>ENOSFI</i>	Downregulated	-1.091890305	0.005476338	-1.250917631	0.002797635
<i>TBXASI</i>	Downregulated	-1.091559389	0.009162067	-1.072733809	0.009911396
<i>FBF1</i>	Downregulated	-1.088918057	0.008578912	-1.343553824	0.003120458
<i>CACNA1G</i>	Downregulated	-1.085662773	0.003954916	-1.002229092	0.005830647
<i>EXTL1</i>	Downregulated	-1.083817631	0.005735474	-1.199723395	0.003491755
<i>FBXW4P1</i>	Downregulated	-1.083147078	0.012304001	-2.270799855	0.000274892
<i>ACCS</i>	Downregulated	-1.073659737	0.007477892	-1.205135995	0.004306548
<i>MMACHC</i>	Downregulated	-1.072624805	0.00264944	-1.464353648	0.000499956
<i>ZDHHC8</i>	Downregulated	-1.072043223	0.00630602	-1.087508572	0.005891599
<i>KIAA1456</i>	Downregulated	-1.052366371	0.002647925	-1.657392552	0.00022236
<i>UBOX5</i>	Downregulated	-1.05228551	0.006874132	-1.320442857	0.002243887
<i>C1QL3</i>	Downregulated	-1.046163145	0.014142439	-2.194076111	0.000329317
<i>LRRK56</i>	Downregulated	-1.039357929	0.000665827	-1.123275393	0.000432185
<i>MGC72080</i>	Downregulated	-1.033445211	0.004386786	-1.072881572	0.003646652
<i>WDR92</i>	Downregulated	-1.025490312	0.004748021	-1.109821167	0.003212576
<i>SCAND2</i>	Downregulated	-1.020136114	0.001425491	-1.061262027	0.001154328
<i>CBR3-AS1</i>	Downregulated	-1.01844139	0.010372414	-1.018734965	0.010359051
<i>SFXN2</i>	Downregulated	-1.009512163	0.000864987	-1.169988214	0.000381527
<i>LOC90784</i>	Downregulated	-1.008077256	0.008872805	-1.391945859	0.001818738
<i>FBXL19-AS1</i>	Downregulated	-1.005520771	0.002147493	-1.506371946	0.000234434
<i>ANO8</i>	Downregulated	-1.003196538	0.009913184	-1.115316121	0.00607344

**Appendix 2: Genes dysregulated by forced  
progerin expression in iPSC-derived neurons  
and differentially expressed in AD brains  
(MSBB and Mayo)**

Gene	Direction in Progerin Transduction	MSBB - BA36 (PHG)				Mayo - Temporal			
		Log2 Fold Change	p value	FDR	Same direction as mDA neurons			p value	q value
					β				
<i>LMNA</i>	Upregulated	0.423845804	0.0000118	0.00046868	Yes	0.34256006	0.01693965	0.0441005	Yes
<i>NOP10</i>	Upregulated	-0.072788447	0.23591894	0.4588814	No	-0.0639772	0.29103487	0.39756322	No
<i>SNHG15</i>	Upregulated	-0.105343862	0.0902455	0.25098394	No	-0.3393466	0.0000632	0.0008818	No
<i>ENHO</i>	Upregulated	0.081923697	0.40191683	0.62708013	Yes	0.0131984	0.9361479	0.95539074	Yes
<i>NDUFB6</i>	Upregulated	-0.063492507	0.31793879	0.54814623	No	-0.1249564	0.00214915	0.01109022	No
<i>ATP5L</i>	Upregulated	-0.214997357	0.00236758	0.02026133	No	-0.2425125	1.05E-07	0.00000844	No
<i>NEDD8</i>	Upregulated	-0.176596246	0.00451516	0.03190707	No	-0.263068	2.44E-07	0.0000148	No
<i>PPIB</i>	Upregulated	0.105110984	0.07082175	0.21416371	Yes	0.13255107	0.01859376	0.04726513	Yes
<i>TMSB10</i>	Upregulated	-0.117637601	0.13777458	0.32954573	No	-0.1310355	0.23131437	0.3328086	No
<i>PRDX4</i>	Upregulated	0.130022718	0.09747172	0.26401953	Yes	0.25103932	0.00453958	0.01784468	Yes
<i>FTL</i>	Upregulated	0.308683094	0.0004565	0.00634544	Yes	0.0763038	0.08455664	0.15102107	Yes
<i>TMSB4X</i>	Upregulated	0.019331329	0.78417077	0.89419593	Yes	-0.1633408	0.0025676	0.01240219	No
<i>ATOXI</i>	Upregulated	0.004716122	0.90996364	0.96071545	Yes	-0.3345547	0.0000699	0.00094775	No
<i>CCDC126</i>	Upregulated	0.077867206	0.3148222	0.54513261	Yes	0.00906084	0.92030745	0.94411569	Yes
<i>PSMB3</i>	Upregulated	#N/A	#N/A	#N/A	#N/A	-0.1460709	0.00330187	0.01450856	No
<i>LOC100128822</i>	Upregulated	#N/A	#N/A	#N/A	#N/A	#N/A	#N/A	#N/A	#N/A

<i>TSNAX</i>	Upregulated	-0.05051895	0.45798988	0.67544337	No	-0.3355095	0.000043	0.00066045	No
<i>TCEAL7</i>	Upregulated	-0.176309289	0.03162359	0.12549578	No	-0.3650857	0.0000283	0.00047899	No
<i>UBC</i>	Upregulated	0.043178469	0.50184632	0.70915414	Yes	0.22011021	0.01253951	0.03541976	Yes
<i>ZNHIT3</i>	Upregulated	#N/A	#N/A	#N/A	#N/A	-0.2741476	5.08E-08	0.00000529	No
<i>PCNA</i>	Upregulated	0.097586464	0.11329524	0.29128895	Yes	0.23790129	0.00043095	0.00366396	Yes
<i>LOC401397</i>	Upregulated	#N/A	#N/A	#N/A	#N/A	#N/A	#N/A	#N/A	#N/A
<i>C4orf52</i>	Upregulated	#N/A	#N/A	#N/A	#N/A	#N/A	#N/A	#N/A	#N/A
<i>NDUFA5</i>	Upregulated	-0.261783655	0.00163475	0.01554243	No	-0.488659	1.46E-07	0.0000106	No
<i>EAPP</i>	Upregulated	-0.085660709	0.1587781	0.36031473	No	-0.1109929	0.00947771	0.02903723	No
<i>COX14</i>	Upregulated	-0.058412285	0.36134692	0.5896232	No	-0.1237511	0.0025838	0.01243739	No
<i>UBE2T</i>	Upregulated	-0.428084105	0.0000188	0.0006451	No	-0.4921291	0.00339636	0.01478856	No
<i>SVIP</i>	Upregulated	-0.05432922	0.41413985	0.63788916	No	-0.3097413	0.00000887	0.00019854	No
<i>CD164</i>	Upregulated	0.250496108	0.00017038	0.00314309	Yes	0.38657707	0.00000101	0.0000408	Yes
<i>RPL12</i>	Upregulated	0.093451335	0.11815181	0.29911513	Yes	-0.0493845	0.4548476	0.56061372	No
<i>SCOC</i>	Upregulated	-0.148703305	0.06789185	0.20830777	No	-0.348943	4.12E-08	0.00000462	No
<i>ARL6IP5</i>	Upregulated	-0.090289386	0.1666827	0.37093862	No	0.02404268	0.68619629	0.76396886	Yes
<i>UBL5</i>	Upregulated	-0.088891397	0.1367227	0.32793058	No	-0.1801727	0.00000121	0.0000464	No
<i>SEC11C</i>	Upregulated	0.160286919	0.01238896	0.06523457	Yes	0.24041459	0.00143885	0.00854996	Yes
<i>VPS25</i>	Upregulated	-0.07778737	0.16418297	0.36761241	No	-0.0183928	0.77837582	0.83770769	No
<i>ITM2C</i>	Upregulated	0.208183514	0.00177489	0.01647452	Yes	0.62373628	0.0000184	0.00034509	Yes
<i>TFAM</i>	Upregulated	0.050410805	0.3373563	0.5674795	Yes	-0.0589131	0.30486625	0.41226559	No
<i>PRDX1</i>	Upregulated	0.166797673	0.00892902	0.05180833	Yes	0.60496455	1.2E-09	4.95E-07	Yes
<i>ABHD10</i>	Upregulated	0.001958963	0.97496534	0.98973165	Yes	-0.2805076	3.76E-07	0.0000199	No

<i>BUD31</i>	Upregulated	-0.047567726	0.51963515	0.72189724	No	-0.0643454	0.09689439	0.16808574	No
<i>TCEB2</i>	Upregulated	#N/A	#N/A	#N/A	#N/A	-0.1331713	0.0002566	0.00249689	No
<i>WRB</i>	Upregulated	0.00107958	0.98588792	0.99432822	Yes	-0.1708161	0.0000335	0.00054712	No
<i>PFNI</i>	Upregulated	0.128322069	0.24434807	0.46857249	Yes	0.19118107	0.00106082	0.00693401	Yes
<i>TCEAL8</i>	Upregulated	-0.1429176	0.0181189	0.0854795	No	-0.0058948	0.9191177	0.9433159	No
<i>RGS2</i>	Upregulated	0.112355332	0.39575363	0.62133634	Yes	-0.2284534	0.10407166	0.17782536	No
<i>C5orf15</i>	Upregulated	0.087053363	0.16285984	0.366032	Yes	0.17741455	0.02093388	0.05166384	Yes
<i>ATP6V1G1</i>	Upregulated	-0.091545452	0.11472838	0.2935815	No	-0.1035841	0.0256638	0.06023619	No
<i>YPEL5</i>	Upregulated	-0.14140961	0.02631548	0.11027686	No	-0.1066361	0.1338998	0.21705822	No
<i>MT3</i>	Upregulated	-0.047965235	0.60266012	0.78018153	No	0.18443302	0.08418481	0.15046186	Yes
<i>UQCR10</i>	Upregulated	-0.141290789	0.03198824	0.12642734	No	-0.1392557	0.00293392	0.0134792	No
<i>TMEM14A</i>	Upregulated	-0.143988821	0.08502484	0.24121938	No	-0.1503527	0.05662619	0.11075349	No
<i>DNAJC8</i>	Upregulated	-0.074459088	0.16161125	0.36428277	No	0.00696087	0.73910246	0.80660397	Yes
<i>SUMO2</i>	Upregulated	0.003875282	0.94225677	0.97599513	Yes	-0.0443417	0.26288035	0.36748544	No
<i>BEX1</i>	Upregulated	-0.362695662	0.00049029	0.00664824	No	-0.9929336	0.00000751	0.0001748	No
<i>NDUFB11</i>	Upregulated	-0.158295783	0.01415871	0.07163154	No	-0.1330292	0.00329139	0.01448821	No
<i>LAMTOR1</i>	Upregulated	0.09638795	0.10326343	0.27463109	Yes	-0.0214289	0.61747989	0.70632109	No
<i>ATP5G3</i>	Upregulated	-0.220177928	0.00281712	0.02285611	No	-0.3514446	0.0000268	0.00046003	No
<i>VBPI</i>	Upregulated	0.010559055	0.88717807	0.94901638	Yes	0.0526952	0.15142342	0.23873896	Yes
<i>QPCT</i>	Upregulated	-0.332417197	0.00246009	0.02084624	No	-0.3983135	0.02077513	0.05138806	No
<i>ZCCHC10</i>	Upregulated	-0.006555794	0.91917343	0.96488461	No	-0.0729858	0.12144862	0.20097614	No
<i>NDUFBI</i>	Upregulated	-0.055047466	0.3631706	0.59122316	No	-0.2701017	0.000018	0.00033898	No
<i>MMADHC</i>	Upregulated	-0.011167876	0.87074984	0.94047921	No	0.14746811	0.00321355	0.01426549	Yes

<i>HSBP1</i>	Upregulated	-0.005979385	0.91785886	0.96433859	No	-0.0820889	0.08883856	0.15706258	No
<i>CAPZA2</i>	Upregulated	0.044712135	0.55710644	0.74935032	Yes	0.10232038	0.12438339	0.20469054	Yes
<i>CNO</i>	Upregulated	#N/A	#N/A	#N/A	#N/A	#N/A	#N/A	#N/A	#N/A
<i>SELT</i>	Upregulated	0.003601443	0.95746369	0.9829743	Yes	0.0280999	0.42161951	0.52939235	Yes
<i>CCDC72</i>	Upregulated	#N/A	#N/A	#N/A	#N/A	#N/A	#N/A	#N/A	#N/A
<i>ATF4</i>	Upregulated	0.170412872	0.07407948	0.22043157	Yes	0.40049282	0.00013634	0.00156064	Yes
<i>GABARAPL2</i>	Upregulated	0.046286333	0.37153657	0.59956794	Yes	-0.032163	0.26856569	0.37377437	No
<i>AASDHPP7</i>	Upregulated	-0.169453784	0.01815626	0.08558237	No	-0.3162165	0.0000636	0.00088494	No
<i>BANFI</i>	Upregulated	-0.117454955	0.28393591	0.51318079	No	-0.001647	0.97144623	0.98078689	No
<i>SUBI</i>	Upregulated	-0.184953674	0.02590674	0.10914247	No	-0.4786434	3.11E-07	0.0000174	No
<i>EID1</i>	Upregulated	-0.116126072	0.12101816	0.30397904	No	0.09518529	0.13823411	0.2224545	Yes
<i>SLIRP</i>	Upregulated	-0.137997763	0.02170815	0.09668048	No	-0.2663583	0.000003	0.0000896	No
<i>PFDN2</i>	Upregulated	-0.314892281	0.00771591	0.04679731	No	-0.3060854	0.0000116	0.00024443	No
<i>EIF3M</i>	Upregulated	-0.07675987	0.12297023	0.3068919	No	-0.2981739	5.33E-10	3.23E-07	No
<i>CYB5A</i>	Upregulated	0.036353061	0.49250709	0.70214913	Yes	-0.004343	0.95013421	0.96567669	No
<i>FDFT1</i>	Upregulated	0.077679135	0.12346583	0.3077563	Yes	0.26343323	0.0003639	0.00323594	Yes
<i>CDC42</i>	Upregulated	-0.023713138	0.69416349	0.84163115	No	-0.0539491	0.14741992	0.23397558	No
<i>DYNLT3</i>	Upregulated	-0.212584399	0.02206326	0.09778014	No	-0.2981199	0.00143413	0.00853606	No
<i>C12orf29</i>	Upregulated	-0.055431181	0.41076853	0.63509369	No	-0.1691907	0.0005969	0.00462909	No
<i>RG9MTD1</i>	Upregulated	#N/A	#N/A	#N/A	#N/A	#N/A	#N/A	#N/A	#N/A
<i>FOS</i>	Upregulated	0.459450771	0.02990429	0.12073039	Yes	1.11015173	0.00029302	0.00275041	Yes
<i>CCT3</i>	Upregulated	-0.017692357	0.76632478	0.88442166	No	0.14135045	0.00979485	0.02973386	Yes
<i>ZCRB1</i>	Upregulated	0.049211935	0.44325894	0.6632312	Yes	0.00214903	0.96271108	0.97431421	Yes

<i>TMBIM6</i>	Upregulated	0.181631557	0.00096151	0.01066805	Yes	0.45627764	1.87E-08	0.00000269	Yes
<i>GTF2B</i>	Upregulated	-0.054327729	0.38775955	0.61442213	No	-0.0241818	0.53493989	0.63381757	No
<i>ILF2</i>	Upregulated	0.032539796	0.53070569	0.73072218	Yes	0.16201432	0.00000197	0.0000665	Yes
<i>POMP</i>	Upregulated	-0.081832056	0.22522228	0.4464219	No	0.02647985	0.42602024	0.53365449	Yes
<i>ZBTB6</i>	Upregulated	0.02768776	0.63647369	0.80233567	Yes	0.12378765	0.02449809	0.05812407	Yes
<i>IDII</i>	Upregulated	-0.008373729	0.90635656	0.95877295	No	0.06012547	0.33066639	0.43898841	Yes
<i>ISCA1</i>	Upregulated	-0.101994905	0.07967967	0.23127578	No	-0.1691563	0.00214053	0.0110599	No
<i>PRDX6</i>	Upregulated	0.32140623	0.00000157	0.00011317	Yes	0.57566361	0.00000178	0.0000612	Yes
<i>TTC33</i>	Upregulated	-0.02136291	0.81193954	0.91030458	No	-0.0538131	0.53805181	0.63674527	No
<i>ANAPC13</i>	Upregulated	-0.155902296	0.01734104	0.08289009	No	-0.1346331	0.00391682	0.01623809	No
<i>DDX24</i>	Upregulated	#N/A	#N/A	#N/A	#N/A	-0.1412909	0.07410395	0.13650521	No
<i>CCNG1</i>	Upregulated	0.227731623	0.00151496	0.01470179	Yes	0.52639737	0.00000008	0.00000707	Yes
<i>TIMM17B</i>	Upregulated	-0.056945559	0.37098184	0.5990319	No	-0.2959365	1.25E-07	0.00000953	No
<i>MRPS35</i>	Upregulated	-0.064741668	0.32409272	0.55435406	No	-0.1258079	0.00168048	0.00945575	No
<i>PGRMC1</i>	Upregulated	-0.097551908	0.16603419	0.37011991	No	-0.1647229	0.0357406	0.07760847	No
<i>CHMP1B</i>	Upregulated	-0.002089077	0.96264225	0.98566075	No	0.05595367	0.25301442	0.35680683	Yes
<i>RPS19BP1</i>	Upregulated	0.07771453	0.2388727	0.46220619	Yes	-0.0331423	0.53865761	0.63727282	No
<i>SRP9</i>	Upregulated	0.031109358	0.68822322	0.83795791	Yes	0.15721766	0.01273264	0.03582927	Yes
<i>CCDC90B</i>	Upregulated	0.023914914	0.60999267	0.78456274	Yes	-0.0239313	0.66972532	0.75016551	No
<i>MORF4L1</i>	Upregulated	-0.029922724	0.5677144	0.75669835	No	-0.0789216	0.00773517	0.02532931	No
<i>EEF1E1</i>	Upregulated	-0.079659017	0.34399692	0.57346419	No	-0.2717687	0.00000201	0.0000675	No
<i>PPP2R1A</i>	Upregulated	-0.134740716	0.05120987	0.17230669	No	-0.3130535	0.0000388	0.00061033	No
<i>PSMA7</i>	Upregulated	0.024922469	0.61339745	0.78688862	Yes	0.04618551	0.19190028	0.28763117	Yes

<i>PDRG1</i>	Upregulated	-0.082139175	0.19033542	0.40301202	No	-0.0426845	0.42688167	0.53446241	No
<i>PKIB</i>	Upregulated	-0.101351147	0.30760804	0.53789245	No	-0.7089726	0.00000674	0.00016129	No
<i>JKAMP</i>	Upregulated	-0.023401349	0.62500641	0.79476977	No	0.08151875	0.1219014	0.20153538	Yes
<i>DPM1</i>	Upregulated	-0.052540073	0.36979838	0.59785856	No	-0.0323755	0.45384345	0.55969776	No
<i>TAF7</i>	Upregulated	0.001564625	0.97669071	0.99052263	Yes	0.06833783	0.23371542	0.33531495	Yes
<i>RMRP</i>	Downregulated	0.222833468	0.94530818	NA	No	0.35946834	0.08778368	0.15556262	No
<i>RPPH1</i>	Downregulated	NA	NA	NA	#N/A	0.02430364	0.9098921	0.93658397	No
<i>MIR3648</i>	Downregulated	#N/A	#N/A	#N/A	#N/A	-0.0971602	0.69683959	0.7724845	Yes
<i>MIR3687</i>	Downregulated	#N/A	#N/A	#N/A	#N/A	0.53900062	0.00512718	0.01929083	No
<i>C3orf72</i>	Downregulated	0.368758815	0.03683358	0.13908883	No	0.73685889	0.00741843	0.02465119	No
<i>TNIP3</i>	Downregulated	-0.66247395	0.00010369	0.00221221	Yes	-0.7141404	0.00837767	0.02669785	Yes
<i>NOSTRIN</i>	Downregulated	#N/A	#N/A	#N/A	#N/A	0.4153297	0.00983147	0.02980896	No
<i>MIR663A</i>	Downregulated	#N/A	#N/A	#N/A	#N/A	-0.3029072	0.22785669	0.32879675	Yes
<i>GVINPI</i>	Downregulated	-0.176262369	0.01615565	0.07884423	Yes	0.26453116	0.142112	0.22729767	No
<i>PRDM1</i>	Downregulated	0.267562455	0.00397887	0.02908029	No	0.23851898	0.12223045	0.20198818	No
<i>C1orf129</i>	Downregulated	#N/A	#N/A	#N/A	#N/A	#N/A	#N/A	#N/A	#N/A
<i>MARCO</i>	Downregulated	0.627355053	0.00584148	0.03828486	No	1.17449251	0.00602984	0.02147829	No
<i>TG</i>	Downregulated	0.209297959	0.18600071	0.3969929	No	-0.2458712	0.22297717	0.32331197	Yes
<i>PEAR1</i>	Downregulated	0.50803347	0.00037834	0.00554853	No	1.02144371	2.27E-08	0.0000031	No
<i>LAMC3</i>	Downregulated	0.313996955	0.00339521	0.02604845	No	0.14691667	0.21296877	0.31223473	No
<i>BCAS1</i>	Downregulated	0.161966479	0.12471131	0.30978791	No	-0.1739568	0.39716138	0.50602431	Yes
<i>LOC285084</i>	Downregulated	#N/A	#N/A	#N/A	#N/A	#N/A	#N/A	#N/A	#N/A
<i>CDHR4</i>	Downregulated	0.292894635	0.4161784	0.63973249	No	-0.418594	0.03240727	0.07199258	Yes

<i>FLI1</i>	Downregulated	0.512775442	5.56E-08	0.0000103	No	0.64527902	0.00021627	0.00219683	No
<i>SLC14A2</i>	Downregulated	-0.111028813	0.30949958	0.54000937	Yes	-0.5379277	0.00069864	0.00519516	Yes
<i>BHMT2</i>	Downregulated	0.327488604	0.00025011	0.00414582	No	0.623695	0.00023773	0.00235643	No
<i>SH3TC2</i>	Downregulated	0.263662965	0.01635454	0.07952854	No	0.23410503	0.30772217	0.41534509	No
<i>OLAHL</i>	Downregulated	0.417242715	0.00326061	0.02532949	No	0.55654306	0.01420622	0.03872883	No
<i>STAB2</i>	Downregulated	0.039346537	0.7324005	0.86376014	No	-0.3675778	0.05776687	0.11245709	Yes
<i>SLC5A1</i>	Downregulated	-0.283624956	0.15424831	0.35422886	Yes	-0.8154017	0.00038694	0.00338421	Yes
<i>SLFN11</i>	Downregulated	0.3982178	0.00000873	0.00038228	No	0.63567626	0.0000838	0.001087	No
<i>VIT</i>	Downregulated	-0.168360875	0.22832083	0.45018376	Yes	-0.3207951	0.10254621	0.17577571	Yes
<i>KIAA1755</i>	Downregulated	0.410956631	0.0000127	0.00049235	No	0.24022008	0.12834718	0.20975863	No
<i>SEC14L4</i>	Downregulated	-0.16847326	0.36656163	0.59455042	Yes	0.37238985	0.05866462	0.11388416	No
<i>LEP</i>	Downregulated	-0.091239307	0.54451455	0.74071589	Yes	-0.1042961	0.64332877	0.72852058	Yes
<i>SHE</i>	Downregulated	0.365840853	0.00010849	0.0022813	No	0.65161661	0.0001037	0.00127294	No
<i>DISC1</i>	Downregulated	0.205805297	0.0007052	0.00853214	No	0.03307413	0.77056399	0.83145097	No
<i>GJA5</i>	Downregulated	0.322415974	0.03705066	0.13962032	No	1.09107625	0.00000897	0.00020042	No
<i>SNORA53</i>	Downregulated	0.501447188	0.00157218	0.01507477	No	0.03680082	0.74919827	0.81469657	No
<i>LOC284801</i>	Downregulated	#N/A	#N/A	#N/A	#N/A	#N/A	#N/A	#N/A	#N/A
<i>APCDD1L</i>	Downregulated	0.183200297	0.15557125	0.35595316	No	-0.2768045	0.23193441	0.33346839	Yes
<i>LOC100507156</i>	Downregulated	#N/A	#N/A	#N/A	#N/A	#N/A	#N/A	#N/A	#N/A
<i>TBXA2R</i>	Downregulated	0.431187318	0.00171479	0.01605014	No	-0.0500474	0.70483274	0.77900875	Yes
<i>FOXD2</i>	Downregulated	0.928100855	0.0000332	0.00097475	No	0.96021954	0.00534236	0.01981694	No
<i>EMR2</i>	Downregulated	#N/A	#N/A	#N/A	#N/A	0.24761699	0.23220485	0.33372376	No
<i>LOC727710</i>	Downregulated	#N/A	#N/A	#N/A	#N/A	#N/A	#N/A	#N/A	#N/A

<i>HOXC8</i>	Downregulated	0.342162135	0.74234802	NA	No	-0.075058	0.70911251	0.78265003	Yes
<i>TGM5</i>	Downregulated	1.116534	0.00103127	0.01121513	No	0.19074957	0.51831346	0.61895664	No
<i>MYH1</i>	Downregulated	-1.063788964	0.0002638	0.00430161	Yes	0.13165352	0.65925394	0.74209325	No
<i>LOC283547</i>	Downregulated	#N/A	#N/A	#N/A	#N/A	#N/A	#N/A	#N/A	#N/A
<i>SGOL1</i>	Downregulated	0.147224413	0.32750448	0.55750381	No	0.76296236	0.01544018	0.04121619	No
<i>LOC100216001</i>	Downregulated	#N/A	#N/A	#N/A	#N/A	#N/A	#N/A	#N/A	#N/A
<i>CMKLR1</i>	Downregulated	0.520204393	0.00000223	0.00014338	No	0.35319106	0.06945337	0.12979092	No
<i>PDGFRA</i>	Downregulated	0.077437204	0.35388039	0.58247002	No	0.43222433	0.02386545	0.05695432	No
<i>HMCN1</i>	Downregulated	0.1558049	0.24049683	0.46437815	No	0.67568087	0.00732075	0.02441098	No
<i>COL6A6</i>	Downregulated	-0.026640174	0.75018549	0.87475929	Yes	-0.2201876	0.12836685	0.20978463	Yes
<i>LIPJ</i>	Downregulated	-0.262190364	0.02225345	0.09828755	Yes	-1.05033	0.0000499	0.00073808	Yes
<i>MFAP5</i>	Downregulated	0.367261398	0.09103322	0.25247166	No	0.8080997	0.00019766	0.00205383	No
<i>WWTR1-AS1</i>	Downregulated	0.251368727	0.19899386	0.41405054	No	1.11748134	3.64E-09	9.81E-07	No
<i>LOC100292680</i>	Downregulated	#N/A	#N/A	#N/A	#N/A	#N/A	#N/A	#N/A	#N/A
<i>GLII</i>	Downregulated	0.146963998	0.3110333	0.54158636	No	0.74305267	0.00273993	0.012922	No
<i>GPRC5A</i>	Downregulated	0.775083563	0.00021008	0.00363247	No	1.17520509	0.001203	0.00756277	No
<i>FLTI</i>	Downregulated	0.347195025	0.00276717	0.02256059	No	1.38719811	1.16E-07	0.00000905	No
<i>RIPK3</i>	Downregulated	0.50027568	0.00032268	0.00495227	No	0.27666877	0.0887088	0.15688789	No
<i>MYOCD</i>	Downregulated	0.36525614	0.02099735	0.09459104	No	0.75595273	0.00045894	0.00384384	No
<i>MEFV</i>	Downregulated	0.206428868	0.07086419	0.2142595	No	-0.0477609	0.79265852	0.84897392	Yes
<i>DNM3OS</i>	Downregulated	0.026734704	0.77819555	0.89086185	No	0.9740733	0.000917	0.0062693	No
<i>MYH11</i>	Downregulated	0.296752706	0.13850517	0.33051401	No	0.49326607	0.00696623	0.02362584	No
<i>ATP6VOA4</i>	Downregulated	0.067684503	0.60900147	0.78405778	No	0.04336485	0.81122818	0.86351352	No

<i>MIRI43HG</i>	Downregulated	0.079683143	0.61257743	0.78650862	No	0.3139639	0.17778307	0.2708696	No
<i>FXYD5</i>	Downregulated	0.469393505	0.0000231	0.00075501	No	0.55249674	0.00047796	0.00395449	No
<i>PIK3R5</i>	Downregulated	0.634013571	4.6E-09	0.00000184	No	0.55296209	0.00697936	0.02364882	No
<i>KCNA7</i>	Downregulated	0.203463176	0.64073448	NA	No	-0.4704187	0.01272075	0.03579942	Yes
<i>LOC642236</i>	Downregulated	#N/A	#N/A	#N/A	#N/A	#N/A	#N/A	#N/A	#N/A
<i>ZNF662</i>	Downregulated	0.039297023	0.48368421	0.69507973	No	0.02018909	0.80682641	0.86004308	No
<i>C7orf58</i>	Downregulated	#N/A	#N/A	#N/A	#N/A	#N/A	#N/A	#N/A	#N/A
<i>TRPA1</i>	Downregulated	-0.467039498	0.0000717	0.00170636	Yes	-0.610279	0.00259565	0.01247461	Yes
<i>LOC100505702</i>	Downregulated	#N/A	#N/A	#N/A	#N/A	#N/A	#N/A	#N/A	#N/A
<i>TMEM154</i>	Downregulated	0.245449038	0.01086419	0.05960273	No	0.17967377	0.32513962	0.43333297	No
<i>IL1R1</i>	Downregulated	0.516167073	0.0000199	0.00067012	No	1.09369416	0.0000037	0.0001047	No
<i>GLP2R</i>	Downregulated	-0.115762153	0.42885919	0.65108431	Yes	-0.7997998	0.0015746	0.00907329	Yes
<i>COL17A1</i>	Downregulated	-0.009956088	0.9111972	0.96129582	Yes	-0.6168521	0.00031551	0.00290627	Yes
<i>SNX29P2</i>	Downregulated	0.306850098	0.17398554	0.38112936	No	0.14959028	0.22210926	0.3223553	No
<i>MSR1</i>	Downregulated	0.866868018	2.35E-09	0.00000113	No	0.8121184	0.00602412	0.02146339	No
<i>GSDMC</i>	Downregulated	0.973009777	0.00180119	0.01663318	No	-0.1123109	0.73927023	0.80670811	Yes
<i>APOL1</i>	Downregulated	0.591942076	6.42E-07	0.0000606	No	0.51370083	0.00210918	0.01094381	No
<i>TMC1</i>	Downregulated	0.362394279	0.00019137	0.00341809	No	0.51063048	0.00984823	0.02983903	No
<i>CYP19A1</i>	Downregulated	0.458004009	0.00606544	0.03929949	No	0.39302594	0.13848385	0.22281138	No
<i>CCBE1</i>	Downregulated	-0.222606809	0.03890452	0.14433895	Yes	-0.6037902	0.00723581	0.02422333	Yes
<i>ALPK2</i>	Downregulated	0.162268921	0.34062062	0.57033784	No	0.02951956	0.89683256	0.92752493	No
<i>LOC100507462</i>	Downregulated	#N/A	#N/A	#N/A	#N/A	#N/A	#N/A	#N/A	#N/A
<i>CCDC36</i>	Downregulated	0.168911713	0.14959806	0.34763025	No	0.30673113	0.1241189	0.20440008	No

<i>PSG5</i>	Downregulated	-0.208398922	0.18042545	0.38979105	Yes	-0.2417691	0.30423241	0.41163809	Yes
<i>MLLT10P1</i>	Downregulated	-0.181310783	0.4049997	0.63018625	Yes	-0.39278	0.06517117	0.12359889	Yes
<i>P2RX7</i>	Downregulated	0.195406201	0.0075313	0.04605709	No	0.8607724	0.0000375	0.00059493	No
<i>DNAJC22</i>	Downregulated	0.488659604	0.00000351	0.00019869	No	0.03669474	0.84118896	0.88683076	No
<i>LOC100506874</i>	Downregulated	#N/A	#N/A	#N/A	#N/A	#N/A	#N/A	#N/A	#N/A
<i>MYPN</i>	Downregulated	-0.107515439	0.61949482	0.79115402	Yes	-0.6345128	0.02136066	0.05244782	Yes
<i>CASP10</i>	Downregulated	0.413196637	0.00000183	0.00012591	No	0.25610228	0.05234033	0.10422456	No
<i>EXO1</i>	Downregulated	-0.14574837	0.1727804	0.37928326	Yes	-0.746283	0.000053	0.00077399	Yes
<i>CSNK1A1P1</i>	Downregulated	-0.07522122	0.47959129	0.6918437	Yes	0.02018886	0.93015489	0.95110248	No
<i>ADAMTS4</i>	Downregulated	0.280681121	0.0493134	0.16858593	No	0.18035456	0.47593502	0.57989541	No
<i>SKA1</i>	Downregulated	#N/A	#N/A	#N/A	#N/A	-0.7266636	2.49E-07	0.000015	Yes
<i>DAND5</i>	Downregulated	0.44033088	0.02332928	0.10150987	No	0.04342108	0.83031529	0.87859749	No
<i>C4orf19</i>	Downregulated	0.55973943	5.63E-10	4.27E-07	No	0.93162748	0.00000227	0.0000734	No
<i>S1PR5</i>	Downregulated	0.394852886	0.00370377	0.02763917	No	0.11216525	0.64574584	0.73053912	No
<i>FLJ43879</i>	Downregulated	#N/A	#N/A	#N/A	#N/A	#N/A	#N/A	#N/A	#N/A
<i>ROSI</i>	Downregulated	-0.692050475	0.0000239	0.00077346	Yes	-0.5010559	0.07686594	0.1404147	Yes
<i>IGSF10</i>	Downregulated	-0.065129837	0.45544839	0.67342273	Yes	-0.3571971	0.00046675	0.00388767	Yes
<i>TPRG1</i>	Downregulated	0.146423892	0.1044159	0.27678453	No	0.1738539	0.37881556	0.48798004	No
<i>SLC2A5</i>	Downregulated	0.341026941	0.00996788	0.05615327	No	0.45412473	0.03677244	0.07933616	No
<i>LOC399715</i>	Downregulated	#N/A	#N/A	#N/A	#N/A	#N/A	#N/A	#N/A	#N/A
<i>GIPC3</i>	Downregulated	0.56226702	0.00024666	0.00410426	No	0.5379832	0.00249362	0.01216504	No
<i>E2F2</i>	Downregulated	0.067524343	0.78924279	0.89731063	No	0.03620876	0.89958082	0.92926746	No
<i>KCNQ1OT1</i>	Downregulated	-0.02706674	0.68932144	0.83867626	Yes	-0.2679292	0.11972083	0.19868898	Yes

<i>RAD51B</i>	Downregulated	0.275636734	0.00018149	0.00328476	No	0.18265561	0.12357478	0.20372665	No
<i>KDR</i>	Downregulated	0.455047898	0.00027646	0.00445544	No	0.44620687	0.00968194	0.02947775	No
<i>CPM</i>	Downregulated	0.652740963	1.4E-12	6.68E-09	No	0.45474913	0.0011744	0.0074437	No
<i>MRVII</i>	Downregulated	0.383768935	0.000008	0.0003603	No	0.86943502	0.00000319	0.0000936	No
<i>SOAT2</i>	Downregulated	0.349030284	0.41851732	NA	No	-0.4102398	0.08927614	0.15762628	Yes
<i>NFATC2</i>	Downregulated	0.497824481	1.38E-09	0.00000075	No	0.58270207	0.00015387	0.00171035	No
<i>TNFRSF1IA</i>	Downregulated	-0.252266386	0.00038298	0.0055928	Yes	-0.6860064	0.0000115	0.0002416	Yes
<i>ITGBL1</i>	Downregulated	0.269715488	0.08112408	0.23414322	No	-0.158796	0.31190313	0.41965422	Yes
<i>MKRN9P</i>	Downregulated	0.005793425	0.99488263	NA	No	-0.2961327	0.1422407	0.22744478	Yes
<i>LOC338817</i>	Downregulated	#N/A	#N/A	#N/A	#N/A	#N/A	#N/A	#N/A	#N/A
<i>AGTR1</i>	Downregulated	0.51567119	0.01345984	0.06919339	No	0.73909409	0.00677856	0.02320391	No
<i>ERG</i>	Downregulated	0.206891968	0.04175764	0.15119916	No	0.68990482	0.0000111	0.00023716	No
<i>MAP1LC3C</i>	Downregulated	0.474176597	0.00157934	0.0151232	No	0.10095984	0.46757552	0.57240812	No
<i>SP7</i>	Downregulated	0.175808937	0.17284234	0.37939148	No	-0.9541304	0.00061224	0.004726	Yes
<i>NOX5</i>	Downregulated	-0.497527743	0.00098758	0.01087417	Yes	-0.3328191	0.13166589	0.21407177	Yes
<i>EGFLAM</i>	Downregulated	0.554694633	0.00110005	0.01172458	No	0.64138202	0.02344833	0.05619052	No
<i>RIBC2</i>	Downregulated	0.083388834	0.55224543	0.74595606	No	0.11555982	0.55003322	0.64728366	No
<i>C3</i>	Downregulated	0.673077579	8.39E-09	0.00000277	No	0.89738839	0.00028039	0.00266103	No
<i>SEC1</i>	Downregulated	#N/A	#N/A	#N/A	#N/A	#N/A	#N/A	#N/A	#N/A
<i>PAPPA2</i>	Downregulated	-0.069260931	0.21926232	0.43896713	Yes	-0.4083156	0.00483706	0.01859198	Yes
<i>ABCA4</i>	Downregulated	0.152547374	0.22164495	0.44173032	No	0.17912757	0.28188472	0.387848	No
<i>DNAH11</i>	Downregulated	0.503485278	0.00077455	0.00909743	No	0.01389262	0.92457911	0.94699285	No
<i>ACTL8</i>	Downregulated	-0.070765551	0.86502471	NA	Yes	-0.67356	0.02369985	0.05665203	Yes

<i>FLT3LG</i>	Downregulated	0.238346504	0.16784013	0.37250479	No	0.2507564	0.01653987	0.04336078	No
<i>PKP1</i>	Downregulated	0.118279447	0.39620329	0.62167013	No	-0.7769722	0.00075811	0.00548026	Yes
<i>LOC100130581</i>	Downregulated	#N/A	#N/A	#N/A	#N/A	#N/A	#N/A	#N/A	#N/A
<i>LINC00311</i>	Downregulated	0.375099437	0.07209836	0.21657468	No	-0.1818232	0.47116813	0.57571499	Yes
<i>ATAD3C</i>	Downregulated	0.339928471	0.01185812	0.06322	No	0.1804804	0.3548165	0.46384874	No
<i>ITK</i>	Downregulated	0.496776086	0.00111204	0.01179937	No	-0.4316114	0.05170602	0.10323799	Yes
<i>C1QTNF2</i>	Downregulated	-0.048749657	0.51941874	0.72178153	Yes	-0.718721	0.00000299	0.0000895	Yes
<i>PAPL</i>	Downregulated	#N/A	#N/A	#N/A	#N/A	0.12469334	0.60094315	0.69236241	No
<i>KCNE3</i>	Downregulated	0.547327822	2.85E-08	0.00000639	No	0.33307204	0.02469449	0.05849047	No
<i>ADCY10</i>	Downregulated	-0.008583484	0.93350469	0.97216503	Yes	-0.1884206	0.27588536	0.3815235	Yes
<i>ELTD1</i>	Downregulated	0.376562899	0.00021754	0.00373348	No	1.06142311	5.91E-07	0.0000271	No
<i>RAET1E</i>	Downregulated	-0.091105709	0.33962958	0.56957253	Yes	0.3487251	0.06373877	0.12144826	No
<i>NOX4</i>	Downregulated	-0.21383856	0.01263462	0.06613355	Yes	-0.5126441	0.0175404	0.04524555	Yes
<i>FKBPIAPI</i>	Downregulated	-0.087087778	0.42844415	0.65076319	Yes	#N/A	#N/A	#N/A	#N/A
<i>TMEM106A</i>	Downregulated	0.31580513	0.00064046	0.00803572	No	0.24428987	0.11169833	0.18802604	No
<i>STX11</i>	Downregulated	0.370419112	0.03797558	0.14197452	No	0.82028182	0.0000806	0.00105524	No
<i>ADAMTSL3</i>	Downregulated	0.386432303	0.000016	0.00058045	No	0.71973021	0.00014669	0.00164669	No
<i>EEF1DP3</i>	Downregulated	-0.136231603	0.07226712	0.21687565	Yes	-0.2373614	0.22289055	0.32325362	Yes
<i>EMCN</i>	Downregulated	0.374577583	0.00114893	0.01208603	No	0.71222655	0.00019735	0.00205274	No
<i>MRI</i>	Downregulated	0.220631837	0.00050755	0.00680693	No	0.44604804	0.00015616	0.00172921	No
<i>HOXD-ASI</i>	Downregulated	0.554670384	0.00270419	0.02222015	No	0.00588612	0.98324231	0.98871104	No
<i>FERIL5</i>	Downregulated	-0.191240368	0.02821494	0.11588247	Yes	-0.2614609	0.07841199	0.14265472	Yes
<i>ADAM20</i>	Downregulated	-0.228694257	0.00511818	0.03489409	Yes	-0.0161714	0.9314277	0.9518628	Yes

<i>GPR183</i>	Downregulated	0.114044996	0.31743584	0.5477785	No	0.45713386	0.17030463	0.26172835	No
<i>PYY</i>	Downregulated	0.202942692	0.44215211	0.66232944	No	-0.4055848	0.01387726	0.03809426	Yes
<i>C10orf54</i>	Downregulated	0.403025164	0.00033767	0.00510619	No	0.73077599	0.0000666	0.00091581	No
<i>MIRLET7BHG</i>	Downregulated	0.243002987	0.00512333	0.03491037	No	#N/A	#N/A	#N/A	#N/A
<i>AURKB</i>	Downregulated	0.674551593	0.07046586	NA	No	-0.4895252	0.09107817	0.16010323	Yes
<i>GSDMA</i>	Downregulated	0.87878291	0.00500177	0.03436592	No	-0.1045381	0.719285	0.79076533	Yes
<i>SCIN</i>	Downregulated	0.602250756	0.00063038	0.00794518	No	0.9838084	0.00257304	0.01241317	No
<i>IQGAP3</i>	Downregulated	-0.102670616	0.41856132	0.6418098	Yes	-0.8836003	0.0000145	0.00028957	Yes
<i>C9orf84</i>	Downregulated	0.107204321	0.35799034	0.58646258	No	0.31680368	0.09084588	0.15982088	No
<i>NEIL3</i>	Downregulated	0.029825471	0.89842678	0.95480531	No	-0.4095298	0.09581886	0.16666123	Yes
<i>MME</i>	Downregulated	-0.250788462	0.0621842	0.19638369	Yes	-0.6517315	0.0023023	0.0115734	Yes
<i>OPNISW</i>	Downregulated	-0.03694373	0.73011633	0.86326589	Yes	-0.2020975	0.12489223	0.20537031	Yes
<i>C6orf99</i>	Downregulated	-0.207627946	0.12028544	0.30271955	Yes	0.23006397	0.12330877	0.2033723	No
<i>LCP1</i>	Downregulated	0.388972055	0.00059647	0.00763775	No	0.71220688	0.00193938	0.01037238	No
<i>NCKAP1L</i>	Downregulated	0.420413894	0.00000781	0.0003532	No	0.32278105	0.12709453	0.20809569	No
<i>ABRA</i>	Downregulated	-0.21079145	0.10526671	0.27814625	Yes	-1.1998782	0.00000472	0.0001251	Yes
<i>CHI3L2</i>	Downregulated	1.522940815	3.14E-09	0.00000137	No	1.31852213	0.00144973	0.008589	No
<i>LILRA6</i>	Downregulated	#N/A	#N/A	#N/A	#N/A	0.63457674	0.00690019	0.02349333	No
<i>CIITA</i>	Downregulated	0.47754803	3.92E-07	0.0000423	No	-0.1646574	0.02600523	0.06082957	Yes
<i>TIE1</i>	Downregulated	0.53552561	0.0000525	0.0013543	No	0.62355693	0.00026748	0.00257174	No
<i>UNQ6975</i>	Downregulated	#N/A	#N/A	#N/A	#N/A	#N/A	#N/A	#N/A	#N/A
<i>USH2A</i>	Downregulated	-0.085410118	0.27262405	0.50134083	Yes	-0.3965054	0.00635968	0.02224348	Yes
<i>TAF4B</i>	Downregulated	-0.16024291	0.02482319	0.1059048	Yes	-0.5656909	0.0000785	0.00103386	Yes

<i>POLQ</i>	Downregulated	-0.321057694	0.00069443	0.00843669	Yes	-0.2931091	0.05459846	0.10763708	Yes
<i>LSP1</i>	Downregulated	0.699865914	0.00000183	0.0001259	No	-0.445583	0.02411537	0.05741392	Yes
<i>ZYG11A</i>	Downregulated	0.142782241	0.39946181	0.62471357	No	-0.1034317	0.66649724	0.74770914	Yes
<i>CD14</i>	Downregulated	0.413500191	0.01203851	0.06396607	No	0.89638385	0.00056402	0.0044493	No
<i>GDNF</i>	Downregulated	0.207237781	0.17327224	0.38003868	No	-0.2607719	0.32495202	0.43317613	Yes
<i>BDKRB1</i>	Downregulated	-0.099043969	0.6700175	0.8256443	Yes	-0.5267704	0.05122348	0.10248373	Yes
<i>ALOX5AP</i>	Downregulated	0.338519476	0.00640914	0.04087212	No	1.20512522	0.0000128	0.00026259	No
<i>GPR156</i>	Downregulated	0.26053531	0.00229682	0.01980764	No	0.13924629	0.31209605	0.41987326	No
<i>ZPI</i>	Downregulated	0.051733898	0.64740716	0.81027836	No	-0.2650536	0.13117664	0.21343191	Yes
<i>SYCP3</i>	Downregulated	-0.043423797	0.61219785	0.78627989	Yes	0.08066582	0.44298188	0.54959719	No
<i>TMEM217</i>	Downregulated	0.129365475	0.27814277	0.50716457	No	0.04552542	0.60769324	0.69823484	No
<i>UHRF1</i>	Downregulated	0.440350502	0.00187574	0.01712165	No	0.61882255	0.00245657	0.01205389	No
<i>GABRR2</i>	Downregulated	0.680249183	0.00017646	0.00321992	No	1.56879553	4.23E-07	0.0000215	No
<i>FGF18</i>	Downregulated	-0.269891483	0.10818429	0.28284263	Yes	-0.3763223	0.04099066	0.08631237	Yes
<i>ADAMTS14</i>	Downregulated	0.277739576	0.09214528	0.2545898	No	-0.1432822	0.61496496	0.70431129	Yes
<i>SLC15A3</i>	Downregulated	0.689538796	2.26E-12	8.57E-09	No	0.12821121	0.19510179	0.29147385	No
<i>CAVI</i>	Downregulated	0.468429273	0.0000104	0.00042924	No	0.66883975	0.00073853	0.0053828	No
<i>COL11A1</i>	Downregulated	-0.11227508	0.10269114	0.27361151	Yes	0.31390528	0.00844771	0.02685349	No
<i>COL13A1</i>	Downregulated	-0.091671366	0.49535413	0.70401748	Yes	-0.235709	0.33373601	0.44221072	Yes
<i>PTPRC</i>	Downregulated	#N/A	#N/A	#N/A	#N/A	0.88007634	0.00133405	0.00813059	No
<i>LRRC19</i>	Downregulated	0.011480017	0.90653595	0.95879827	No	-0.0033689	0.98589746	0.99044502	Yes
<i>ACSM5</i>	Downregulated	0.505457733	0.0000178	0.00062195	No	0.26159844	0.17323185	0.26535807	No
<i>LOC648987</i>	Downregulated	#N/A	#N/A	#N/A	#N/A	#N/A	#N/A	#N/A	#N/A

<i>C8orf46</i>	Downregulated	-0.111186378	0.03865386	0.14375978	Yes	-0.1239907	0.07676763	0.14028108	Yes
<i>ANKRD26P1</i>	Downregulated	-0.117628174	0.65497295	0.81547183	Yes	-0.1996114	0.51320856	0.61441121	Yes
<i>GTF2IRD2P1</i>	Downregulated	0.26716323	0.20160603	0.41764942	No	-0.0637628	0.69567353	0.77160941	Yes
<i>SLC2A4</i>	Downregulated	0.627210839	0.00000399	0.00021578	No	0.78367659	0.00015914	0.00175531	No
<i>TXNRD3NB</i>	Downregulated	NA	NA	NA	#N/A	0.00670053	0.94421526	0.96145931	No
<i>LOC100506810</i>	Downregulated	#N/A	#N/A	#N/A	#N/A	#N/A	#N/A	#N/A	#N/A
<i>HGF</i>	Downregulated	0.28637717	0.02169242	0.0966558	No	0.92148999	0.00072282	0.00531193	No
<i>HNRNPA3P1</i>	Downregulated	0.335284013	0.78262235	NA	No	-0.1309383	0.3160097	0.42406404	Yes
<i>SKA3</i>	Downregulated	0.339839533	0.02920503	0.11880469	No	-0.6867612	0.0000199	0.00036704	Yes
<i>BRIP1</i>	Downregulated	-0.0123155	0.9057128	0.9584404	Yes	-0.807485	0.0000227	0.00040591	Yes
<i>SVEP1</i>	Downregulated	-0.273822131	0.00812905	0.04850337	Yes	-0.2245947	0.30979593	0.41744361	Yes
<i>CCDC168</i>	Downregulated	-0.220417538	0.24559132	0.47017266	Yes	0.0354198	0.88077203	0.91572173	No
<i>GIPC2</i>	Downregulated	-0.096035716	0.2897578	0.51951086	Yes	-0.2674136	0.01913556	0.04830982	Yes
<i>TNS4</i>	Downregulated	0.246506795	0.51392516	NA	No	-0.4519474	0.13668174	0.22050166	Yes
<i>PTPRB</i>	Downregulated	0.059208475	0.43227582	0.65383161	No	0.71127981	0.0000893	0.00113671	No
<i>CD40</i>	Downregulated	0.386677459	0.0000262	0.0008234	No	0.52648086	0.0000734	0.00098193	No
<i>LOC100134368</i>	Downregulated	#N/A	#N/A	#N/A	#N/A	#N/A	#N/A	#N/A	#N/A
<i>EN1</i>	Downregulated	-0.583365187	0.21674214	NA	Yes	-0.1397086	0.62897221	0.71630733	Yes
<i>LOC148696</i>	Downregulated	#N/A	#N/A	#N/A	#N/A	#N/A	#N/A	#N/A	#N/A
<i>FERMT1</i>	Downregulated	0.045585775	0.63075256	0.79814038	No	0.0297457	0.86161954	0.90162642	No
<i>ITGB2</i>	Downregulated	0.594805276	6.11E-07	0.0000583	No	0.64993897	0.00679895	0.02325427	No
<i>COL6A3</i>	Downregulated	0.426841659	0.04348549	0.15523402	No	0.46499165	0.09141694	0.16058736	No
<i>ATP8B5P</i>	Downregulated	0.202511322	0.22751192	0.44927093	No	-0.3894864	0.00047736	0.00395118	Yes

<i>OTOA</i>	Downregulated	-0.132185708	0.22532523	0.44657557	Yes	-0.6196993	0.00067727	0.00508027	Yes
<i>PCDHGA12</i>	Downregulated	0.215043683	0.02065848	0.0936317	No	0.30184082	0.00016405	0.00179621	No
<i>TBX15</i>	Downregulated	0.443360636	0.00375639	0.02793009	No	1.42267542	2.32E-08	0.00000314	No
<i>PTPN22</i>	Downregulated	0.217508464	0.02101959	0.09461306	No	0.11287863	0.50130863	0.60341884	No
<i>INHBA</i>	Downregulated	1.034984552	0.00000302	0.000177	No	-0.0930317	0.5822795	0.67619712	Yes
<i>BIRC3</i>	Downregulated	0.300188296	0.00265124	0.02191312	No	0.37644235	0.02364544	0.05656078	No
<i>BCL11B</i>	Downregulated	-0.098089894	0.21924535	0.43896713	Yes	-0.6419024	0.000039	0.0006122	Yes
<i>CASC5</i>	Downregulated	#N/A	#N/A	#N/A	#N/A	-0.2951085	0.10682789	0.18150584	Yes
<i>AXDND1</i>	Downregulated	0.23237127	0.07455108	0.22128035	No	-0.2528807	0.33146316	0.43977374	Yes
<i>CYP27B1</i>	Downregulated	0.059105654	0.64975188	0.81200399	No	-0.453362	0.0000317	0.00052267	Yes
<i>LOC440028</i>	Downregulated	#N/A	#N/A	#N/A	#N/A	#N/A	#N/A	#N/A	#N/A
<i>PIP5K1P1</i>	Downregulated	0.091529445	0.52126082	0.72304411	No	0.00810806	0.97337897	0.982098	No
<i>CYP11A1</i>	Downregulated	0.229109569	0.04106134	0.14950517	No	0.01989777	0.90180183	0.93090298	No
<i>ANKRD20A9P</i>	Downregulated	-0.172288665	0.53645185	0.73482365	Yes	-0.119852	0.58955382	0.68249824	Yes
<i>BCL11A</i>	Downregulated	-0.377739047	3.77E-07	0.0000413	Yes	-0.6699523	0.00042128	0.00359979	Yes
<i>DQX1</i>	Downregulated	-0.023374357	0.8339513	0.92086121	Yes	-0.2465916	0.15450374	0.24262126	Yes
<i>DPT</i>	Downregulated	-0.063999411	0.60966979	0.78443376	Yes	-0.5406114	0.001911	0.0102748	Yes
<i>RORI</i>	Downregulated	-0.149039039	0.08193364	0.23565544	Yes	0.06568377	0.66073833	0.74314902	No
<i>SH2D4A</i>	Downregulated	0.058361875	0.3809972	0.60819178	No	0.6910437	0.0000144	0.00028774	No
<i>MOCOS</i>	Downregulated	0.080252326	0.47000913	0.68520883	No	0.13287346	0.50301658	0.60499143	No
<i>PLIN1</i>	Downregulated	0.64050055	0.0000537	0.00137654	No	0.79749738	0.00039824	0.00345373	No
<i>TPTE2</i>	Downregulated	-0.130170659	0.38024027	0.60759289	Yes	-0.908342	0.0000165	0.00032015	Yes
<i>SLC38A4</i>	Downregulated	0.212954234	0.1731731	0.37991204	No	0.43836287	0.13569348	0.21923285	No

<i>COL24A1</i>	Downregulated	-0.616398085	3.32E-08	0.00000719	Yes	-0.3438051	0.14048201	0.22526452	Yes
<i>TRIM29</i>	Downregulated	-0.083568582	0.60979588	0.78443376	Yes	-0.5362202	0.00983189	0.02980896	Yes
<i>CD101</i>	Downregulated	-0.087594459	0.27374622	0.50248664	Yes	-0.7785195	5.27E-08	0.00000541	Yes
<i>HYMA1</i>	Downregulated	-0.145994167	0.18275435	0.39290012	Yes	#N/A	#N/A	#N/A	#N/A
<i>SP110</i>	Downregulated	0.210352452	0.00676469	0.04255006	No	0.35124747	0.00512436	0.01928415	No
<i>CAGE1</i>	Downregulated	-0.201127992	0.36158216	0.58985687	Yes	-0.0024081	0.9908263	0.99380294	Yes
<i>HHIP</i>	Downregulated	0.176685771	0.09215918	0.2545898	No	0.24153606	0.32421222	0.43245877	No
<i>CYP2B7P1</i>	Downregulated	#N/A	#N/A	#N/A	#N/A	#N/A	#N/A	#N/A	#N/A
<i>CLCF1</i>	Downregulated	0.225185233	0.01841433	0.08640097	No	0.58699454	0.00142346	0.00849295	No
<i>ODF3L2</i>	Downregulated	0.229506012	0.13191366	0.32056929	No	-0.0914372	0.54387458	0.64189219	Yes
<i>TMC2</i>	Downregulated	-0.187943553	0.02427494	0.10423474	Yes	-0.2462453	0.08590724	0.15293992	Yes
<i>MKX</i>	Downregulated	-0.146263145	0.11866596	0.30001651	Yes	-0.5290396	0.00249587	0.01216872	Yes
<i>LOC153684</i>	Downregulated	#N/A	#N/A	#N/A	#N/A	#N/A	#N/A	#N/A	#N/A
<i>BIRC5</i>	Downregulated	0.531128918	0.00236244	0.02023391	No	-0.0292897	0.86659707	0.90545858	Yes
<i>FHAD1</i>	Downregulated	-0.154435172	0.13049421	0.31847875	Yes	-0.5336393	0.00101581	0.00674659	Yes
<i>PSTPIP1</i>	Downregulated	0.286732585	0.00027098	0.00438205	No	0.032336	0.80037718	0.85511392	No
<i>EGF</i>	Downregulated	0.177267159	0.05138887	0.17263397	No	0.63726725	0.00053319	0.00427691	No
<i>C20orf152</i>	Downregulated	#N/A	#N/A	#N/A	#N/A	#N/A	#N/A	#N/A	#N/A
<i>LOC100133985</i>	Downregulated	#N/A	#N/A	#N/A	#N/A	#N/A	#N/A	#N/A	#N/A
<i>KLHL10</i>	Downregulated	-0.087339247	0.47822915	0.69106069	Yes	-0.1905404	0.13685045	0.22069723	Yes
<i>FAM129C</i>	Downregulated	0.188221393	0.09674401	0.26270459	No	-0.1653343	0.33306068	0.44148375	Yes
<i>FMO4</i>	Downregulated	0.480601834	0.0000333	0.00097632	No	0.21329164	0.23366104	0.33525038	No
<i>EVC2</i>	Downregulated	0.491909804	0.0000025	0.00015616	No	0.57151578	0.00282582	0.01317325	No

<i>LYG2</i>	Downregulated	-0.182729827	0.04878832	0.16739395	Yes	0.20418689	0.33440262	0.44286246	No
<i>COL5A3</i>	Downregulated	0.098074735	0.33898243	0.56911971	No	0.5371478	0.00300393	0.01368583	No
<i>SP100</i>	Downregulated	-0.345148712	0.24350902	0.46776705	Yes	0.54532049	0.0003242	0.00296474	No
<i>C4orf22</i>	Downregulated	0.058221413	0.70272423	0.84698195	No	-1.0277523	0.00026448	0.00255083	Yes
<i>CDC25C</i>	Downregulated	-0.136769767	0.42297992	0.64540402	Yes	-0.1059096	0.31907727	0.42727555	Yes
<i>IL15</i>	Downregulated	0.224086136	0.03963583	0.14607432	No	0.14761196	0.26129046	0.36570301	No
<i>LOC100288637</i>	Downregulated	#N/A	#N/A	#N/A	#N/A	#N/A	#N/A	#N/A	#N/A
<i>FLJ42289</i>	Downregulated	#N/A	#N/A	#N/A	#N/A	#N/A	#N/A	#N/A	#N/A
<i>ITGB4</i>	Downregulated	0.793239917	1.04E-08	0.00000302	No	1.22774373	7.72E-07	0.0000332	No
<i>LOC100130872</i>	Downregulated	#N/A	#N/A	#N/A	#N/A	#N/A	#N/A	#N/A	#N/A
<i>PLCG2</i>	Downregulated	0.372307885	0.00000442	0.00023435	No	0.43360605	0.00283996	0.01322185	No
<i>VEPH1</i>	Downregulated	-0.143367925	0.14475479	0.34073807	Yes	-0.7102948	0.00132742	0.00809844	Yes
<i>LILRB3</i>	Downregulated	#N/A	#N/A	#N/A	#N/A	0.59489336	0.0175104	0.04518376	No
<i>ANO3</i>	Downregulated	-0.5221847	0.0000276	0.00085057	Yes	-1.1112537	0.00010982	0.00133313	Yes
<i>FLJ14107</i>	Downregulated	#N/A	#N/A	#N/A	#N/A	#N/A	#N/A	#N/A	#N/A
<i>STAB1</i>	Downregulated	0.379237344	0.00689669	0.0431586	No	0.93303203	0.0000243	0.00042864	No
<i>ADH6</i>	Downregulated	0.222462621	0.13547478	0.32574025	No	-0.0389665	0.86801773	0.90634362	Yes
<i>FBXW10</i>	Downregulated	-0.036297142	0.73681185	0.86659302	Yes	-0.293066	0.08978619	0.15837137	Yes
<i>FLJ38109</i>	Downregulated	#N/A	#N/A	#N/A	#N/A	#N/A	#N/A	#N/A	#N/A
<i>NLRP14</i>	Downregulated	0.052914754	0.69764951	0.8439391	No	0.26986113	0.55632563	0.65285595	No
<i>PCDHGA9</i>	Downregulated	-0.013284462	0.79795913	0.90294686	Yes	0.30168419	0.0001968	0.00204851	No
<i>ABCG2</i>	Downregulated	0.313077984	0.02134327	0.0956842	No	0.69498358	0.00562704	0.02050731	No
<i>LRRK1</i>	Downregulated	-0.175648699	0.00815144	0.04857136	Yes	-0.1282658	0.3004451	0.40764143	Yes

<i>SOX7</i>	Downregulated	0.347744553	0.00317583	0.02485778	No	0.48875498	0.00018984	0.00199334	No
<i>KIF6</i>	Downregulated	0.389969603	0.00000422	0.00022643	No	-0.2370383	0.19823953	0.29508618	Yes
<i>LOC149773</i>	Downregulated	#N/A	#N/A	#N/A	#N/A	#N/A	#N/A	#N/A	#N/A
<i>FAM176A</i>	Downregulated	#N/A	#N/A	#N/A	#N/A	#N/A	#N/A	#N/A	#N/A
<i>KIAA1875</i>	Downregulated	-0.097386512	0.40868852	0.63341998	Yes	-0.0612547	0.68623184	0.76399319	Yes
<i>SLC26A8</i>	Downregulated	-0.213366476	0.01241596	0.06534047	Yes	-0.5651671	0.00062257	0.00478389	Yes
<i>CDK15</i>	Downregulated	-0.16316398	0.20491871	0.42179537	Yes	-0.6125283	0.0153362	0.04100537	Yes
<i>TM4SF18</i>	Downregulated	0.451307744	0.00068619	0.00836879	No	1.02084336	0.00000418	0.00011453	No
<i>KIF4B</i>	Downregulated	-0.12167777	0.26076164	0.48810718	Yes	-0.214905	0.31130474	0.41901089	Yes
<i>ASB2</i>	Downregulated	#N/A	#N/A	#N/A	#N/A	-1.0664607	0.0000034	0.0000982	Yes
<i>KCNJ14</i>	Downregulated	0.117565046	0.17293548	0.37953008	No	-0.0992504	0.35917404	0.46819507	Yes
<i>LRRIQ4</i>	Downregulated	-0.332709965	0.01591731	0.07800201	Yes	-0.1655619	0.50508758	0.60682777	Yes
<i>LOC152742</i>	Downregulated	#N/A	#N/A	#N/A	#N/A	#N/A	#N/A	#N/A	#N/A
<i>PAQR5</i>	Downregulated	0.285672024	0.00713097	0.04428882	No	0.58238569	0.00247127	0.01209555	No
<i>LOC100506655</i>	Downregulated	#N/A	#N/A	#N/A	#N/A	#N/A	#N/A	#N/A	#N/A
<i>SND1-IT1</i>	Downregulated	-0.071892227	0.31584216	0.54630056	Yes	#N/A	#N/A	#N/A	#N/A
<i>NLRC5</i>	Downregulated	0.504651342	0.00000107	0.0000884	No	0.69621221	0.00000433	0.00011743	No
<i>GLI2</i>	Downregulated	0.557516345	0.0000194	0.00065577	No	0.98111212	5.3E-08	0.00000543	No
<i>DYSF</i>	Downregulated	0.199007565	0.019059	0.08856089	No	0.092646	0.67773708	0.75693899	No
<i>EPSTI1</i>	Downregulated	0.307255559	0.00398871	0.02912746	No	0.24274684	0.2101863	0.30895962	No
<i>BARD1</i>	Downregulated	0.207161584	0.0034068	0.0261057	No	0.38248915	0.00019836	0.0020588	No
<i>DENND2D</i>	Downregulated	0.510838082	0.0000112	0.00045084	No	0.52094826	0.00806349	0.02599707	No
<i>CDC45</i>	Downregulated	0.547365461	0.00242817	0.02066336	No	0.4749377	0.0344582	0.0754586	No

<i>FUT2</i>	Downregulated	-0.074436811	0.2987995	0.52865483	Yes	-0.187829	0.04156035	0.0872553	Yes
<i>OSCAR</i>	Downregulated	#N/A	#N/A	#N/A	#N/A	-0.0596063	0.6367262	0.72277012	Yes
<i>TINAGL1</i>	Downregulated	0.537970259	0.00027579	0.00444659	No	0.60669342	0.00120056	0.0075551	No
<i>INMT</i>	Downregulated	0.402680631	0.03205416	0.12659557	No	0.13726519	0.46618303	0.57119756	No
<i>HNMT</i>	Downregulated	0.294352702	0.0000478	0.00126647	No	0.2584666	0.01321737	0.03680506	No
<i>C19orf35</i>	Downregulated	#N/A	#N/A	#N/A	#N/A	0.52156286	0.0028233	0.01316765	No
<i>DTL</i>	Downregulated	0.482020882	0.00196921	0.01774442	No	-0.1918402	0.29086507	0.39744811	Yes
<i>LOC100129931</i>	Downregulated	#N/A	#N/A	#N/A	#N/A	#N/A	#N/A	#N/A	#N/A
<i>SATB2</i>	Downregulated	-0.247320473	0.00041082	0.00588603	Yes	-0.3916954	0.00805798	0.02598802	Yes
<i>PRAMI</i>	Downregulated	0.434302145	0.0000478	0.00126647	No	0.04295825	0.78051567	0.8395245	No
<i>SLC12A1</i>	Downregulated	-0.410890153	0.00077395	0.00909677	Yes	-0.8565587	0.00000228	0.0000736	Yes
<i>ALPK1</i>	Downregulated	0.361041252	0.00033046	0.00503039	No	0.55106041	0.00023749	0.00235525	No
<i>EMX2OS</i>	Downregulated	0.401831855	0.000038	0.0010635	No	0.99519881	0.00000423	0.0001154	No
<i>PRRG4</i>	Downregulated	0.597603813	0.0000224	0.00073842	No	0.78263086	0.00068881	0.00513783	No
<i>SPDY5</i>	Downregulated	-0.013495106	0.87446675	0.94220206	Yes	#N/A	#N/A	#N/A	#N/A
<i>S1PRI</i>	Downregulated	0.341462532	0.00047563	0.00653584	No	0.91017564	2.77E-08	0.00000355	No
<i>SP140L</i>	Downregulated	0.259219245	0.00041554	0.00592691	No	0.3420866	0.00175605	0.00974135	No
<i>TDRD9</i>	Downregulated	-0.159739789	0.11422907	0.29279733	Yes	-0.364512	0.02266481	0.05478148	Yes
<i>ZMYND15</i>	Downregulated	0.590610516	0.00000197	0.00013224	No	0.09170389	0.53442375	0.6333524	No
<i>C14orf182</i>	Downregulated	#N/A	#N/A	#N/A	#N/A	-0.3789874	0.05673372	0.11093267	Yes
<i>MIP</i>	Downregulated	-0.062019773	0.71621113	0.85473312	Yes	-0.1343611	0.20588341	0.30401323	Yes
<i>DLGAP5</i>	Downregulated	0.947769429	0.00312569	0.02463295	No	-0.4336474	0.11660709	0.19459974	Yes
<i>APOBEC3D</i>	Downregulated	0.390920527	0.0240874	0.10375816	No	0.44313517	0.01077954	0.0317515	No

<i>PSMB9</i>	Downregulated	0.461870914	0.0000107	0.00043711	No	0.31846934	0.0150448	0.04043956	No
<i>LOC440600</i>	Downregulated	#N/A	#N/A	#N/A	#N/A	#N/A	#N/A	#N/A	#N/A
<i>CDRT1</i>	Downregulated	-0.256410916	0.12741507	0.31411141	Yes	0.02488711	0.86824443	0.9064494	No
<i>LOC400891</i>	Downregulated	#N/A	#N/A	#N/A	#N/A	#N/A	#N/A	#N/A	#N/A
<i>MEII</i>	Downregulated	-0.144040059	0.08872507	0.2484302	Yes	-0.4314779	0.01179477	0.0338758	Yes
<i>GPR39</i>	Downregulated	-0.422965395	0.00093196	0.01044414	Yes	0.02749944	0.86684876	0.90556015	No
<i>IGSF6</i>	Downregulated	0.210911004	0.00180324	0.01664737	No	0.5383316	0.01515746	0.04066202	No
<i>HOGA1</i>	Downregulated	0.391654057	0.00000727	0.00033496	No	0.00724182	0.96031865	0.97254612	No
<i>LOC285540</i>	Downregulated	#N/A	#N/A	#N/A	#N/A	#N/A	#N/A	#N/A	#N/A
<i>ZBTB20</i>	Downregulated	0.317444653	0.00000569	0.00027991	No	0.60934102	0.0000135	0.00027486	No
<i>ZNF850</i>	Downregulated	0.162898157	0.0011213	0.01187111	No	0.02893529	0.815255	0.86667476	No
<i>CCDC158</i>	Downregulated	-0.308983308	0.0000592	0.00147747	Yes	-0.3509558	0.00768386	0.02522499	Yes
<i>ERAP2</i>	Downregulated	0.244492211	0.0370495	0.13962032	No	0.20862883	0.4624411	0.56788903	No
<i>KCTD19</i>	Downregulated	0.026459879	0.85832602	0.9344085	No	-0.3304184	0.04904936	0.09909399	Yes
<i>ITGA11</i>	Downregulated	0.070209868	0.27154257	0.50012746	No	0.39904261	0.00117134	0.00742988	No
<i>TMPRSS5</i>	Downregulated	0.48271906	0.00105688	0.01140216	No	0.46205627	0.11298261	0.18971986	No
<i>ARHGAP6</i>	Downregulated	0.082073278	0.43655645	0.65773743	No	-0.0201481	0.87873745	0.91422013	Yes
<i>NKX3-1</i>	Downregulated	0.30197116	0.0027183	0.02229746	No	0.31891914	0.01451633	0.03937578	No
<i>GREM1</i>	Downregulated	0.1253725	0.39114028	0.61718896	No	0.14324071	0.59566204	0.68781288	No
<i>DIAPH3</i>	Downregulated	0.245066282	0.0303143	0.12195769	No	0.20441611	0.26957481	0.37490741	No
<i>FRRS1</i>	Downregulated	0.407495128	0.00729786	0.0450452	No	0.79686295	0.00633275	0.0221827	No
<i>TLR5</i>	Downregulated	0.550935325	0.00000324	0.00018613	No	0.68147621	0.00018896	0.00198802	No
<i>LRTM1</i>	Downregulated	-0.256570729	0.00803256	0.04811727	Yes	-0.0686	0.7827973	0.84134372	Yes

<i>ALS2CRI1</i>	Downregulated	-0.01008674	0.89408389	0.95218755	Yes	-0.1882409	0.15279004	0.24043128	Yes
<i>KIF20A</i>	Downregulated	0.055336032	0.63053694	0.79798766	No	-0.4073967	0.0029297	0.01346869	Yes
<i>BTBD18</i>	Downregulated	0.00478308	0.94734016	0.97830976	No	0.01758754	0.89854461	0.92861737	No
<i>PRR5L</i>	Downregulated	0.396640624	0.000032	0.00094748	No	0.06660838	0.73005681	0.79934504	No
<i>RPGRIP1</i>	Downregulated	0.072868569	0.53843089	0.73617948	No	-0.4986569	0.00439622	0.01747205	Yes
<i>MALAT1</i>	Downregulated	-0.057625435	0.38853192	0.61489202	Yes	0.94415683	0.0000428	0.00065738	No
<i>GOLGA6L10</i>	Downregulated	-0.084543709	0.64127855	0.8063972	Yes	0.07983839	0.75177939	0.81668829	No
<i>RERGL</i>	Downregulated	0.178503015	0.26111324	0.48840401	No	0.1071664	0.68878474	0.76607054	No
<i>GALM</i>	Downregulated	0.269490151	0.00018756	0.00336571	No	0.35269737	0.00156781	0.00905007	No
<i>PPP1R36</i>	Downregulated	0.269388762	0.01102063	0.06008866	No	-0.1623479	0.3398001	0.44849784	Yes
<i>COLEC11</i>	Downregulated	-0.075355207	0.66715864	0.82377966	Yes	0.27469995	0.29506691	0.40183741	No
<i>COX7AI</i>	Downregulated	-0.200356781	0.02661704	0.11113566	Yes	-0.0973956	0.39273503	0.5015882	Yes
<i>RAD21-ASI</i>	Downregulated	-0.089708212	0.57141471	0.75889289	Yes	0.31978533	0.01671139	0.04370971	No
<i>PRR11</i>	Downregulated	0.06596666	0.42180604	0.64444192	No	-0.1347796	0.29055946	0.39706118	Yes
<i>VDR</i>	Downregulated	0.131701875	0.40963998	0.63406217	No	-0.2922441	0.1737977	0.26601144	Yes
<i>SPTBN5</i>	Downregulated	0.171346924	0.073004	0.21829306	No	0.04718578	0.73435921	0.80293627	No
<i>HAS2</i>	Downregulated	0.230452315	0.05477771	0.18050859	No	-0.0320734	0.88269174	0.91717035	Yes
<i>NCAPH</i>	Downregulated	0.088119496	0.40974835	0.63415843	No	-0.3116332	0.0984716	0.17017756	Yes
<i>LOC158376</i>	Downregulated	#N/A	#N/A	#N/A	#N/A	#N/A	#N/A	#N/A	#N/A
<i>SERPINE3</i>	Downregulated	0.258671111	0.02819923	0.11583046	No	-0.2398837	0.00437581	0.01742574	Yes
<i>CPSI</i>	Downregulated	0.166424153	0.01073068	0.05912778	No	0.13840502	0.25747297	0.36158703	No
<i>CAPN12</i>	Downregulated	-0.116548877	0.54638777	0.74179655	Yes	-0.3933422	0.0000404	0.00062922	Yes
<i>ACTR3C</i>	Downregulated	-0.008853786	0.9075202	0.95932013	Yes	-0.2725822	0.01722735	0.04464872	Yes

<i>NCF2</i>	Downregulated	0.497638992	0.0000175	0.00061369	No	0.9204783	0.00010172	0.00125373	No
<i>CX3CRI</i>	Downregulated	0.242895616	0.10500521	0.27776469	No	-0.0570647	0.86347165	0.90291322	Yes
<i>ENDOU</i>	Downregulated	0.138436681	0.12915704	0.31656611	No	0.09054643	0.49309139	0.59592074	No
<i>IGFN1</i>	Downregulated	0.05338518	0.8052548	0.90698402	No	-0.2976786	0.27988021	0.38577541	Yes
<i>ADAMTS9-AS2</i>	Downregulated	-0.002853814	0.97289012	0.9892478	Yes	0.36930626	0.01193903	0.0341914	No
<i>HJURP</i>	Downregulated	0.433248258	0.11238851	0.28991175	No	-0.395252	0.08732484	0.1549465	Yes
<i>SGCG</i>	Downregulated	-0.126063363	0.19298634	0.40649334	Yes	-0.3447332	0.08318759	0.14910973	Yes
<i>LOC646626</i>	Downregulated	#N/A	#N/A	#N/A	#N/A	#N/A	#N/A	#N/A	#N/A
<i>C6orf97</i>	Downregulated	#N/A	#N/A	#N/A	#N/A	#N/A	#N/A	#N/A	#N/A
<i>TAT</i>	Downregulated	-0.221576396	0.26779857	0.49616924	Yes	-0.4073237	0.01920157	0.04844355	Yes
<i>WNK4</i>	Downregulated	0.214217987	0.05367386	0.17780726	No	-0.2062338	0.13409284	0.21732059	Yes
<i>GLIS1</i>	Downregulated	0.039946226	0.719611	0.85709269	No	0.0663645	0.59518368	0.68744559	No
<i>LOC100505826</i>	Downregulated	#N/A	#N/A	#N/A	#N/A	#N/A	#N/A	#N/A	#N/A
<i>RGS20</i>	Downregulated	0.075535251	0.38690879	0.61373753	No	0.23435437	0.18638987	0.28107953	No
<i>TMEM204</i>	Downregulated	0.274616454	0.01509371	0.07508084	No	0.49109615	0.00481452	0.01854602	No
<i>CPNE6</i>	Downregulated	-0.017562876	0.8362782	0.92201469	Yes	-0.1758216	0.26425234	0.36896858	Yes
<i>FGF7</i>	Downregulated	-0.022040996	0.87713792	0.94401864	Yes	-0.5250586	0.00023956	0.00236947	Yes
<i>POTEKP</i>	Downregulated	0.379371549	0.61116789	NA	No	-0.3449001	0.10045145	0.17285797	Yes
<i>RUNX2</i>	Downregulated	0.045781491	0.4614996	0.67827431	No	-0.1180054	0.34905804	0.45800673	Yes
<i>NAT1</i>	Downregulated	0.360474873	0.00523107	0.0354599	No	0.52606391	0.00257425	0.01241411	No
<i>CFB</i>	Downregulated	#N/A	#N/A	#N/A	#N/A	0.68702537	0.0000969	0.00120894	No
<i>ROCK1PI</i>	Downregulated	-0.22348142	0.07971229	0.23135278	Yes	-0.0197184	0.84054436	0.88639339	Yes
<i>LOC100507178</i>	Downregulated	#N/A	#N/A	#N/A	#N/A	#N/A	#N/A	#N/A	#N/A

<i>RSPO1</i>	Downregulated	-0.404065482	0.17266275	0.37908497	Yes	-0.4055066	0.00190532	0.01025058	Yes
<i>TROAP</i>	Downregulated	0.638732314	0.07105865	0.21460697	No	-0.1125901	0.69386109	0.77014948	Yes
<i>MCTP2</i>	Downregulated	-0.203624959	0.03239642	0.12754914	Yes	0.51229409	0.00792696	0.02573084	No
<i>KIF14</i>	Downregulated	0.208969254	0.13109353	0.31929177	No	0.13276483	0.52345531	0.62357436	No
<i>TWIST1</i>	Downregulated	-0.11480304	0.22473345	0.44580219	Yes	-0.4420828	0.00881364	0.02766812	Yes
<i>CRISPLD2</i>	Downregulated	0.144715982	0.30056165	0.53051606	No	0.41247982	0.02428722	0.05773678	No
<i>MYLK2</i>	Downregulated	-0.024036982	0.90385628	0.95759718	Yes	-0.6299893	0.00823632	0.02636644	Yes
<i>PXDNL</i>	Downregulated	-0.232657732	0.00336808	0.02589267	Yes	-0.36888	0.01374066	0.03782581	Yes
<i>C21orf7</i>	Downregulated	#N/A	#N/A	#N/A	#N/A	#N/A	#N/A	#N/A	#N/A
<i>LOC100499405</i>	Downregulated	#N/A	#N/A	#N/A	#N/A	#N/A	#N/A	#N/A	#N/A
<i>ACRV1</i>	Downregulated	-0.407354353	0.00055396	0.00723755	Yes	-0.6769944	0.0000835	0.00108429	Yes
<i>E2F8</i>	Downregulated	0.076498215	0.65958071	0.81868422	No	-0.0874837	0.72431262	0.79479219	Yes
<i>NUF2</i>	Downregulated	-0.029852637	0.76357965	0.88265135	Yes	-0.26086	0.06257462	0.11974159	Yes
<i>CD163</i>	Downregulated	0.644568655	0.00279936	0.0227381	No	1.69124701	0.00020085	0.00207801	No
<i>FGF5</i>	Downregulated	-0.370024065	0.00881121	0.05132301	Yes	-0.749815	0.00000583	0.00014551	Yes
<i>DNAH5</i>	Downregulated	-0.024133321	0.81173328	0.91015337	Yes	-0.4742934	0.00430651	0.01726196	Yes
<i>ANKRD31</i>	Downregulated	-0.131293179	0.08458576	0.24042298	Yes	-0.425525	0.01854448	0.04717883	Yes
<i>CC2D2B</i>	Downregulated	-0.052801579	0.65995908	0.81904673	Yes	0.04024153	0.7854889	0.84331993	No
<i>MFSD7</i>	Downregulated	0.317415005	0.00063317	0.00796905	No	0.0824916	0.30944241	0.41707813	No
<i>PTGS1</i>	Downregulated	0.395916852	0.0000463	0.00123742	No	0.3303322	0.04901059	0.09903721	No
<i>RAD54L</i>	Downregulated	-0.082910119	0.41836831	0.64156569	Yes	-0.2520907	0.01199184	0.03431027	Yes
<i>NDE1</i>	Downregulated	0.324390134	0.00062816	0.0079365	No	0.37315317	0.03635816	0.0786364	No
<i>ADAM32</i>	Downregulated	#N/A	#N/A	#N/A	#N/A	-0.6066482	3.43E-07	0.0000186	Yes

<i>C8orf31</i>	Downregulated	-0.093817379	0.22249056	0.44288073	Yes	-0.2840332	0.00126259	0.00781318	Yes
<i>ANP32A-IT1</i>	Downregulated	#N/A	#N/A	#N/A	#N/A	#N/A	#N/A	#N/A	#N/A
<i>ATP10A</i>	Downregulated	0.255009913	0.04484816	0.15831165	No	0.56703718	0.00235343	0.01174312	No
<i>HKDC1</i>	Downregulated	0.406756682	0.00830721	0.04923359	No	0.00642198	0.97312914	0.98188355	No
<i>MSTIP2</i>	Downregulated	0.1193413	0.24179377	0.46598155	No	0.05571418	0.64823045	0.73271659	No
<i>IMPG1</i>	Downregulated	0.067896119	0.50843655	0.71368027	No	0.10491781	0.43405134	0.54121596	No
<i>PLAC8</i>	Downregulated	0.079487682	0.74416802	0.87142583	No	0.34758322	0.2509576	0.35457888	No
<i>LINC00315</i>	Downregulated	0.213207839	0.12896253	0.31629362	No	0.73012075	0.00859673	0.02718047	No
<i>TBX3</i>	Downregulated	0.387099926	0.01035267	0.05759679	No	0.87432533	0.0000118	0.00024722	No
<i>COL11A2</i>	Downregulated	#N/A	#N/A	#N/A	#N/A	-0.1440993	0.29677797	0.40355956	Yes
<i>CDCP1</i>	Downregulated	0.293855166	0.01035572	0.05760531	No	0.41369771	0.0278031	0.06395173	No
<i>CCNB2</i>	Downregulated	0.050581828	0.65334525	0.81429155	No	-0.1696229	0.4458062	0.55221905	Yes
<i>EDNRA</i>	Downregulated	0.223090763	0.00640895	0.04087212	No	0.47493487	0.00034612	0.00311514	No
<i>LOC100132215</i>	Downregulated	#N/A	#N/A	#N/A	#N/A	#N/A	#N/A	#N/A	#N/A
<i>DIO2</i>	Downregulated	-0.278281631	0.02885499	0.11783311	Yes	-0.0569324	0.82292426	0.87268131	Yes
<i>MPL</i>	Downregulated	0.185132194	0.10720046	0.28125856	No	0.03363988	0.83083783	0.87900029	No
<i>FBXO43</i>	Downregulated	0.089214575	0.59579131	0.77581444	No	-0.4375	0.07996393	0.14467094	Yes
<i>ASPM</i>	Downregulated	-0.06890352	0.5485589	0.74311898	Yes	-0.5114816	0.00614812	0.02175231	Yes
<i>CAPN14</i>	Downregulated	-0.239415286	0.01571459	0.07728337	Yes	-0.1411076	0.361531	0.47065126	Yes
<i>EYS</i>	Downregulated	-0.092743586	0.21053056	0.42881167	Yes	0.26800755	0.03074021	0.06911929	No
<i>CCDC38</i>	Downregulated	-0.138285947	0.26999975	0.49844693	Yes	-0.2994461	0.07974361	0.1444176	Yes
<i>CDCA2</i>	Downregulated	0.306389401	0.11716076	0.29754083	No	0.20270492	0.42336442	0.53106046	No
<i>TLR1</i>	Downregulated	0.342871817	0.00096157	0.01066805	No	0.79723892	0.00086305	0.0060165	No

<i>MSTIR</i>	Downregulated	-0.039000951	0.75152813	0.87557254	Yes	-0.029796	0.83467654	0.88183626	Yes
<i>TNFSF13B</i>	Downregulated	0.119081032	0.19906843	0.41413305	No	0.01547748	0.90443106	0.93277086	No
<i>HLA-F-AS1</i>	Downregulated	#N/A	#N/A	#N/A	#N/A	0.22842747	0.05006156	0.10070833	No
<i>GSG2</i>	Downregulated	#N/A	#N/A	#N/A	#N/A	0.03722362	0.86853351	0.90663237	No
<i>HOXC4</i>	Downregulated	0.252712416	0.36970208	0.59772835	No	0.36165939	0.14328227	0.22873781	No
<i>CCDC147</i>	Downregulated	0.242735218	0.01748184	0.08330267	No	-0.2812533	0.05636077	0.11035049	Yes
<i>PLAUR</i>	Downregulated	0.150525483	0.2941201	0.52352081	No	0.43690005	0.00706908	0.02384271	No
<i>C9orf47</i>	Downregulated	0.151930439	0.07783465	0.22755633	No	0.49397457	0.00048265	0.00398264	No
<i>APOBEC3F</i>	Downregulated	0.423292772	0.00119157	0.0123972	No	0.3018453	0.06508274	0.12345217	No
<i>CLDN11</i>	Downregulated	0.451498937	0.00046329	0.00641037	No	0.26312519	0.2604928	0.36478806	No
<i>LOC401074</i>	Downregulated	#N/A	#N/A	#N/A	#N/A	#N/A	#N/A	#N/A	#N/A
<i>SSPO</i>	Downregulated	0.165584086	0.09741594	0.26401953	No	0.25376237	0.07384167	0.13612102	No
<i>TBX1</i>	Downregulated	0.293097778	0.12670847	0.31303087	No	0.32564658	0.11466612	0.19199749	No
<i>CCDC150</i>	Downregulated	0.164604733	0.11542623	0.29463225	No	-0.3426092	0.07251817	0.1342583	Yes
<i>SLC11A1</i>	Downregulated	0.46291138	0.01113196	0.06051309	No	0.85706032	0.00830521	0.02651695	No
<i>IL21R</i>	Downregulated	0.232184997	0.2474548	0.47271489	No	-0.0870029	0.68450534	0.76257352	Yes
<i>PODN</i>	Downregulated	0.491678942	0.0000654	0.00159127	No	0.58709795	0.00035396	0.00316675	No
<i>PRG4</i>	Downregulated	0.1910818	0.2294965	0.45156877	No	-0.4162505	1.27E-07	0.00000961	Yes
<i>FLJ12825</i>	Downregulated	#N/A	#N/A	#N/A	#N/A	#N/A	#N/A	#N/A	#N/A
<i>MEIS1</i>	Downregulated	0.11452587	0.11623045	0.29602809	No	-0.2389058	0.09703733	0.16823948	Yes
<i>LOC100134713</i>	Downregulated	#N/A	#N/A	#N/A	#N/A	#N/A	#N/A	#N/A	#N/A
<i>XRCC2</i>	Downregulated	-0.076650831	0.31185135	0.54244646	Yes	-0.1550928	0.14567116	0.23181326	Yes
<i>ENAM</i>	Downregulated	-0.34656096	0.16245548	0.36542614	Yes	-0.2776553	0.29379111	0.40038661	Yes

<i>ABCA6</i>	Downregulated	0.169684704	0.19912014	0.41420902	No	0.31781864	0.26624016	0.37121424	No
<i>ITGA1</i>	Downregulated	0.253629763	0.00799393	0.04793832	No	0.84493169	0.00000463	0.00012328	No
<i>BRCA2</i>	Downregulated	0.125532061	0.1169478	0.29719698	No	-0.0342477	0.82672704	0.87573457	Yes
<i>TRPV4</i>	Downregulated	0.34617083	0.05723992	0.18577765	No	0.35008133	0.09419453	0.16441505	No
<i>TLCD2</i>	Downregulated	#N/A	#N/A	#N/A	#N/A	0.62003962	0.0003479	0.00312809	No
<i>KIF2C</i>	Downregulated	0.25555144	0.0033276	0.02569988	No	-0.2728141	0.01173819	0.03374971	Yes
<i>ANKRD1</i>	Downregulated	0.005715605	0.97481874	0.98973165	No	-0.6281484	0.01177182	0.03382024	Yes
<i>PRH2</i>	Downregulated	0.060600551	0.54765199	0.74258096	No	-0.4690218	0.0030482	0.01381364	Yes
<i>BHMT</i>	Downregulated	-0.219494478	0.05084864	0.17162426	Yes	-0.4088881	0.05255489	0.10451743	Yes
<i>NOTUM</i>	Downregulated	0.013520039	0.92387194	0.96709369	No	0.10877871	0.49778003	0.6002211	No
<i>C6orf132</i>	Downregulated	-0.175871366	0.37587525	0.60359506	Yes	-0.5184683	0.0132741	0.03691878	Yes
<i>PKD1L1</i>	Downregulated	-0.057229187	0.52213128	0.72374897	Yes	0.10338103	0.43152601	0.53886146	No
<i>BDKRB2</i>	Downregulated	0.025848342	0.83552729	0.92158101	No	-0.5295624	0.0319183	0.07114278	Yes
<i>CEP55</i>	Downregulated	0.745833654	0.01166482	0.06249668	No	-0.1985305	0.5054676	0.60717723	Yes
<i>C2orf65</i>	Downregulated	#N/A	#N/A	#N/A	#N/A	#N/A	#N/A	#N/A	#N/A
<i>CCDC144A</i>	Downregulated	-0.065981644	0.64171068	0.80671349	Yes	-0.4503984	0.00154911	0.00897278	Yes
<i>MOV10L1</i>	Downregulated	-0.247515979	0.00352517	0.02673561	Yes	-0.4184437	0.00034507	0.00310822	Yes
<i>PIWIL2</i>	Downregulated	0.149034685	0.15193784	0.35102728	No	-0.2124652	0.24621768	0.34919146	Yes
<i>LOC100505806</i>	Downregulated	#N/A	#N/A	#N/A	#N/A	#N/A	#N/A	#N/A	#N/A
<i>TGFBI</i>	Downregulated	0.572398101	0.00014216	0.00275852	No	0.93922516	0.00157094	0.00905937	No
<i>MCM10</i>	Downregulated	0.363867767	0.06373732	0.19961471	No	-0.442283	0.02285618	0.05511738	Yes
<i>LOC100132774</i>	Downregulated	#N/A	#N/A	#N/A	#N/A	#N/A	#N/A	#N/A	#N/A
<i>PTPN14</i>	Downregulated	0.00974174	0.84205285	0.92508164	No	0.03485631	0.65675077	0.73990292	No

<i>CAV2</i>	Downregulated	0.370307243	0.00015196	0.00289978	No	0.34879071	0.00827236	0.02645205	No
<i>LOC388692</i>	Downregulated	#N/A	#N/A	#N/A	#N/A	#N/A	#N/A	#N/A	#N/A
<i>FLJ35024</i>	Downregulated	#N/A	#N/A	#N/A	#N/A	#N/A	#N/A	#N/A	#N/A
<i>FLJ12334</i>	Downregulated	#N/A	#N/A	#N/A	#N/A	#N/A	#N/A	#N/A	#N/A
<i>PLIN4</i>	Downregulated	0.536167092	0.0000265	0.00082989	No	0.77327694	0.00000383	0.00010756	No
<i>CTSW</i>	Downregulated	0.130069947	0.30971888	0.5401898	No	0.06920708	0.67638101	0.75580294	No
<i>ABCA17P</i>	Downregulated	-0.122197239	0.08923228	0.24915811	Yes	-0.4032236	0.00021125	0.00216147	Yes
<i>KIAA0101</i>	Downregulated	#N/A	#N/A	#N/A	#N/A	-0.1424097	0.31817471	0.42632511	Yes
<i>LDHAL6A</i>	Downregulated	-0.210421049	0.02941932	0.11933804	Yes	0.10636575	0.51508489	0.61605117	No
<i>FKBP9L</i>	Downregulated	-0.249818132	0.16455213	0.36811339	Yes	-0.1022334	0.22619398	0.32693829	Yes
<i>HTR4</i>	Downregulated	-0.389086671	2.89E-07	0.0000343	Yes	-0.6643339	0.00206935	0.01080862	Yes
<i>LINC00482</i>	Downregulated	0.306321379	0.17008164	0.37562854	No	0.30832941	0.18744608	0.28231345	No
<i>ANKFNI</i>	Downregulated	0.396045488	0.0000184	0.0006347	No	0.5672367	0.00355126	0.01521471	No
<i>MYH15</i>	Downregulated	0.220584973	0.00811937	0.04846088	No	-0.2602076	0.07940958	0.14401381	Yes
<i>TOB2P1</i>	Downregulated	0.489579169	0.04286252	0.15384556	No	0.4850618	0.06373721	0.12144826	No
<i>EXPH5</i>	Downregulated	0.186937965	0.02129622	0.09551452	No	-0.0412739	0.7999335	0.85469629	Yes
<i>AGAP11</i>	Downregulated	0.864047275	0.0018514	0.01694835	No	0.37323727	0.00398997	0.01643262	No
<i>ESPL1</i>	Downregulated	0.564588644	0.00243342	0.02069876	No	0.00307416	0.98732178	0.99136094	No
<i>METTL7A</i>	Downregulated	0.385085579	0.0000307	0.00091956	No	0.75299568	3.76E-07	0.0000199	No
<i>IFI44L</i>	Downregulated	0.635962755	0.00012198	0.00247183	No	0.35317499	0.18711316	0.28196908	No
<i>NFIB</i>	Downregulated	0.077379656	0.12130823	0.30434509	No	0.12706723	0.12827867	0.20968965	No
<i>COL8AI</i>	Downregulated	0.268748804	0.10804386	0.28259228	No	1.09134822	0.000015	0.00029754	No
<i>PII6</i>	Downregulated	0.711770709	1.63E-08	0.00000426	No	0.4150814	0.10352372	0.17704645	No

<i>NR5A2</i>	Downregulated	-0.069791397	0.69385965	0.84150021	Yes	0.14330863	0.66227951	0.74453283	No
<i>KIF23</i>	Downregulated	-0.010873932	0.894795	0.95265083	Yes	-0.3050689	0.03635925	0.0786364	Yes
<i>MYO15A</i>	Downregulated	-0.119614971	0.1949478	0.40931426	Yes	-0.4882674	0.00079319	0.00566628	Yes
<i>RFX8</i>	Downregulated	-0.336991798	0.00890359	0.05169486	Yes	-0.6417171	0.00190484	0.01025058	Yes
<i>BLM</i>	Downregulated	0.050244515	0.43532268	0.6565477	No	0.03052953	0.76831195	0.82951863	No
<i>ABI3BP</i>	Downregulated	0.288713357	0.01170397	0.06266128	No	0.65012999	0.00119281	0.00752586	No
<i>RAC2</i>	Downregulated	0.26952303	0.05675885	0.18481685	No	0.62235726	0.00383128	0.01600654	No
<i>LOC729020</i>	Downregulated	#N/A	#N/A	#N/A	#N/A	#N/A	#N/A	#N/A	#N/A
<i>FLJ41484</i>	Downregulated	#N/A	#N/A	#N/A	#N/A	#N/A	#N/A	#N/A	#N/A
<i>COLEC10</i>	Downregulated	-0.42357306	0.00349445	0.02658732	Yes	-0.5636567	0.03721447	0.08001427	Yes
<i>ANGPT1</i>	Downregulated	0.813578885	1.33E-08	0.0000036	No	1.10985855	4.76E-08	0.00000511	No
<i>PRDM6</i>	Downregulated	0.31136898	0.00787266	0.04752649	No	0.4010766	0.0616071	0.11826356	No
<i>PRELID2</i>	Downregulated	0.067155606	0.36778807	0.59570584	No	-0.3313952	0.00294021	0.01350031	Yes
<i>ACSL5</i>	Downregulated	0.308553723	0.00066197	0.00819389	No	0.94731079	0.00000234	0.0000749	No
<i>FRK</i>	Downregulated	0.212916905	0.02280722	0.09996825	No	0.04745613	0.78397364	0.84216693	No
<i>HCG25</i>	Downregulated	#N/A	#N/A	#N/A	#N/A	-0.1515446	0.00546804	0.02011453	Yes
<i>LRRC2</i>	Downregulated	-0.370908864	0.0000526	0.00135501	Yes	-0.8593104	0.0000194	0.00035917	Yes
<i>PARPBP</i>	Downregulated	-0.141118741	0.24213889	0.46623614	Yes	-0.4110141	0.0050625	0.01914371	Yes
<i>ACYI</i>	Downregulated	-0.036667871	0.7264273	0.86101832	Yes	-0.2485199	0.0000547	0.00079297	Yes
<i>GRB7</i>	Downregulated	-0.490017319	0.00343151	0.02623149	Yes	-0.9025985	0.00055396	0.00439378	Yes
<i>AOXI</i>	Downregulated	0.273270371	0.00719292	0.04458601	No	0.5727228	0.00380514	0.01593865	No
<i>FANCD2</i>	Downregulated	-0.010997877	0.90530078	0.95821813	Yes	-0.3260548	0.00505954	0.0191358	Yes
<i>COL12A1</i>	Downregulated	-0.426056555	5.09E-07	0.0000512	Yes	-0.3388025	0.02849707	0.06520634	Yes

<i>MGC23270</i>	Downregulated	#N/A	#N/A	#N/A	#N/A	#N/A	#N/A	#N/A	#N/A
<i>CHEK2</i>	Downregulated	0.292374489	0.00029784	0.00469661	No	0.08172569	0.33274563	0.4412025	No
<i>BMPER</i>	Downregulated	-0.366743485	5.86E-07	0.0000566	Yes	-0.5721475	0.00069195	0.00515777	Yes
<i>ACRC</i>	Downregulated	#N/A	#N/A	#N/A	#N/A	0.08552027	0.59476482	0.6871339	No
<i>PKN3</i>	Downregulated	0.458563883	0.00042168	0.00598738	No	0.59197088	0.0000543	0.00078917	No
<i>CLEC14A</i>	Downregulated	0.229789335	0.04141246	0.15033655	No	0.62907011	0.00032848	0.00299553	No
<i>LOC100128788</i>	Downregulated	#N/A	#N/A	#N/A	#N/A	#N/A	#N/A	#N/A	#N/A
<i>JPH2</i>	Downregulated	0.404560192	0.01673533	0.08074913	No	0.73579975	0.00278382	0.01305423	No
<i>IGFI</i>	Downregulated	-0.341887243	0.00182068	0.01674794	Yes	-1.0951469	0.0000113	0.00023956	Yes
<i>IGFBP3</i>	Downregulated	0.07932602	0.52638106	0.72735526	No	0.17348572	0.390947	0.49983	No
<i>MBOAT1</i>	Downregulated	0.580790458	0.0000826	0.00187818	No	0.22462506	0.29859251	0.40555222	No
<i>EFCAB5</i>	Downregulated	-0.067428958	0.35421353	0.58274036	Yes	-0.3350828	0.00034404	0.00310093	Yes
<i>FAM160A1</i>	Downregulated	-0.124950025	0.10709558	0.28113332	Yes	-0.4598102	0.02475754	0.05861574	Yes
<i>KLHL30</i>	Downregulated	0.307810715	0.13131319	0.31962167	No	0.06010002	0.80926669	0.86211689	No
<i>ARHGAP9</i>	Downregulated	0.136360568	0.1053994	0.27836119	No	0.21013096	0.0496282	0.10000252	No
<i>ANPEP</i>	Downregulated	0.543337335	0.00151542	0.01470249	No	0.61274097	0.00211331	0.01095933	No
<i>DENND2C</i>	Downregulated	0.101975076	0.16643883	0.3706301	No	-0.2001439	0.04732846	0.09644646	Yes
<i>TRPC4</i>	Downregulated	-0.039593746	0.588744	0.77055203	Yes	0.36662711	0.02508863	0.05918517	No
<i>FLJ31813</i>	Downregulated	#N/A	#N/A	#N/A	#N/A	#N/A	#N/A	#N/A	#N/A
<i>LOC100129845</i>	Downregulated	#N/A	#N/A	#N/A	#N/A	#N/A	#N/A	#N/A	#N/A
<i>LINC00312</i>	Downregulated	#N/A	#N/A	#N/A	#N/A	-0.2163074	0.15522755	0.24351602	Yes
<i>RAD51</i>	Downregulated	0.043328661	0.66929977	0.82516172	No	-0.0180428	0.84450348	0.88934057	Yes
<i>PABPC4L</i>	Downregulated	0.548264576	0.00011168	0.00232521	No	0.83493972	0.00021102	0.00215958	No

<i>CNTD2</i>	Downregulated	-0.138167163	0.4037768	0.62879306	Yes	-0.2504342	0.14449673	0.23026464	Yes
<i>MARK2P9</i>	Downregulated	-0.186295393	0.34438406	0.57383233	Yes	0.09979547	0.72164853	0.79270727	No
<i>HERC2P3</i>	Downregulated	0.306506634	0.03550449	0.13577204	No	1.29436192	0.00000284	0.000086	No
<i>CYP2A6</i>	Downregulated	-0.087854716	0.39744574	0.62285042	Yes	0.1535068	0.34692272	0.45571971	No
<i>STARD13</i>	Downregulated	-0.072777674	0.08850343	0.24799255	Yes	0.19044641	0.02345898	0.05621122	No
<i>GHRLOS</i>	Downregulated	-0.056894894	0.59028096	0.77176353	Yes	-0.0335528	0.83620661	0.88288774	Yes
<i>GSG1</i>	Downregulated	-0.17981454	0.04100725	0.14935124	Yes	-0.9371047	1.62E-08	0.00000245	Yes
<i>SLC26A4</i>	Downregulated	-0.365777142	0.00017968	0.00326343	Yes	-0.5694823	0.00119418	0.00753162	Yes
<i>SHCBP1</i>	Downregulated	-0.098924572	0.42728364	0.64967243	Yes	-0.4333351	0.00166204	0.00939938	Yes
<i>CXorf69</i>	Downregulated	#N/A	#N/A	#N/A	#N/A	#N/A	#N/A	#N/A	#N/A
<i>COL7A1</i>	Downregulated	0.166070805	0.02431214	0.10433586	No	0.15642997	0.2522435	0.35596994	No
<i>MYLK3</i>	Downregulated	0.559444393	0.01177504	0.06291608	No	-0.5416361	0.02288894	0.055163	Yes
<i>LOC731275</i>	Downregulated	#N/A	#N/A	#N/A	#N/A	#N/A	#N/A	#N/A	#N/A
<i>CI9orf40</i>	Downregulated	#N/A	#N/A	#N/A	#N/A	-0.2164986	0.10481713	0.1787923	Yes
<i>ALS2CL</i>	Downregulated	-0.208243703	0.0163102	0.07937394	Yes	-0.0847548	0.49569155	0.59820736	Yes
<i>ENTPD3-AS1</i>	Downregulated	0.096112061	0.07136178	0.21516983	No	-0.0399489	0.61868087	0.70731272	Yes
<i>CLCNKB</i>	Downregulated	0.050879152	0.7841521	0.89419593	No	0.18239129	0.40847373	0.51681178	No
<i>FAM53A</i>	Downregulated	0.161296194	0.08901321	0.24885145	No	-0.1922846	0.23514231	0.33693801	Yes
<i>LOC100133315</i>	Downregulated	#N/A	#N/A	#N/A	#N/A	#N/A	#N/A	#N/A	#N/A
<i>SLC35F2</i>	Downregulated	0.216627834	0.00137622	0.01374557	No	-0.022142	0.79618332	0.85164503	Yes
<i>CLDN2</i>	Downregulated	0.050747553	0.722733	0.85887057	No	0.01830688	0.93817083	0.95687727	No
<i>TNFAIP8</i>	Downregulated	0.466064102	0.0000953	0.00208039	No	0.31077337	0.09407953	0.16427089	No
<i>FLJ32224</i>	Downregulated	#N/A	#N/A	#N/A	#N/A	#N/A	#N/A	#N/A	#N/A

<i>VTCN1</i>	Downregulated	-0.039679593	0.86763035	0.93906072	Yes	-0.4921044	0.03106122	0.06969214	Yes
<i>LYN</i>	Downregulated	0.401002571	0.00000814	0.0003625	No	0.54309639	0.00277367	0.01302194	No
<i>TSHZ2</i>	Downregulated	-0.110831824	0.16629228	0.37037911	Yes	-0.4009632	0.01413423	0.0385771	Yes
<i>TM6SF2</i>	Downregulated	-0.271785273	0.15461781	0.3548627	Yes	-0.4032964	0.00130784	0.0080114	Yes
<i>ETS1</i>	Downregulated	0.262183571	0.00118522	0.01235093	No	0.66704591	0.00000138	0.0000509	No
<i>LOC100101266</i>	Downregulated	#N/A	#N/A	#N/A	#N/A	#N/A	#N/A	#N/A	#N/A
<i>ZNF90</i>	Downregulated	0.089392939	0.3453455	0.57465224	No	-0.2816599	0.01008363	0.03033467	Yes
<i>NME9</i>	Downregulated	-0.129783577	0.00427938	0.03065096	Yes	-0.3600219	0.00000201	0.0000674	Yes
<i>UNC13D</i>	Downregulated	0.422641361	0.0000146	0.00054514	No	0.07069244	0.63258448	0.71923123	No
<i>ANKRD18B</i>	Downregulated	-0.150519202	0.16683137	0.37111228	Yes	-0.6010988	0.00036196	0.00322282	Yes
<i>EBLN2</i>	Downregulated	0.154952423	0.12288553	0.30674103	No	0.71585532	0.0000405	0.00063082	No
<i>TP53TG5</i>	Downregulated	0.040584491	0.49424934	0.70335634	No	-0.1498552	0.44994474	0.55605814	Yes
<i>DAPK2</i>	Downregulated	0.087722021	0.2762465	0.5049198	No	-0.4065328	0.00409842	0.01671752	Yes
<i>HELB</i>	Downregulated	0.169064294	0.06766727	0.20783713	No	0.83758198	0.0000079	0.00018212	No
<i>ORC1</i>	Downregulated	0.070151672	0.55100044	0.74512474	No	-0.1547626	0.35368005	0.46266682	Yes
<i>SEPT7L</i>	Downregulated	#N/A	#N/A	#N/A	#N/A	#N/A	#N/A	#N/A	#N/A
<i>DLEU2</i>	Downregulated	0.046979455	0.51934133	0.72175323	No	-0.1437891	0.23655906	0.338507	Yes
<i>PPP1R13L</i>	Downregulated	0.648254682	1.79E-07	0.0000239	No	0.34218405	0.01129987	0.03282479	No
<i>NUDT13</i>	Downregulated	-0.019443676	0.78139852	0.89263924	Yes	0.07331666	0.40462935	0.51327556	No
<i>MMP12</i>	Downregulated	0.226268555	0.60325057	NA	No	-0.2470884	0.19233488	0.28818187	Yes
<i>NOS3</i>	Downregulated	0.584979467	0.00027786	0.00447243	No	0.71044993	0.0000878	0.00112322	No
<i>CEP128</i>	Downregulated	0.130623003	0.00837742	0.04953369	No	-0.0455905	0.70601634	0.78000766	Yes
<i>BCL2L15</i>	Downregulated	-0.216235236	0.02823164	0.11592595	Yes	-0.3313353	0.01162118	0.03351083	Yes

<i>RPS10P7</i>	Downregulated	0.295860478	0.0011708	0.01225657	No	0.29141734	0.05947222	0.11515256	No
<i>LOC100506068</i>	Downregulated	#N/A	#N/A	#N/A	#N/A	#N/A	#N/A	#N/A	#N/A
<i>GYPCK</i>	Downregulated	0.636840646	5E-11	7.91E-08	No	0.38437616	0.0112253	0.03266927	No
<i>AGMAT</i>	Downregulated	-0.147012196	0.04856779	0.16687866	Yes	-0.6903174	0.0000154	0.00030276	Yes
<i>CCRL1</i>	Downregulated	#N/A	#N/A	#N/A	#N/A	#N/A	#N/A	#N/A	#N/A
<i>TDRD6</i>	Downregulated	-0.111195481	0.10598714	0.27926923	Yes	-0.1289657	0.22953395	0.33081463	Yes
<i>SLC19A3</i>	Downregulated	0.299143906	0.00089872	0.010173	No	0.43688015	0.0054888	0.02017226	No
<i>WDR65</i>	Downregulated	-0.107595603	0.38300654	0.61003946	Yes	-0.3916993	0.0000703	0.00095187	Yes
<i>MYOM3</i>	Downregulated	0.727324554	0.01087747	0.05961713	No	0.43174182	0.1789031	0.27218929	No
<i>SLC17A9</i>	Downregulated	0.377195235	0.00240604	0.02053027	No	0.54820304	0.00019	0.00199461	No
<i>DHRS3</i>	Downregulated	0.295921536	0.00019628	0.00347133	No	0.46312062	0.00040599	0.00350731	No
<i>MATN1</i>	Downregulated	0.044876891	0.75140749	0.87553863	No	-0.1019114	0.58535371	0.67870696	Yes
<i>BTN3A2</i>	Downregulated	0.433080061	0.0000617	0.00152456	No	0.26371309	0.08164666	0.1469429	No
<i>TBX2</i>	Downregulated	0.576244128	0.0000374	0.00105186	No	0.48931831	0.00122721	0.00766316	No
<i>CD37</i>	Downregulated	0.489636458	1.33E-07	0.0000192	No	0.39612239	0.00919466	0.02843988	No
<i>PCDHGB3</i>	Downregulated	0.063534403	0.38188619	0.60904733	No	0.28363324	0.00034328	0.00309556	No
<i>MKI67</i>	Downregulated	0.772663199	0.00855287	0.05022679	No	-0.3361862	0.23890724	0.34113173	Yes
<i>FAIM3</i>	Downregulated	0.560660962	0.01875323	0.08754736	No	0.27217218	0.27590103	0.38152809	No
<i>LOC100128881</i>	Downregulated	#N/A	#N/A	#N/A	#N/A	#N/A	#N/A	#N/A	#N/A
<i>DNAH12</i>	Downregulated	0.341771063	0.00786908	0.04751244	No	-0.1342593	0.47818962	0.58212573	Yes
<i>SYPL2</i>	Downregulated	0.147439329	0.2091435	0.42714396	No	0.54465357	0.00211774	0.01097671	No
<i>HLA-DPA1</i>	Downregulated	#N/A	#N/A	#N/A	#N/A	0.67624782	0.00621029	0.02189405	No
<i>ABCA10</i>	Downregulated	-0.280749122	0.0012907	0.01315443	Yes	-0.4813228	0.00002	0.00036825	Yes

<i>MSH5-SAPCD1</i>	Downregulated	#N/A	#N/A	#N/A	#N/A	-0.4169418	0.0000413	0.00063954	Yes
<i>PCOLCE2</i>	Downregulated	0.114704699	0.32688757	0.55701493	No	0.29679808	0.09103805	0.16004798	No
<i>SNORA48</i>	Downregulated	NA	NA	NA	#N/A	0.79333057	0.0000593	0.00084341	No
<i>EFCAB6</i>	Downregulated	-0.092362833	0.04814859	0.16583074	Yes	-0.4553084	0.0000285	0.00048186	Yes
<i>SYNPO2</i>	Downregulated	0.038515185	0.56495988	0.75491084	No	-0.0327629	0.74217363	0.80883159	Yes
<i>PRO0611</i>	Downregulated	#N/A	#N/A	#N/A	#N/A	#N/A	#N/A	#N/A	#N/A
<i>MPP4</i>	Downregulated	-0.240247782	0.01438829	0.07261605	Yes	-0.4209466	0.00692094	0.02353096	Yes
<i>MELK</i>	Downregulated	0.704176886	0.00715539	0.04441138	No	-0.0852369	0.75913227	0.82242648	Yes
<i>CASS4</i>	Downregulated	0.278568054	0.01696439	0.08163155	No	0.62566391	0.00286929	0.01330294	No
<i>C3orf35</i>	Downregulated	-0.159073422	0.05135363	0.17261302	Yes	-0.2065849	0.16892076	0.26005557	Yes
<i>ITIH2</i>	Downregulated	0.267632537	0.02486696	0.10602119	No	0.5002047	0.01207242	0.03446366	No
<i>SLC2A9</i>	Downregulated	0.378856379	1.26E-07	0.0000186	No	0.44131472	0.00309033	0.01393596	No
<i>LOC641298</i>	Downregulated	#N/A	#N/A	#N/A	#N/A	#N/A	#N/A	#N/A	#N/A
<i>KCNAB3</i>	Downregulated	-0.179677391	0.05191176	0.17389753	Yes	-0.5904215	0.00040799	0.00351754	Yes
<i>INPP4B</i>	Downregulated	-0.052178797	0.3165664	0.54698217	Yes	-0.1182981	0.22734107	0.32818011	Yes
<i>SYT15</i>	Downregulated	-0.161702289	0.11005279	0.28628812	Yes	-0.1030697	0.32319711	0.43138338	Yes
<i>ITGB3</i>	Downregulated	0.185753531	0.16369104	0.36696572	No	0.59597938	0.00052132	0.00420647	No
<i>CCDC33</i>	Downregulated	0.477484604	0.07711777	0.2261573	No	-0.3382672	0.21360926	0.31298446	Yes
<i>ENPP3</i>	Downregulated	-0.086556043	0.30960644	0.54006816	Yes	-0.2993887	0.0132712	0.03691254	Yes
<i>PVRL4</i>	Downregulated	-0.496166947	0.16226278	NA	Yes	-0.4499596	0.05886646	0.11421764	Yes
<i>NOXRED1</i>	Downregulated	0.077452902	0.29658826	0.52638349	No	-0.0376261	0.74558259	0.81174086	Yes
<i>SIX1</i>	Downregulated	0.821725449	0.00060391	0.00770961	No	0.97177496	0.00399969	0.01645561	No
<i>LOC100268168</i>	Downregulated	#N/A	#N/A	#N/A	#N/A	#N/A	#N/A	#N/A	#N/A

<i>LOC389641</i>	Downregulated	#N/A	#N/A	#N/A	#N/A	#N/A	#N/A	#N/A	#N/A
<i>COL4A3</i>	Downregulated	0.001492851	0.98637232	0.99459722	No	0.61293923	0.00044441	0.00375148	No
<i>SLC7A5P2</i>	Downregulated	NA	NA	NA	#N/A	0.45014331	0.00092916	0.00632326	No
<i>SHOX2</i>	Downregulated	1.051705233	0.00797641	0.04789379	No	-0.3143182	0.21683387	0.31665242	Yes
<i>MSLN</i>	Downregulated	0.058258217	0.6933933	0.84106901	No	-0.3642396	0.15710387	0.24575606	Yes
<i>FOXH1</i>	Downregulated	-0.147843427	0.5090624	0.714057	Yes	-0.1891229	0.07811841	0.14220412	Yes
<i>C1orf38</i>	Downregulated	#N/A	#N/A	#N/A	#N/A	#N/A	#N/A	#N/A	#N/A
<i>ADAP2</i>	Downregulated	0.327608649	0.00014828	0.00285104	No	0.12856467	0.33179095	0.44015647	No
<i>EMP2</i>	Downregulated	0.487815798	0.00000169	0.00012052	No	0.51067003	0.00142493	0.00849988	No
<i>BMP3</i>	Downregulated	-0.326703282	0.00586082	0.03832708	Yes	-0.7628843	0.00101024	0.00672168	Yes
<i>DUOXA1</i>	Downregulated	0.105365111	0.13879676	0.33097483	No	-0.16417	0.193729	0.28978856	Yes
<i>MYBL2</i>	Downregulated	0.839603575	0.01428494	0.07219314	No	-0.3881085	0.19726178	0.29399182	Yes
<i>FERMT3</i>	Downregulated	0.425805198	0.0001062	0.00224857	No	0.42995009	0.00520852	0.01950082	No
<i>RANBP3L</i>	Downregulated	0.348576685	0.0000968	0.00210622	No	1.30136989	1.42E-08	0.00000227	No
<i>USP18</i>	Downregulated	0.131264416	0.17924935	0.38829004	No	0.15812768	0.09039374	0.15916606	No
<i>LRRC8E</i>	Downregulated	-0.136029462	0.70907934	NA	Yes	-0.2034865	0.31034677	0.41800793	Yes
<i>FOXM1</i>	Downregulated	0.275488032	0.00745506	0.04572552	No	-0.0714629	0.50463745	0.60645686	Yes
<i>KANK4</i>	Downregulated	0.251694246	0.05004534	0.1701685	No	0.17285231	0.44211038	0.54888235	No
<i>ZNF587B</i>	Downregulated	-0.005795234	0.93949943	0.97448104	Yes	-0.1413091	0.12599929	0.206703	Yes
<i>RGPD3</i>	Downregulated	-0.037061708	0.81868958	0.91384461	Yes	0.31770823	0.05426869	0.10714228	No
<i>PTH1R</i>	Downregulated	0.40631721	0.00038445	0.0056121	No	0.39323703	0.00545164	0.02007011	No
<i>SLC28A3</i>	Downregulated	0.135677417	0.51393882	0.7178648	No	0.14031535	0.59906434	0.69074016	No
<i>MTM1I</i>	Downregulated	0.258118496	0.00015527	0.00294812	No	0.38467603	0.00037407	0.00329906	No

<i>ANKRD19P</i>	Downregulated	-0.273231287	0.00449506	0.03179972	Yes	-0.2943972	0.05804222	0.11291308	Yes
<i>WFIKKN1</i>	Downregulated	0.128453185	0.32812401	0.5581212	No	-0.0443509	0.77033221	0.83126522	Yes
<i>LOC729799</i>	Downregulated	#N/A	#N/A	#N/A	#N/A	#N/A	#N/A	#N/A	#N/A
<i>CDH15</i>	Downregulated	0.065038439	0.82551184	0.9168739	No	-0.6684972	0.03085305	0.0693255	Yes
<i>ADAM12</i>	Downregulated	0.268422465	0.00076616	0.00904187	No	0.84924591	2.57E-07	0.0000153	No
<i>CCDC88B</i>	Downregulated	0.303485944	0.00224333	0.01949904	No	-0.0133338	0.90932431	0.93617236	Yes
<i>HR</i>	Downregulated	0.015882296	0.86366571	0.93717496	No	-0.4208683	0.0000403	0.00062798	Yes
<i>FAM194A</i>	Downregulated	-0.156563878	0.17725388	0.38544138	Yes	-0.446269	0.00536347	0.01987013	Yes
<i>NPEPL1</i>	Downregulated	0.124312118	0.12308471	0.30708704	No	0.04465848	0.67452632	0.75435031	No
<i>ATP8B4</i>	Downregulated	0.152408537	0.06225287	0.19653513	No	-0.093771	0.53602156	0.63484118	Yes
<i>RNF125</i>	Downregulated	0.316569621	0.00042334	0.0060042	No	-0.02442	0.89946743	0.9292158	Yes
<i>CASQ1</i>	Downregulated	-0.34123449	0.00064594	0.00807268	Yes	-0.5978553	0.00061308	0.00473117	Yes
<i>FAM65C</i>	Downregulated	#N/A	#N/A	#N/A	#N/A	0.73024089	0.00022906	0.00229411	No
<i>CLSPN</i>	Downregulated	-0.400963308	0.00000554	0.00141284	Yes	-0.6005544	0.00621226	0.02189724	Yes
<i>DMC1</i>	Downregulated	0.065104313	0.55637545	0.74884478	No	-0.259804	0.0945241	0.16486128	Yes
<i>POLN</i>	Downregulated	-0.046355298	0.43365828	0.65503711	Yes	0.05803277	0.5176141	0.61835987	No
<i>C8orf73</i>	Downregulated	#N/A	#N/A	#N/A	#N/A	#N/A	#N/A	#N/A	#N/A
<i>IL17RA</i>	Downregulated	0.28084079	0.00033967	0.00513006	No	0.31475511	0.00157222	0.00906363	No
<i>NEB</i>	Downregulated	0.121114751	0.16450196	0.36806213	No	0.04396244	0.71556768	0.78796816	No
<i>CASP8</i>	Downregulated	0.103340561	0.11024716	0.28649793	No	0.0751072	0.48385934	0.58719444	No
<i>C2</i>	Downregulated	#N/A	#N/A	#N/A	#N/A	0.16048632	0.25838	0.36259433	No
<i>SOX6</i>	Downregulated	0.125726648	0.01073807	0.05914274	No	0.18641641	0.06813058	0.12792782	No
<i>RBL1</i>	Downregulated	0.175351835	0.00059502	0.00762699	No	0.40956481	0.0302825	0.06833263	No

<i>SECTM1</i>	Downregulated	0.775217907	0.00075337	0.00893821	No	0.3997135	0.15761129	0.24640465	No
<i>RRN3P2</i>	Downregulated	0.209806145	0.02097822	0.09455022	No	0.10099818	0.25731981	0.36141581	No
<i>FOXP3</i>	Downregulated	0.137267316	0.324171	0.55441537	No	-0.2879417	0.00012018	0.0014227	Yes
<i>GINS4</i>	Downregulated	0.28506035	0.00383393	0.02833198	No	0.05720154	0.73813256	0.80584518	No
<i>CNTD1</i>	Downregulated	0.059637953	0.41974605	0.6428955	No	-0.2794608	2.29E-08	0.00000312	Yes
<i>LINC00471</i>	Downregulated	0.065695322	0.4936506	0.70275004	No	-0.5194196	0.00095847	0.00647138	Yes
<i>ZNF69</i>	Downregulated	0.12171204	0.08957582	0.24967031	No	0.22973387	0.0856032	0.15250805	No
<i>C22orf43</i>	Downregulated	#N/A	#N/A	#N/A	#N/A	-0.1644607	0.3560488	0.46520884	Yes
<i>CD4</i>	Downregulated	0.354060454	0.000012	0.00047327	No	0.27508899	0.10303593	0.17643182	No
<i>LOC100287036</i>	Downregulated	#N/A	#N/A	#N/A	#N/A	#N/A	#N/A	#N/A	#N/A
<i>IFI16</i>	Downregulated	0.348930115	0.00071205	0.00858214	No	0.71878821	0.00000812	0.00018546	No
<i>ARHGAP10</i>	Downregulated	0.172129351	0.00300207	0.02393344	No	-0.0578203	0.61733906	0.70621795	Yes
<i>TBC1D3P1-DHX40P1</i>	Downregulated	0.062151996	0.98154124	NA	No	0.25799725	0.00290103	0.01339766	No
<i>MYBPHL</i>	Downregulated	-0.126458862	0.19905655	0.41413305	Yes	-0.0790547	0.62950492	0.7167747	Yes
<i>ECT2L</i>	Downregulated	-0.01430191	0.86537636	0.93795854	Yes	-0.317914	0.00666574	0.02294165	Yes
<i>FGF1</i>	Downregulated	0.482027151	0.00000135	0.00010276	No	0.15412426	0.32280788	0.43096704	No
<i>3-Mar</i>	Downregulated	#N/A	#N/A	#N/A	#N/A	#N/A	#N/A	#N/A	#N/A
<i>PPARG</i>	Downregulated	0.08882323	0.16681695	0.37110196	No	-0.3034448	0.00606784	0.02156802	Yes
<i>NLRP1</i>	Downregulated	-0.073235562	0.28270562	0.5119428	Yes	-0.468485	0.0000259	0.00044984	Yes
<i>LOC284454</i>	Downregulated	#N/A	#N/A	#N/A	#N/A	#N/A	#N/A	#N/A	#N/A
<i>ALDH3B1</i>	Downregulated	0.324981488	0.0000573	0.00144816	No	-0.0073578	0.94946707	0.96522055	Yes
<i>KL</i>	Downregulated	-0.08735626	0.43424804	0.65556064	Yes	-0.0469274	0.72337464	0.79409948	Yes
<i>SUSD2</i>	Downregulated	0.377674598	0.01640525	0.07965649	No	0.21929886	0.29914498	0.40618385	No

<i>IRF7</i>	Downregulated	0.455836318	0.0000109	0.00044146	No	0.65147328	0.0000257	0.0004464	No
<i>MXRA5</i>	Downregulated	0.15439467	0.28323112	0.51255205	No	0.3798021	0.08401688	0.15023878	No
<i>KCNJ2</i>	Downregulated	0.372893192	0.0000213	0.00070748	No	0.33446293	0.09055791	0.15939976	No
<i>LOC100130093</i>	Downregulated	#N/A	#N/A	#N/A	#N/A	#N/A	#N/A	#N/A	#N/A
<i>PGM5P2</i>	Downregulated	0.008136071	0.91514384	0.96321047	No	0.15079638	0.27622264	0.38186679	No
<i>TMOD4</i>	Downregulated	NA	NA	NA	#N/A	0.32736703	0.02903124	0.06613149	No
<i>PKDREJ</i>	Downregulated	0.214896078	0.13127594	0.31957199	No	0.24468896	0.31735036	0.42547796	No
<i>DKFZP564C196</i>	Downregulated	#N/A	#N/A	#N/A	#N/A	#N/A	#N/A	#N/A	#N/A
<i>HLA-DMA</i>	Downregulated	#N/A	#N/A	#N/A	#N/A	0.28621011	0.05489072	0.10807567	No
<i>LRRK70</i>	Downregulated	0.030655125	0.79494696	0.90080065	No	0.39958468	0.01305965	0.03649529	No
<i>TMPRSS9</i>	Downregulated	0.026125794	0.81055404	0.90965969	No	-0.6548843	1.44E-07	0.0000105	Yes
<i>MICALCL</i>	Downregulated	0.044083916	0.79883151	0.90336842	No	-0.221236	0.23395244	0.33560389	Yes
<i>DEPDC1</i>	Downregulated	-0.124614918	0.27811683	0.50715169	Yes	-0.8426	0.0000162	0.00031542	Yes
<i>COL15A1</i>	Downregulated	0.382672533	0.00259527	0.02162454	No	0.40931731	0.03234878	0.0718982	No
<i>MUC5B</i>	Downregulated	0.189010827	0.25445686	0.48105478	No	0.00931995	0.96969668	0.97944618	No
<i>FAM18B2</i>	Downregulated	#N/A	#N/A	#N/A	#N/A	#N/A	#N/A	#N/A	#N/A
<i>WDR76</i>	Downregulated	0.273214706	0.00012389	0.00249586	No	0.10329097	0.30189488	0.40916472	No
<i>ITGA5</i>	Downregulated	0.433714586	0.00015488	0.00294501	No	1.08198323	5.41E-08	0.00000549	No
<i>IRFI</i>	Downregulated	0.592340203	1.71E-07	0.0000234	No	0.45428182	0.00539366	0.01994223	No
<i>DGKH</i>	Downregulated	-0.171338598	0.00183602	0.01683198	Yes	-0.3233259	0.00052658	0.00423911	Yes
<i>NUDT4</i>	Downregulated	-0.106708144	0.04243896	0.15283232	Yes	-0.0836335	0.41882334	0.52675675	Yes
<i>GBP1</i>	Downregulated	0.939389988	3.25E-09	0.0000014	No	0.86957664	0.0001125	0.00135417	No
<i>SLC28A2</i>	Downregulated	-0.077904548	0.67021706	0.82570443	Yes	-0.2767312	0.16133544	0.25083428	Yes

<i>TNFRSF10A</i>	Downregulated	0.389483063	0.00474175	0.03310065	No	1.1077883	5.06E-07	0.0000244	No
<i>BMP6</i>	Downregulated	0.351899915	0.00783076	0.04731869	No	1.14967971	0.00000781	0.00018063	No
<i>HLA-L</i>	Downregulated	#N/A	#N/A	#N/A	#N/A	-0.0898326	0.22647038	0.32719431	Yes
<i>CSGALNACTI</i>	Downregulated	0.085194169	0.04775217	0.1649573	No	0.3150539	0.00317365	0.01414446	No
<i>ESCO2</i>	Downregulated	0.118561465	0.28173764	0.51101889	No	-0.7125855	0.00018387	0.00195089	Yes
<i>HEATR4</i>	Downregulated	0.02659937	0.63466516	0.8010669	No	-0.1508987	0.056748	0.11094504	Yes
<i>LOC729177</i>	Downregulated	#N/A	#N/A	#N/A	#N/A	#N/A	#N/A	#N/A	#N/A
<i>KIF15</i>	Downregulated	0.054858417	0.40310401	0.62820931	No	-0.0213855	0.817423	0.8683669	Yes
<i>DNAH17</i>	Downregulated	0.315401933	0.00300974	0.023968	No	-0.1281589	0.44900327	0.55518997	Yes
<i>APOL6</i>	Downregulated	0.538399454	0.00000112	0.0000911	No	0.81002459	0.000037	0.00058891	No
<i>LOC387723</i>	Downregulated	#N/A	#N/A	#N/A	#N/A	#N/A	#N/A	#N/A	#N/A
<i>FAM54A</i>	Downregulated	#N/A	#N/A	#N/A	#N/A	#N/A	#N/A	#N/A	#N/A
<i>LOC100129858</i>	Downregulated	#N/A	#N/A	#N/A	#N/A	#N/A	#N/A	#N/A	#N/A
<i>CHRNA10</i>	Downregulated	-0.123840042	0.31058549	0.54103	Yes	-0.158077	0.41304073	0.52130065	Yes
<i>EMX2</i>	Downregulated	0.411941141	0.02305081	0.10066394	No	0.79038801	0.0000146	0.00029194	No
<i>LRRK2</i>	Downregulated	-0.112319429	0.08745497	0.2459262	Yes	0.13188526	0.22076257	0.32091037	No
<i>PCDHB19P</i>	Downregulated	-0.145422246	0.05798182	0.18724393	Yes	0.42195841	0.00594744	0.02127628	No
<i>LINC00173</i>	Downregulated	0.196136696	0.03542656	0.13556963	No	-0.217778	0.15394506	0.24189999	Yes
<i>RELL1</i>	Downregulated	0.520003439	2.86E-08	0.00000639	No	1.48743223	1.31E-10	1.33E-07	No
<i>ASB3</i>	Downregulated	-0.028840076	0.53900712	0.73656931	Yes	0.37751628	2.89E-07	0.0000165	No
<i>GALNTL2</i>	Downregulated	#N/A	#N/A	#N/A	#N/A	#N/A	#N/A	#N/A	#N/A
<i>AGPAT9</i>	Downregulated	0.000115045	0.99915373	0.99968051	No	-0.5471479	0.00258286	0.012435	Yes
<i>WDR62</i>	Downregulated	0.115383703	0.2348258	0.45761853	No	-0.1053822	0.4121372	0.52034876	Yes

<i>GRAMD2</i>	Downregulated	#N/A	#N/A	#N/A	#N/A	-0.0040292	0.97729284	0.98497749	Yes
<i>OTOG</i>	Downregulated	-0.580165101	0.00000038	0.0000413	Yes	-0.5858493	0.00219045	0.01122168	Yes
<i>ANGPTL4</i>	Downregulated	0.245538496	0.15873988	0.36024955	No	1.22817476	0.00000634	0.00015518	No
<i>LCNL1</i>	Downregulated	0.290807465	0.01072671	0.05911448	No	0.47618656	0.01040342	0.03099606	No
<i>SNORD116-20</i>	Downregulated	NA	NA	NA	#N/A	0.55873804	0.00178452	0.00984152	No
<i>BUB1</i>	Downregulated	0.243430555	0.08831857	0.24762082	No	-0.3102743	0.14679484	0.23322865	Yes
<i>DKK1</i>	Downregulated	-0.140465983	0.29475551	0.524283	Yes	-0.4141237	0.00720049	0.02414425	Yes
<i>DPF3</i>	Downregulated	0.185130169	0.00561691	0.03726999	No	0.03381098	0.71232586	0.78540612	No
<i>RGS5</i>	Downregulated	0.196810544	0.04114975	0.14976962	No	0.36699698	0.0258652	0.06058394	No
<i>EBF2</i>	Downregulated	-0.176483979	0.3581613	0.58653739	Yes	-0.4066835	0.05010366	0.10076032	Yes
<i>CENPF</i>	Downregulated	-0.232562675	0.01385376	0.07064432	Yes	-0.5734957	0.00915908	0.02838336	Yes
<i>PHACTR3</i>	Downregulated	0.110815146	0.0615646	0.19515081	No	0.01113283	0.88691937	0.92025972	No
<i>ITIH4</i>	Downregulated	-0.016558941	0.89834904	0.95477415	Yes	-0.1597859	0.20119	0.29846609	Yes
<i>RHBDL2</i>	Downregulated	0.084995521	0.11048731	0.28681256	No	-0.126611	0.43080774	0.5381787	Yes
<i>HSF4</i>	Downregulated	-0.01154986	0.8597907	0.93532757	Yes	0.13271158	0.20973064	0.30846754	No
<i>C21orf49</i>	Downregulated	#N/A	#N/A	#N/A	#N/A	-0.0095283	0.94640963	0.96291999	Yes
<i>GTSE1</i>	Downregulated	0.430201182	0.00955126	0.05445523	No	-0.3534848	0.07925388	0.14382993	Yes
<i>KIAA1656</i>	Downregulated	#N/A	#N/A	#N/A	#N/A	#N/A	#N/A	#N/A	#N/A
<i>PRIMA1</i>	Downregulated	#N/A	#N/A	#N/A	#N/A	0.36051708	0.13029955	0.21231462	No
<i>SLC25A34</i>	Downregulated	0.084437555	0.32249518	0.55276982	No	0.07341905	0.50435294	0.60618027	No
<i>COL4A4</i>	Downregulated	0.077727694	0.33867065	0.56886042	No	0.6157636	0.00015836	0.00174871	No
<i>C6orf163</i>	Downregulated	-0.157040556	0.04983527	0.16968224	Yes	-0.0069783	0.95514118	0.96892185	Yes
<i>MCM9</i>	Downregulated	0.124200762	0.00314844	0.02471985	No	0.11102608	0.08816169	0.15611341	No

<i>TOMM20L</i>	Downregulated	0.051536369	0.68396993	0.83486829	No	-0.5261113	7.65E-10	3.91E-07	Yes
<i>ZNF490</i>	Downregulated	-0.061388592	0.18156752	0.39141278	Yes	0.02871253	0.65918444	0.74204082	No
<i>CACNA2D3</i>	Downregulated	-0.329683401	0.00000132	0.00010119	Yes	-0.4385997	0.00749673	0.02481109	Yes
<i>IMPA2</i>	Downregulated	0.23318238	0.00168323	0.01585639	No	0.47104378	0.00036473	0.00323976	No
<i>RPL19P12</i>	Downregulated	0.006239357	0.95463539	0.9817448	No	-0.3271435	0.00564731	0.02055442	Yes
<i>LMOD1</i>	Downregulated	0.38234129	0.00283249	0.02295141	No	0.33334813	0.06149514	0.11809923	No
<i>CCDC163P</i>	Downregulated	#N/A	#N/A	#N/A	#N/A	0.26743572	0.13260954	0.21534228	No
<i>PHEX</i>	Downregulated	0.365761732	0.0000105	0.00043084	No	0.43191931	0.0178325	0.04582518	No
<i>KLRG1</i>	Downregulated	0.046430166	0.51561536	0.71931432	No	-0.0657242	0.62959622	0.71681301	Yes
<i>KIAA1462</i>	Downregulated	-0.08737416	0.30552206	0.53557731	Yes	0.25241708	0.05445912	0.10745355	No
<i>ERBB3</i>	Downregulated	0.283495687	0.00467265	0.03270249	No	0.10528185	0.63512907	0.72137413	No
<i>NFATC1</i>	Downregulated	0.555632804	5.13E-08	0.00000984	No	0.18468642	0.13810807	0.22232225	No
<i>MLN</i>	Downregulated	0.145844942	0.51706757	0.72012266	No	0.04015723	0.88516171	0.91907758	No
<i>OXT</i>	Downregulated	-0.373861408	0.4429653	0.6630212	Yes	-0.4140732	0.13566738	0.21920338	Yes
<i>TAGAP</i>	Downregulated	-0.03335149	0.56539867	0.75513878	Yes	-0.0530247	0.65908678	0.74201354	Yes
<i>LY6G5C</i>	Downregulated	#N/A	#N/A	#N/A	#N/A	0.00964792	0.91860399	0.94300967	No
<i>GP1BA</i>	Downregulated	0.184771842	0.04188284	0.15146462	No	-0.0047399	0.96588333	0.97660325	Yes
<i>SYCP2</i>	Downregulated	0.03010014	0.70634016	0.84941419	No	0.07143665	0.33299409	0.44147191	No
<i>C15orf42</i>	Downregulated	#N/A	#N/A	#N/A	#N/A	#N/A	#N/A	#N/A	#N/A
<i>ZNF469</i>	Downregulated	0.237432438	0.06010195	0.19181882	No	0.15018682	0.27905434	0.38495111	No
<i>C3orf49</i>	Downregulated	-0.184992925	0.0027127	0.0222695	Yes	-0.3376557	0.01902557	0.04808658	Yes
<i>CCDC7</i>	Downregulated	0.084657609	0.28234206	0.51167505	No	-0.1315434	0.10714064	0.18192635	Yes
<i>KCNK6</i>	Downregulated	0.170404725	0.02845041	0.11662241	No	-0.0824855	0.4553394	0.56109584	Yes

<i>PKD1L3</i>	Downregulated	0.055659301	0.5812002	0.76595281	No	-0.1636278	0.13356009	0.21658309	Yes
<i>CEP152</i>	Downregulated	0.07442241	0.33865291	0.56886042	No	0.31540776	0.0159747	0.04226801	No
<i>KRT15</i>	Downregulated	0.387401012	0.15704557	0.35787678	No	0.96338522	0.00180402	0.00990834	No
<i>PLCB3</i>	Downregulated	0.380772802	0.00015742	0.00297538	No	0.38561032	0.00026815	0.00257557	No
<i>TAS2R20</i>	Downregulated	0.025273886	0.82189086	0.9155869	No	0.13672415	0.45517692	0.56095762	No
<i>KIAA1614</i>	Downregulated	0.132682107	0.0498449	0.16969978	No	-0.1326413	0.12314313	0.20317809	Yes
<i>MYO15B</i>	Downregulated	0.395344742	0.0000319	0.00094696	No	0.11603289	0.4285052	0.5359415	No
<i>ARHGAP31</i>	Downregulated	0.360939169	0.00000867	0.00037982	No	1.01811804	3.97E-09	0.00000103	No
<i>IZUMO4</i>	Downregulated	0.115893195	0.11588562	0.29542738	No	-0.0564515	0.65529985	0.73865636	Yes
<i>LOC221442</i>	Downregulated	#N/A	#N/A	#N/A	#N/A	#N/A	#N/A	#N/A	#N/A
<i>USP43</i>	Downregulated	-0.208136729	0.00337534	0.02593271	Yes	-0.378239	0.00361484	0.01540423	Yes
<i>PDE1A</i>	Downregulated	-0.224683975	0.0232735	0.10134494	Yes	-0.7139314	0.0000381	0.00060198	Yes
<i>ATP8B3</i>	Downregulated	0.027496332	0.81785076	0.91321555	No	-0.2448696	0.11018545	0.18599194	Yes
<i>BAIAP2L2</i>	Downregulated	-0.075122797	0.39193822	0.61796375	Yes	-0.4450411	0.0000105	0.00022657	Yes
<i>ABCC3</i>	Downregulated	0.497113369	0.00025304	0.00418475	No	0.51022331	0.00773926	0.02533215	No
<i>SPATA5</i>	Downregulated	0.106608661	0.00810908	0.04842263	No	0.13754596	0.07933633	0.14394025	No
<i>AGBL2</i>	Downregulated	0.605367226	0.00026283	0.00429239	No	-0.0152121	0.94553017	0.96227258	Yes
<i>FAM71F2</i>	Downregulated	-0.124057283	0.14778496	0.34506493	Yes	0.08868885	0.50249044	0.60454369	No
<i>CAPN3</i>	Downregulated	0.352515986	0.00048584	0.00661628	No	0.09170644	0.66755974	0.74848096	No
<i>RARB</i>	Downregulated	-0.030863603	0.69901876	0.84468492	Yes	-0.2463133	0.06622645	0.12514479	Yes
<i>PDGFRB</i>	Downregulated	0.33239346	0.00046866	0.00646112	No	0.79196746	3.28E-07	0.000018	No
<i>C10orf140</i>	Downregulated	#N/A	#N/A	#N/A	#N/A	#N/A	#N/A	#N/A	#N/A
<i>GPR126</i>	Downregulated	0.186549949	0.04666865	0.16256075	No	0.95672729	0.0000344	0.00055899	No

<i>KRTAP5-7</i>	Downregulated	-0.026699719	0.87108111	0.94055322	Yes	-0.6174012	0.00037955	0.00333419	Yes
<i>RHOJ</i>	Downregulated	0.125161563	0.09898264	0.2668409	No	0.84441656	4.41E-08	0.00000485	No
<i>HERC2P7</i>	Downregulated	0.147840016	0.9636985	NA	No	-0.2725465	0.18413153	0.27838922	Yes
<i>SNX22</i>	Downregulated	0.020063973	0.81317429	0.91104645	No	-0.1823553	0.05084702	0.10189872	Yes
<i>RBMS3</i>	Downregulated	0.172235925	0.00422651	0.03037551	No	0.31981112	0.00227015	0.0114807	No
<i>NLRC3</i>	Downregulated	-0.001359319	0.98074868	0.99199089	Yes	-0.2041104	0.02862357	0.06541929	Yes
<i>GRIN2C</i>	Downregulated	0.144035757	0.14489781	0.34087847	No	0.2508739	0.13067208	0.21281344	No
<i>FAM129A</i>	Downregulated	0.296353169	0.01106458	0.06027232	No	0.68981958	0.00082502	0.00582054	No
<i>SH3D21</i>	Downregulated	-0.111265254	0.22644981	0.44794268	Yes	0.16894712	0.10872803	0.18409475	No
<i>TPTE2P1</i>	Downregulated	-0.271923329	0.00044174	0.00619633	Yes	-0.676956	4.78E-07	0.0000233	Yes
<i>NMI</i>	Downregulated	0.369134525	0.0000428	0.00115891	No	0.54250185	0.0000292	0.00048991	No
<i>UCP3</i>	Downregulated	-0.068992023	0.47247131	0.68703024	Yes	-0.1446557	0.26552945	0.37041783	Yes
<i>ADAMTS6</i>	Downregulated	-0.081688342	0.293487	0.52298774	Yes	0.18017694	0.30769425	0.41533435	No
<i>CFD</i>	Downregulated	#N/A	#N/A	#N/A	#N/A	0.07013129	0.66196868	0.74426969	No
<i>ARAP3</i>	Downregulated	0.034783583	0.76663801	0.88467556	No	0.33552441	0.00228983	0.0115389	No
<i>LOC439949</i>	Downregulated	#N/A	#N/A	#N/A	#N/A	#N/A	#N/A	#N/A	#N/A
<i>CLMP</i>	Downregulated	-0.008793316	0.91679584	0.96406698	Yes	0.12848643	0.520076	0.62055636	No
<i>AFAP1L1</i>	Downregulated	0.381750928	0.00028418	0.00454331	No	0.83429866	0.0000106	0.00022743	No
<i>ABCA9</i>	Downregulated	-0.020875033	0.8102376	0.90951932	Yes	0.00616761	0.95763035	0.97070457	No
<i>LOC100506746</i>	Downregulated	#N/A	#N/A	#N/A	#N/A	#N/A	#N/A	#N/A	#N/A
<i>THSD4</i>	Downregulated	0.30652174	0.01000556	0.05630948	No	0.90869582	0.00045632	0.00382593	No
<i>RAB41</i>	Downregulated	0.162300434	0.0409559	0.14920839	No	0.28301065	0.00590856	0.02117891	No
<i>DUSP19</i>	Downregulated	0.029658733	0.70100971	0.84603544	No	-0.2387369	0.05072685	0.10168349	Yes

<i>DLC1</i>	Downregulated	0.125692131	0.02283025	0.1000461	No	0.50406935	7.27E-08	0.0000067	No
<i>LDB3</i>	Downregulated	0.076118994	0.49088924	0.70068484	No	-0.6255398	0.01590602	0.04213314	Yes
<i>LOC648809</i>	Downregulated	#N/A	#N/A	#N/A	#N/A	#N/A	#N/A	#N/A	#N/A
<i>GSTM2P1</i>	Downregulated	0.110325533	0.79297811	NA	No	0.09942957	0.71239963	0.78545687	No
<i>PCDHB11</i>	Downregulated	-0.005203989	0.92389656	0.96709369	Yes	0.55140166	0.00023632	0.00234741	No
<i>LOC728377</i>	Downregulated	#N/A	#N/A	#N/A	#N/A	#N/A	#N/A	#N/A	#N/A
<i>RASA4</i>	Downregulated	0.177449678	0.0942867	0.25817454	No	0.02326318	0.79148272	0.84801611	No
<i>NPHP3</i>	Downregulated	0.094104975	0.23257124	0.454917	No	0.09474061	0.43037906	0.53779057	No
<i>LOC388849</i>	Downregulated	#N/A	#N/A	#N/A	#N/A	#N/A	#N/A	#N/A	#N/A
<i>E2F7</i>	Downregulated	0.128112719	0.3023599	0.53223469	No	0.09509735	0.64555802	0.73040713	No
<i>LOC619207</i>	Downregulated	#N/A	#N/A	#N/A	#N/A	#N/A	#N/A	#N/A	#N/A
<i>EHBP1L1</i>	Downregulated	0.265457068	0.00162505	0.01547696	No	0.33135643	0.00036444	0.00323853	No
<i>ABCA1</i>	Downregulated	0.560290503	6.94E-10	4.47E-07	No	0.92564657	3.44E-08	0.00000414	No
<i>MUC1</i>	Downregulated	0.54352099	0.00016229	0.00304182	No	0.856342	0.00000298	0.0000894	No
<i>PHACTR2</i>	Downregulated	0.090467394	0.10718643	0.28125856	No	0.0763726	0.42813123	0.53560593	No
<i>FMN1</i>	Downregulated	-0.257498643	0.00423288	0.03040978	Yes	-0.4682806	0.00661431	0.02282776	Yes
<i>CARNS1</i>	Downregulated	0.27275724	0.04901262	0.16781461	No	-0.2367648	0.40023139	0.50906421	Yes
<i>ATP2C2</i>	Downregulated	-0.117558723	0.14685399	0.34371585	Yes	-0.3318028	0.00156086	0.00902252	Yes
<i>STL</i>	Downregulated	#N/A	#N/A	#N/A	#N/A	#N/A	#N/A	#N/A	#N/A
<i>COL16A1</i>	Downregulated	0.281475848	0.00072936	0.00873251	No	0.06113058	0.67485341	0.75459504	No
<i>LAMA4</i>	Downregulated	0.259961946	0.00071816	0.00863931	No	0.36880364	0.00067577	0.0050724	No
<i>MND1</i>	Downregulated	0.308071873	0.01387392	0.07069963	No	-0.1863143	0.41562726	0.52369974	Yes
<i>GLI3</i>	Downregulated	0.225125425	0.00902305	0.05221423	No	0.53300465	0.00071079	0.0052507	No

<i>NFKBIZ</i>	Downregulated	0.276688066	0.0056581	0.03746465	No	0.51008826	0.00020956	0.00214702	No
<i>LOC100505894</i>	Downregulated	#N/A	#N/A	#N/A	#N/A	#N/A	#N/A	#N/A	#N/A
<i>LMOD3</i>	Downregulated	0.027834785	0.77134594	0.88718902	No	-0.4792226	0.00099882	0.00666949	Yes
<i>CATSPER3</i>	Downregulated	-0.040695533	0.77795179	0.89068339	Yes	0.05469229	0.56383797	0.65974166	No
<i>LINC00174</i>	Downregulated	0.066195349	0.37750421	0.60518162	No	-0.175358	0.20651005	0.30476097	Yes
<i>DOCK5</i>	Downregulated	0.322721403	0.00043478	0.00613221	No	0.47128832	0.03225996	0.07173225	No
<i>NRXN3</i>	Downregulated	-0.323079056	0.00010587	0.00224609	Yes	-0.945232	1.23E-08	0.00000209	Yes
<i>ITGA10</i>	Downregulated	0.417138799	0.00019453	0.003455	No	1.15305859	3.28E-09	9.39E-07	No
<i>TTN</i>	Downregulated	-0.059141683	0.4389731	0.65956393	Yes	-0.3061261	0.07982538	0.1444906	Yes
<i>MYOZ3</i>	Downregulated	-0.350792452	0.0000532	0.00136918	Yes	-0.8948707	0.00000161	0.0000569	Yes
<i>TAS2R31</i>	Downregulated	0.036384067	0.734245	0.86496787	No	0.17137179	0.42176231	0.52953926	No
<i>IL27RA</i>	Downregulated	0.187804038	0.06068417	0.19318964	No	0.20754234	0.0456256	0.09368339	No
<i>SCARNA12</i>	Downregulated	0.096502798	0.97629945	NA	No	0.47527579	0.00655083	0.02267152	No
<i>PDE6C</i>	Downregulated	0.025238137	0.79376968	0.90002667	No	0.07470008	0.57856177	0.67286074	No
<i>OPLAH</i>	Downregulated	0.377174701	0.00012398	0.00249632	No	0.32634581	0.01418904	0.03869299	No
<i>NPR3</i>	Downregulated	-0.124644127	0.22037528	0.4401808	Yes	-0.9469944	0.00020417	0.00210458	Yes
<i>PRSS36</i>	Downregulated	-0.019293503	0.86955027	0.93987899	Yes	-0.5928245	0.00000476	0.00012595	Yes
<i>DPH3PI</i>	Downregulated	NA	NA	NA	#N/A	-0.0572301	0.74137002	0.8083192	Yes
<i>TAF1L</i>	Downregulated	-0.255484617	0.19048272	0.40321905	Yes	-0.023757	0.87263751	0.90980352	Yes
<i>KIAA1530</i>	Downregulated	#N/A	#N/A	#N/A	#N/A	#N/A	#N/A	#N/A	#N/A
<i>DOK3</i>	Downregulated	0.234891143	0.01807751	0.08533753	No	0.26891431	0.03420798	0.07503366	No
<i>LOC387646</i>	Downregulated	#N/A	#N/A	#N/A	#N/A	#N/A	#N/A	#N/A	#N/A
<i>MIR940</i>	Downregulated	#N/A	#N/A	#N/A	#N/A	-0.4715933	0.00011118	0.00134439	Yes

<i>HSPB6</i>	Downregulated	0.374233693	0.00920827	0.05296116	No	0.22868352	0.09091297	0.15990862	No
<i>P2RX5-TAX1BP3</i>	Downregulated	-0.036537255	0.61376273	0.78712747	Yes	0.04837748	0.54402178	0.64202516	No
<i>CENPN</i>	Downregulated	0.121677787	0.0254719	0.10786127	No	-0.0153895	0.82047183	0.87080941	Yes
<i>FBXO32</i>	Downregulated	0.265662808	0.00019138	0.00341809	No	0.06917344	0.53001271	0.62936892	No
<i>LOC285593</i>	Downregulated	#N/A	#N/A	#N/A	#N/A	#N/A	#N/A	#N/A	#N/A
<i>APOLD1</i>	Downregulated	0.499569856	0.0021638	0.01897962	No	0.79266842	0.00000484	0.00012766	No
<i>LRGUK</i>	Downregulated	-0.217776887	0.00135864	0.01361655	Yes	0.0295223	0.8654702	0.90448458	No
<i>CDCA7</i>	Downregulated	0.201624921	0.0759586	0.22391709	No	0.01597874	0.91918059	0.94333574	No
<i>IL1RAP</i>	Downregulated	-0.031019416	0.6548608	0.81535951	Yes	0.20871929	0.16172016	0.25128527	No
<i>NIDI</i>	Downregulated	0.286169079	0.00844441	0.0497992	No	1.04888786	1.34E-07	0.0000099	No
<i>ATP2A1</i>	Downregulated	0.018568665	0.86545945	0.93799848	No	-0.1785132	0.14019561	0.22494235	Yes
<i>PCDH12</i>	Downregulated	-0.00222126	0.96925577	0.98775497	Yes	0.01337384	0.8660876	0.90501106	No
<i>EFNA4</i>	Downregulated	0.315146705	0.00759512	0.04634486	No	0.52085652	0.00027495	0.00262366	No
<i>SAMD9</i>	Downregulated	0.195661647	0.04425223	0.15690854	No	0.68927488	0.00031214	0.00288287	No
<i>ASF1B</i>	Downregulated	0.26665871	0.03380027	0.1315181	No	0.01300431	0.94987631	0.96553095	No
<i>ULK4</i>	Downregulated	0.043272117	0.53359102	0.73267659	No	-0.1169679	0.30901893	0.41666886	Yes
<i>CDC6</i>	Downregulated	-0.167558695	0.05699423	0.18529714	Yes	-0.4670642	0.00036982	0.00326936	Yes
<i>HSF2BP</i>	Downregulated	-0.113502907	0.13815326	0.33011011	Yes	-0.1273549	0.30427434	0.41167484	Yes
<i>RFTN2</i>	Downregulated	0.351497372	0.0000409	0.00111803	No	0.59066739	0.00018321	0.00194458	No
<i>MCC</i>	Downregulated	0.235827456	0.00012082	0.00245747	No	0.3826532	0.00605981	0.02154651	No
<i>C3orf32</i>	Downregulated	#N/A	#N/A	#N/A	#N/A	#N/A	#N/A	#N/A	#N/A
<i>HAR1A</i>	Downregulated	-0.135821196	0.16069845	0.36294809	Yes	-0.7690718	0.00019738	0.00205274	Yes
<i>TNFRSF25</i>	Downregulated	-0.004819936	0.96340641	0.9860308	Yes	0.10694237	0.60119932	0.6926003	No

<i>LOC100506649</i>	Downregulated	#N/A	#N/A	#N/A	#N/A	#N/A	#N/A	#N/A	#N/A
<i>FLJ39653</i>	Downregulated	#N/A	#N/A	#N/A	#N/A	#N/A	#N/A	#N/A	#N/A
<i>ADM2</i>	Downregulated	0.116318103	0.66348338	0.82116507	No	0.67335449	0.0045327	0.0178228	No
<i>KLHL34</i>	Downregulated	-0.14898524	0.08972948	0.24995112	Yes	-0.0174338	0.92890223	0.95012421	Yes
<i>MGC16275</i>	Downregulated	#N/A	#N/A	#N/A	#N/A	#N/A	#N/A	#N/A	#N/A
<i>LTBR</i>	Downregulated	0.543917387	0.00000126	0.000098	No	0.50408858	0.00013494	0.00155092	No
<i>LAMA3</i>	Downregulated	0.073080263	0.26307439	0.49096353	No	0.50276872	0.0000143	0.00028612	No
<i>CORO6</i>	Downregulated	-0.221308603	0.02437012	0.10449584	Yes	-0.165726	0.32000964	0.42819501	Yes
<i>LOC100288846</i>	Downregulated	#N/A	#N/A	#N/A	#N/A	#N/A	#N/A	#N/A	#N/A
<i>C9orf100</i>	Downregulated	#N/A	#N/A	#N/A	#N/A	#N/A	#N/A	#N/A	#N/A
<i>JAK3</i>	Downregulated	-0.040339956	0.70312196	0.84701398	Yes	-0.2125791	0.12395014	0.20417644	Yes
<i>ANGPTL6</i>	Downregulated	-0.156174761	0.13627758	0.32717307	Yes	-0.0931163	0.09084354	0.15982088	Yes
<i>HSD17B11</i>	Downregulated	-0.009361026	0.88525754	0.94820074	Yes	0.1664435	0.01926844	0.04858249	No
<i>CI6orf74</i>	Downregulated	0.190360561	0.10270773	0.27363254	No	-0.2869981	0.03866416	0.08244873	Yes
<i>CHDH</i>	Downregulated	0.396704611	4.3E-08	0.00000872	No	0.54736641	0.00015577	0.00172669	No
<i>ZHX2</i>	Downregulated	0.277011111	0.00043778	0.00616123	No	0.42216977	0.0003206	0.00294142	No
<i>ENPEP</i>	Downregulated	0.167062188	0.21594376	0.43500502	No	0.47334036	0.03993073	0.08455027	No
<i>LOC100507501</i>	Downregulated	#N/A	#N/A	#N/A	#N/A	#N/A	#N/A	#N/A	#N/A
<i>MAK</i>	Downregulated	-0.058097599	0.47428028	0.68836841	Yes	-0.016333	0.89228736	0.92417844	Yes
<i>SLC39A11</i>	Downregulated	#N/A	#N/A	#N/A	#N/A	0.49745423	0.00000995	0.00021709	No
<i>LOC100506451</i>	Downregulated	#N/A	#N/A	#N/A	#N/A	#N/A	#N/A	#N/A	#N/A
<i>ATG9B</i>	Downregulated	-0.246302773	0.01960653	0.09035379	Yes	-0.0611253	0.50262964	0.60462542	Yes
<i>UCKL1-AS1</i>	Downregulated	0.246377866	0.04344544	0.15513484	No	#N/A	#N/A	#N/A	#N/A

<i>MMS22L</i>	Downregulated	0.149736614	0.0358685	0.1367644	No	-0.1713982	0.09411361	0.16430256	Yes
<i>TMC3</i>	Downregulated	-0.136077485	0.3102228	0.54067118	Yes	-0.7792366	0.0000315	0.00052043	Yes
<i>GPR179</i>	Downregulated	#N/A	#N/A	#N/A	#N/A	-0.4325144	0.00456073	0.01789502	Yes
<i>CCNE1</i>	Downregulated	-0.107931747	0.10126165	0.27095916	Yes	-0.3913584	0.0000431	0.00066103	Yes
<i>SARDH</i>	Downregulated	0.074196404	0.45396324	0.67235262	No	0.13255598	0.33051544	0.43881935	No
<i>ATHL1</i>	Downregulated	0.508651728	0.00000963	0.00041057	No	0.66315224	0.0000854	0.00110149	No
<i>PLEKHG4B</i>	Downregulated	0.140514726	0.35324879	0.58175842	No	-0.2903796	0.18929211	0.28457872	Yes
<i>ARHGEF26</i>	Downregulated	0.339946552	1.38E-07	0.0000198	No	0.62616339	0.0000674	0.00092314	No
<i>ALDH8A1</i>	Downregulated	-0.145285907	0.19126252	0.40434932	Yes	-0.2795216	0.0759616	0.13914564	Yes
<i>AMH</i>	Downregulated	0.300286559	0.03160134	0.12544685	No	-0.2103727	0.26934213	0.37463989	Yes
<i>MIR137HG</i>	Downregulated	-0.34667905	0.00113611	0.01197776	Yes	-0.4760836	0.01378783	0.0379142	Yes
<i>PIWIL4</i>	Downregulated	0.02273285	0.66990131	0.82555472	No	-0.0233481	0.74401343	0.81044061	Yes
<i>C5</i>	Downregulated	0.208303272	0.00213787	0.01883493	No	0.04393463	0.70918851	0.7827058	No
<i>CATSPER2</i>	Downregulated	-0.216145635	0.01084281	0.05952957	Yes	-0.2506824	0.04319264	0.08989692	Yes
<i>RNF144B</i>	Downregulated	0.273934386	0.00259638	0.02162454	No	0.54128267	0.00036008	0.00320973	No
<i>AIFM3</i>	Downregulated	0.330873021	0.00048396	0.00660492	No	0.38284361	0.00450232	0.0177474	No
<i>FAM186B</i>	Downregulated	0.084735169	0.28015333	0.50940411	No	0.21831789	0.12302276	0.20300266	No
<i>RAPGEF3</i>	Downregulated	0.320882509	0.00026206	0.00428162	No	0.53667768	0.0003158	0.002908	No
<i>TUBD1</i>	Downregulated	0.101444744	0.04310135	0.15435995	No	0.02915807	0.6942227	0.7704895	No
<i>GALNT6</i>	Downregulated	0.280066994	0.02555708	0.10810136	No	-0.0193405	0.93681192	0.95589345	Yes
<i>LOC389791</i>	Downregulated	#N/A	#N/A	#N/A	#N/A	#N/A	#N/A	#N/A	#N/A
<i>ERBB4</i>	Downregulated	-0.04935812	0.34308847	0.57242746	Yes	-0.0753755	0.42787479	0.53534517	Yes
<i>LRP5L</i>	Downregulated	0.116975913	0.10491207	0.27767312	No	0.0518963	0.63963142	0.72530587	No

<i>C7orf10</i>	Downregulated	#N/A	#N/A	#N/A	#N/A	#N/A	#N/A	#N/A	#N/A
<i>TPX2</i>	Downregulated	-0.299467302	0.00037486	0.00551022	Yes	-0.5588601	0.0000177	0.00033583	Yes
<i>C8orf51</i>	Downregulated	#N/A	#N/A	#N/A	#N/A	#N/A	#N/A	#N/A	#N/A
<i>PFN1P2</i>	Downregulated	-0.131315794	0.17435725	0.38167927	Yes	-0.146932	0.50057773	0.60278632	Yes
<i>CCDC102B</i>	Downregulated	-0.121310997	0.03772499	0.14138583	Yes	-0.3835596	0.0000615	0.00086447	Yes
<i>PLBI</i>	Downregulated	-0.011761703	0.8883715	0.94954102	Yes	-0.2379299	0.03905738	0.08310216	Yes
<i>SNORD22</i>	Downregulated	NA	NA	NA	#N/A	-0.4469963	0.00418091	0.01692643	Yes
<i>SPHK1</i>	Downregulated	0.724332644	9.18E-09	0.0000028	No	0.81006994	0.00016534	0.00180686	No
<i>LGALS3</i>	Downregulated	0.297107757	0.00182779	0.01677664	No	0.58997524	0.00057864	0.00453448	No
<i>CYP20A1</i>	Downregulated	0.298088974	0.00000136	0.00010282	No	0.16959982	0.08380111	0.14994431	No
<i>FBXO36</i>	Downregulated	0.084030246	0.13094677	0.31920179	No	0.08058832	0.38013396	0.48930532	No
<i>ANO9</i>	Downregulated	0.206240453	0.22002887	0.4397012	No	-0.0079032	0.9691654	0.97908043	Yes
<i>GNN</i>	Downregulated	#N/A	#N/A	#N/A	#N/A	#N/A	#N/A	#N/A	#N/A
<i>AIM1</i>	Downregulated	0.025722478	0.70361858	0.84748626	No	0.14668564	0.14798926	0.23465829	No
<i>CD27</i>	Downregulated	0.111501435	0.38133906	0.60850716	No	0.0395904	0.68418552	0.76226292	No
<i>RPL23AP64</i>	Downregulated	0.02706184	0.78765964	0.89647744	No	0.02281981	0.86384976	0.90312965	No
<i>PNPLA7</i>	Downregulated	0.12991212	0.09297192	0.25616379	No	-0.0897572	0.39538608	0.50428065	Yes
<i>SERPINF2</i>	Downregulated	#N/A	#N/A	#N/A	#N/A	0.15350222	0.35199595	0.46095042	No
<i>ZNF563</i>	Downregulated	-0.046915409	0.47337673	0.68771635	Yes	-0.0466423	0.47169595	0.57615385	Yes
<i>MDM4</i>	Downregulated	0.118628212	0.01803565	0.08519291	No	0.03707858	0.74463452	0.81100623	No
<i>CDH23</i>	Downregulated	0.472673667	0.0000119	0.00047164	No	0.66229011	0.00058057	0.00454422	No
<i>TAF8</i>	Downregulated	0.09178026	0.10218573	0.27258626	No	0.07925858	0.13547354	0.21899173	No
<i>DCHS2</i>	Downregulated	-0.253249226	0.00064229	0.00804002	Yes	0.06383825	0.65464479	0.73819733	No

<i>LOC100132247</i>	Downregulated	#N/A	#N/A	#N/A	#N/A	#N/A	#N/A	#N/A	#N/A
<i>LOC646214</i>	Downregulated	#N/A	#N/A	#N/A	#N/A	#N/A	#N/A	#N/A	#N/A
<i>HAPLN3</i>	Downregulated	0.511177237	0.00114033	0.01200557	No	0.35685524	0.03280137	0.07268625	No
<i>ISPD</i>	Downregulated	-0.045675602	0.43305086	0.65460774	Yes	-0.1841837	0.08207498	0.14754232	Yes
<i>FBLN2</i>	Downregulated	-0.052828058	0.66107429	0.81952961	Yes	0.2122113	0.22944445	0.33071129	No
<i>DHRS4L1</i>	Downregulated	0.311455698	0.00599308	0.03893555	No	#N/A	#N/A	#N/A	#N/A
<i>P2RX5</i>	Downregulated	-0.298961859	0.00251347	0.02118184	Yes	-0.5514858	0.000397	0.00344786	Yes
<i>ATG16L2</i>	Downregulated	0.220931036	0.00138491	0.01381783	No	0.10658678	0.13503412	0.21844607	No
<i>SH2D3A</i>	Downregulated	0.623748164	0.00341648	0.02616408	No	0.66248622	0.00609643	0.02163322	No
<i>ARRDC2</i>	Downregulated	0.365966681	0.00090819	0.01024966	No	0.44188221	0.01450519	0.03935338	No
<i>GHR</i>	Downregulated	-0.113816224	0.11120749	0.28804812	Yes	-0.14623	0.15302152	0.24072023	Yes
<i>BRCA1</i>	Downregulated	0.247276879	0.0001578	0.00298119	No	0.00933827	0.94518237	0.96204019	No
<i>NRG4</i>	Downregulated	-0.193218376	0.04603522	0.16111131	Yes	-0.3733103	0.00143474	0.00853606	Yes
<i>LPIN3</i>	Downregulated	0.293557157	0.01040786	0.05781906	No	0.23465936	0.09587241	0.16672787	No
<i>LOC645166</i>	Downregulated	#N/A	#N/A	#N/A	#N/A	#N/A	#N/A	#N/A	#N/A
<i>B3GNT7</i>	Downregulated	0.307937563	0.01259249	0.06599347	No	0.23071862	0.17246329	0.26446268	No
<i>SLCO2A1</i>	Downregulated	0.08109819	0.43351016	0.65494166	No	0.11078106	0.48153401	0.58506015	No
<i>MYLK4</i>	Downregulated	-0.051114525	0.45515705	0.67330218	Yes	-0.3714316	0.00055201	0.00438303	Yes
<i>LOC400680</i>	Downregulated	#N/A	#N/A	#N/A	#N/A	#N/A	#N/A	#N/A	#N/A
<i>MYLK</i>	Downregulated	0.320098238	0.0000158	0.00057723	No	0.42710762	0.00576432	0.02082924	No
<i>SCNN1D</i>	Downregulated	0.057579525	0.44250784	0.66257942	No	-0.0271719	0.73099197	0.80008615	Yes
<i>CA13</i>	Downregulated	-0.056931728	0.29578546	0.52552389	Yes	-0.3612571	0.0000252	0.00043946	Yes
<i>CENPL</i>	Downregulated	0.125342198	0.01780552	0.08432446	No	-0.0906501	0.17861762	0.27189181	Yes

<i>FST</i>	Downregulated	0.004635856	0.97922038	0.99153904	No	-0.8405434	0.00023303	0.0023218	Yes
<i>PCSK5</i>	Downregulated	0.049283685	0.394859	0.62062785	No	0.45555215	0.0000144	0.00028875	No
<i>VWCE</i>	Downregulated	0.112810535	0.21327428	0.43201859	No	0.05792963	0.64481255	0.72981544	No
<i>NR6A1</i>	Downregulated	-0.077946241	0.08128982	0.2344255	Yes	-0.1136548	0.19649928	0.29310924	Yes
<i>FHOD1</i>	Downregulated	0.125768981	0.0564512	0.18417119	No	0.06132119	0.36835619	0.47750733	No
<i>XPNPEP3</i>	Downregulated	0.098188987	0.06284877	0.19785684	No	-0.2092179	0.00013388	0.00154228	Yes
<i>MAP7D3</i>	Downregulated	0.240486164	0.00066384	0.00819867	No	0.15973241	0.13490905	0.21833243	No
<i>TMOD1</i>	Downregulated	-0.209838476	0.00100535	0.01100573	Yes	-0.1316001	0.1117905	0.18816008	Yes
<i>NEK8</i>	Downregulated	0.201267597	0.05267222	0.17556175	No	-0.1521933	0.23584181	0.337706	Yes
<i>ESR2</i>	Downregulated	-0.170565856	0.01636088	0.07953092	Yes	0.18821058	0.15503096	0.24329157	No
<i>DMKN</i>	Downregulated	-0.264395945	0.00557535	0.03711056	Yes	-0.5752633	0.0000141	0.0002842	Yes
<i>PLCE1</i>	Downregulated	0.428686087	1.98E-11	3.96E-08	No	0.68053176	7.53E-08	0.00000685	No
<i>C18orf56</i>	Downregulated	#N/A	#N/A	#N/A	#N/A	-0.2318951	0.25828083	0.36247892	Yes
<i>SLC25A35</i>	Downregulated	0.233122513	0.02140295	0.09583853	No	-0.2019536	0.0000189	0.00035286	Yes
<i>FANCI</i>	Downregulated	-0.072887916	0.27122256	0.49980487	Yes	-0.2497506	0.00148575	0.00873284	Yes
<i>CCDC154</i>	Downregulated	0.207749865	0.06524004	0.20282768	No	0.06278145	0.6975962	0.77315629	No
<i>LOC100506023</i>	Downregulated	#N/A	#N/A	#N/A	#N/A	#N/A	#N/A	#N/A	#N/A
<i>PTGIS</i>	Downregulated	0.159964769	0.21721982	0.43664854	No	-0.1446032	0.28646976	0.39282853	Yes
<i>PRRX1</i>	Downregulated	0.388580089	0.00013878	0.00270399	No	0.73133553	0.0000285	0.00048232	No
<i>C9orf3</i>	Downregulated	0.028290222	0.58233898	0.76642256	No	-0.2049669	0.06806163	0.12782848	Yes
<i>DNAH7</i>	Downregulated	-0.040905836	0.6101027	0.78457132	Yes	0.20514362	0.26357095	0.36820159	No
<i>FBXO17</i>	Downregulated	0.036538759	0.53230706	0.73176074	No	-0.0330029	0.64623689	0.73091805	Yes
<i>MIR149</i>	Downregulated	-0.245939867	0.19891576	0.41404237	Yes	0.11488728	0.52462044	0.62466872	No

<i>CD44</i>	Downregulated	0.975681759	9.07E-08	0.0000146	No	2.06106114	1.23E-08	0.00000209	No
<i>FGFR4</i>	Downregulated	0.223533025	0.0668593	0.20624008	No	0.19352662	0.23308061	0.33466697	No
<i>TEPI</i>	Downregulated	0.353589776	3.25E-07	0.0000372	No	0.57692153	1.37E-07	0.00001	No
<i>GNL3L</i>	Downregulated	-0.05869916	0.2121501	0.43074653	Yes	0.49123885	6.01E-08	0.00000591	No
<i>TRIM38</i>	Downregulated	0.427117209	3.85E-07	0.0000417	No	0.51944296	0.00082073	0.00579611	No
<i>CLMN</i>	Downregulated	0.30154039	0.00134212	0.01349152	No	0.75396037	0.00055042	0.00437283	No
<i>CHST5</i>	Downregulated	-0.193805011	0.06825198	0.20905784	Yes	-0.3294015	0.00181996	0.0099572	Yes
<i>LTB4R</i>	Downregulated	0.140363041	0.09579302	0.26103736	No	-0.044095	0.70521303	0.77932092	Yes
<i>HMBOX1</i>	Downregulated	0.277823216	1.85E-10	1.82E-07	No	0.40376655	0.0000821	0.00107091	No
<i>ZNF573</i>	Downregulated	0.004385385	0.9181642	0.96445717	No	0.16118628	0.01775877	0.04566728	No
<i>PLEKHG6</i>	Downregulated	0.349202705	0.03847934	0.14332138	No	0.77112017	0.00013427	0.00154551	No
<i>MACROD2</i>	Downregulated	-0.261244114	0.00056217	0.00731698	Yes	-0.6905671	0.00000055	0.0000259	Yes
<i>LOC344967</i>	Downregulated	#N/A	#N/A	#N/A	#N/A	#N/A	#N/A	#N/A	#N/A
<i>GMEB1</i>	Downregulated	0.044636103	0.21641726	0.43570447	No	-0.1663726	0.0024572	0.01205486	Yes
<i>GATSL2</i>	Downregulated	#N/A	#N/A	#N/A	#N/A	0.11523193	0.19356884	0.28964157	No
<i>ZNF221</i>	Downregulated	-0.015021498	0.74218341	0.87016029	Yes	0.23519904	0.01522579	0.04079897	No
<i>C10orf103</i>	Downregulated	#N/A	#N/A	#N/A	#N/A	#N/A	#N/A	#N/A	#N/A
<i>SGK494</i>	Downregulated	#N/A	#N/A	#N/A	#N/A	0.05669384	0.67487331	0.75460215	No
<i>HYAL1</i>	Downregulated	0.087093634	0.24910046	0.47469114	No	0.31529603	0.01093007	0.03208808	No
<i>LOC100507053</i>	Downregulated	#N/A	#N/A	#N/A	#N/A	#N/A	#N/A	#N/A	#N/A
<i>LOC283440</i>	Downregulated	#N/A	#N/A	#N/A	#N/A	#N/A	#N/A	#N/A	#N/A
<i>ITGB1BP2</i>	Downregulated	0.020855351	0.87961511	0.94541539	No	-0.1115244	0.55141115	0.64856299	Yes
<i>LOC100131067</i>	Downregulated	#N/A	#N/A	#N/A	#N/A	#N/A	#N/A	#N/A	#N/A

<i>DNAH1</i>	Downregulated	-0.050982511	0.52935593	0.72960653	Yes	-0.139684	0.25597444	0.35999775	Yes
<i>C20orf132</i>	Downregulated	#N/A	#N/A	#N/A	#N/A	#N/A	#N/A	#N/A	#N/A
<i>MMP25</i>	Downregulated	0.211431862	0.07687044	0.2258508	No	0.41551874	0.00084142	0.00590485	No
<i>CDCA8</i>	Downregulated	-0.021261367	0.79375762	0.90002667	Yes	-0.1326934	0.16790611	0.25880555	Yes
<i>EDARADD</i>	Downregulated	0.209401119	0.39017594	0.61618348	No	0.09269227	0.46737791	0.57221235	No
<i>EFNA5</i>	Downregulated	-0.266583376	0.00181621	0.01672367	Yes	-0.4496951	0.00204802	0.01073914	Yes
<i>BNC2</i>	Downregulated	0.623022272	0.00000475	0.00024484	No	0.99444348	0.00011955	0.00141616	No
<i>NEK2</i>	Downregulated	-0.134520492	0.50643494	0.71242519	Yes	-1.18221	0.0000122	0.00025264	Yes
<i>PDE11A</i>	Downregulated	0.200534489	0.02689017	0.11195583	No	-0.2941528	0.07313077	0.13514458	Yes
<i>RYR3</i>	Downregulated	0.243430865	0.00095674	0.0106377	No	0.76690183	0.0000225	0.00040203	No
<i>DDR2</i>	Downregulated	0.576008207	7.4E-12	2.2E-08	No	0.95599569	1.33E-07	0.00000985	No
<i>JMJD7</i>	Downregulated	-0.065717599	0.54012923	0.73743892	Yes	0.11275345	0.14727484	0.23383416	No
<i>ZAK</i>	Downregulated	#N/A	#N/A	#N/A	#N/A	#N/A	#N/A	#N/A	#N/A
<i>CCDC18</i>	Downregulated	0.100469175	0.1646442	0.36827568	No	0.29886617	0.0000291	0.00048972	No
<i>COL9A2</i>	Downregulated	0.411246385	0.0000297	0.00089998	No	0.07444639	0.66218669	0.74447767	No
<i>MYL3</i>	Downregulated	0.45853089	0.00000797	0.00035953	No	0.43931488	0.01360842	0.03757309	No
<i>LOC100131655</i>	Downregulated	#N/A	#N/A	#N/A	#N/A	#N/A	#N/A	#N/A	#N/A
<i>SRCRB4D</i>	Downregulated	0.08962184	0.36558938	0.59362839	No	-0.3440951	0.00335286	0.01466557	Yes
<i>DDX60L</i>	Downregulated	0.334855933	0.00017043	0.00314309	No	0.45309899	0.00141729	0.00847364	No
<i>MTL5</i>	Downregulated	-0.238173998	0.02979964	0.1204361	Yes	-0.5440372	0.00870013	0.02740881	Yes
<i>MOB3B</i>	Downregulated	0.25231695	0.00502288	0.0344496	No	0.38670624	0.03373748	0.07424775	No
<i>C4orf47</i>	Downregulated	-0.075476365	0.44243664	0.66254647	Yes	0.09338214	0.53861234	0.63723278	No
<i>DSCR6</i>	Downregulated	#N/A	#N/A	#N/A	#N/A	#N/A	#N/A	#N/A	#N/A

<i>YJEFN3</i>	Downregulated	-0.167638537	0.08581072	0.24282235	Yes	-0.2550571	4.21E-07	0.0000215	Yes
<i>KIFC1</i>	Downregulated	0.044909445	0.81773317	0.91321142	No	-0.0908353	0.62318769	0.7114052	Yes
<i>PILRB</i>	Downregulated	0.307226518	0.0240563	0.10367125	No	0.23187939	0.0812454	0.14644859	No
<i>LOC100288198</i>	Downregulated	#N/A	#N/A	#N/A	#N/A	#N/A	#N/A	#N/A	#N/A
<i>PROC</i>	Downregulated	-0.016506641	0.88975954	0.95000798	Yes	-0.1773825	0.18975266	0.2850943	Yes
<i>ACACB</i>	Downregulated	0.376138557	0.00012328	0.00248745	No	0.47429897	0.00137249	0.00828454	No
<i>SSPN</i>	Downregulated	0.447084242	0.00000108	0.0000884	No	0.90434523	4.51E-07	0.0000225	No
<i>SLC26A1</i>	Downregulated	0.091901272	0.26366216	0.49152522	No	0.22081262	0.00604428	0.02150638	No
<i>IBA57</i>	Downregulated	0.116415605	0.02969137	0.1201905	No	0.05657948	0.34293552	0.45164193	No
<i>C17orf53</i>	Downregulated	0.017158313	0.8605847	0.93557902	No	-0.1894481	0.07061778	0.13151994	Yes
<i>LOC728989</i>	Downregulated	#N/A	#N/A	#N/A	#N/A	#N/A	#N/A	#N/A	#N/A
<i>GRHL1</i>	Downregulated	-0.269432121	0.00031975	0.00492395	Yes	-0.6170886	0.00000691	0.00016422	Yes
<i>CYP2D6</i>	Downregulated	#N/A	#N/A	#N/A	#N/A	0.24044112	0.08569466	0.15261735	No
<i>TTLL3</i>	Downregulated	0.113736997	0.08109129	0.23408419	No	-0.0345075	0.7377199	0.80556156	Yes
<i>FAM46C</i>	Downregulated	0.18079951	0.13324212	0.32234204	No	0.31852129	0.07984098	0.14451323	No
<i>CPT1A</i>	Downregulated	0.245587063	0.0010493	0.01135244	No	0.63471738	0.0000154	0.00030276	No
<i>ZSCAN22</i>	Downregulated	0.035729507	0.48311597	0.69460503	No	-0.0507676	0.46432279	0.56949738	Yes
<i>PIEZ01</i>	Downregulated	0.452325348	0.00000774	0.00035127	No	0.74374698	9.68E-11	1.15E-07	No
<i>AKR7A3</i>	Downregulated	0.070170885	0.37391607	0.60156022	No	-0.058301	0.51998801	0.6204912	Yes
<i>C1orf101</i>	Downregulated	-0.004482511	0.94758494	0.97841664	Yes	-0.1101544	0.2974558	0.40431364	Yes
<i>TONSL</i>	Downregulated	0.072378064	0.38835512	0.61478139	No	-0.0938698	0.17441295	0.26676272	Yes
<i>LOC285456</i>	Downregulated	#N/A	#N/A	#N/A	#N/A	#N/A	#N/A	#N/A	#N/A
<i>CILP2</i>	Downregulated	-0.18470829	0.17701449	0.38513093	Yes	-0.6453283	0.00020655	0.00212397	Yes

<i>ASB14</i>	Downregulated	-0.024880332	0.72633214	0.86101628	Yes	0.06974298	0.25806573	0.36223536	No
<i>RTDRI</i>	Downregulated	#N/A	#N/A	#N/A	#N/A	-0.3184838	0.0000443	0.00067373	Yes
<i>TIAM2</i>	Downregulated	-0.201462166	0.00279421	0.02270908	Yes	-0.3703509	0.0008811	0.006108	Yes
<i>POLR2J3</i>	Downregulated	-0.02680313	0.80951435	0.90912669	Yes	-0.0476549	0.68314897	0.76134596	Yes
<i>CCDC77</i>	Downregulated	0.057356068	0.21941233	0.43917472	No	-0.0649564	0.47997822	0.58362772	Yes
<i>LOC728758</i>	Downregulated	#N/A	#N/A	#N/A	#N/A	#N/A	#N/A	#N/A	#N/A
<i>ARHGEF1</i>	Downregulated	0.261059503	0.00059294	0.00761571	No	0.07232343	0.57767722	0.67210542	No
<i>PRR16</i>	Downregulated	-0.227240978	0.00446805	0.03167622	Yes	-0.6320689	0.00000301	0.0000899	Yes
<i>TENI-CDK3</i>	Downregulated	0.358318715	0.01272391	0.0664726	No	-0.068438	0.41446979	0.52258596	Yes
<i>LOC100131208</i>	Downregulated	#N/A	#N/A	#N/A	#N/A	#N/A	#N/A	#N/A	#N/A
<i>FAM13A-AS1</i>	Downregulated	-0.003842656	0.96165751	0.9852012	Yes	0.10775372	0.21568307	0.31534353	No
<i>NPAS2</i>	Downregulated	-0.150880607	0.01411691	0.07150584	Yes	-0.1014949	0.26311251	0.36774544	Yes
<i>PION</i>	Downregulated	#N/A	#N/A	#N/A	#N/A	#N/A	#N/A	#N/A	#N/A
<i>FMNL3</i>	Downregulated	0.326204927	0.00000201	0.00013376	No	0.21480392	0.01490049	0.04014651	No
<i>NOXO1</i>	Downregulated	0.541497221	0.65760205	NA	No	-0.0099513	0.92263869	0.94578841	Yes
<i>ASPRV1</i>	Downregulated	0.226843815	0.00048233	0.00659445	No	0.09621377	0.40176885	0.51056465	No
<i>SIRT4</i>	Downregulated	-0.061448469	0.49460494	0.70353724	Yes	-0.1512273	0.23541776	0.33719405	Yes
<i>DCDC2B</i>	Downregulated	0.049785723	0.58882607	0.77057805	No	-0.0282346	0.81437716	0.8659562	Yes
<i>MYO7A</i>	Downregulated	0.063597716	0.48003729	0.69219849	No	0.0609865	0.55008394	0.64732968	No
<i>C10orf68</i>	Downregulated	-0.058975171	0.38286707	0.6098685	Yes	#N/A	#N/A	#N/A	#N/A
<i>RRM2</i>	Downregulated	0.598089468	0.0358733	0.13676899	No	-0.1697891	0.54219812	0.64032022	Yes
<i>OBSCN</i>	Downregulated	-0.02226612	0.7878957	0.89661169	Yes	-0.0315747	0.7847688	0.84271733	Yes
<i>RGS11</i>	Downregulated	0.015861481	0.83658773	0.92216874	No	-0.2168438	0.06407319	0.12197708	Yes

<i>LOC440300</i>	Downregulated	#N/A	#N/A	#N/A	#N/A	#N/A	#N/A	#N/A	#N/A
<i>FAM70B</i>	Downregulated	#N/A	#N/A	#N/A	#N/A	#N/A	#N/A	#N/A	#N/A
<i>ATAD5</i>	Downregulated	-0.048745042	0.47967248	0.69192437	Yes	-0.2375694	0.00660235	0.02279385	Yes
<i>LENG8</i>	Downregulated	#N/A	#N/A	#N/A	#N/A	0.18262899	0.12678004	0.20766004	No
<i>NBEAL2</i>	Downregulated	0.264946014	0.00151631	0.01470361	No	0.59922496	4.55E-07	0.0000226	No
<i>C8orf77</i>	Downregulated	#N/A	#N/A	#N/A	#N/A	#N/A	#N/A	#N/A	#N/A
<i>POLE</i>	Downregulated	0.102444223	0.21507777	0.43409899	No	0.02821976	0.83409607	0.88136035	No
<i>LINC00085</i>	Downregulated	#N/A	#N/A	#N/A	#N/A	#N/A	#N/A	#N/A	#N/A
<i>C15orf52</i>	Downregulated	0.445414907	0.00000218	0.00014221	No	0.21717882	0.06420138	0.12217106	No
<i>LOC401010</i>	Downregulated	#N/A	#N/A	#N/A	#N/A	#N/A	#N/A	#N/A	#N/A
<i>LOC642846</i>	Downregulated	#N/A	#N/A	#N/A	#N/A	#N/A	#N/A	#N/A	#N/A
<i>CYP27C1</i>	Downregulated	0.331035744	0.10930999	0.28494879	No	-0.4902762	0.02861127	0.06540632	Yes
<i>ANKRD36</i>	Downregulated	-0.076718195	0.29260486	0.52231293	Yes	-0.0263561	0.76377845	0.82600503	Yes
<i>TMC7</i>	Downregulated	0.324785797	0.0000561	0.0014257	No	0.09586365	0.6041704	0.69523301	No
<i>PDZD2</i>	Downregulated	-0.113688023	0.07633466	0.2245896	Yes	0.21410216	0.03843521	0.08204423	No
<i>GAL3ST4</i>	Downregulated	0.246229817	0.01943088	0.08980512	No	0.29413867	0.03333712	0.07357866	No
<i>HYDIN</i>	Downregulated	0.154847181	0.0605904	0.19290731	No	0.14161641	0.26392841	0.36859936	No
<i>CSMD2</i>	Downregulated	-0.111439752	0.09349942	0.257076	Yes	0.02319527	0.7856584	0.84342523	No
<i>RNF112</i>	Downregulated	-0.161492776	0.01713528	0.0822502	Yes	-0.3935327	0.0008972	0.0061781	Yes
<i>LAMP3</i>	Downregulated	0.30426589	0.0378137	0.1416204	No	0.04784476	0.82750535	0.87638384	No
<i>LOC100130987</i>	Downregulated	#N/A	#N/A	#N/A	#N/A	#N/A	#N/A	#N/A	#N/A
<i>LOC100289019</i>	Downregulated	#N/A	#N/A	#N/A	#N/A	#N/A	#N/A	#N/A	#N/A
<i>OAF</i>	Downregulated	0.158901366	0.19839996	0.41349032	No	0.34431189	0.0309317	0.06945743	No

<i>LEPREL1</i>	Downregulated	0.177677336	0.00162627	0.0154801	No	0.3855077	0.00150587	0.00880835	No
<i>AGER</i>	Downregulated	#N/A	#N/A	#N/A	#N/A	-0.106306	0.37447064	0.4836233	Yes
<i>ROBO3</i>	Downregulated	0.208245645	0.00614874	0.03966167	No	0.18241157	0.10082695	0.1734185	No
<i>FDXACB1</i>	Downregulated	-0.118867981	0.07896095	0.22987528	Yes	-0.1982208	0.00529096	0.01970016	Yes
<i>CDKN3</i>	Downregulated	-0.226061312	0.0113016	0.06117241	Yes	-0.5679776	0.0000104	0.0002242	Yes
<i>LOC100132832</i>	Downregulated	#N/A	#N/A	#N/A	#N/A	#N/A	#N/A	#N/A	#N/A
<i>RREB1</i>	Downregulated	0.457585912	5.75E-09	0.00000208	No	0.66393682	8.13E-07	0.0000346	No
<i>LOC100507577</i>	Downregulated	#N/A	#N/A	#N/A	#N/A	#N/A	#N/A	#N/A	#N/A
<i>EML3</i>	Downregulated	0.410991174	0.0000105	0.00042954	No	0.30945121	0.0109659	0.03215435	No
<i>TRPC3</i>	Downregulated	-0.033376913	0.72469468	0.86004701	Yes	-0.0518921	0.71707162	0.78908862	Yes
<i>LOC646851</i>	Downregulated	#N/A	#N/A	#N/A	#N/A	#N/A	#N/A	#N/A	#N/A
<i>FZD4</i>	Downregulated	-0.001038855	0.98725115	0.99478182	Yes	0.41723329	0.00037677	0.00331759	No
<i>NPIPL3</i>	Downregulated	#N/A	#N/A	#N/A	#N/A	#N/A	#N/A	#N/A	#N/A
<i>TMEM30B</i>	Downregulated	0.608970998	0.00238622	0.02040184	No	0.70732007	0.05970968	0.11550805	No
<i>MEGF6</i>	Downregulated	0.3506892	0.0015054	0.01465023	No	0.12115435	0.36746069	0.476557	No
<i>HIF3A</i>	Downregulated	0.368475576	0.0011762	0.01229449	No	0.84200277	0.000087	0.00111749	No
<i>PCSK4</i>	Downregulated	0.00930976	0.91684211	0.9640872	No	-0.0682113	0.37919923	0.48835018	Yes
<i>CENPE</i>	Downregulated	-0.017396876	0.8274149	0.91794174	Yes	-0.4522563	0.00656178	0.0226875	Yes
<i>SSC5D</i>	Downregulated	0.518436121	0.00010043	0.00215723	No	0.46913853	0.00082657	0.00582778	No
<i>DEPDC4</i>	Downregulated	-0.070005316	0.44428538	0.66442363	Yes	-0.1724353	0.09652784	0.16759066	Yes
<i>FRMPD4</i>	Downregulated	-0.385620487	0.00000525	0.00026366	Yes	-0.721726	0.00135052	0.00820702	Yes
<i>B3GALT5</i>	Downregulated	0.126970815	0.14630031	0.34282163	No	0.09735449	0.39857933	0.50741351	No
<i>TMEM51</i>	Downregulated	0.300379579	0.00051405	0.0068602	No	0.2526007	0.05623203	0.11015991	No

<i>SLC12A8</i>	Downregulated	-0.136771486	0.12858591	0.31581891	Yes	-0.3941542	0.00047378	0.00392746	Yes
<i>ETV6</i>	Downregulated	0.076039406	0.20818544	0.42590934	No	0.22780564	0.02900303	0.06608471	No
<i>LOC283922</i>	Downregulated	#N/A	#N/A	#N/A	#N/A	#N/A	#N/A	#N/A	#N/A
<i>NTN3</i>	Downregulated	0.221755066	0.06470009	0.20160313	No	0.71602449	0.0000021	0.0000698	No
<i>ARID3A</i>	Downregulated	0.139812625	0.04613083	0.16134765	No	-0.1031814	0.1839918	0.27823763	Yes
<i>FES</i>	Downregulated	0.370358919	0.0001027	0.00219589	No	0.55696955	0.0000198	0.00036477	No
<i>LRRC16A</i>	Downregulated	-0.022987915	0.62979025	0.79748638	Yes	0.50800966	0.00010656	0.00130003	No
<i>CLCNKA</i>	Downregulated	0.400060197	0.07453888	0.22126143	No	0.62708921	0.0151262	0.04060745	No
<i>UTRN</i>	Downregulated	0.311322444	9.43E-08	0.000015	No	0.52948867	0.00000596	0.00014806	No
<i>MACC1</i>	Downregulated	0.122006758	0.27134261	0.499929	No	-0.2542246	0.06026237	0.11629253	Yes
<i>ARHGAP25</i>	Downregulated	0.214281819	0.0051208	0.03489941	No	-0.0331636	0.78505238	0.84298938	Yes
<i>NRIP2</i>	Downregulated	0.225580944	0.0029419	0.02357124	No	0.14200876	0.32188622	0.43000427	No
<i>GPLD1</i>	Downregulated	-0.234044474	0.0000647	0.00158229	Yes	-0.10905	0.28199744	0.3879648	Yes
<i>BMP8A</i>	Downregulated	0.021674161	0.81065519	0.90969213	No	-0.2478264	0.00870899	0.02742917	Yes
<i>MAF</i>	Downregulated	0.324244955	0.0000118	0.00046868	No	0.30056947	0.02297003	0.0553098	No
<i>TTF2</i>	Downregulated	0.270834093	0.0003885	0.00565592	No	0.05642121	0.60655509	0.69715699	No
<i>SGK1</i>	Downregulated	0.306848779	0.00186003	0.0170028	No	0.55544222	0.00457063	0.01791495	No
<i>TRMT2B</i>	Downregulated	0.038872252	0.32578906	0.55575522	No	0.08687225	0.18181156	0.27559908	No
<i>MCM8</i>	Downregulated	0.131126268	0.01496275	0.07462497	No	0.25718725	0.04308185	0.08973333	No
<i>ZNF276</i>	Downregulated	0.23031857	0.00033055	0.00503039	No	-0.0033672	0.97117907	0.98061073	Yes
<i>PDE7B</i>	Downregulated	0.035244422	0.5788198	0.76430876	No	-0.0791829	0.50810227	0.60954343	Yes
<i>MAP3K5</i>	Downregulated	0.111992188	0.00535211	0.03608703	No	0.54005366	0.00000277	0.0000844	No
<i>LIPT1</i>	Downregulated	0.046151566	0.43855251	0.65924866	No	0.00252915	0.97758728	0.9851852	No

<i>TENCI</i>	Downregulated	#N/A	#N/A	#N/A	#N/A	0.15618287	0.24334967	0.34611883	No
<i>BCO2</i>	Downregulated	-0.065392569	0.29201724	0.52173527	Yes	-0.0971849	0.37442731	0.48357854	Yes
<i>KCNMB3</i>	Downregulated	0.09167546	0.24790009	0.47335111	No	-0.3156601	0.00063354	0.00484348	Yes
<i>CNIH3</i>	Downregulated	-0.259466187	0.00000284	0.00017053	Yes	-0.7266843	0.00000875	0.00019658	Yes
<i>RTKN2</i>	Downregulated	-0.424268773	0.00120432	0.01248187	Yes	-0.9476606	0.0000066	0.00015914	Yes
<i>KNTC1</i>	Downregulated	-0.048028146	0.49590322	0.70432493	Yes	-0.1756903	0.02465217	0.05841258	Yes
<i>HRC</i>	Downregulated	0.412088908	0.01028996	0.05738113	No	-0.0350798	0.84093397	0.88668627	Yes
<i>SLC16A4</i>	Downregulated	0.120218118	0.04704418	0.16334413	No	0.65210338	7.02E-07	0.000031	No
<i>SYTL2</i>	Downregulated	-0.319830343	0.0000392	0.00108865	Yes	0.07805478	0.6308553	0.71776284	No
<i>CCDC84</i>	Downregulated	-0.108052825	0.1117113	0.28891931	Yes	-0.2864699	0.00546157	0.02009604	Yes
<i>PLAGL1</i>	Downregulated	-0.18782868	0.01214572	0.0643286	Yes	-0.0386539	0.69485414	0.77096668	Yes
<i>PPFIBP2</i>	Downregulated	0.283847884	0.00029077	0.00461679	No	0.26231266	0.07750071	0.14128726	No
<i>NFIA</i>	Downregulated	0.291925404	0.0000408	0.00111803	No	0.36194972	0.00041732	0.00357586	No
<i>HSPG2</i>	Downregulated	0.517071023	0.00054351	0.00713542	No	0.64777682	0.0000369	0.00058804	No
<i>SERINC4</i>	Downregulated	NA	NA	NA	#N/A	0.28160757	0.00013933	0.00158699	No
<i>ADAMTS16</i>	Downregulated	0.048563896	0.65834511	0.81787188	No	-0.5217318	0.00193447	0.01035604	Yes
<i>VAMP8</i>	Downregulated	0.394665508	0.00035616	0.00531352	No	0.41550551	0.01660517	0.043493	No
<i>MGC27345</i>	Downregulated	#N/A	#N/A	#N/A	#N/A	#N/A	#N/A	#N/A	#N/A
<i>PPIEL</i>	Downregulated	-0.089049075	0.26246876	0.49020443	Yes	-0.2003847	0.0757451	0.13885823	Yes
<i>CNKSRI</i>	Downregulated	0.209000876	0.04133698	0.15010595	No	-0.2441019	0.10696702	0.18170648	Yes
<i>OIP5</i>	Downregulated	0.273620756	0.02934717	0.11916576	No	0.01241942	0.91515491	0.94057729	No
<i>CROCC</i>	Downregulated	0.203034358	0.01968222	0.09057443	No	0.02354717	0.79617634	0.85164503	No
<i>MYOM1</i>	Downregulated	0.426008709	4.26E-07	0.0000454	No	0.13548793	0.30665125	0.4142775	No

<i>LOC146880</i>	Downregulated	#N/A	#N/A	#N/A	#N/A	#N/A	#N/A	#N/A	#N/A
<i>BDNF-AS1</i>	Downregulated	#N/A	#N/A	#N/A	#N/A	#N/A	#N/A	#N/A	#N/A
<i>BUB1B</i>	Downregulated	-0.051431011	0.68103194	0.83288929	Yes	-0.5903783	0.00548213	0.02015308	Yes
<i>LOC441454</i>	Downregulated	#N/A	#N/A	#N/A	#N/A	#N/A	#N/A	#N/A	#N/A
<i>ZNF530</i>	Downregulated	-0.00399578	0.95293123	0.98082881	Yes	-0.371304	0.0000748	0.0009963	Yes
<i>RCN3</i>	Downregulated	0.191269955	0.03398365	0.13197745	No	-0.0371076	0.65919406	0.74204082	Yes
<i>CCDC142</i>	Downregulated	0.0932367	0.13024552	0.3180632	No	-0.0179761	0.70349961	0.77793626	Yes
<i>DDX58</i>	Downregulated	0.267784296	0.00000466	0.00024246	No	0.42381252	0.00000213	0.0000703	No
<i>LOC286437</i>	Downregulated	#N/A	#N/A	#N/A	#N/A	#N/A	#N/A	#N/A	#N/A
<i>AP1G2</i>	Downregulated	-0.020365222	0.81976853	0.91432292	Yes	0.2105537	0.15006727	0.23704472	No
<i>IKBKB</i>	Downregulated	0.218578326	0.00000669	0.00031518	No	0.2746935	0.00395816	0.01634508	No
<i>CTAGE1</i>	Downregulated	-0.13943346	0.82242594	NA	Yes	-0.3337281	0.13786538	0.22201668	Yes
<i>HSPBAP1</i>	Downregulated	0.052920719	0.33535229	0.56556147	No	-0.1726569	0.04108944	0.08647176	Yes
<i>KCND1</i>	Downregulated	-0.00142534	0.98416396	0.99353545	Yes	0.02127699	0.8177366	0.86865039	No
<i>PPARGC1B</i>	Downregulated	-0.149462203	0.00259598	0.02162454	Yes	-0.2804207	0.00912729	0.0283209	Yes
<i>NEXN</i>	Downregulated	0.077751357	0.33742897	0.56755058	No	0.27399899	0.01778409	0.04571763	No
<i>MSS51</i>	Downregulated	-0.295912257	0.00015137	0.00289102	Yes	-0.074877	0.55804189	0.65449806	Yes
<i>RTTN</i>	Downregulated	0.189862161	0.0072585	0.04485329	No	0.09380687	0.34332146	0.45201967	No
<i>GSDMB</i>	Downregulated	-0.123963884	0.13566832	0.3261023	Yes	0.01241468	0.93805515	0.95682929	No
<i>FBLNI</i>	Downregulated	0.37221779	0.00067646	0.00829013	No	0.80640395	0.00000804	0.00018406	No
<i>FBXL13</i>	Downregulated	0.02217509	0.67640402	0.83007346	No	0.11055129	0.16233337	0.2519923	No
<i>CCDC69</i>	Downregulated	0.235812844	0.01755947	0.08358864	No	0.37423944	0.00395681	0.01634191	No
<i>FAM72B</i>	Downregulated	-0.019520924	0.91895032	0.96488461	Yes	-0.283869	0.09620212	0.16715727	Yes

<i>SLC25A45</i>	Downregulated	0.00878475	0.89776458	0.95454183	No	-0.6121878	0.00000028	0.0000162	Yes
<i>FRZB</i>	Downregulated	0.398660907	0.00431369	0.0308327	No	0.49012205	0.0297506	0.06742326	No
<i>POLE2</i>	Downregulated	0.128495473	0.10048623	0.26958749	No	-0.2394336	0.0209857	0.05175737	Yes
<i>LOC100131691</i>	Downregulated	#N/A	#N/A	#N/A	#N/A	#N/A	#N/A	#N/A	#N/A
<i>PLK4</i>	Downregulated	-0.141064414	0.21462064	0.43358236	Yes	-0.4466962	0.00606137	0.02154931	Yes
<i>LOC401321</i>	Downregulated	#N/A	#N/A	#N/A	#N/A	#N/A	#N/A	#N/A	#N/A
<i>RAD9A</i>	Downregulated	-0.051286088	0.42591039	0.64810372	Yes	-0.3286741	0.00000208	0.0000692	Yes
<i>CASP6</i>	Downregulated	0.172591318	0.01456953	0.07323159	No	0.47235994	0.0000359	0.00057681	No
<i>TPK1</i>	Downregulated	-0.07891343	0.1675499	0.37217546	Yes	-0.3670639	0.00000219	0.0000716	Yes
<i>LRRC37A4</i>	Downregulated	#N/A	#N/A	#N/A	#N/A	#N/A	#N/A	#N/A	#N/A
<i>GLDC</i>	Downregulated	0.010403634	0.85360411	0.93175006	No	0.16718487	0.11620035	0.19404196	No
<i>MTBP</i>	Downregulated	-0.097637414	0.338829	0.569048	Yes	-0.1528791	0.06666133	0.12576197	Yes
<i>CHRD</i>	Downregulated	-0.110237007	0.07323298	0.21870207	Yes	-0.2435492	0.03002282	0.06788127	Yes
<i>C9orf169</i>	Downregulated	0.216116936	0.06359109	0.19932739	No	-0.2532235	0.01049926	0.03118457	Yes
<i>B3GNTL1</i>	Downregulated	#N/A	#N/A	#N/A	#N/A	-0.4691573	2.83E-08	0.0000036	Yes
<i>TOMM10L</i>	Downregulated	-0.2157498	0.00021071	0.00364176	Yes	-0.4022265	1.18E-07	0.00000914	Yes
<i>SLC26A5</i>	Downregulated	0.296287479	0.02068526	0.09370833	No	0.63511784	0.0044153	0.01752668	No
<i>IFIT3</i>	Downregulated	0.208742537	0.0046425	0.03253351	No	0.46155087	0.00015382	0.00171016	No
<i>DNAH10</i>	Downregulated	0.063985638	0.31731695	0.54762857	No	0.08151467	0.40837382	0.51674733	No
<i>SCUBE3</i>	Downregulated	0.066357648	0.28744873	0.51679879	No	0.47618747	0.00183001	0.01000336	No
<i>PROM2</i>	Downregulated	0.059173501	0.45014826	0.66947207	No	0.01077917	0.93069914	0.95136238	No
<i>ERNI</i>	Downregulated	0.168996568	0.00069842	0.00847419	No	0.18381851	0.01065255	0.03150225	No
<i>MIR210HG</i>	Downregulated	-0.1437565	0.32648475	0.55654176	Yes	-0.0349329	0.85872407	0.89954193	Yes

<i>HEATR7A</i>	Downregulated	#N/A	#N/A	#N/A	#N/A	#N/A	#N/A	#N/A	#N/A
<i>BAHCC1</i>	Downregulated	0.24118401	0.00735068	0.0452388	No	#N/A	#N/A	#N/A	#N/A
<i>HIFX-AS1</i>	Downregulated	0.108216224	0.1849162	0.39555038	No	-0.1895586	0.00710626	0.02393768	Yes
<i>CLEC16A</i>	Downregulated	-0.002177424	0.95381581	0.98131514	Yes	-0.0043064	0.92895263	0.95013452	Yes
<i>ATP8B1</i>	Downregulated	0.00349904	0.95653836	0.98266225	No	0.00055917	0.99496546	0.99648993	No
<i>SNTB2</i>	Downregulated	0.036267057	0.48230325	0.69412976	No	0.27465971	0.00109082	0.0070622	No
<i>FAM26F</i>	Downregulated	0.383224982	0.02037458	0.09266384	No	0.02351201	0.9088529	0.93594625	No
<i>EDA</i>	Downregulated	0.228186502	0.00288971	0.02324958	No	0.24064749	0.02642215	0.06154718	No
<i>TRPS1</i>	Downregulated	0.231307334	0.0000342	0.00098946	No	0.74029642	2.03E-08	0.00000287	No
<i>STC2</i>	Downregulated	0.022524985	0.91386838	0.96276335	No	0.20205389	0.42235556	0.53009528	No
<i>C19orf57</i>	Downregulated	0.11883447	0.07714473	0.22620143	No	-0.0521027	0.34089423	0.44958012	Yes
<i>FUT4</i>	Downregulated	0.082783123	0.05394065	0.17843873	No	0.02867935	0.72738841	0.79700248	No
<i>SLC13A3</i>	Downregulated	0.242424131	0.00173132	0.01616897	No	0.13850655	0.35833471	0.46737415	No
<i>PRKD3</i>	Downregulated	0.171279286	0.00140081	0.01394712	No	0.66305146	1.79E-08	0.00000261	No
<i>ENOSF1</i>	Downregulated	0.1909921	0.09973281	0.26830782	No	-0.4270017	0.07365584	0.13588063	Yes
<i>TBXASI</i>	Downregulated	0.500726846	2.04E-08	0.00000506	No	0.28415185	0.09207582	0.16145992	No
<i>FBF1</i>	Downregulated	0.105436687	0.09271799	0.25566831	No	0.01875794	0.78107387	0.83998125	No
<i>CACNA1G</i>	Downregulated	-0.047527631	0.63448427	0.80094513	Yes	-0.3536526	0.02843016	0.06507192	Yes
<i>EXTL1</i>	Downregulated	-0.280366102	0.00102699	0.01118779	Yes	-0.414019	0.01308338	0.03654282	Yes
<i>FBXW4P1</i>	Downregulated	0.10448103	0.262858	0.49070447	No	0.09514819	0.46611711	0.57113278	No
<i>ACCS</i>	Downregulated	-0.06690486	0.48872664	0.6990176	Yes	-0.0260879	0.86823998	0.9064494	Yes
<i>MMACHC</i>	Downregulated	0.035325388	0.40751176	0.63247416	No	-0.138218	0.06711608	0.12645302	Yes
<i>ZDHHC8</i>	Downregulated	0.033940386	0.67637674	0.83007346	No	-0.0612258	0.14037939	0.22515299	Yes

<i>KIAA1456</i>	Downregulated	-0.216562422	0.0040566	0.02951203	Yes	-0.5116997	0.00059429	0.00461749	Yes
<i>UBOX5</i>	Downregulated	0.018889138	0.73704848	0.86681761	No	-0.238729	0.0011244	0.00720434	Yes
<i>C1QL3</i>	Downregulated	-0.405249888	0.00061965	0.00786296	Yes	-0.5533329	0.11145808	0.18768556	Yes
<i>LRRK56</i>	Downregulated	0.07039551	0.49598667	0.70437877	No	-0.2882218	0.00852371	0.02702465	Yes
<i>MGC72080</i>	Downregulated	#N/A	#N/A	#N/A	#N/A	#N/A	#N/A	#N/A	#N/A
<i>WDR92</i>	Downregulated	-0.075241687	0.08108551	0.23408419	Yes	-0.2231766	0.000119	0.00141196	Yes
<i>SCAND2</i>	Downregulated	#N/A	#N/A	#N/A	#N/A	#N/A	#N/A	#N/A	#N/A
<i>CBR3-AS1</i>	Downregulated	-0.098803761	0.15238238	0.35164267	Yes	-0.417409	0.000011	0.00023461	Yes
<i>SFXN2</i>	Downregulated	0.01957112	0.77731055	0.89030524	No	-0.2640373	0.0043636	0.01739821	Yes
<i>LOC90784</i>	Downregulated	#N/A	#N/A	#N/A	#N/A	#N/A	#N/A	#N/A	#N/A
<i>FBXL19-AS1</i>	Downregulated	0.115779008	0.24465802	0.46890625	No	-0.1676507	0.14838371	0.23510989	Yes
<i>ANO8</i>	Downregulated	0.192230789	0.01231402	0.06495417	No	0.39642087	0.00000131	0.0000488	No

**Appendix 3: Common variants near LMNA  
and ZMPSTE24 are not associated with risk  
for AD in IGAP Stage 1**

Gene	# Variant ID	IGAP P value Stage 1
<i>LMNA</i>	rs71630614	0.05618
<i>LMNA</i>	rs75088561	0.094
<i>LMNA</i>	rs74116482	0.09867
<i>LMNA</i>	rs138130536	0.09987
<i>LMNA</i>	rs6669212	0.1016
<i>LMNA</i>	rs12144377	0.1061
<i>LMNA</i>	rs116755477	0.1178
<i>LMNA</i>	rs77778388	0.1298
<i>LMNA</i>	rs56106339	0.1757
<i>LMNA</i>	rs41310120	0.196
<i>LMNA</i>	rs116394986	0.197
<i>LMNA</i>	rs11584621	0.1994
<i>LMNA</i>	rs74610158	0.2004
<i>LMNA</i>	rs114427537	0.2058
<i>LMNA</i>	rs76017998	0.2235
<i>LMNA</i>	rs12035654	0.24
<i>LMNA</i>	rs11264435	0.2407
<i>LMNA</i>	rs11578696	0.2654
<i>LMNA</i>	rs12035615	0.2673
<i>LMNA</i>	rs547915	0.2725
<i>LMNA</i>	rs11590832	0.2731
<i>LMNA</i>	rs35997354	0.2745
<i>LMNA</i>	rs6700693	0.2762
<i>LMNA</i>	rs9919256	0.2791
<i>LMNA</i>	rs584025	0.2797
<i>LMNA</i>	rs520973	0.3095
<i>LMNA</i>	rs581342	0.3103
<i>LMNA</i>	rs509551	0.3125
<i>LMNA</i>	rs665979	0.3139

---

<i>LMNA</i>	rs553016	0.3193
<i>LMNA</i>	rs693671	0.3196
<i>LMNA</i>	rs6657367	0.3224
<i>LMNA</i>	rs594028	0.3264
<i>LMNA</i>	rs471679	0.3274
<i>LMNA</i>	rs2485666	0.3281
<i>LMNA</i>	rs577492	0.332
<i>LMNA</i>	rs671728	0.3321
<i>LMNA</i>	rs2485665	0.3391
<i>LMNA</i>	rs28653480	0.3394
<i>LMNA</i>	rs610918	0.3434
<i>LMNA</i>	rs7531942	0.3439
<i>LMNA</i>	rs1962065	0.3504
<i>LMNA</i>	rs2485668	0.3537
<i>LMNA</i>	rs2485676	0.3573
<i>LMNA</i>	rs78261031	0.3576
<i>LMNA</i>	rs505058	0.3578
<i>LMNA</i>	rs955383	0.3637
<i>LMNA</i>	rs2430415	0.3661
<i>LMNA</i>	rs2430416	0.3664
<i>LMNA</i>	rs609625	0.3696
<i>LMNA</i>	rs2993267	0.3756
<i>LMNA</i>	rs543235	0.3817
<i>LMNA</i>	rs500940	0.387
<i>LMNA</i>	rs528636	0.3879
<i>LMNA</i>	rs513043	0.3932
<i>LMNA</i>	rs4661147	0.3972
<i>LMNA</i>	rs520910	0.4008
<i>LMNA</i>	rs672200	0.4027
<i>LMNA</i>	rs2993269	0.4035
<i>LMNA</i>	rs675661	0.4061
<i>LMNA</i>	rs501791	0.4064

---

---

<i>LMNA</i>	rs6691659	0.4065
<i>LMNA</i>	rs544627	0.4083
<i>LMNA</i>	rs10159320	0.4087
<i>LMNA</i>	rs2485667	0.4093
<i>LMNA</i>	rs116251020	0.4105
<i>LMNA</i>	rs2485675	0.4111
<i>LMNA</i>	rs503815	0.4117
<i>LMNA</i>	rs517606	0.4162
<i>LMNA</i>	rs6686943	0.4164
<i>LMNA</i>	rs569025	0.4189
<i>LMNA</i>	rs623189	0.419
<i>LMNA</i>	rs653969	0.4218
<i>LMNA</i>	rs2485674	0.423
<i>LMNA</i>	rs521354	0.4231
<i>LMNA</i>	rs7339	0.4262
<i>LMNA</i>	rs2475758	0.428
<i>LMNA</i>	rs545731	0.4288
<i>LMNA</i>	rs568036	0.429
<i>LMNA</i>	rs593987	0.4297
<i>LMNA</i>	rs538089	0.4313
<i>LMNA</i>	rs2993266	0.4328
<i>LMNA</i>	rs2430417	0.4361
<i>LMNA</i>	rs10158206	0.4385
<i>LMNA</i>	rs2485664	0.4413
<i>LMNA</i>	rs140762385	0.4466
<i>LMNA</i>	rs646840	0.4505
<i>LMNA</i>	rs666869	0.4507
<i>LMNA</i>	rs508641	0.4515
<i>LMNA</i>	rs534807	0.452
<i>LMNA</i>	rs111340905	0.4536
<i>LMNA</i>	rs476000	0.4539
<i>LMNA</i>	rs582690	0.4625

---

---

<i>LMNA</i>	rs9427236	0.4658
<i>LMNA</i>	rs16837187	0.4669
<i>LMNA</i>	rs141257912	0.4756
<i>LMNA</i>	rs2485672	0.4836
<i>LMNA</i>	rs573739	0.492
<i>LMNA</i>	rs573735	0.4924
<i>LMNA</i>	rs56702163	0.499
<i>LMNA</i>	rs7542186	0.5
<i>LMNA</i>	rs11264443	0.5056
<i>LMNA</i>	rs11264442	0.5057
<i>LMNA</i>	rs74116489	0.5191
<i>LMNA</i>	rs2430414	0.5238
<i>LMNA</i>	rs622834	0.5292
<i>LMNA</i>	rs12063072	0.5563
<i>LMNA</i>	rs12073543	0.5609
<i>LMNA</i>	rs2485662	0.5691
<i>LMNA</i>	rs11264434	0.5698
<i>LMNA</i>	rs915180	0.5841
<i>LMNA</i>	rs113487506	0.5991
<i>LMNA</i>	rs112941217	0.601
<i>LMNA</i>	rs11803917	0.6141
<i>LMNA</i>	rs139860915	0.6255
<i>LMNA</i>	rs12063564	0.643
<i>LMNA</i>	rs6661281	0.6609
<i>LMNA</i>	rs12076700	0.6623
<i>LMNA</i>	rs10737170	0.6802
<i>LMNA</i>	rs6691151	0.6925
<i>LMNA</i>	rs6691151	0.6925
<i>LMNA</i>	rs11264437	0.7089
<i>LMNA</i>	rs12565130	0.7168
<i>LMNA</i>	rs4661146	0.7549
<i>LMNA</i>	rs4641	0.7577

---

<i>LMNA</i>	rs12131777	0.7593
<i>LMNA</i>	rs61813324	0.8164
<i>LMNA</i>	rs915179	0.8994
<i>LMNA</i>	rs11264447	0.8997
<i>LMNA</i>	rs536857	0.9264
<i>LMNA</i>	rs72708262	0.9336
<i>LMNA</i>	rs682267	0.9519
<i>LMNA</i>	rs480886	0.952
<i>ZMPSTE24</i>	rs114052415	0.03941
<i>ZMPSTE24</i>	rs80160325	0.09068
<i>ZMPSTE24</i>	rs60640112	0.1034
<i>ZMPSTE24</i>	rs77081740	0.1166
<i>ZMPSTE24</i>	rs111781530	0.1595
<i>ZMPSTE24</i>	rs11207778	0.174
<i>ZMPSTE24</i>	rs71648511	0.242
<i>ZMPSTE24</i>	rs12725815	0.256
<i>ZMPSTE24</i>	rs79638111	0.2903
<i>ZMPSTE24</i>	rs12757549	0.2974
<i>ZMPSTE24</i>	rs16827109	0.302
<i>ZMPSTE24</i>	rs11811980	0.3261
<i>ZMPSTE24</i>	rs16827106	0.3302
<i>ZMPSTE24</i>	rs7517840	0.3339
<i>ZMPSTE24</i>	rs3765483	0.3367
<i>ZMPSTE24</i>	rs2284447	0.3367
<i>ZMPSTE24</i>	rs7548758	0.3372
<i>ZMPSTE24</i>	rs6691598	0.4041
<i>ZMPSTE24</i>	rs6676644	0.4346
<i>ZMPSTE24</i>	rs149885289	0.4351
<i>ZMPSTE24</i>	rs1579150	0.4822
<i>ZMPSTE24</i>	rs74938879	0.4935
<i>ZMPSTE24</i>	rs6600324	0.5127
<i>ZMPSTE24</i>	rs6600323	0.514

ZMPSTE24	rs6682701	0.5423
ZMPSTE24	rs12134085	0.5513
ZMPSTE24	rs10889220	0.5567
ZMPSTE24	rs2092735	0.5685
ZMPSTE24	rs9326050	0.6201
ZMPSTE24	rs12121804	0.6311
ZMPSTE24	rs11589157	0.6575
ZMPSTE24	rs140585118	0.688
ZMPSTE24	rs55674553	0.6906
ZMPSTE24	rs7516571	0.7033
ZMPSTE24	rs720793	0.7253
ZMPSTE24	rs6664294	0.7535
ZMPSTE24	rs6677717	0.7756
ZMPSTE24	rs7556313	0.7848
ZMPSTE24	rs11207771	0.8402
ZMPSTE24	rs74763199	0.8579
ZMPSTE24	rs2284446	0.8593
ZMPSTE24	rs12144229	0.8622
ZMPSTE24	rs6698320	0.8727
ZMPSTE24	rs10489432	0.8789
ZMPSTE24	rs926830	0.8862
ZMPSTE24	rs7514099	0.8873
ZMPSTE24	rs11580085	0.8908
ZMPSTE24	rs11207716	0.8943
ZMPSTE24	rs10489430	0.9341
ZMPSTE24	rs10489431	0.9423
ZMPSTE24	rs2076697	0.9428
ZMPSTE24	rs12117796	0.9766



# Curriculum Vitae

Matthew James Rosene

[mjrosene@wustl.edu](mailto:mjrosene@wustl.edu)

PhD Candidate

Department of Psychiatry

Washington University in St. Louis School of Medicine

425 S. Euclid Ave, Campus Box 8134

St Louis, MO 63110

**Citizenship:** USA

## **Education:**

**Washington University**, St Louis, MO, US

PhD Candidate, Molecular Cell Biology

Mentor: Dr. Celeste M Karch

**Luther College**, Decorah, Iowa, USA

BA, *cum laude*, Biology, May 2015

## **Positions:**

2018-present Doctoral student in the laboratory of Celeste Karch, St Louis, MO

2016-2018 Doctoral student in the laboratory of Zhongsheng You, St Louis, MO

2015-present PhD Student in the Division of Biology and Biomedical Sciences at Washington University, St. Louis, MO

2014 Undergraduate research intern in the laboratory of Bryan Phillips, Iowa City, IA

2013 Undergraduate research intern in the laboratory of Thomas Rutkowski, Iowa City, IA

## **Selected Honors:**

2021 Travel Fellowship, Alzheimer's Association International Conference

2016-2018 Cell and Molecular Biology Training Grant Recipient

2014 University of Iowa Summer Undergraduate Research Program Intern

**Supervising, Teaching, and Science Outreach:**

2019 Summer Mentor for the Biomed RAP Undergraduate Research Program, Madhavi Jere

2017 Teaching Assistant for General Biology, Washington University in St. Louis, St Louis, MO

2014 Undergraduate Lab Assistant, Molecular Biology, Luther College, Decorah, IA

**Conference Abstracts**

2021 Defining the role of phospholipase D3 in Alzheimer disease pathogenesis (Talk), AAIC Next Virtual Conference

2021 Defining the role of phospholipase D3 in Alzheimer disease pathogenesis (Talk), Alzheimer's Association International Conference, Denver, CO

2021 LMNA-mediated nucleoskeleton dysregulation in Alzheimer's disease (Poster), Alzheimer's Association International Conference, Denver, CO

2021 Defining the role of phospholipase D3 in Alzheimer disease pathogenesis (Talk), Chan-Zuckerberg Initiative Neurodegenerative Challenge Network Virtual Conference

2021 LMNA-mediated nucleoskeleton dysregulation in Alzheimer's disease (Poster), Washington University Virtual Psychiatry Residency Research Education Program Research Day Symposium

2020 LMNA-mediated nucleoskeleton dysregulation in Alzheimer's disease (Poster), Cold Springs Harbor Laboratory Virtual Conference for Neurodegenerative Diseases: Biology and Therapeutics

2020 LMNA-mediated nucleoskeleton dysregulation in Alzheimer's disease (Poster), Chan-Zuckerberg Initiative Neurodegenerative Challenge Network Virtual Conference

2014 Prevalence of Multi-Drug Resistant (MDR) Bacteria in North East Iowa Streams (Talk), Iowa Academy of Sciences Research Symposium, Fort Dodge, IA

**Professional Service:**

2020-Present Member of the LouHealth Advocacy group Criminal Justice Reform Team

2019 Poster Judge, Biomed RAP Summer Symposium

**Societal Membership:**

βββ Biological Honor Society

**Technical Skills:**

**Molecular Biology:** SDS-PAGE, Western blotting, protein purification, PCR, RNA purification, reverse transcription and quantitative PCR, plasmid construction and cloning, DNA radiolabeling

**Cell and Tissue Biology:** Mammalian cell culture, stable and transient transfections, virus production and transduction, immunocytochemistry, confocal and fluorescence microscopy

**Animals:** *Xenopus laevis* handling, extract preparation from *Xenopus laevis* eggs, *Caenorhabditis elegans* handling, *mus musculus* handling, *Mus musculus* brain tissue harvesting

**Peer-Reviewed Publications:**

**Matthew J. Rosene**, Natalie Wen, Zeran Li, Logan Brase, Simon Hsu, Carlos Cruchaga, Sally Temple, Oscar Harari, Celeste M. Karch. *LMNA*-mediated nucleoskeleton dysregulation in Alzheimer disease. In Revision.

**Matthew J. Rosene**, Simon Hsu, Shih Feng You, Logan Brase, Anthony Verbeck, Rita Martinez, Clare E. Wallace, Zeran Li, Ping Yan, Nina M. Dräger, Sydney M. Sattler, Abhirami K. Iyer, Shannon L. Macauley, David Holtzman, Bruno A. Benitez, Martin Kampmann, Carlos Cruchaga, Oscar Harari, John Cirrito, Jin-Moo Lee, Alison Goate, Celeste M. Karch. Phospholipase D3 contributes to Alzheimer's disease risk via disruption of A $\beta$  clearance and inflammatory response. In Revision. medRxiv:

<https://doi.org/10.1101/2022.01.31.22270175>

Simon Hsu, Anna A. Pimenova, Kimberly Hayes, Juan A. Villa, **Matthew J. Rosene**, Madhavi Jere, Alison M Goate, Celeste M. Karch (2020). Systematic Validation of Variants of Unknown Significance in APP, PSEN1 and PSEN2. *Neurobiology of Disease* (In Press. DOI: <https://doi.org/10.1016/j.nbd.2020.104817>)

Justina P. Tavana\*, **Matthew Rosene** \*, Nick O. Jensen, Perry G. Ridge, John S.K. Kauwe, Celeste M. Karch (2019). RAB10: an Alzheimer's disease resilience locus and potential drug target. *Clinical Interventions in Aging* 14: 73-79.